ACTA UNIVERSITATIS SZEGEDIENSIS

ACTA
MINERALOGICA-PETROGRAPHICA

ABSTRACT SERIES

Volume 7 Miskolc, 2012

JOINT MSCC+CEMC 2012

5th Mineral Sciences in the Carpathians Conference
3rd Central-European Mineralogical Conference

Co-organiser

Scientific sponsors:

Published by the Department of Mineralogy, Geochemistry and Petrology, University of Szeged

ACTA MINERALOGICA-PETROGRAPHICA
established in 1922

ABSTRACT SERIES

HU ISSN 1589-4835
HU ISSN 0324-6523

Editorial Address
H-6701 Szeged, Hungary
P.O. Box 651
E-mail: asviroda@geo.u-szeged.hu

Abbreviated title:
Acta Mineral. Petrogr. Abstr. Ser., Szeged

The Acta Mineralogica-Petrographica is published by the Department of Mineralogy, Geochemistry and Petrology, University of Szeged, Szeged, Hungary

---

On the cover: The main entrance of the University of Miskolc.
On the logo of the conference: Euchroite from Ľubietová, Slovakia (after Grailich & Lang, 1857).

JOINT
5th MINERAL SCIENCES IN THE CARPATHIANS CONFERENCE (MSCC)
and
3rd CENTRAL-EUROPEAN MINERALOGICAL CONFERENCE (CEMC)
Miskolc, Hungary, 19–21 April 2012

ABSTRACTS

Edited by

Béla Fehér

Abstracts revised by

Ferenc Mádai, Csaba Szabó, Sándor Szakáll, Pavel Uher, Tamás G. Weiszburg and Norbert Zajzon

Sponsored by

CBGA Commission on Mineralogy and Geochemistry
Czech Geological Society
Herman Ottó Museum
Mineralogical and Geochemical Branch of the Hungarian Geological Society
Mineralogical Society of Poland
Mineralogical Society of Romania
Slovak Geological Society
Ukrainian Mineralogical Society

Organizer

University of Miskolc

Co-organizer

Slovak Mineralogical Society

International Scientific Board

Igor Broska
Geological Institute, Slovak Academy of Sciences, Bratislava, Slovakia

Corina Ionescu
Babeş-Bolyai University, Cluj-Napoca, Romania

Friedrich Koller
University of Vienna, Vienna, Austria

Victor Kvasnytsya
Institute of Geochemistry, Mineralogy and Ore Formation, National Academy of Sciences, Kyiv, Ukraine

Milan Novák
Masaryk University, Brno, Czech Republic

Adam Pieczka
AGH – University of Science and Technology, Cracow, Poland

Mihály Pósfai
University of Pannonia, Veszprém, Hungary

Local Organizing Committee

Sándor Szakáll (chairman)
János Földessy, Ferenc Mádai, Viktor Mádai and Norbert Zajzon
University of Miskolc, Miskolc, Hungary

Béla Fehér
Herman Ottó Museum, Miskolc, Hungary

MINERALOGY AND MINERAL CHEMISTRY OF HORNBLENDITES FROM THE DITRĂU ALKALINE MASSIF (ROMANIA) AND ITS PETROGENETIC RELATIONS

ALMÁSI, E.E.*, PÁL-MOLNÁR, E. & BATKI, A.
Department of Mineralogy, Petrology and Geochemistry, University of Szeged, Egyetem Street 2, H-6722 Szeged, Hungary
* E-mail: almasieniko@geo.u-szeged.hu

The Ditrău Alkaline Massif [DAM] is a Mesozoic alkaline igneous complex, which is situated in the S-SW part of the Ghiurghiu Mountains in the Eastern Carpathians (Romania). Petrographically the DAM is exceptionally diverse, and consists of different type of rocks: hornblendites, gabbros, diorites, monzodiorites, monzonites, nepheline syenites, granites, monzosyenites, syenites, quartz syenites, alkali feldspar syenites, lamprophyres and tinguaites. The massif is the result of a long lasting (Middle Triassic–Lower Cretaceous), two phased (Middle Triassic–Upper Triassic and Lower Cretaceous) magmatic process (PÁL-MOLNÁR, 2010*)*.

Horblendites are representative primitive rocks of the massif, thus the determination of their mineralogy and mineral chemical composition is essential for understanding the magma processes, which formed the DAM. Several varieties can be found here such as olivine-pyroxene hornblendite, pyroxene-hornblendite, plagioclase-bearing hornblendite and pure hornblendite.

The aim of this paper is the discussion of mineralogy and mineral chemistry of hornblendites and the estimation of their impact on the petrogenesis of the rocks.

Chemical analysis of the minerals were performed on a Cameca SX-50 (acceleration voltage of 15kV, and probe current 20 nA) electron microprobe at the University of Bern, Switzerland.

The main rock forming minerals are amphibole, pyroxene, plagioclase, biotite and a small amount of apatite titanite and magnetite.

Olivine is often altered and can be found only in olivine-pyroxene hornblendite. The Fo content varies between 74–98%, referring to a crystallization from a relatively primitive magma.

The amphibole content could reach even 90 wt% among the other rock forming minerals. The following amphibole types were identified: pargasites, kaersutites, ferrokaersutites and magnesiohastingsites.

Among the plagioclases albite ($Ab_{78–98}$) is dominating, due to late stage processes.

Biotites are represented by annite, which present in all the samples except in olivine-pyroxene-hornblendites.

Pyroxenes are mainly diopsides, aegirine-augites and augites. Additionally ferro-enstatite occurs in olivine-pyroxene hornblendite. The pyroxenes are zoned, in some cases as a diopside core and augite and/or aegirine augite rim, suggesting metasomatic alteration of pyroxenes among rim and cleavages.

The composition of clinopyroxenes is a sensitive indicator of the nature of magma and crystallization history. Ti vs. Al ratios (0.191–0.246) in the pyroxenes indicate high crystallization pressure. The pyroxenes formed under the following p-T conditions: max. 1150°C and 18–22 kbar (using the thermobarometry of NIMIS, 1999).

According to the thermometry of RIDOLFI *et al*. (2010), amphibole composition is estimated at max. 1000°C, and 7–10 kbar using the method of ANDERSON & SMITH (1995) and HOLLISTER *et al*. (1987).

The mineralogical composition of the different types of hornblendites indicates a fractionational crystallization process. Thus, the most primitive rock is olivine-pyroxene hornblendite, whilst the most differentiated one is plagioclase-bearing hornblendite.

Based on the evaluated pressure and temperature values of amphiboles and pyroxenes magnesiohastingsite and pargasite could have crystallised at around 50 km depth, whilst diopside and augite could have formed at around 60–65 km depth. The composition of amphiboles and pyroxenes of the DAM hornblendites suggests that the primitive melt originated from the upper mantle, more than 70 km depth.

References

ANDERSON, J.L. & SMITH, D.R. (1995): American Mineralogist, 80: 549–559.

HOLLISTER, L.S., GRISSOM, G.C., PETERS, E.K., STOWELL, H.H. & SISSON, V.B. (1987): American Mineralogist, 72: 231–239.

NIMIS, P. (1999): Contributions to Mineralogy and Petrology, 135: 62–74.

PÁL-MOLNÁR, E. (2010): Rock-forming minerals of the Ditrău alkaline massif. In: SZAKÁLL, S. & KRISTÁLY, F. (eds.): Mineralogy of Székelyland, Eastern Transylvania, Romania. Csík County Nature and Conservation Society, Sfântu Gheorghe–Miercurea-Ciuc–Târgu Mureş, pp. 63–88.

RIDOLFI, F., RENZULLI, A. & PUERINI, M. (2010): Contributions to Mineralogy and Petrology, 160: 45–66.

GEOCHEMISTRY OF THE SKARN FROM MRACONIA VALLEY, ROMANIA

ANASON, A.[1]*, MARINCEA, Şt.[1], BILAL, E.[2], DUMITRAS, D.G.[1] & IANCU, A.M.[1]
[1] Geological Institute of Romania, 1 Caransebes Str., RO-012271, Bucharest, Romania
[2] Centre SPIN, Ecole Nationale Supérieure des Mines de Saint-Etienne, 158, Cours Fauriel, F-42023 Saint-Etienne Cedex 2, France
* E-mail: angela.anason@yahoo.com

The research area is of the hydrographic basin of the Mraconia Valley, it is bounded by the alignment Poiana Mraconia and Lugojistea at north; at east by the Satului Valley; southern limit is the Ponicova Valley and the western limit is Cracul Radului-Cracul Urzicea. The studied rock belongs to two generations of intrusions corresponding to the acid magmatic phase, followed by basic dykes, including kersantite and spessartite. The crystalline schist of the Poiana Mraconia Series (CODARCEA *et al*., 1934) suffered a progressive amphibolite with almandine facies metamorphism, a kyanite-almandine-muscovite sub-facies, together revealed the meta-pelite paragenesis including kyanite, green hornblende, andesine and almandine. The primary metamorphism was followed by regressive metamorphism of the Assyntic orogeny and Varisc cycles (BERCIA & BERCIA, 1975). The amphibolite paragneiss and the micaceous paragneiss (with biotite and garnet) associated with the quartz-feldspar gneiss were affected by the arteritic migmatization. The endoskarns can be distinguished from their high levels of Al, Na, K, Fe, Mg, Mn, Cu, Pb and Mo, however, the exoskarns are characterized by their high content of W. So we see a duality related to host rock (limestone, hornfels, granitoids) through which the metasomatic fluids were filtered. The skarns in the systems ACF and CaO-SiO_2-MgO show clearly the difference between endoskarns and exoskarns, and the influence of the crystallization of garnet and pyroxene on the evolution of fluids between the igneous rocks and limestones. Some exoskarns show the presence of wollastonite in this equilibrium. Finally, endoskarns are characterized by the presence of sulphides of Mo, Pb, Cu, Zn; the other hand, the exoskarns are much richer in scheelite. The garnet is contemporary of sulphidization phase affecting the pyroxene. There has been a syn-crystallization of andradite and sulphides, and silicification associated with sulphides (pyrite, pyrrhotite). The andradite-quartz-sulphide assemblage results from the transformation of pyroxene in the presence of sulphide. If the fugacity of sulphur increases during the transformation, the pyrrhotite is unstable and only pyrite is present (ANASON *et al.,* 2011).The main metallic mineral from Mraconia Valley is scheelite and molybdenite. The skarn is richer in garnet (andradite) and ferroactinolite, magnetite, epidote, apatite, vesuvianite and wollastonite.

References

ANASON, A., BILAL, E., MARINCEA, Şt., DUMITRAS, D.G., (2011): 17th Meeting of the Association of European Geological Societies (MAEGS-17), Belgrade, 215–217.

BERCIA, I. & BERCIA, E. (1975): Revue Roumanie de Géologie, Géophisique et Géographie, Série de Géologie, 24:

CODARCEA *et al.* (1934): C.R. Inst. Geol. Roum., 21:

DISTRIBUTION OF PLATINUM-GROUP ELEMENTS IN UPPER MANTLE XENOLITHS FROM THE CARPATHIAN-PANNONIAN REGION

ARADI, L.[1]*, HATTORI, K.[2], GRIFFIN, W.[3], O'REILLY, S.[3], SZABÓ, Á.[1] & SZABÓ, Cs.[1]
[1] Lithosphere Fluid Research Lab, Department of Petrology and Geochemistry, Eötvös Loránd University, Pázmány Péter sétány 1/C, H-1117 Budapest, Hungary
[2] Department of Earth Sciences, University of Ottawa, Canada
[3] GEMOC, Department of Earth and Planetary Sciences, Macquarie University, Australia
* E-mail: aradi.laszloelod@gmail.com

The geochemical behaviour of platinum-group elements (PGE) is widely debated due to their geochemical significance and economic importance. Laboratory experiments revealed that the abundances of PGEs in the silicate Earth are several orders of magnitude higher than is expected, and their Pd/Ir and Ru/Pt ratios are nearly chondritic. A widely accepted model for this high level of PGEs in the silicate Earth is the "Late Veneer" model, which assumes that after formation of the core, and during the "Late Heavy Bombardment" (4–3.8 Ga), an influx of chondritic meteorites caused the anomalous PGE abundances and chondritic ratios. PGEs are used to trace melting and metasomatic events in Earth's mantle. 90% of the PGE content of the mantle resides in sulphides (e.g., monosulphide solid solution, pentlandite, chalcopyrite); by analyzing the PGE contents of these sulphides, in basalt-, kimberlite- and lamprophyre-hosted ultramafic xenoliths, the PGE budget of the mantle can be estimated.

We chose 15 sulphide-bearing peridotite xenoliths from the Carpathian-Pannonian region (CPR), including the Styrian Basin, Bakony-Balaton Highland, Nógrád-Gömör and East-Transylvanian Basin. Petrographically all of them are lherzolites; a few samples contain rare metasomatic amphibole. Their textures are representative for their source region, varying from protogranular to equigranular and some of them show poikilitic textures.

Geochemical features of the bulk rock compositions and clinopyroxenes reveal that partial melting and refertilization processes affected the mantle, which is widely known in this region. These processes also affect the PGE budget of the mantle, which is studied first in our work in the CPR.

Os, Ir, Ru, Rh, Pt and Pd contents were determined in lherzolite xenoliths and in their sulphide grains. Total whole-rock PGE contents range between 7 and 21 ppb regardless of location. Ir-type PGEs are overall high, 5–12 ppb, which confirms the residual-mantle nature of the xenoliths. Pt and Pd contents and their ratios with Ir-type PGEs correlate with Al, as expected, due to the incompatible nature of Pt and Pd during partial melting. In situ PGE analyses on sulphide grains show positive correlations between Os, Ir, Ru and Rh, except in sulphides from the Bakony-Balaton-Highland and some sulphides from Nógrád-Gömör and East-Transylvania, whereas Pt and Pd correlate poorly with the Ir-type PGEs. The total concentrations of PGEs range between 4 and 796 ppm. All these data reveal that the PGE distribution in the mantle under the CPR is heterogeneous, and each of the xenolith localities studied has its own PGE pattern. Most of the PGE patterns show high and variable abundances of Os, Ir, Ru and Rh, with decreasing abundance from Rh to Au and a strong negative Pt anomaly. This distribution could be explained by different degrees of melting and metasomatism beneath the CPR.

MINERALOGY, PETROGRAPHY AND ORIGIN OF A HYDROTHERMAL BRECCIA IN THE RECSK PORPHYRY-EPITHERMAL ORE COMPLEX, ILONA VALLEY, PARÁD (NE-HUNGARY)

ARATÓ, R.[1]*, KISS, G.[1] & MOLNÁR, F.[2]
[1] Department of Mineralogy, Eötvös Loránd University, Pázmány P. sétány 1/c, H-1117 Budapest, Hungary
[2] Geological Survey of Finland, PO. Box 96, FI-02151 Espoo, Finland
* E-mail: arato.robi@gmail.com

The Recsk Igneous Complex is the north-easternmost member of the Palaeogene magmatic range along the Periadriatic-Balaton Lineament (MOLNÁR, 2007). It is located in the north-eastern forelands of the Mátra Mountains, NE-Hungary. In this complex, four volcanic and three related intrusive stages were distinguished by FÖLDESSY *et al.* (2008). The focus of this study was a hydrothermal breccia dyke, located in the Ilona Valley (south of Parád village, in the Recsk Orefield). The host rock of the dyke is a dacite tuff, which formed in the second phase of the Palaeogene volcanism in this area. An interesting aspect of this hydrothermal breccia is that – as MOLNÁR *et al.* (2008) showed by K-Ar studies – its age is Lower Oligocene, which finding opens up a new ground of geological evaluation of the Recsk porphyry-epithermal system.

Following the fieldwork, macroscopic and microscopic observations together with XPD, Raman-spectroscopy and SEM+EDS analyses were carried out in order to characterize the hydrothermal breccia.

Four main types of fragments were detected in the breccia, all of which have suffered a strong hydrothermal alteration. The most abundant clasts are round, intensively altered (to clay minerals and adularia) andesite fragments with 1.5–3 mm size, probably representing the first stage submarine lava flows of the volcanic complex. The second group of fragments consists of mostly argillitised-silicified dacitic tuff (>3 cm size) and idiomorphic feldspar crystals, representing fragments of the host dacitic tuff. Rarely occurring coarse-grained fragments of diorite/quartz-diorite clasts had probably originated from the subvolcanic intrusion below the volcanic sequence. Completely sericitic-silicic fragments with relict sedimentary texture were also recognized probably originating from the basement sedimentary units. The matrix consists mostly of hydrothermal quartz and sericite, however, adularia also occurs. Disseminated pyrite is abundant in both the matrix and the rock fragments, while a small amount of sphalerite is present in the former, and galena occurs in the latter one. Anatase is a common hydrothermal accessory mineral in the andesite fragments, mostly replacing feldspar together with pyrite, but it is completely absent in the matrix and in the other fragments. In addition to these minerals, barite, zircon and monazite fragments were detected in the andesite by the SEM.

According to these results, the hydrothermal breccia dyke most likely started its way from the depth of the basement sedimentary rocks and the subvolcanic intrusion and cut through the first and second phase volcanic rocks. The observable alteration- and partly the ore mineral paragenesis imply, that the formation of the breccia can be related to a low-sulphidation (LS) epithermal system, which is also supported by the previous work of MOLNÁR *et al.* (2008). In contrast, the occurrence of barite and anatase is characteristic to more acidic environments (HEDENQUIST & ARRIBAS, 1999). Three kinds of environments could be assumed for the presence of this kind of acidic fluids: 1.) the deeper part that belong to the subvolcanic intrusion of the system, 2.) a shallower environment, the high sulphidation-type epithermal part, or 3.) a steam heated zone, representing also a shallower part of the system. The known geological background supports shallower depth for the processes that happened during the earlier stages of the evolution of the volcanic sequence. This phenomena – effecting only on the older rock fragments of the breccia – is newly discovered in the area of Parád and is almost completely overprinted by the products of the LS-system.

This work was supported by the Baross Gábor Program of the National Research and Technology Agency (NKTH).

References

FÖLDESSY, J., ZELENKA, T., BENEDEK, K. & PÉCSKAY, Z. (2008): Miskolci Egyetem Közleményei, Geosciences, Series A, Mining, 73: 7–21.

HEDENQUIST, J.W. & ARRIBAS, A. (1999): Guidebook Series of the Society of Economic Geologists, 31: 13–64.

MOLNÁR, F. (2007): Proceedings of the Ninth Biennial SGA Symposium, Dublin, 2007, 153–157.

MOLNÁR, F., JUNG, P., KUPI, L., POGÁNY, A., VÁGÓ, E., VIKTORIK, O., PÉCSKAY, Z. & HURAI, V. (2008): Miskolci Egyetem Közleményei, Geosciences, Series A, Mining, 73: 99–128.

TENNANTITE-TETRAHEDRITES FROM MADAN Pb-Zn HYDROTHERMAL DEPOSITS (BULGARIA): CRYSTAL MORPHOLOGY AND MINERAL TEXTURES

ATANASSOVA, R. & VASSILEVA, R.D.*
Geological Institute, Bulgarian Academy of Sciences, BG-1113 Sofia, Bulgaria
* E-mail: rosivas@geology.bas.bg

The sulphosalt minerals usually occur as massive, coarse aggregates or small (< l mm) anhedral grains and inclusions. Tennantite-tetrahedrite polyhedral crystals are rarely reported in literature (KOSTOV & KOSTOV, 1999). Representative samples from the Petrovitsa and Gradishte base metal deposits, Madan ore region, Central Rhodopes, Bulgaria are studied. Tennantite-tetrahedrites from Madan deposits are formed in the late phases of the main quartz-sulphide stage with galena, sphalerite, pyrite and chalcopyrite, showing complex chemical compositions (VASSILEVA *et al.*, 2012). In the studied materials sulphosalts are presented as remarkable size crystals with polyhedral morphologies.

The tennantite-tetrahedrite in the Gradishte samples are observed as idiomorphic crystals and postdate the aggregates of large chalcopyrite, pyrite and quartz. In polished sections the inclusions of chalcopyrite are crosscut by the sulphosalts, showing their later formation. Under SEM it was observed that crystals are developed by negative and small positive tetrahedra. The {110} acting mostly as a modifying form. Tennantite-tetrahedrite overgrows (112) chalcopyrite faces with parallel mutual orientation, due to the similar basic structural motifs (BONEV, 1973). Characteristic penetration twins on {111} are observed (Fig. 1).

Macroscopically, the tetrahedrite from Petrovitsa occurs as well-shaped crystals, where two characteristic morphologies are observed: (i) Tennantite-tetrahedrite crystals, composing peculiar crust, completely overgrow and resemble the shape of the main sulphides. These perimorhoses are composed by subparallel crystals, which are from 0.5–1 to 3–4 mm in size, with tetrahedral habit and bounded by the faces of *o*{111}, *d*{110}, *a*{100} and small *n*{211}. In cross section, the central parts of the crusts contain aggregates of chalcopyrite-galena-sphalerite-tetrahedrite association, together with carbonates and minor quartz. The galena and chalcopyrite crystals situated under these mineral crusts are affected probably by natural dissolution, which process has not left macroscopic marks on the tetrahedrite crystals. In polished sections galena occur as characteristic vertex formations growing with chalcopyrite and sphalerite. Tetrahedrite corrodes slightly sphalerite and galena or penetrates chalcopyrite. The textural relationships among the three minerals change considerably in different places of an aggregate, suggesting complex intergrowth mechanism of formation and metasomatic replacement. (ii) Single crystals, up to 1 mm, observed preferably on cubo-octahedral galena crystals (2–3 mm). Tetrahedrite overgrows galena cubo-octahedra following the scheme galena (100) [100] // tetrahedrite (001) [110], represented the one of the cases of epitaxy, described by MINCHEVA-STEFANOVA (1960). According to the textural characteristics and spatial position these tetrahedrites are formed shortly after the polyhedral crusts.

Acknowledgements. The authors are grateful for the financial support of the BG051PO001-3.3.05-0001 Project of the Bulgarian Ministry of Science and Education and SCOPES IZ73Z0-128089 project of the Swiss National Fund.

References

BONEV, I.K. (1973): Bulletin of the Geological Institute, Series Geochemistry, Mineralogy, Petrography, 22: 91–105.

KOSTOV, I. & KOSTOV, R. (1999): Crystal habits of minerals, Prof. Martin Drinov Acadademic Publishing House & Pensoft, Sofia, 415 p.

MINCHEVA-STEFANOVA, J. (1960): Zapiski Vsesoyuznogo Mineralogicheskogo Obshchestva, 89: 213–219.

VASSILEVA, R.D., ATANASSOVA, R. & KOUZMANOV, K. (2012): Acta Mineralogica-Petrographica, Abstract Series, 7: this volume.

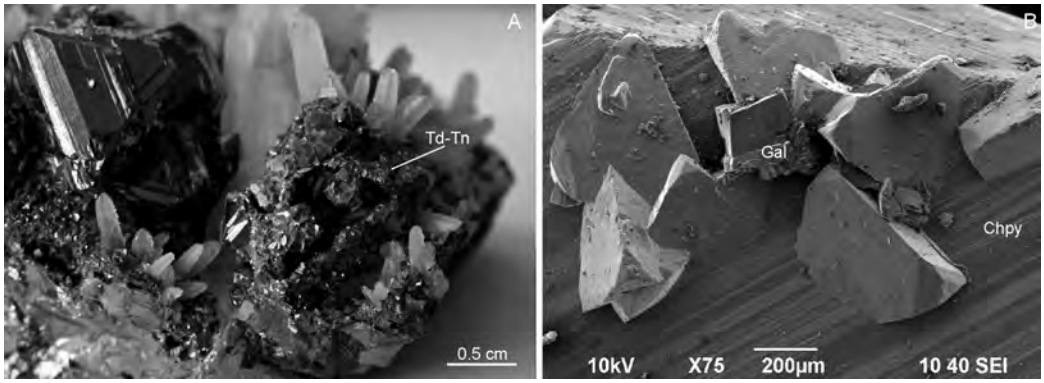

Fig. 1. *A) Tetrahedrite crust resampling sphalerite morphology, Petrovitsa; B) SEM image of Gradishte sulphosalts on chalcopyrite (Chpy).*

ENVIRONMENTAL IMPACT OF ACID MINE DRAINAGE ON THE ROŞIA RIVER (ROŞIA MONTANĂ MINING AREA, ROMANIA): A MINERALOGICAL AND GEOCHEMICAL APPROACH

AZZALI, E.[1]*, MARESCOTTI, P.[1], CARBONE, C.[1], DINELLI, E.[2], PORRO, S.[3], DE CAPITANI, L.[3] & SERVIDA, D.[3]
[1] Dip. Te. Ris., University of Genova, Corso Europa 26, Genova, Italy
[2] Dip. Scienze della Terra, University of Bologna, Piazza di Porta San Donato, Bologna, Italy
[3] Dip. Scienze della Terra, University of Milano, Via Botticelli 23, Milano, Italy
* E-mail: eva.azzali@unige.it

The development of Acid Mine Drainage (AMD), as a result of the oxidative weathering of sulphides, and the release of Potentially Toxic Elements (PTE) in the environment are one of the main problem affecting the natural watercourses in mining areas (NORDSTROM, 2011).

The studied area is within the Roşia Montană mine site, a hydrothermal gold deposit hosted in andesites and dacites of Neogene age, piercing the prevolcanic sedimentary basement as breccia pipes (WALLIER *et al.*, 2006).

In this study a mineralogical and geochemical characterization of the ochreous precipitates and coupled waters occurring in the Roşia River was carried out in order to evaluate both the mineralogical variations and the PTE partitioning between contaminated waters and secondary minerals. Twelve samples of ochreous precipitates, associated to mine waters and soils were collected starting from the adit of the "Sf. Cruci din Orlea" gallery up to the confluence between Roşia and Abrud Rivers. The mineralogy of the precipitates was determined by means of XRPD, whereas the bulk chemistry by ICP-MS. Temperature, pH and Eh were measured in situ, whereas the chemical analysis on mine waters were made by means of ICP-OES, AAS and chromatography.

Ochreous precipitates consist of a mixture of jarosite and schwertmannite and are characterized by high concentrations of PTE (V, Zn, Cd, As, Pb). Moreover a positive correlation between Fe and S with As, V and Pb suggests an effective control of schwertmannite and jarosite on the mobility of specific PTE. Waters flowing from "Sf. Cruci din Orlea" gallery (ASW) are characterized by the lowest pH values and the highest Eh values and PTE contents (Zn, Cr, Cu, Ni, Co, Cd). Soils close to the Roşia River are probably affected by the leakage of ASW, as they show average concentrations of PTE one order of magnitude higher than those of non-contaminated soils (KABATA-PENDIAS & PENDIAS, 2001).

Results show that PTE mobility in precipitates and soils is strongly affected by water pH related to the different geochemical behaviour of elements.

References

KABATA-PENDIAS, A. & PENDIAS, H. (2001): Trace elements in soils and plants. CRC, Boca Raton.

NORDSTROM, D.K. (2011): Applied Geochemistry, 26: 1777–1791.

WALLIER, S., RAY, R., KOUZMANOV, K., PETTKE, T., HEINRICH, C.A., LEARY, S., O'CONNOR, G., CALIN, G.T, VENNEMAN, T. & ULLRICH, T. (2006): Economic Geology, 101: 923–954.

CRYSTAL CHEMISTRY OF V-, Cr- AND Mn-BEARING SILICATE MINERALS IN ČIERNA LEHOTA, STRÁŽOVSKÉ VRCHY MTS., SLOVAK REPUBLIC

BAČÍK, P.*, UHER, P., OZDÍN, D. & ŠTEVKO, M.
Department of Mineralogy and Petrology, Comenius University, Mlynská dolina G, 842 15 Bratislava, Slovakia
* E-mail: bacikp@fns.uniba.sk

Assemblage of silicate minerals enriched in V, Cr and Mn including amphiboles, garnets, minerals of the epidote group, titanite and chamosite accompanied by feldspars (plagioclase and hyalophane) occur in Lower Paleozoic metamorphosed deep-marine volcanics with the sedimentary admixture near Čierna Lehota village, Strážovské vrchy Mountains, Slovak Republic.

Amphiboles are highly magnesian, X_{Mg} (Mg/(Mg+Fe)) is higher than 0.95 in tremolite and between 0.82 and 0.97 in magnesiohornblende but it decreases with an increase of tetrahedral Al in younger magnesiohornblende. Amphiboles are generally enriched in Cr and V which increase from tremolite to magnesiohornblende, up to 3.8 wt% Cr_2O_3 (0.43 *apfu*) and 1.8 wt% V_2O_3 (0.21 *apfu*), respectively.

Grossular garnet verges to goldmanite with an increased V content (up to 12.0 wt%, 0.79 *apfu*). The content of Mn (spessartine component) and Cr (uvarovite component) is also relatively high, up to 19.4 wt% MnO (1.30 *apfu*) and 9.0 wt% Cr_2O_3 (0.58 *apfu*), respectively. Dominant substitutions include $MnCa_{-1}$ in the *A* site and VAl_{-1} and $CrAl_{-1}$ in the *B* site.

Minerals of epidote group also have an increased content of V (up to 5.3 wt% V_2O_3, 0.34 *apfu*) and REE (up to 0.74 *apfu*); they are represented mostly by clinozoisite. Vanadium-rich clinozoisite attains the composition of mukhinite owing to the VAl_{-1} substitution. The enrichment in REE is due to the $REEFe^{2+}(CaAl)_{-1}$ substitution which results in allanite-(La) composition since La is the most abundant REE. Negative Ce and slightly positive Eu anomalies are displayed in chondrite-normalized pattern.

Chamosite has X_{Mg} between 0.54 and 0.61, and locally it is also enriched in V (1.8 wt% V_2O_3, 0.16 *apfu*), Cr (1.4 wt% Cr_2O_3, 0.12 *apfu*), and Mn (1.5 wt% MnO, 0.14 *apfu*). Four types of feldspars include albite with $An_{<0.01,}$ plagioclase with $An_{0.30–0.52}$, and hyalophane with between 0.45 and 0.54 *apfu* Ba, which is overgrown by hyalophane with up to 0.32 *apfu* Ba.

In the Western Carpathians, similar V- and Cr-rich silicate mineralization was described from Pezinok–Rybníček in Malé Karpaty Mts. where rare V- and Cr-bearing goldmanite, mukhinite and dissakisite-(La) occurs in pre-Hercynian basic metavolcanics with the sedimentary admixture (UHER *et al.,* 2008; BAČÍK & UHER, 2010) and also in Chvojnica with V-enriched dravite to magnesiofoitite (BAČÍK *et al.,* 2011) and V-rich muscovite to roscoelite (MÉRES & IVAN, 2007). All occurrences shares the common features including V- and Cr- enrichment, high X_{Mg} in majority of silicate minerals and accompanying sulphide mineralization with dominant pyrite and pyrrhotite. Moreover, the same negative Ce and slightly positive Eu anomalies as in allanite-(La) from Čierna Lehota also occur in dissakisite-(La) from Pezinok–Rybníček. Negative Ce anomaly is also pronounced in bulk-rock composition of metachert in Chvojnica. However, there are some differences to Pezinok–Rybníček (mineral assemblage with tourmaline and white mica in Chvojnica is significantly different, thus it is not taken into account now): Fe-dominant allanite-(La) in Čierna Lehota but Mg-dominant dissakisite-(La) in Pezinok–Rybníček; chamosite in Čierna Lehota but clinochlore in Pezinok–Rybníček; significant spessartine component in garnets from Čierna Lehota, whereas Mn attains only up to 0.29 *apfu* in goldmanite to grossular from Pezinok–Rybníček. It suggests slight differences in protolith (Mn-enrichment) and also metamorphic or hydrothermal evolution (Fe-enriched phases in later stages) of silicate mineralization in Čierna Lehota compared to that from Pezinok–Rybníček.

Acknowledgements: Authors are indebted to grants APVV-0081-10 and VEGA-1/0255/11.

References

BAČÍK, P. & UHER, P. (2010): Canadian Mineralogist, 48: 523–536.

BAČÍK, P., MÉRES, Š. & UHER, P. (2011): Canadian Mineralogist, 49: 195–206.

MÉRES, Š. & IVAN, P. (2007): Mineralogia Polonica – Special Papers, 31: 211–214.

UHER, P., KOVÁČIK, M., KUBIŠ, M., SHTUKENBERG, A. & OZDÍN, D. (2008): American Mineralogist, 93: 63–73.

TECHNOLOGICAL EXAMINATION OF 18TH to 19TH CENTURY COBALT-BLUE DECORATIVE CERAMICS FROM TRANSYLVANIA (ROMANIA)

BAJNÓCZI, B.*, NAGY, G. & TÓTH, M.
Institute for Geological and Geochemical Research, Research Centre for Astronomy and Earth Sciences, Hungarian Academy of Sciences; Budaörsi út 45, H-1112 Budapest, Hungary
* E-mail: bajnoczi@geochem.hu

The so-called "cobalt-blue ceramics" are elegant and decorative type of pottery with white incisions on dark blue base. This pottery (mostly jugs and plates) was produced between 1766 and 1840, mainly from 1785 to 1815 in Transylvania, most probably in Saschiz (Szászkézd) (VIDA, 2011).

The production technology, particularly the method used to form the decorations has been the matter of debate from the 1880s both among the Transylvanian and the Hungarian researchers. Some technological details have not yet been clarified up to this day. It is generally accepted that the reddish body of the ceramics was covered by a white engobe. Then a blue layer was applied, which is regarded as glaze or mixture of engobe and glaze/blue smalt. White decorations were made either by removing the blue layer with scratching (sgraffito technique) or by making drawings using wax, to which the blue layer does not adhere (wax-resist/batik technique). Finally a transparent (lead) glaze was applied over the object. Based on electron microscopy analysis of the glaze Horst Klusch questioned the order of layers suggesting that the transparent glaze was applied first, then it was covered by the blue layer (see recently ROŞKA & KLUSCH, 2010). The use of white tin glaze (instead of engobe) and blue-coloured tin glaze was suggested by KATONA (1976). Therefore archaeometric analysis should answer the following technological questions: (a) what is the actual order of layers? (b) what is the blue layer? (c) was tin glaze applied? (d) at what stage did firing occur? (e) how were decorations made?

Detailed analysis was performed on two cobalt-blue plates of the Ceramic Collection of the Ethnographic Museum in Budapest. Detached glaze pieces represent blue areas, white decorations as well as their transitions, and also contain the light-coloured engobe. Microtextural and chemical analysis was performed on glaze pieces in cross section using an electron microprobe coupled with an energy-dispersive X-ray spectrometer. Crystalline phases of the glaze and the engobe were determined by X-ray powder diffraction analysis.

The lower and upper parts of the blue glaze pieces contain different amounts of inclusions and their vitreous matrix has different chemical composition. The lower, inclusion-rich (e.g. newly formed cristobalite) part of the glaze is strongly coloured with cobalt and contains low amounts of lead, while the upper part of the glaze is more enriched in lead and less coloured. The lower and the upper glaze parts meet with more or less sharp boundary indicating that two glaze layers were applied. Going towards the decorations the glaze becomes thinner and contains only one layer: the blue, cobalt-rich part disappears and a colourless or slightly coloured, lead-rich glaze covers the light-coloured engobe.

According to its chemical composition and microstructure the blue layer is proved to be glaze and does not contain engobe [e.g. the blue layer is very poor in Al ($\leq$ 1 wt% Al_2O_3), while the engobe has elevated Al content ($\geq$ 30 wt% Al_2O_3)]. Nickel-cobalt-rich particles and arsenate inclusions, the latter crystallized during the firing and subsequent cooling, indicate the use of zaffre cobalt pigment for colouring. The blue layer is actually a glaze rich in potassium and silicon, poor in lead (maybe originally lead-free?) and coloured with zaffre. Tin above detection limit or tin oxide particles were not found in the blue glaze, therefore it is not a blue-coloured tin glaze.

The light-coloured layer under the glaze is proved to be fine-grained engobe containing quartz, K-feldspar and a small amount of titan oxide (anatase ± rutile). High-temperature phases or relicts of decomposed clay minerals were not detected by XRD analysis most probably due to the very small amount of samples. Usage of white tin glaze can be unambiguously denied.

Based on the above results, layers were applied in the following order: engobe, then blue (cobalt-rich) glaze, finally transparent lead glaze. Accordingly the generally supposed layer sequence is appropriate, while our analysis did not confirm the layer sequence determined by Horst Klusch. Firing might have occurred after applying the engobe, then after applying the transparent lead glaze. During the last firing the chemical composition of both glaze layers was modified through element diffusion.

Future microstructural investigations on glazes of tentatively produced vessels will help to determine the technique (sgraffito or batik method) used for making the decorations.

References

KATONA, I. (1976): A habán kerámia Magyarországon. 2. kiadás, Képzőművészeti Alap Kiadóvállalata, Budapest, 227 p.

ROŞKA, K. & KLUSCH, H. (2010): Keramik aus Siebenbürgen. Keramikerzeugnisse der Zünfte, der Manufakturen, der Habanerwerkstatt aus Siebenbürgen. Honterus Verlag, Hermannstadt, 328 p.

VIDA, G. (2011): Néprajzi Értesítő, 93: in press.

PRELIMINARY STUDY OF EUCLASE FROM RN, BRAZIL

BARETTO, S. de B.[1]*, ZEBEC, V.[2], ČOBIĆ, A.[3], BEGIĆ, V.[3], WEGNER, R.[4], KAMPIĆ, Š.[3] & BERMANEC, V.[3]
[1] Department of Geology, Federal University of Pernambuco, Av. Academico Hélio Ramos. S/N. 5 andar., Cidade Universitária, Recife, PE, Brazil
[2] Croatian Natural History Museum, Zagreb, Croatia
[3] Institute of Mineralogy and Petrology, Faculty of Science, Zagreb, Croatia
[4] Univ. Federal de Campina Grande, Centro de Ciências e Tecnologia, Dep. de Min. e Geol., Campina Grande, PB, Brazil
* E-mail: sandrabrito@smart.net.br

Euclase is a nesosilicate with general formula $BeAlSiO_4(OH)$. It crystallizes in monoclinic system, space space group $P2_1/a$. Investigated crystals were collected in two distinct pegmatite bodies near the city of Equador, RN, Brazil: Jacu and Mina do Santino pegmatites.

XRD patterns of natural samples and samples heated at 1025°C were analyzed using X'Pert High Score programme (PANALYTICAL, 2004). All crystals are confirmed as single phase euclase with small differences in unit cell parameters. Unit cell parameters were calculated using Unit cell programme (HOLLAND & REDFERN, 1997). For natural sample from Jacu pegmatite (sample: 2018) they are: a = 4.7814(2) Å, b = 14.3355(7) Å, c = 4.6348(2) Å and β = 100.331(5)° and for natural sample from Mina do Santina pegmatite (sample: 1474): a = 4.7842(3) Å, b = 14.3391(6) Å, c = 4.6356(2) Å and β = 100.311(5)°. High accuracy of unit cell parameters is due to pure euclase phase with no inclusions which is observed by very sharp lines in XRD pattern. Heating of euclase samples at 1025°C for 3 h yields break down of euclase structure to several products: coesite (SiO_2), phenakite (Be_2SiO_4), mullite ($Al_{4+2x}Si_{2-2x}O_{10-x}$) and beryllium aluminium silicate ($2BeO \cdot 3.67Al_2O_3 \cdot 6SiO_2$, JCPDS card 18-204, also reported in literature: GRAZIANI & GUIDI, 1980).

Crystals of euclase were measured using two-circle goniometer. They are well developed with following forms: {100}, {120}, {010}, {111}, {011}, {021}, {031}, $\{\bar{1}31\}$, $\{\bar{2}21\}$ and $\{\bar{6}31\}$. Identification of forms was done using axial ratio a:b:c=0.3237:1:0.3332 after GOLDSCHMIDT (1916).

Wet chemical analysis show common euclase chemistry (GRAZIANI & GUIDI, 1980), but these investigations also showed the unexpected presence of calcium.

Samples from both localities are colourless with colored domains in every crystal. As for samples from the Jacu pegmatite, these domains are greyish blue and in crystals from Mina do Santino pegmatite are greenish blue.

Chemical and optical study as well as a study about the inclusions will be carried out.

References

GOLDSCHMIDT, V. (1916): Atlas der Krystallformen. Band III. Carl Winters Universitätsbuchhandlung, Heidelberg.

GRAZIANI, G. & GUIDI, G. (1980): American Mineralogist, 65: 183–187.

HOLLAND, T.J.B. & REDFERN, S.A.T. (1997): Mineralogical Magazine, 61: 65–77.

PANALYTICAL (2004): X'Pert High Score Plus, version 2.1, Panalytical, Almelo, The Netherlands.

COMPOSITIONAL VARIATIONS OF CLINOPYROXENE FROM IJOLITE, DITRĂU ALKALINE MASSIF, ROMANIA

BATKI, A.[1]*, PÁL-MOLNÁR, E.[1], MARKL, G.[2] & WENZEL, T.[2]
[1] Department of Mineralogy, Geochemistry and Petrology, Univ. of Szeged; Egyetem str. 2, H-6722 Szeged, Hungary
[2] Fachbereich Geowissenschaften, Universität Tübingen; Wilhelmstrasse 56, D-72074 Tübingen, Germany
* E-mail: batki@geo.u-szeged.hu

The Ditrău Alkaline Massif in the Eastern Carpathians (Romania) is a Mesozoic alkaline igneous complex formed during an extensional event of the Alpine evolution associated with a rifted continental margin. The massif comprises a series of ultramafic to mafic rocks, felsic silica-saturated and oversaturated syenites and granites, as well as undersaturated alkaline rocks. Numerous dykes, including lamprophyres, tinguaites, alkali feldspar syenites and nepheline syenites, cut the whole complex. Additionally, small discrete rounded mafic aggregates, here named ijolites, occur within some of the tinguaite dykes. In the present study we use major element compositions of clinopyroxenes of the ijolite aggregates in order to discuss their chemical variations and try to define their possible magma sources.

Globular to lenticular dark grey ijolite aggregates with sharp margins vary in diameter from 1 to 9 centimetres. They have a porphyritic, fine-grained texture, and are composed of clinopyroxene (diopside, hedenbergite, augite, aegirine-augite), biotite, K-feldspar, cancrinite and accessory titanite, apatite and magnetite. Clinopyroxenes show several generations. Euhedral to anhedral phenocrysts show oscillatory or patchy zoning (Fig. 1). Their rims are resorbed and overgrown by a later clinopyroxene generations in all cases (Fig. 1). Small euhedral to anhedral diopside and aegirine-augite grains also appear as groundmass minerals.

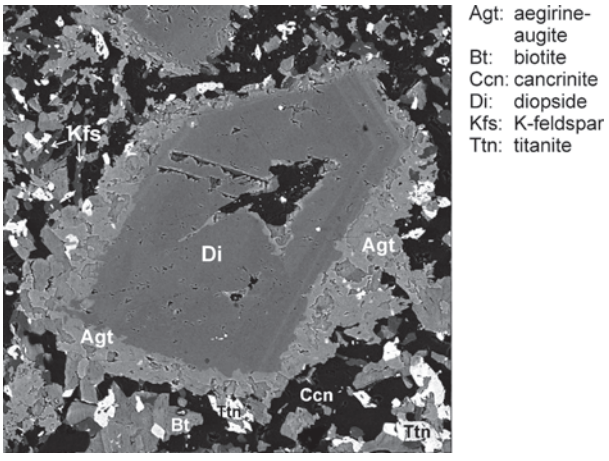

Fig. 1. *BSE image of an oscillatory-zoned Cr-diopside phenocryst overgrown by aegirine-augite in ijolite.*

Clinopyroxenes were analyzed with a JEOL 8900 electron microprobe in wavelength-dispersion mode at the Department of Geosciences, Universität Tübingen, Germany, using a beam current of 15 nA and an acceleration voltage of 15 kV. Additional mineral compositions were obtained with a JEOL JCXA-733 electron microprobe at the Institute for Geochemical Research, Hungarian Academy of Sciences, Budapest, Hungary.

Clinopyroxenes are classified in terms of quadrilateral and sodic components. They are mainly of diopsidic to augitic composition. They have variable diopside and aegirine contents of $Di_{10–94}Aeg_{2–63}$, while the hedenbergite content varies only in a narrow range ($Hd_{0.5–40}$). The highest Di-contents belong to chromian diopsides (up to 0.68 wt% Cr_2O_3), whereas pyroxenes with the highest Aeg-contents reach relatively high Zr-contents as well (up to 0.67 wt% ZrO_2). All the pyroxenes exhibit high Al-content (up to 8.90 wt% Al_2O_3). Ti/Al ratios of the phenocrysts fall between 0.125 and 0.250 indicating a relatively high crystallization pressure. Both groundmass diopside and aegirine-augite, and most of the aegirine-augite rims overgrowing phenocrysts have Ti/Al ratios above 0.25, which probably indicates a low crystallization pressure. Diopsides in ijolite have the same composition as clinopyroxenes in camptonites and hornblendites of the massif (Fig. 2) which suggest the same initial basanitic magma source for these rocks. The sodic fractionation trend from Di_{94} towards Aeg_{63} in the clinopyroxenes of ijolite approaches the aegirine composition in nepheline syenites of the massif (Fig. 2). The latter Na-enrichment of the ijolite clinopyroxenes could be a testimony of mixing between basanitic and nepheline syenitic magma.

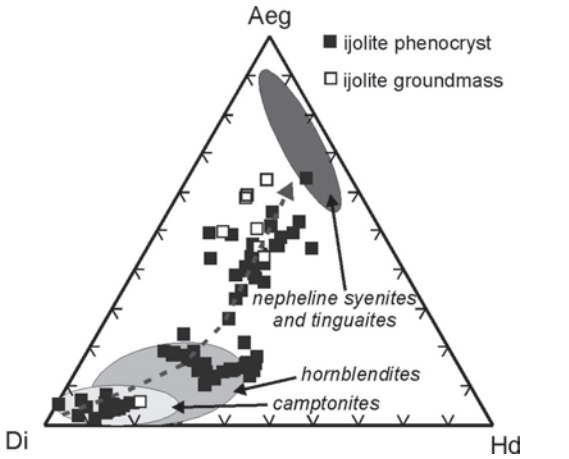

Fig. 2. *Compositional variation of clinopyroxenes of the Ditrău Alkaline Massif in terms of Di-Hd-Aeg end member mol%.*

CHARNOCKITIZATION OF GRANITOID ROCKS IN THE FOOTWALL OF THE DULUTH COMPLEX (MINNESOTA, USA)

BENKÓ, Zs.[1]*, MOLNÁR, F.[2], MOGESSIE, A.[1], SEVERSON, M.[3], HAUCK, S.[3] & AREHART, G.[4]
[1] Institute of Earth Sciences, Mineralogy and Petrology, Karl-Franzens-University of Graz, A-8010 Graz, Austria
[2] Geological Survey of Finland, PO. Box 96, FI-02151 Espoo, Finland
[3] Natural Resources Research Centre, Duluth, 55811 Minnesota, USA
[4] University of Nevada, Reno, 89557 Nevada, USA
* Email: zsolt.benko@uni-graz.at

The South Kawishiwi Intrusion (SKI) is a part of the Mesoproterozoic (1.1 Ga) Duluth Complex. The footwall of the SKI consists of Archaean granite-gneiss, diorite, granodiorite (Giant Range Batholith), thin condensed sequences of Paleoproterozoic shale (Virginia Fm.), as well as banded iron formation (Biwabik Iron Fm.).

The footwall granite in some zones contains Cu and PGE mineralization, whereas fluids and melts emerging from the contact-metamorphosed footwall probably played an important role in the distribution of PGE and base metals in the SKI. The aim of our study was to understand the metamorphic history in the partially melted (charnockitised) footwall rocks and to show that this process released fluids from the footwall. Detailed drill core logging, petrographic analysis, mineral chemistry and whole rock geochemical analysis have been carried out on the granitic footwall rocks in the NM-57 drill hole.

In the studied drill hole, the footwall consists of foliated metagranite that is intersected by mafic (dioritic) dykes of older age than the SKI. In the proximal contact zones the orthopyroxene + clinopyroxene + plagioclase + quartz + Fe-Ti-oxide porphyroblasts embedded in a plagioclase + K-feldspar + orthopyroxene + apatite matrix, indicating pyroxene-hornfels facies conditions in the mafic dykes. Non-equilibrium metamorphic mineral is assemblage characterized by abundant relict mineral phases as well as quartz grains showing dynamic recrystallisation that can be related to the rapid upheating and retrograde metamorphism. Partial melting in the vicinity of the magmatic complex is revealed by the euhedral crystal faces of plagioclase and pyroxene against anhedral quartz crystals, quartz-K-feldspar symplectites (granophyres) and occurrence of plagioclase ± biotite leucosome segregations. Sulphide mineralization is localized on the diorite dykes in form of disseminated chalcopyrite ± millerite ± sphalerite.

Two generations of biotite have been distinguished on the basis of their petrographic positions and fluorine contents. High modal proportion of F-rich biotite suggests to a fluid rich environment during retrograde metamorphism after the de-volatilization of peak metamorphism.

Syntectonic fluid flow was restricted on some mylonitic shear zones defined by extremely high modal proportion of F-poor biotite with lepidoblastic texture.

Apatite is an omnipresent accessory mineral in all rock types, with up to 1–3% modal proportion. Crystal habit is columnar or rarely needle-like. X_{Cl}/X_F and X_{OH}/X_F ratios of apatite were compared with depth in the drill hole and in relation to the host rock type. Apatite in the metagranite and in the dioritic dykes is fluorine-rich ($X_{Fgranite} \approx 1.27–1.63$; $X_{Fmafic\ dyke} \approx 1.51–1.83$) and their $X_{Cl}/X_{Fgranite} \approx 0.083$ to 0.051 and $X_{Cl}/X_{Fmafic\ dyke} \approx 0.051$ to 0.044 ratios decrease towards the distal parts of the contact. Apatite in biotite-rich mylonite, as well as in the porphyroblasts of mafic dykes, is extremely depleted in chlorine- and hydroxyl-anions ($X_{Cl}/X_{Fmylonite} \approx 0.02$ and $X_{OH}/X_{Fmylonite} \approx 0.14$), whereas apatite in felsic dykes and in the in-source leucosome are enriched in hydroxyl and chlorine relative to fluorine ($X_{Cl}/X_{Ffelsic\ vein} \approx 0.21$ and $X_{OH}/X_{Ffelsic\ vein} \approx 0.37$). These variations suggest release of chlorine enriched fluids from the partially melted contact zones and movement and enrichments of these fluids in migration channels of partial melts.

It has been for a long time accepted that sulphur originated from the metamorphosed Virginia Formation played an essential role in the sulphur saturation and sulphide segregation at the bottom of the gabbroic intrusions in the northwestern marginal zones of the Duluth Complex. Our study proves that the granitic footwall was also an important source of aqueous fluids and melts.

GEOCHEMICAL COMPOSITION OF CHROMITE – AN EFECTIVE TOOL FOR THE CHROMITE ORE EXPLORATION (CASE STUDY: ULTRAMAFIC MASSIF OF BULQIZA, ALBANIA)

BEQIRAJ, A. & BEQIRAJ (GOGA), E.*
Department of Earth Sciences, Polytechnic University of Tirana, Rruga Elbasani, Tirana, Albania
* E-mail: ea_beqiraj@yahoo.com

The ultramafic massif of Bulqiza belongs to the eastern belt of the Jurassic ophiolites in Albania. Its geological section, from the bottom to the top, consists of three rock sequences: (a) tectonic sequence (harzburgite and dunite); (b) transitional zone (massive dunite) and (c) magmatic sequence (wehrlite, pyroxenite and gabbro). The Bulqiza massif is the most noted due to its chromium-bearing potential. Four main podiform occurrences of chromite have been distinguished which are associated from the bottom to the top with: basal harzburgites (lower tectonite sequence) (a_1), dunitic lens-bearing harzbugites (middle-upper tectonite sequence) (a_2), layered chromitite-bearing dunites of transitional zone (b), and the stratigraphically lowermost part of the magmatic section (c) (CINA, 1987; BEQIRAJ *et al.*, 2000).

The most economically important chromite ore bodies, which belong to the metallurgical type, are found in the upper part of the tectonite sequence (a_2) and in the transitional zone (b). Chromite compositions similar to those of other podiform chromites are bimodal (BEQIRAJ *et al.*, 2000). Thus, chromites from occurrences (b) and (c) are richer in Cr than chromites from the other two occurrences.

Accessory chromite disseminated throughout the massif display ranges of the Cr/(Cr + Al) (0.40–0.83) and Mg/(Mg + Fe^{2+}) (0.35–0.68) similar to that of orebody chromites from the type-III Alpine peridotites (DICK & BULLEN, 1984). In addition, accessory chromite is richer in Fe than ore body chromite, due to the subsolidus re-equilibration with olivine (IRVINE, 1967; LEHMAN, 1983), where olivine is enriched in magnesium and nickel there chromite became richer in iron and manganese.

Both ore bodies and accessory chromites show compositional ranges correlating with host-rock compositions, i.e., the Cr-rich chromites are hosted by the most refractory ultramafic rocks, that is, with the most depleted tectonic sequence rocks, which suffered high partial melting.

The Cr/(Cr + Al) ratio of chromite seems to reflect the position of the sample in the sequence (CINA, 1987; BEQIRAJ *et al.*, 2000) and it can be assumed to characterize the stratigraphic level of the various chromite occurrences. Thus, the lower this ratio is, the deeper the chromitite occurs in the tectonite section and, vice-versa in the magmatic section. On the other hand, as the variation of the Cr/Fe^{tot} and Mg/Fe^{tot} ratios is controlled by ore abundance (LEHMAN, 1983), these ratios correlate positively with ore grade and, to some extent, with tonnage at a given stratigraphic level. Therefore, these ratios can be useful for exploration of high-grade, metallurgical chromite ore at Bulqiza and in other massifs of similar geodynamic setting.

References

BEQIRAJ, A., MASI, U. & VIOLO, M. (2000): Exploration and Mining Geology, 9: 149–156.

CINA, A. (1987): Bulleti i Shkencave Gjeologjike, 4: 99–131.

DICK, H.J.B. & BULLEN, T. (1984): Contributions to Mineralogy and Petrology, 86: 54–76.

IRVINE, T.N. (1967): Canadian Journal of Earth Sciences, 4: 71–103.

LEHMAN, J. (1983): Earth and Planetary Science Letters, 64: 123–138.

GEOCHEMICAL COMPOSITION OF ZEOLITIC ROCKS FROM MUNELLA REGION (OPHIOLITIC COMPLEX OF ALBANIA)

BEQIRAJ (GOGA), E.* & BEQIRAJ, A.
Department of Earth Sciences, Polytechnic University of Tirana, Rruga Elbasani, Tirana, Albania
* E-mail: ea_beqiraj@yahoo.com

Zeolitic rocks are found between the supra subduction zone (SSZ) type volcanic rocks of the Munella region, in the northeastern part of the Mirdita geotectonic zone (Jurassic Albanian Ophiolitic Complex). From the bottom to the top, the volcanic section consists of basalts, basaltic andesites, dacites and rhyolites. Zeolitic rocks crop out as up to 2–3 m thick, separated layers, intercalated with rhyolites, dacites and andesites of the uppermost part of the volcanic sequence (SHALLO, 1994; BECCALUVA *et al*., 1994).

Based on the SiO_2 content, the zeolitic rocks of Munella belong to andesite-rhyodacite group, bearing low Ti, saturated in Si. In the Na_2O+K_2O – SiO_2 diagram (not shown) they fall in the sub-alkaline field, whereas in the SiO_2 – FeO*/MgO diagram (not shown) they clearly display calc-alkaline features (BEQIRAJ GOGA, 2005).

Sample	Mu1	Mu2/3	Mu3/5	Mu4/1	Mu5	Mu6
SiO_2	60.95	72.70	60.20	65.26	64.77	69.97
Al_2O_3	11.97	10.08	12.44	11.63	11.40	10.10
Fe_2O_3	5.84	4.13	5.69	4.27	5.48	3.21
MnO	0.056	0.053	0.072	0.083	0.092	0.080
MgO	2.07	0.82	1.19	0.97	0.90	0.37
CaO	5.18	2.90	6.15	4.72	4.71	4.72
Na_2O	0.27	1.82	0.39	0.98	0.58	0.28
K_2O	0.09	1.01	0.14	0.54	0.80	0.27
TiO_2	0.378	0.308	0.411	0.362	0.364	0.305
P_2O_5	0.10	0.08	0.16	0.09	0.09	0.07
LOI	13.01	6.48	13.27	11.00	1.11	10.84
Total	99.92	100.38	100.11	99.89	100.28	100.23

In addition, in FeO^{tot} – FeO^{tot} /MgO and K_2O – SiO_2 diagrams (not shown) the zeolitic rocks fall within the field of tholeiite. As a whole, the zeolitic rocks show a geochemical character similar with that of the host medium-acid volcanic rocks.

In general, the contents of REE in the Munella zeolitic rocks are low, almost near the values expected for the MORB. Their normalized values to MORB are 4–5 times lower than the expected concentration in the host medium-acid volcanic rocks. The nearly flat patterns of their normalized values to MORB show neither differentiation nor fractionation.

References

BECCALUVA, L. (1994): Ofioliti, 19(1): 77–96.
BEQIRAJ (GOGA), E. (2005): PhD Thesis. Polytechnic University of Tirana, 173 p.
SHALLO, M. (1994): Ofioliti, 19(1): 57–75.

CO_2-RICH FLUIDS IN THE MANTLE: A COMPARATIVE FLUID INCLUSION STUDY

BERKESI, M.[1]*, PINTÉR, Zs.[1], KÁLDOS, R.[1], PARK, M.[2], GUZMICS, T.[1], CZUPPON, Gy.[3] & SZABÓ, Cs.[1]
[1] Lithosphere Fluid Research Lab, Eötvös University, Budapest, Hungary
[2] School of Earth and Environmental Sciences, Seoul National University, Seoul, Republic of Korea
[3] Institute for Geological and Geochemical Research, Budapest, Hungary
* E-mail: marta.berkesi@gmail.com

Study of negative crystal shaped fluid inclusions enclosed in spinel lherzolites from five different locations all around the world were the subject of a detailed fluid inclusion study. Samples were studied from: the Central Pannonian Basin (Hungary), Cameroon Volcanic Line (Cameroon), Jeju Island (S-Korea), Rio Grande Rift (New Mexico, USA) and from Queensland (Australia). As a result, CO_2-rich fluids within the fluid inclusions could be studied and compared. The main aim to study fluid inclusion of mantle xenoliths (from the aforementioned locations) was to understand the properties of fluids and processes (e.g., interaction) in the deep lithosphere.

High (spectral) resolution Raman spectroscopy (available at Eötvös Loránd University, Budapest, Hungary) at different temperatures revealed that fluids in inclusions are heterogeneous and contain in small amounts species other than CO_2. One of the main advantages of the use of high spectral resolution Raman microspectrometer was the discovery of nitrogen (N_2) in some of the fluid inclusions. We prove, in addition, that nitrogen can be present in the dense fluid and is more common than that was previously thought. Sulphur in the fluid at room temperature can be present either as H_2S or as SO_2, however these species never occur together at the same location. In addition, following fluid inclusion exposure by the FIB-SEM (Focused Ion Beam-Scanning Electron Microscopy, available at Eötvös Loránd University, Budapest, Hungary) technique, the complexity of S-bearing solid phases has also been identified: sulphides and sulphates were also found within the fluid inclusion cavity. OH-bearing solids were also identified in some cases within the fluid inclusions.

H_2O is present in almost all of the inclusions, and was identified by the combination of stepwise heating experiments and Raman spectroscopy (BERKESI *et al*., 2009). Our results show that, although H_2O is a minor component in mantle fluids, its relative amount varies among different locations, which has not been previously recognized.

However, using only Raman spectroscopy, no information can be obtained for the volume percentages of the solid phases, which is crucial to model the entrapped fluid composition. Stepwise exposure technique, involving FIB-SEM, was able to obtain highly precise volume proportions of even submicron-sized solid phases from mantle-derived fluid inclusions. The exposure procedure was carried out in two steps. After having exposed the inclusions, Raman spectroscopy was applied for precise identification of solid phases. As a result, combination of Raman spectroscopy with FIB-SEM technique proved the presence of carbonates (magnesite in enstatite-hosted fluid inclusions, whereas dolomite in diopside-hosted ones) and α-quartz that are interpreted as a reaction product of the trapped CO_2 and the host pyroxene.

We can conclude that, similar to the solid phases involved in the composition of the subcontinental lithospheric mantle, the coexisting fluid can also be heterogeneous in the mantle, although the dominant component in each case is CO_2.

Reference

BERKESI, M., HIDAS, K., GUZMICS, T., DUBESSY, J., BODNAR, R.J., SZABÓ, Cs., VAJNA, B., & TSUNOGAE, T. (2009): Journal of Raman Spectroscopy, 40: 1461–1463.

THE ULTRAMAFIC COMPLEX OF NAUDERS (LOWER ENGADINE WINDOW, EASTERN ALPS, AUSTRIA)

BERTLE, R.J.[1], KOLLER, F.[2]* & MELCHER, F.[3]
[1] GEOGNOS Bertle ZT GmbH, Schruns, Austria
[2] Department of Lithospheric Research, University of Vienna, Altanstraße 14, A-1090 Vienna, Austria
[3] Federal Institute for Geoscience and Natural Resources, Hannover, Germany
* E-mail: friedrich.koller@univie.ac.at

Ultramafic complexes of Mesozoic age are widespread within the Penninic Windows of the Eastern Alps. Most of them are related to ophiolitic fragments representing former Penninic oceanic crust. All of these mantle fragments are highly serpentinized and show in the Eastern Alps harzburgitic composition. Only few exceptions are composed of rather undepleted lherzolitic rocks. They occur in the zone of Matrei (a tectonic zone between Penninic and Austroalpine nappes) south of the Tauern window, and in the north in the Lower Austroalpine Reckner complex. An additional lherzolite complex occurs close to Nauders at the southern margin of the Lower Engadine Window.

The ultramafic complex SW Nauders is located between pumpellyite-bearing greenschists and sediments to the north, both related to the North Penninic zone of Pfunds, and granitic to gabbroic rocks of the Middle Penninic Tasna nappe to the south. The ultramafic body of Nauders is situated in a middle Penninic position as is demonstrated by recent geological mapping (BERTLE, 2004). Locally, small gabbroic intrusions and synfoliational layers with commonly pyroxenitic composition and more rarely with preserved volcanic texture are connected to the lherzolites. The coarse-grained lherzolite of Nauders carries a well-preserved magmatic assemblage of olivine ($Fo_{0.90}$), clinopyroxene (X_{Mg} = 0.90 to 0.91, with up to 2 wt% Na_2O and 6–7 wt% Al_2O_3), orthopyroxene (En 0.89–0.90, with 0.4–0.6 wt% CaO and 4–5 wt% Al_2O_3) and a green spinel (with a Cr# = 0.065 and a X_{Mg} = 0.796).This assemblage is partly replaced by pure diopside (rimming clinopyroxene), minor amphibole (Na- and Ti-rich pargasite), serpentine and carbonate as well as brown spinel. Na concentrations are considerably higher (up to 0.23 wt% Na_2O) than in all other Penninic lherzolitic complexes. Chondrite-normalized REE patterns of the ultramafic rock of Nauders are rather flat with slightly depleted LREE (MELCHER *et al*., 2002), similar to other lherzolitic samples of the Mesozoic units.

Small gabbroic bodies and rare cross-cutting basaltic dikes are associated with the ultramafic rocks. Based on their less mobile trace element (HFSE) geochemistry, they more likely represent with-in plate magmas than typical mid-ocean ridge basalts.

Based on the differences in preservation and geological setting, and in the geochemical composition of associated mafic rocks the ultramafic complex of Nauders might better correspond to tectonic setting such as, e.g. the Valmalenco complex (MÜNTENER *et al*., 2000, MANATSCHAL *et al*., 2006), which is currently interpreted as a fragment of a pre-oceanic subcontinental mantle of the Brianconnais microplate, emplaced and denudated during late Jurassic to early Cretaceous time (BERTLE, 2004).

References

BERTLE, R. (2004): PhD thesis, University of Vienna.
MANATSCHAL, G., MÜNTENER, O., PÉRON-PINVODIC, G., JAMMES, S. & MOHN, G. (2006): Excursion guide IODP-Workshop 2006.
MELCHER, F., MEISEL, T., PUHL, J. & KOLLER, F. (2002): Lithos, 65: 69–112.
MÜNTENER, O., HERMANN, J. & TROMMSDORFF, V. (2000): Journal of Petrology, 41: 175–200.

POSSIBLE MAGMA AND METAL SOURCES OF PORPHYRY Mo-Cu DEPOSITS FROM EASTERN TRANSBAIKALIA (RUSSIA)

BERZINA, A.N.*, BERZINA, A.P. & GIMON, V.O.
Institute of Geology and Mineralogy, Koptyug Av. 3, 630090 Novosibirsk, Russia
* E-mail: anitansk@gmail.com

Southern Siberia (Russia) is a part of the Central Asian Orogenic Belt, it accommodates a series of porphyry-type Mo-rich (Cu) deposits. Among them there are the Zhireken and Shakhtama deposits in Eastern Transbaikalia (Fig. 1A). The occurrence of porphyry Cu-Mo mineralization in Eastern Transbaikalia is related to active processes in the interaction zone of the Siberian continent with the Mongol-Okhotsk (Pz_2–Mz) Ocean. The northern margin of Eastern Transbaikalia is regarded as an active continental margin related to northward subduction of the Mongol-Okhotsk Ocean plate under the Siberian continent during Late Triassic-Middle Jurassic time. The ocean closed in the Middle-Late Jurassic as a result of the collision of the Siberian and Khingan-Bureya continents. Collision was accompanied by calc-alkaline magmatism and formation of large barren Mesozoic granitic plutons, followed by the emplacement of post-collisional shallow level mineralized porphyritic intrusions.

$^{40}Ar/^{39}Ar$ age of the Zhireken plutonic rocks ranges from 188 to 168 Ma, the granitic porphyries have an age range from 164 to 158 Ma. Shakhtama pluton has been dated from 202 to 167 Ma and porphyritic stock from 160 to 150 Ma. The Re-Os age for molybdenite samples has been dated at 163–162 Ma for Zhireken and 159–158 Ma for Shakhtama. The Zhireken deposit shows $(^{87}Sr/^{86}Sr)_0$ values of 0.70495–0.70642 indicating mantle-crust interaction, the Shakhtama deposit is dominated by a crustal source component with $(^{87}Sr/^{86}Sr)_0$ = 0.70741–0.70782.

S-Pb isotopic results together with Re-Os and $^{40}Ar/^{39}Ar$ isotopic dating indicate that the mineralization is genetically related to the emplacement of late orogenic post-collisional granitic porphyries. The sources of two magmatic systems – Zhireken and Shakhtama – were remarkably different with respect to the degree of crustal involvement in magma genesis. Pb isotope data show a linear trend in the plumbotectonic framework diagram ranging from radiogenic Pb at the Shakhtama deposit to mantle Pb at the Zhireken (Fig. 1B). The higher Pb-isotopic values for Shakhtama suggest an increasing involvement of crustal material in the source region. In both deposits Sr and Pb isotopic fingerprints show close values and narrow ranges for the ore-bearing porphyries and plutonic rocks in which the porphyries were emplaced, suggesting that they could have been generated from similar or the same source rocks. Lead isotope heterogeneity in the sulphides from Zhireken and Shakhtama indicates that not all Pb, and probably, other metals were deposited from one isotopically homogenous magmatic fluid. At least two sources of Pb with different isotopic compositions participated in the ore formation at Zhireken and Shakhtama. The Pb isotopic fingerprint of Cu-Fe sulphides (chalcopyrite from Shakhtama and pyrite from Zhireken) is consistent with a magmatic metal source. The more radiogenic Pb isotope compositions of molybdenite from both deposits are compatible with derivation of Pb from an external source.

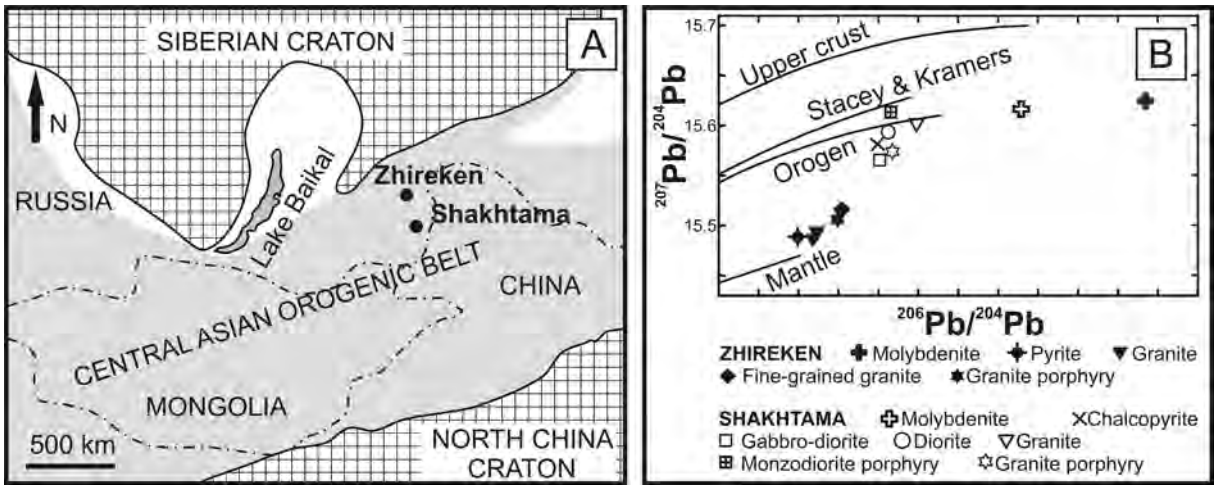

Fig. 1. *(A) Location of the studied ore deposits within the Central Asian Orogenic Belt; (B) Lead isotope compositions of sulphides and rocks from the Zhireken and Shakhtama porphyry Mo-Cu deposits.*

DISTRIBUTION OF AUTHIGENIC CLAY MINERALS IN ROTLIEGEND AEOLIAN SANDSTONES FROM THE FORE-SUDETIC MONOCLINE, SW POLAND

BIERNACKA, J.
Institute of Geology, University of Poznan, Makow Polnych 16, 61-606 Poznan, Poland
E-mail: julbier@amu.edu.pl

The amount, distribution pattern and morphology of clay minerals are of key importance for reservoir properties of sandstones. These parameters vary regionally, even for one sedimentary basin, and are dependent on a number of agents. The distribution of clay mineral cements was studied for aeolian sandstones of the Fore-Sudetic Monocline, one of gas-perspective areas in Poland, by a combination of XRD, optical microscopy and SEM. Illite, chlorite and kaolinite constitute the most ubiquitous cements in the sandstones studied. Their distribution pattern shows distinct relation to a palaeogeographic pattern, *i.e*. the location of sand dunes with regard to a playa lake and a local high (Wolsztyn High), the latter dividing the dune field into the Eastern Erg (facing the playa) and the Southern Erg.

Chlorite

Chlorite is a common mineral in the entire belt of the Eastern Erg, *i.e*. the dune field located between the playa lake and the Wolsztyn High, *ca*. 100 km long and 40 km wide. Conversely, the mineral is absent (or almost absent) in sandstones of the Southern Erg, separated from the playa by the Wolsztyn High. Because the amount of chlorite increases towards the playa, most probably the mineral crystallized from solutions derived from this lake during early diagenesis. Diffraction patterns of chlorite suggest the occurrence of Mg-rich variety. Chlorite forms flakes and platelets on the surface of grains.

Illite

Illite is the most ubiquitous authigenic mineral in the Rotliegend sandstones, it occurred in each sandstone studied. The XRD studies confirmed the occurrence of almost pure illite, with only minor admixture of highly ordered mix-layered illite-smectite. Some sandstones from the eastern part of the Southern Erg contain exclusively illite, without noticeable amounts of other clay minerals. The morphology of authigenic illite is variable – from play to hairy and fibrous. Fibrous illite is a late diagenetic phase; it grows on plates of earlier illite.

Kaolinite

Kaolinite occurs only in sandstones of the Southern Erg and it is unevenly distributed. The mineral shows a negative correlation with the content of feldspar, coming arguably from its destruction. The uneven distribution of kaolinite, even in sandstones lying at the same depth in geographically close areas, suggests its growth from acid fluids flowing along faults. Probably, the acid fluids were derived from basement Carboniferous coal-bearing rocks. Kaolinite forms pseudohexagonal plates, usually stacked into vermicular aggregates.

PETROLOGICAL AND GEOCHEMICAL STUDY OF THE LOWER TRIASSIC SILICICLASTIC SUCCESSION OF THE RUDABÁNYA ORE DEPOSIT (NE HUNGARY)

BODOR, S.* & FÖLDESSY, J.
Institute of Mineralogy and Geology, University of Miskolc, H-3515 Miskolc-Egyetemváros, Hungary
* E-mail: bodors@gmail.com

The open pit and underground mining in the iron and base metal ore deposit of Rudabánya went on from 1872 until 1985. The ore deposit is located in the Lower-Middle Triassic siliciclastic and carbonatic succession, the majority of the ore is metasomatic siderite and limonite, which was generated by the oxidation of the siderite. Beside the iron ore a probably synsediment, stratiform Pb-Zn ore deposit, and furthermore another Pb-, Zn-, Ag- and Cu enrichments also occur. The Oligocene-Miocene, NNE-SSW strike slip faults of Darnó Zone comminuted the ore bearing formations (FÖLDESSY *et al*., 2010).

We present the petrological and geochemical study of the oldest formations of the Rudabánya ore deposit (Lower Triassic Bódvaszilas Sandstone and Szin Marl Formation). The aim of our work was to get more acquainted with the complex ore-forming system of Rudabánya. We studied the drill cores from the open pit, and the similar formations from the non-ore bearing areas (drill cores from Aggtelek Mts., samples from type localities and other surface outcrops) to describe the alterations in the succession generated through ore formation.

The older formation, the Bódvaszilas Sandstone is built up from sandstone, siltstone and claystone. In the Aggtelek Mts. in Bódvaszilas Sandstone the monocrystalline quartz and muscovite are the most abundant constituents, and feldspars (plagioclase, K-feldspar) also occur in contrast to the samples of Rudabánya where they are almost absent. In the quantity and quality of the accessory minerals there are no notable differences in both areas. There is a great amount of carbonate cement in the formation, which is calcite in the type locality, but magnesite-ankerite in the drill cores of Aggtelek Mts., and magnesite-ankerite-siderite in Rudabánya where these cementing minerals are dominant. Some mineral phases, which have not been mentioned in the former publications, were also identified.

The Szin Marl Formation is built up from marl, slaty marl and calcareous marl. The clasts are similar to Bódvaszilas Sandstone and there are carbonate fragments also which are dolomite and ankerite. In the Rudabánya area the amount of clay minerals is very low, or they are completely absent in many samples. We have observed the previously mentioned synsediment sulphide accumulation along the laminae.

As a result of our research we were able to separate the posterior alterations, such as the ore-forming processes of Rudabánya from the non-ore-bearing formations; and to outline their regional extension.

Reference

FÖLDESSY, J., NÉMETH, N. & GERGES, A. (2010): Földtani Közlöny, 140: 281–292.

MODELING THE EFFECTS OF DRILLING FLUIDS WITH HEAT TREATED CORE SAMPLES

BORS, V.[1]* & TÓTH, J.[2]
[1] Department of Mineralogy, Eötvös Loránd University, Pázmány Péter sétány 1/c, H-1117 Budapest, Hungary
[2] Engineering and Technology Development, MOL PLC, EPD IFA, Hungary
* E-mail: bors.viktoria.orsolya@gmail.com

The aims of the modeling/work

The first and most important task of the selected drilling fluid is to prevent the reservoir rocks, namely to avoid damage, preserve the initial features and parameters of reservoir rocks (CAENN & CHILLINGAR, 1996; VAN OORT, 2003; ANDERSON *et al*, 2010). The modeling of the conditions inside the borehole has two pillars; one is to recognize in large scale the traits of the reservoir rocks and the applied drilling fluid; the other element is to relate and interpret their features (DORMÁN, 2010). Our primary aim is to recognize and evaluate the initial composition of samples and to demonstrate the possible mineral changes in the heat treated core samples.

The experimental conditions

The initial core sample was a grey, middle hard, micaceous mudstone. The mineral phase composition of the samples in order of decreasing quantity: illite/muscovite, quartz, chlorite, albite. During the experiment the chemical agent was designed to be more and more similar to the field-used water based drilling fluid. There were four agents applied: distilled water, 0.1% NaOH + 0.3% $Ca(OH)_2$, 0.1% KOH + 5% KCl and Synthetic HPHT fluid. The heat treatments were done at 175°C, 200°C and 220°C in runs of 24 and 72 hours.

Results

In heat-treated samples, mineral phase changes were monitored by X-ray powder diffraction. Sylvine appeared in samples treated by synthetic HPHT fluid and KOH + KCl agent at almost all temperatures. Analcime and calcite appeared as new phases in the sample which was treated by KOH + KCl at 220°C. In connection with the original clay fraction reactions, new phases (mainly zeolite) were recognized in several samples.

Though changes in the ion concentrations between the agents and samples were expected during the experiments, only in a few cases were found correlations between the ion changes and the appearance of the new mineral phases.

Scanning electron microscopy was used for characterising both the untreated, initial samples and the samples treated at 220°C, where particularly the shape and size of the new mineral phases were studied.

The impact of the drilling fluid on the swelling clays, namely whether it prevented or reduced the clay-swelling, was studied as well, with particular interest on the different dissolution marks on the surface of the samples.

Interesting phenomena occurred during the experiment when the heavy metals accumulated on the illite/muscovite dissolution surface. The reason for those phenomena was that the samples which were treated with the "simply" agent could not stabilize adequately the clay minerals. Therefore, during the heat-treatment the samples could disintegrate and the heavy metals could be fixed on the illite/muscovite surface on drying.

Conclusions

During our model experiments only a small amount of new minerals were formed in the heat-treated samples, and even these new phases appeared on the surface of the samples and not as void-fillers. Therefore, the above mentioned chemical agents are suitable drilling fluids, as their components have only a minimal effect on the reservoir rocks and even that effect is not long-lasting.

That modeling was just a first step in these testing, our methods should be improved in the future.

References

ANDERSON, R.L., RATCLIFFE, I., GREENWELL, H.C., WILLIAMS, P.A., CLIFFE, S. & COVENEY, P.V. (2010): Earth-Science Reviews, 98: 201–216.

CAENN, R. & CHILLINGAR, G.V. (1996): Journal of Petroleum Science and Engineering, 14: 221–230.

DORMÁN, J. (2010): MOL Scientific Magazine, 2010/3: 4–12.

VAN OORT, E. (2003): Journal of Petroleum Science and Engineering, 38: 213–235.

PARAGENESIS OF TYPOMORPHIC ACCESSORY MINERALS VS. TYPOLOGY OF GRANITIC ROCKS: EXAMPLES FROM WESTERN CARPATHIANS, SLOVAKIA

BROSKA, I.[1]*, PETRÍK, I.[1] & UHER, P.[2]
[1] Geological Institute, Slovak Academy of Sciences, Dúbravská cesta 9, 840 05 Bratislava, Slovakia
[2] Department of Mineralogy and Petrology, Comenius University, Mlynská dolina G, 842 15 Bratislava, Slovakia
* E-mail: geolbros@savba.sk

Assemblages of accessory minerals are important criterion for the typological division of granitic rocks. On the example of the West-Carpathian granite suites have been shown that the most critical assemblages for granite classifications are the magmatic accessory paragenesis reflecting the primary character of former melts. The accessory minerals determining the character of primary melts are the typomorphic. Detailed study of accessory minerals in Variscan I- and S-type and post-Variscan Permian specialized S- and A-types granites in Tatric, Veporic and Gemeric Units of the Western Carpathians enable us to characterize their differences and petrogenetic impact to origin of the suites (BROSKA *et al.*, 2011). Primarily relationship between *monazite* and *allanite* is important for the recognition of I- and S-type granitic rocks: monazite-(Ce) dominates in the S-type granites, on the other hand higher water and Ca activities stabilises allanite-(Ce) in the I-type granites. Exceptions represent more fractionated I-type granites where monazite-(Ce) is common. Although monazite-(Ce) in the hypersolvus A-type granites almost absent, in subsolvus granites occurs locally. Except xenotime-(Y), which may locally be abundant in S-type granites, A-type granitic rocks contain further Y-B-silicate phases (gadolinite and hingganite).

Magnetite as a typical mineral of the I-type granitoid paragenesis indicate higher oxidation level. In such rocks Ti-rich magnetite occurs first, which is in late-magmatic stage replaced by nearly pure magnetite in association with titanite. This is interpreted as result of late- to post-magmatic oxidation due to separation of fluid phase and following water dissociation. Another important basis for division is composition of *apatites* (hydroxylapatite to fluorapatite): low contents of Fe and Mn are typical of apatites from I-type granites, in contrast to S-type granite apatites, which are enriched in these elements. Similarly, apatite from A-type granites is commonly rich in Fe. The highest Mn contents accompanied by Sr are found in apatites from specialised S-type granites from the Gemeric unit

Zircon composition and its morphology are the important markers for granite typology. Restite zircon holds many features of former granitic magma. A morphological boundary may be derived from comparison of monazite/allanite antagonistic relationship and zircon morphology based on I.T parameter equal 350; I.T < 350 indicates S-type granites, while I.T > 350 is characteristic of I-type granites, I.A parameter is close to 300 for both granitic types. A higher I.A parameter close to 400 indicates specialised S-type granites. The A-type granites have values in the range 650–700. Hypersolvus granites contain commonly zircon subtypes D and P5 with high I.T parameter around 700, whereas subsolvus A-type granites show lower I.T parameter, close to 300. Orthomagmatic zircons show Zr/Hf_{wt} ratio in S- and I-type granites roughly 35–45, late-magmatic zircons in leucogranites have a lower ratio due to increase of Hf with differentiations. High Zr/Hf_{wt} ratio (> 50), but low Y, REE, U, Th concentrations in early magmatic zircons from hypersolvus A-type granites are in contrast to lower temperature subsolvus members. Similarly, highly fractionated S-type granites show Zr/Hf_{wt} ratio under 30, and contents of P, Y, REE U, and Th are commonly ≥ 0.5 wt%.

Tourmaline supergroup minerals indicate increased boron and other volatile elements in the primary melt. Schorl to foitite occur in Permian, post-orogenic specialized S-type Gemeric granites, locally are present also in some Veporic Permian S-type granites. Highly fractionated members of the specialised S-type granites contain *Nb-Ta oxide* minerals (mainly columbite-group minerals), Nb-Ta rutile, cassiterite and ferberite. Such mineralization typically occurs in greisenised granites. However, scarce Nb-Ta rutile, Ti-rich ixiolite, Fe-rich columbite-tantalite, and ferrotapiolite occur also in fractionated S-type leucogranites in the Tatric Unit. Moreover, some granitic pegmatites derived from S- and rarely I-type granitic magmas contain beryl and accessory minerals of columbite, rarely tapiolite and wodginite groups (Tatric Unit). This Nb-Ta-Sn-(Ti) suite is typical of granites-pegmatites of S- and I-type, in contrast to Y-REE-Ti-Nb-(Ta) suite [fergusonite-(beta)/samarskite-(Y), aeschynite/polycrase-(Y), Nb-rich rutile?] in the hypersolvus A-type granites (Turčok, Gemeric Unit). A special group of rare phosphates was found in Li-F-P topaz- and Li-mica-bearing granite from the Hnilec area (Gemeric Unit) comprising lacroixite, arrojadite, viitaniemiite, gorceixite and goyazite.

Reference

BROSKA, I. PETRÍK, I. & UHER, P. (2011): Accessory minerals in the granitic rocks of the Western Carpathians. Veda Pub. (Bratislava), 250 pp, in press. (In Slovak with English summary)

AGE OF POST-COLLISIONAL EVENTS IN THE DANUBIAN DOMAIN (SOUTH CARPATHIANS, ROMANIA): MOTRU DYKE SWARM

CAMPEANU, M.[1]*, BALICA, C.[1], STREMȚAN, C.[2] & BALINTONI, I.[1]
[1] Department of Geology, "Babeș-Bolyai" University, Cluj-Napoca, Romania
[2] Department of Geology, University of South Florida, Tampa, USA
* E-mail: campeanu.mara@gmail.com

This study is aimed at providing a better understanding of the emplacement age and genesis of Motru Dyke Swarm (South Carpathians, Romania) using geochemical and radiogenic isotope data.

The metamorphic basement of the Alpine Danubian nappes of South Carpathians (Romania) consists of Neoproterozoic high grade metamorphic rocks and several granitoid plutons also of Neoproterozoic age (LIÉGEOIS *et al.,* 1996; BALINTONI *et al.,* 2011), underlying low grade Ordovician to early Carboniferous formations (*e.g.,* IANCU *et al.,* 2005). The entire sequence is intruded by late Variscan post-collisional granitoid plutons (BALICA *et al.,* 2007). An extensive system of dykes, known as the Motru Dyke Swarm (MDS), penetrates through the whole Danubian basement in a presumed pre-Ordovician thermo-tectonic event (BERZA & IANCU, 1994). According to FÉMÉNIAS *et al*. (2008), this system is characteristic for a sub-volcanic event occurred in the early Palaeozoic (Cambrian-Ordovician). The MDS crosscut the Variscan post-collisional granitoid plutons and are covered by low grade metamorphic sediments. New zircon U/Pb ages on some components of MDS together with already published data reported by BALINTONI *et al.* (2011) does not confirm any Variscan or Late Variscan age, since the entire zircon population is inherited. Yet the cross-cutting relation of MDS with proven post-collisional late Variscan plutons constrain the age of these dykes to Upper Paleozoic, most likely Carboniferous. Age distribution patterns of these inherited zircons indicate a Pan-African origin and a peri-Amazonian provenance for the possible crustal source of MDS.

The distribution area of these dykes is of about 2000 km². They are characterized by heterogeneous geochemical composition and are represented by the calc-alkaline, medium-K to shoshonitic suites (*e.g.,* FÉMÉNIAS *et al.,* 2008). Furthermore this dyke system consists of numerous subvolcanic dykes defining a complete differentiation series, ranging from basaltic andesites to rhyolites (50–72% wt% SiO_2). Petrologically the MDS is comprised mainly of andesitic, trachiandesitic and dacitic dykes. Basaltic andesites with porphyry texture (euhedral amphiboles and zoned plagioclase phenocrysts) are the most common type in the MDS composition (*e.g.,* FÉMÉNIAS *et al.,* 2008).

In what concern the mineralogical aspects of the MDS, their main feature is represented by the absence of olivine and the presence of brownish amphibole phenocrysts. The primary minerals observed are: plagioclase, green hornblende and resorbed quartz**.** The Mn-enriched ilmenite is the main oxide present.

Based on the trace elements distribution and REE patterns, and also on U/Th, Nb/Ta and Zr/Hf ratios constant throughout the MDS, an ocean arc setting was inferred, dominantly sourced in an unique and homogeneous enriched mantle reservoir (subduction related and the absence of any upper/lower crustal contamination, FÉMÉNIAS *et al.,* 2008). Our Rb/Sr and Sm/Nd isotope data does not fully confirm this assumption, yet indicate a heterogeneous source of mixed mantle and crustal origin, the latter being the most prominent. The involvement of a crustal component is also suggested by the large presence of inherited zircon grains in MDS.

Therefore, we can conclude that MDS was emplaced during a Late Paleozoic (Carboniferous) post-collisional extensional event. The post-collisional tectonic setting in relation with a possible delamination could have triggered the partial melting of the uppermost mantle, which in turn could have induced the partial melting of crustal components.

References

BALICA, C., HANN, H.P., CHEN, F., BALINTONI, I. & ZAHARIA, L. (2007): Eos Trans. AGU, 88(52): Abstract T31B-0476.

BALINTONI, I., BALICA, C., DUCEA, M. & STREMȚAN, C. (2011): Gondwana Research, 19: 945–957.

BERZA, T. & IANCU, V. (1994): Romanian Journal of Tectonics and Regional Geology, 75, suppl. no. 2 [ALCAPA II – Geological evolution of the Alpine-Carpathian-Pannonian system (field guidebook)]: 93–104.

FÉMÉNIAS, O., BERZA, T., TATU, M., DIOT, H. & DEMAIFFE, D. (2008): International Journal of Earth Sciences (Geologische Rundschau), 97: 479–476.

IANCU, V., BERZA, T., SEGHEDI, A. & MĂRUNȚIU, M. (2005): Geologica Belgica, 8(4): 48–68.

LIÉGEOIS, J.P., BERZA, T., TATU, M. & DUCHESNE, J.C. (1996): Precambrian Research, 80: 281–301.

FERRIMOLYBDITE IN DIVINO DE UBÁ PEGMATITE, MINAS GERAIS, BRAZIL

CÂNDIDO FILHO, M.[1], SCHOLZ, R.[2], ŽIGOVEČKI GOBAC, Ž.[3]*, BELOTTI, F.M.[4] & BERMANEC, V.[3]
[1] Mining Department, Mining School, Federal University of Ouro Preto, Campus do Morro do Cruzeiro, Ouro Preto, MG, Brazil
[2] Geology Department, Mining School, Federal University of Ouro Preto, Campus do Morro do Cruzeiro, Ouro Preto, MG, Brazil
[3] Institute of Mineralogy and Petrography, Department of Geology, Faculty of Science, University of Zagreb, Horvatovac 95, Zagreb, Croatia
[4] Federal University of Itajubá, Campus Itabira, MG, Brazil
* E-mail: zeljkaz@geol.pmf.hr

Introduction

Ferrimolybdite is a hydrated ferric molybdate, with an uncertain water content, probably $Fe_2(MoO_4)_3 \cdot 8H_2O$ (PALACHE *et al.,* 1957). It is a secondary mineral, commonly formed by the alteration of molybdenite (PALACHE *et al.,* 1957). Ferrimolybdite was found as a greenish yellow coating on well-developed crystals of samarskite and euxenite in Divino de Ubá pegmatite, in southeast of Minas Gerais State, Brazil. The samples were obtained from the collection of the Geology Department, of the School of Mines, Federal University of Ouro Preto.

Experimental

In order to perform elemental analysis, a sample of greenish yellow material found in Divino de Ubá pegmatite was investigated using a JEOL-JSM840A scanning electron microscope (SEM). The SEM analysis in the EDS (electron dispersive spectrometer) mode was obtained with variable operating conditions of current and voltage. Fragments of crystals were prepared on carbon tape in a copper stub.

Results

SEM analysis of the sample, combined with EDS confirmed that it contains iron and molybdenum (Fig. 1). Such result could be interpreted as ferrimolybdite, but more accurate chemical composition and diffraction data would lead to better description of this extremely rare mineral species.

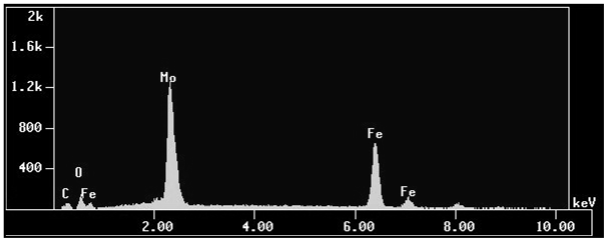

Fig. 1. *EDS spectrum of ferrimolybdite.*

Discussion and conclusion

Ferrimolybdite is usually found in the oxidized portions of hydrothermal vein and porphyry-type molybdenum-bearing deposits (ANTHONY *et al.,* 2003). Such a yellow coating is frequently found on sulphide ores of molybdenum (KERR *et al.,* 1963). Although molybdenite is a common mineral in Brazilian emerald deposits (GIULIANI *et al.,* 1994), but molybdenum rich mineral species are uncommon in granitic pegmatites. This is the first report of ferrimolybdite from Brazilian pegmatites.

References

ANTHONY, J.W., BIDEAUX, R.A., BLADH, K.W. & NICHOLS, M.C. (2003): Handbook of Mineralogy, 5: 222.

GIULIANI, G., ZIMMERMANN, J.L. & MONTIGNY, R. (1994): Journal of South American Earth Sciences, 7: 149–165.

KERR, P.F., THOMAS, A.W. & LANGER, A.M. (1963): American Mineralogist, 48: 14–32.

PALACHE, C., BERMAN, H. & FRONDEL, C. (1951): Dana's system of mineralogy, (7th edition), 2: 1095–1097.

THE CRYSTAL CHEMISTRY OF NEW SYNTHETIC COMPOUNDS $CsNaCu(P_2O_7)$ AND $Rb_2Cu(P_2O_7)$

CHERNYATIEVA, A.P.*, SPIRIDONOVA, D.V. & KRIVOVICHEV, S.V.
Faculty of Geology, St. Petersburg State University, University Emb. 7/9, 199034 St. Petersburg, Russia
* Email: nastya250@yandex.ru

In this work we describe preliminary results of the synthesis and of a crystal-chemical study of synthetic phosphates with transition metals. Due to the increasing requirements for environmental safety specialists from various industries, we are searching for sustainable forms of immobilization of hazardous waste during storage. We are also developing a component-based waste for new materials. In our continued exploratory synthesis of compounds containing transition-metals, we were able to produce the new phosphate phases $CsNaCu(P_2O_7)$ and $Rb_2Cu(P_2O_7)$.

A crystal chemical study has allowed us to identify the new phosphates. Crystals of $CsNaCu(P_2O_7)$ (Phase 1) and $Rb_2Cu(P_2O_7)$ (Phase 2) have been obtained by high-temperature reaction of $CsNO_3$, $Cu(NO_3)_2$, NaOH and $(NH_4)_4P_2O_7$. The reagents were mixed in an agate mortar in ratios of Cs:Na:Cu:P 1:1:3:4 (1) and Rb:Cu:P 1:3:3 (2). The mixtures were heated up to 650°C and kept at this temperature for 8 hours in air, followed by cooling down to 25°C at a cooling rate of 25°C/h. The product consisted of blue platy crystals of compounds (1) and (2). Synthetic crystals of the phosphate of copper and rubidium were studied in detail by us on the structures of $Rb_2Cu(P_2O_7)$ and $Rb_2Cu_3(P_2O_7)_2$ – new alkali metal copper diphosphates (CHERNYATIEVA *et al.*, 2008).

The structures of these synthetic compounds were solved using single-crystal X-ray diffraction and a computer program from SHELDRICK (1997). $CsNaCu(P_2O_7)$ (1) is orthorhombic, crystallizes in space group $Pmn2_1$, with a = 5.147(8), b = 15.126(2), c = 9.717(2) Å, V = 756.20 Å^3, $R1$ = 0.066 for 1221 unique reflections [$I > 2\sigma(I)$]. The structure is based upon 2-D layers of Cu square pyramids and P_2O_7 groups. Additional distortion occurs in the [6]-coordinated Cu pyramids due to JAHN & TELLER (1937). $Rb_2Cu(P_2O_7)$ (2) is orthorhombic as well, crystallizes in space group *Pmcn*, with a = 5.183(8), b = 10.096(1), c = 15.146(3) Å, V = 793.55 Å^3, $R1$ = 0.063 for 1326 unique reflections [$I > 2\sigma(I)$]. The structure is based upon 2-D layers of Cu square pyramids and groups of P_2O_7, similar to the structure of compound (1). However, the latter structure consists of different layers, with the scheme ABAB. A qualitative chemical analysis was performed with an electron microscope Quanta200 3D (FEI, Galanda), a microprobe analysis was performed on the microprobe EDAX (USA) at an accelerating voltage of ~20 kV.

Here we report the synthesis, the structure and the properties of the title compounds and we compare these phases with the previously discovered $K_2CuP_2O_7$ (ELMAADI *et al.*, 1995) and $CsNaMnP_2O_7$ (HUANG *et al.*, 1998). These structures crystallize in other space groups, although their structures are also based on 2-D layers, formed by P_2O_7 groups combined with polyhedra of the transition metals.

This work was supported by the Russian Ministry of Science and Education 3.37.84.2011.

References

CHERNYATIEVA, A.P., KRIVOVICHEV, S.V. & SPIRIDONOVA, D.V. (2008): International conference "Inorganic Materials" Dresden, 2008: P3–143.

ELMAADI, A., BOUKHARI, A. & HOLT, E.M. (1995): Journal of Alloys Compounds, 223: 13–17.

HUANG, Q., HWU, S.J. & MO, X.H. (1998): Angewandte Chemie – International Edition, 40: 1690–1693.

JAHN, H.A. & TELLER, E. (1937): Proceedings of the Royal Society of London, Series A., 161: 220–235.

SHELDRICK, G.M. (1997): SHELX-97: program for the solution and refinement of crystal structures. Siemens Energy and Automation, Madison, Wisconsin.

HYDROTHERMAL ALTERATION OF THE ACTIVE SEAMOUNTS IN TONGA VOLCANIC ARC, SOUTHERN LAU BASIN, SOUTHWESTERN PACIFIC

CHO, H.G.[1]* & CHOI, H.[2]
[1] Department of Earth and Environmental Sciences and Research Institute of Natural Science, Gyeongsang National University, Jinju 660-701, Korea
[2] Petroleum & Marine Research Division, Korea Institute of Geosciences & Mineral Resources, Daejeon 305-350, Korea
* E-mail: hgcho@gsnu.ac.kr

The Lau Basin in the south-western Pacific is an active back-arc and relatively shallow water depth (2,000~3,000 m) basin located in a subduction zone between the Pacific plate and Indo-Australian plate. The Tonga Volcanic Arc in southern Lau Basin is an interesting place where a back-arc spreading center closely approaches an active volcanic front (MARTINEZ & TAYLOR, 2003). In the last few decades, many active seamounts were found, and some of them have hydrothermal vents (DE RONDE *et al.*, 2001, 2005; STOFFERES *et al.*, 2003, 2006; ARCULUS, 2005). The hydrothermal vent fluids may produce massive sulfide deposits on the seafloor (MASSOTH *et al.*, 2007).

In this study, we interpret hydrothermal alteration around seamounts in the Tonga Arc using X-ray diffraction for clay fraction. We used two core samples from two seamounts (TA 12 and TA 26) and 19 TV guided grab samples (GTV) from five seamounts (TA 12, TA 19, TA 22, TA 25, and TA 26). Based on the downcore variation of mineral assemblages, TA 12 core can be divided into 3 zones; upper gypsum zone, middle smectite zone, and lower smectite + kaolinite + talc zone. TA 25 core can be divided into 5 zones from top to bottom; gypsum zone, smectite zone, smectite + kaolinite zone, smectite + talc zone, and smectite + kaolinite + talc zone. Most zones except gypsum zone correspond to argillic alteration zone. GTV samples are mostly composed of smectite in TA 12 and TA 25, kaolinite in TA 26, and smectite + kaolinite + illite in TA 22. These clay mineral assemblages correspond to argillic alteration. This study suggests that argillic hydrothermal alteration occurred and a high probability of massive sulfide deposits in the seafloor of the studied seamounts.

References

ARCULUS, R.J. (2005): New Zealand Minerals Conferences Proceedings: 45–50.

DE RONDE, C.E.J., BAKER, E.T., MASSOTH, G.J., LUPTON, J.E., WRIGHT, I.C., FEELY, R.A. & GREENE, R.R. (2001): Earth and Planetary Science Letters, 193: 359–369.

DE RONDE, C.E.J., HANNINGTON, M.D., STOFFERS, P., WRIGHT, I.C., DITCHBURN, R.G., REYES, A.G., BAKER, E.T., MASSOTH, G.J., LUPTON, J.E., WALKER, S.L., GREENE, R.R., SOONG, C.W.R., ISHIBASHI, J., LEBON, G.T., BRAY, C.J. & RESING, J.A. (2005): Economic Geology, 100: 1097–1134.

MARTINEZ, F. & TAYLOR, B. (2003): Geological Society of London Special Publication, 219: 19–54.

MASSOTH, G., BAKER, E., WORTHINGTON, T., LUPTON, J., DE RONDE, C., ARCULUS, R., WALKER, S., NAKAMURA, K., ISHIBASHI, J., STOFFERS, P., RESING, J., GREENE, R. & LEBON, G. (2007): Geochemistry Geophysics Geosystems, 8, Q11008: 26 pp.

STOFFERS, P., WORTHINGTON, T.J. & SHIPBOARD SCIENTIFIC PARTY (2003): Cruise Report Sonne, 167: 276 pp.

STOFFERS, P., WORTHINGTON, T.J., SCHWARZ-SCHAMPERA, U., HANNINGTON, M.D., MASSOTH, G.J., HEKINIAN, R., SCHMIDT, M., LUNDSTEN, L.J., EVANS, L.J., VAIOMO'UNGA, R. & KERBY, T. (2006): Geology, 34: 453–456.

MINERALOGICAL CHARACTERISTICS OF CERAMICS

ČOBIĆ, A.[1]*, BARETTO, S. DE B.[2] & BERMANEC, V.[1]
[1] Institute of Mineralogy and Petrology, Department of Geology, Faculty of Science, Zagreb, Croatia
[2] Department of Geology, Federal University of Pernambuco, Av. Academico Hélio Ramos S/N. 5 andar., Cidade Universitária, Recife, PE, Brazil
* E-mail: ancobic@geol.pmf.hr

Ten samples of recent ceramics' fragments were analyzed using XRPD method. The ceramics are variably coloured as well as multicoloured. Two fragments are completely brownish red; two fragments are red with a thin black film on the one side and six fragments are black in the middle and red on the outer sides. Black and red parts were analyzed separately.

XRPD analyses were performed using X'Pert High Score software (PANALYTICAL, 2004) and yielded the following results. Every sample contains albite, microcline and quartz (quartz is macroscopically visible as grains in the ceramics). Nine samples (regardless of their colour) contain muscovite, which can also be macroscopically seen, and one sample contains a mineral of the biotite series and illite. All red samples contain hematite which is the probable cause of the red colour. Also, all black samples contain a spinel group mineral which is, as well, the probable cause of black colour. Fig. 1 depicts XRPD patterns of a red ceramics' fragment (sample RK_6; Fig. 1a) and a black ceramics' fragment (RK_8 sample; Fig. 1b). Another reason for appearance of different colours could be in the sintering temperature. After reaching a certain temperature, the hematite is reduced to magnetite nevertheless of the oxidizing atmosphere. Thus, the presence of a spinel group member could be due to the appearance of reducing conditions. Estimated temperature for black layers formation is over 1300°C which is in agreement with findings of SLOVENEC *et al*. (1997).

References

PANALYTICAL (2004): X'Pert High Score Plus, version 2.1, Panalytical, Almelo, The Netherlands.

SLOVENEC, D., POPOVIĆ, S. & TADEJ, N. (1997): Neues Jahrbuch für Mineralogie, Abhandlungen, 171: 323–339.

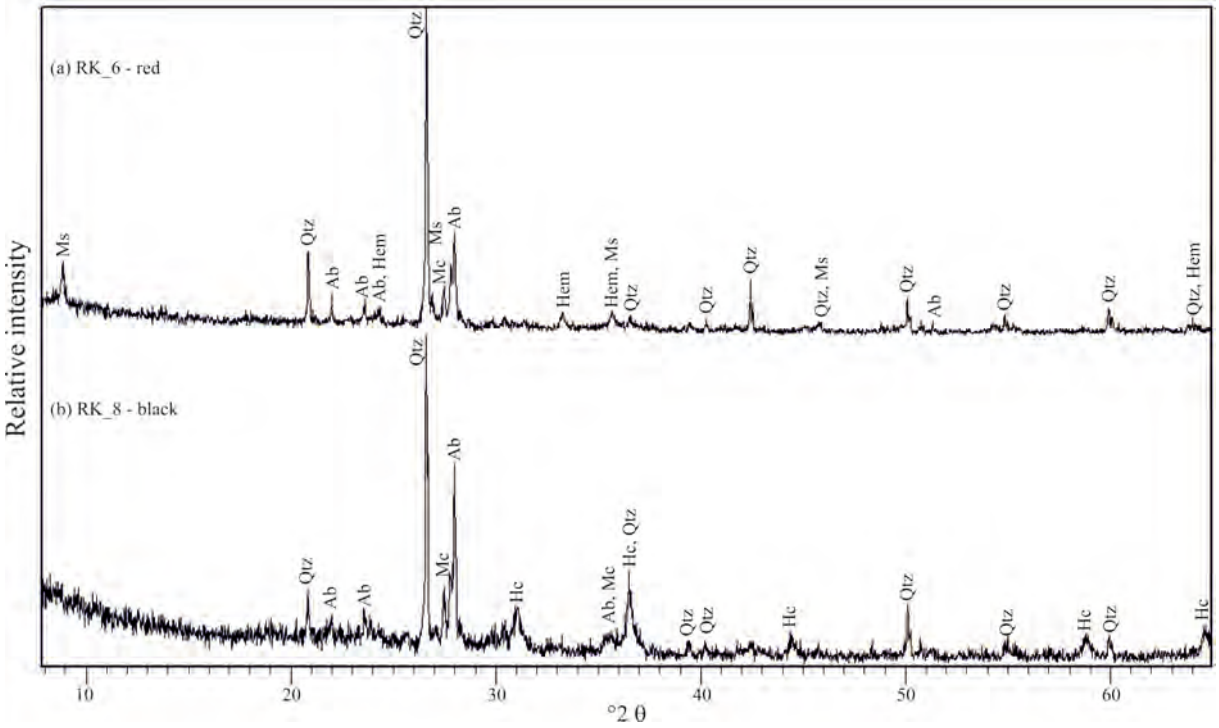

Fig. 1. *(a) sample RK_6 – red; (b) sample RK_8 – black; Qtz – quartz; Ms – muscovite; Mc – microcline; Ab – albite; Hem – hematite; Hc – hercynite.*

FORMATION OF AUTHIGENIC MONAZITE AND XENOTIME IN VERY LOW-GRADE METASEDIMENTS: ROLE OF THE CHEMICAL COMPOSITION OF HOST ROCK

ČOPJAKOVÁ, R.
Czech Geological Survey and Institute of Geological Sciences, Masaryk University, Kotlářská 2, Brno, Czech Republic
E-mail: copjakova@sci.muni.cz

Monazite (monoclinic $LREEPO_4$) and xenotime (tetragonal YPO_4) are common accessory minerals in medium- to high-grade metamorphic rocks, however, studies dealing with formation of monazite and xenotime at diagenetic to low-grade metamorphic conditions are rather sporadical.

Irregular aggregates of authigenic monazite (up to 150 μm) and xenotime (typically < 30 μm), have been found in shales and graywackes from the Moravo-Silesian Culm Basin (Bohemian Massif, Czech Republic). The Moravo-Silesian Culm Basin belongs to the Variscan foreland basin deposited as an axial turbidite system at ~ 330–325 Ma ago. Xenotime is far less common (1:10). Both Y+REE phosphates can intergrowth. Monazite and xenotime aggregates enclose a variety of authigenic (quartz, anatase, Fe-oxide/ hydroxide, chlorite, illite) and detrital minerals (quartz and K-feldspar) identical to those of the sediment matrix. Rarely, authigenic monazite encloses relics of detrital monazite with a chemical composition typical for high-grade monazite.

Authigenic monazite and xenotime growth was almost synchronous and they formed in relation to deep burial and very low-grade metamorphism of basin sediments at a maximum temperature ~200–300°C in the southern part of the Moravo-Silesian Basin (Drahany Upland) and ~200–350°C in the northern part of the Moravo-Silesian Basin (Nízký Jeseník Mts.). Monazite and xenotime precipitation can relate to decreasing $REEPO_4$ solubility in aqueous solutions with increasing temperature in this temperature range 200–300°C (WOOD & WILLIAMS-JONES, 1994; POITRASSON *et al.*, 2004). Authigenic monazite and xenotime appears only in Ca-poor rocks (< 0.5 wt% CaO), which underwent a temperature overprint corresponding to very low-grade metamorphism in the presence of REE-remobilization. In Ca-rich graywackes and shales (0.60–2.70 CaO), which underwent the same low-temperature metamorphic overprint and REE remobilization, authigenic synchysite-(Ce) or parisite-(Ce) are common instead. Decreasing the thermal overprint of shales and graywackes to T ~150–200°C decrease also remobilisation of REE's and authigenic monazite and xenotime did not precipitate even in the Ca-poor sediments. These results along with data from RASMUSSEN & MUHLING (2009); ČOPJAKOVÁ *et al.* (2011) indicate that metamorphic monazite and xenotime in sub-amphibolite-facies siliciclastic sediments is stabilized by a low whole-rock Ca content. The presence of authigenic monazite and xenotime does not show any apparent relationship to the whole-rock ΣREE+Y and REE patterns, or to the whole-rock variability in other major elements (Al, Fe, Mg).

Chemical composition of low-grade authigenic monazite and xenotime differs from that of higher temperature magmatic or metamorphic monazite and xenotime. Authigenic monazite shows low concentrations of Th, U, Ca, Y+HREE, and a low Eu anomaly. The central parts are enriched in Nd + MREE, whereas the outer parts are enriched in La and Ce. Zoning pattern in monazite and textural relation between monazite and xenotime suggest an evolution in fluid chemistry during diagenesis/very low-grade metamorphism or it relates to different solubility of the individual REE phosphates. Very low-grade xenotime is enriched in MREE and HREE (0.18–0.28 *apfu*) and shows flat chondrite normalized REE pattern from Gd to Lu with high Gd/Yb ratio (avg. 1.4) and a weak negative Eu anomaly. Authigenic xenotime typically has low concentrations of Th and U with relatively high Th/U ratio (0.4–2). The major source of REE's in the pore fluids are probably detrital minerals mainly monazite. A portion of the Y+REEs may have originated from other partly dissolved detrital minerals (xenotime, allanite, titanite, garnet). Other minor sources of REE's probably include Fe-oxide/hydroxide and/or clay minerals, which could have contributed to the Nd + MREE-rich cores in the authigenic monazite.

This abstract was supported by the research project GAČR 205/07/474 to RČ.

References

ČOPJAKOVÁ, R., NOVÁK, M. & FRANCŮ, E. (2011): Lithos, 127: 373–385.

POITRASSON, F., OELKERS, E., SCHOTT, J. & MONTEL, J.M. (2004): Geochimica et Cosmochimica Acta, 68: 2207–2221.

RASMUSSEN, B. & MUHLING, J.R. (2009): Chemical Geology, 264: 311–327.

WOOD, S.A. & WILLIAMS-JONES, A.E. (1994): Chemical Geology, 115: 47–60.

DISTRIBUTION OF REE IN TOURMALINE FROM TOURMALINITES AND HOST MICA SCHISTS: IMPLICATIONS FOR EVOLUTION AND GENESIS

ČOPJAKOVÁ, R.[1]*, NOVÁK, M.[1] & VAŠINOVÁ GALIOVÁ, M.[2]
[1] Department of Geological Sciences, Masaryk University, Kotlářská 2, Brno, Czech Republic
[2] Department of Chemistry, Masaryk University, Kotlářská 2, Brno, Czech Republic
* E-mail: copjakova@sci.muni.cz

Tourmaline is the most common borosilicate occurring in a variety of rock types of highly varying compositions and geological settings. The large compositional range in both major and trace elements makes tourmaline an excellent indicator of the chemical and physical properties in its host environment (VAN HINSBERG *et al.,* 2011). Interpretation of the REE compositional record in tourmaline depends on availability of REE data for tourmaline of different genesis and REE partitioning between tourmaline, coexisting minerals, melts and fluids.

We analysed REE+Y contents in tourmaline from tourmalinites and host mica schists from the Svratka Unit, Bohemian Massif to use REE for genetic interpretations. Tourmalinites (Tu + Qtz + Ms ± Grt ± Bt ± Ky ± Sil) form stratiform layers (< 1 cm to up to 1 m) hosted in mica schists (Qtz + Ms + Bt ± Grt ± Tu ± Ky ± Sil ± St ± Pl). The tourmaline from tourmalinites usually exhibits three compositional domains, (i) brecciated chemically heterogeneous schorl core interpreted as an older, low-temperature hydrothermal tourmaline; (ii) dravite-rich tourmaline overgrowing schorl core crystallizing during the Variscan amphibolite-facies prograde metamorphic event; (iii) outermost Al-rich schorl-dravite rim, growing most likely during exhumation of the Svratka Unit accompanied by decreasing pressure and temperature (ČOPJAKOVÁ *et al.,* 2009). The tourmaline from the host mica schists corresponds to dravite-rich tourmaline rimed by schorl-dravite and show similar chemical composition and evolution as metamorphic tourmaline (ii+iii) from tourmalinites.

Total REE contents in tourmaline are rather low to medium 1–60 ppm. Systematic variations were observed in the absolute abundance of REE and in chondrite normalized REE-patterns in tourmaline from both rock types and different tourmaline zones. The highest ΣREE contents are in (i) schorl tourmaline cores and the lowest in (ii) metamorphic dravite from tourmalinites. The REE patterns in tourmaline from tourmalinites are relatively flat (La_N/Yb_N = 0.1–5), commonly with slight MREE enrichment (Sm-Gd) yielding none or weak positive Eu anomaly (Eu/Eu* = 1–3). The (i) schorl cores show systematically slightly higher La_N/Yb_N ratio compared with (ii+iii) metamorphic outer zones. Total REE contents in tourmaline from mica schists are 3–27 ppm, REE patterns are LREE enriched with steep La-Dy pattern (avg. La_N/Dy_N = 13) and significant positive Eu anomaly (avg. Eu/Eu* = 10) accompanied by increasing contents of HREE from Ho to Lu. The La_N/Yb_N ratio (1.8–23) is higher compared with tourmaline from tourmalinites. Tourmaline from mica schists shows rimward increase in REE. All tourmalines are Y-depleted with significant Y anomaly compared with Dy and Ho.

The REE patterns in tourmaline do not reflect whole rock (tourmalinite and mica schist) REE patterns. Eu-enriched chondrite-normalized REE patterns are rather a hydrothermal fluid signature of tourmaline. Metamorphic tourmaline (ii+iii) from tourmalinites and hosted mica schists show distinct REE-patterns, but rimward REE enrichment was observed in both rock types. This rimward increase of REE probably reflects tourmaline growth during decreasing PT conditions. The REE patterns for metamorphic tourmaline in tourmalinites (ii+iii) and mica schists indicate crystallization of tourmaline from metamorphic fluids, where REE were donated by wall rocks. The major REE source for (ii+iii) metamorphic tourmaline in tourmalinites was probably (i) schorl core. Relative enrichment in HREE and depletion in LREE in younger (ii+iii) tourmaline compared with (i) schorl core can relates to elevated contents of F^- in tourmalinite layers and, hence, stronger complexation of HREE by F-rich metamorphic fluids. The REE patterns in metamorphic tourmaline from mica schists agree with preferential fractionation of Eu and LREE into metamorphic fluids during metamorphic processes in pelitic rocks (JIANG *et al.,* 2004).

REE contents in garnets showing simple compositional zoning with rimward decreasing of REE+Y, increasing of Tb/Lu ratio and deepening of negative Eu anomaly confirm garnet growth during prograde metamorphism (BEA & MONTERO, 1999). No relation between presence of garnet and REE-distribution in metamorphic tourmaline from tourmalinites and mica schists was observed.

This abstract was supported by the research project GAČR P210/10/0743 to RČ and MN and by the European Regional Development Fund project "CEITEC" (CZ.1.05/1.1.00/02.0068) to MVG.

References

BEA, F. & MONTERO, P. (1999): Geochimica et Cosmochimica Acta, 63: 1133–1153.

ČOPJAKOVÁ, R., BURIÁNEK, D., ŠKODA, R. & HOUZAR, S. (2009): Journal of Geosciences, 54: 221–243.

JIANG, S.Y., YU, J.M. & LU, J.J. (2004): Chemical Geology, 209: 193–213.

VAN HINSBERG, V.J., HENRY, D.J. & DUTROW, B.L. (2011): Elements, 7: 327–332.

HYDROTHERMAL ALTERATION OF TOURMALINE FROM TOURMALINITES IN THE KRKONOŠE CRYSTALLINE UNIT, BOHEMIAN MASSIF, CZECH REPUBLIC

ČOPJAKOVÁ, R.[1]*, ŠKODA, R.[1] & BURIÁNEK, D.[2]
[1] Department of Geological Sciences, Masaryk University, Kotlářská 2, Brno, Czech Republic
[2] Czech Geological Survey, Leitnerova 22, Brno, Czech Republic
* E-mail: copjakova@sci.muni.cz

Tourmaline is the most common borosilicate occurring in a variety of rock types with variable composition and geological setting. Tourmaline shows a wide stability field from diagenetic zone to granulite-facies metamorphism. It is usually consider to be resistant to weathering and low-temperature hydrothermal alteration. Only some studies report tourmaline breakdown during hydrothermal alteration in pegmatites (AHN & BUSECK, 1998) or in ore deposits (SLACK, 1996).

This abstract deals with the hydrothermal alteration of the tourmaline from tourmalinites in the Krkonoše Crystalline Unit, Bohemian Massif investigated by electron microprobe. Tourmalinites composed of major tourmaline and quartz and minor muscovite and chlorite form stratiform layers in surrounding metasediments (mica schists). Accessory minerals include monazite, apatite, rutile and zircon. The host mica schists are composed of quartz, muscovite, garnet, chlorite ± tourmaline ± biotite. Based on petrographic and electron microprobe data, three generations of tourmaline were distinguished. The early (i) Mg-rich tourmaline [Al-rich dravite with Mg/(Mg + Fe) = 0.81–0.99 and 6.19–7.12 *apfu* Al] reflects growth from Mg-rich hydrothermal fluids in the submarine hydrothermal system. This Mg-rich tourmaline is overgrown by (ii) schorl-dravite [avg. Mg/(Mg + Fe) = 0.61; avg. 6 *apfu* Al; low X-site vacancy avg. 0.09 *pfu*; enriched in F avg. 0.25 *apfu* F]. The third generation of tourmaline, (iii) schorl-dravite [avg. Mg/(Mg + Fe) = 0.56; with varying Al 5.79–6.68 *apfu* and X-site vacancy 0.05–0.36 *pfu*; poor in F avg. 0.17 *apfu* F] replaced early tourmaline. It was developed in relation to the Variscan regional metamorphic overprint and associated K-rich metasomatism. The calculated P-T conditions for this metamorphic event from mica schist (Qtz + Ms + Bt + Chl + Grt) hosted tourmalinite layer yielded T = 553 ± 30°C and P = 13 ± 2.5 kbar (calculated by THERMOCALC in average PT mode; HOLLAND & POWELL, 1998).

Tourmaline from tourmalinite layers has undergone metasomatic replacement reactions in some cases. They include: a) replacement of early tourmaline by newly formed schorl-dravite (type iii) + muscovite + quartz; b) replacement of schorl-dravite (type ii and iii) by chlorite ± muscovite. The type of replacement reaction seems to be dependent on the tourmaline chemistry. The replacement reaction (a) was observed preferentially in Mg-rich tourmaline cores (i). Chloritization of tourmaline (b) was observed exclusively in tourmaline of schorl-dravite composition (ii).

Muscovite replacing tourmaline contains higher Si, Mg, F and lower Al and Na contents compared with the matrix muscovite. The sum of oxides and cation occupancy in T+A sites (~ 6 *apfu*) in muscovite formed after tourmaline indicate that this muscovite does not contain significant B content. Chlorites correspond to Al-rich chamosite [2.69–2.86 *apfu* Al; Mg/(Mg + Fe) = 0.23–0.47], although the Mg/(Mg + Fe) ratio vary significantly from sample to sample. Chemical composition of chlorite replacing tourmaline differs from chlorite in tourmalinite matrix and is quite similar to fan-like chlorite from quartz-chlorite veins. Chlorite replacing tourmaline and chlorite from quartz-chlorite veins contain higher Si and lower Fe compared to chlorite from the matrix and the contents of Ca and Na were usually detectable by electron microprobe.

Positive correlation between degree of alteration of tourmaline to muscovite [replacement reaction (a)] and amount of muscovite in tourmalinite matrix and presence of muscovite-rich layers suggest that this alteration was caused by K-rich fluids. Intensive K-rich metasomatism and replacement reaction (a) relates probably to the Variscan metamorphic event. Our observations indicate that chloritization of tourmaline [replacement reaction (b)] occurred in relation to younger hydrothermal fluid flux together with quartz-chlorite vein formation. The empirical chlorite thermometer (JOWETT, 1991) indicates T = 246–260°C for formation quartz-chlorite veins.

This abstract was supported by the research project GAČR P210/10/0743 to RČ and RŠ.

References

AHN, J.H. & BUSECK, P.R. (1998): American Mineralogist, 83: 535–541.

HOLLAND, T.J.B. & POWELL R. (1998): Journal of Metamorphic Geology, 8: 89–124.

JOWETT, E.C. (1991): GAC/MAC/SEG Joint Annual Meeting (Toronto), Program with Abstracts, 16: A62.

SLACK, J.F. (1996): Reviews in Mineralogy, 33, 559–643.

PETROGRAPHIC ANALYSIS OF LITHIC ARTEFACTS FROM LIMBA (ROMANIA) TO CONFIRM NEOLITHIC TRADE PATTERNS

CRANDELL, O.N.
Department of Geology, Babeş-Bolyai University, 1 Kogălniceanu Str., RO-400084 Cluj-Napoca, Romania
E-mail: otis.crandell@ubbcluj.ro

An important question in prehistoric archaeology is the intersettlement and intercultural interactions of settlements. Trade and procurement can often give us insights into the economic aspects of interaction. For this study, 440 knapped lithic artefacts from the Early to Middle Neolithic settlement site near Limba (Alba County, western Romania) were analyzed to help to verify their sources and thereby to determine the intensity of trade with different regions. Within and adjacent to the Transylvanian Basin, there are three main knappable materials that are considered as high quality and were imported in large quantities during the Neolithic. These are the "Carpathian obsidian", "Moldavian flint" and "Balkan flint" (Fig. 1). Within a day's travel by walking or by boat from Limba there are also materials of various quality that are suitable for knapping. The Criş and Vinča cultures, that occupied the Limba settlement, were extended to the south in the region of the Danube. Since two of the high quality materials i.e. Moldavian flint and Carpathian obsidian are outside of their cultural territory and the third i.e. the Balkan flint is within, this is an ideal assemblage for at the analysis of intra- and intercultural economic interactions.

The entire set of artefacts was compared macroscopically with material samples from potential source outcrops. Thirty of the artefacts were analysed petrographically and compared by thin sections with raw material samples. Obsidian was not analysed under microscope, but can be clearly distinguished from microcrystalline quartz and other studies indicate that its source was correctly identified. One artefact based on macroscopic assessment was considered as Balkan flint and two were considered as local, however these were not proved by petrography. In other cases, the petrographic analyses supported the macroscopic categories.

Although there are numerous local and near-local sources of lithic material, a large portion of the artefacts appear to be made from non-local materials. Only 38% of the artefacts came from sources within a day's travel distance from the settlement. Regarding to the imported materials, 24% of the whole assemblage is Moldavian flint, and 26% is Carpathian obsidian. Contrary, only 7% is Balkan flint. This suggests more economic contacts with the North, outside of their cultural territories. The results of this study indicate that economic contacts and interactions were not limited to the given culture. In fact, it is likely that there were other more important factors involved in choosing trade partners. The large proportion of imported material suggests that trade routes may have already existed in the Neolithic.

Acknowledgements. The artefacts used in this study were provided by the "1 Decembrie 1918" University in Alba Iulia. Information regarding their cultural origins and stratigraphic context was given by Iuliu Paul, the scientific director of the site from 1996 to 2001. Raw material samples were taken from the Romanian Lithotheque Project collection, housed at Babeş-Bolyai University, Cluj-Napoca. This study was financed by the ID-2241/2008 project (Romanian Ministry of Education and Research).

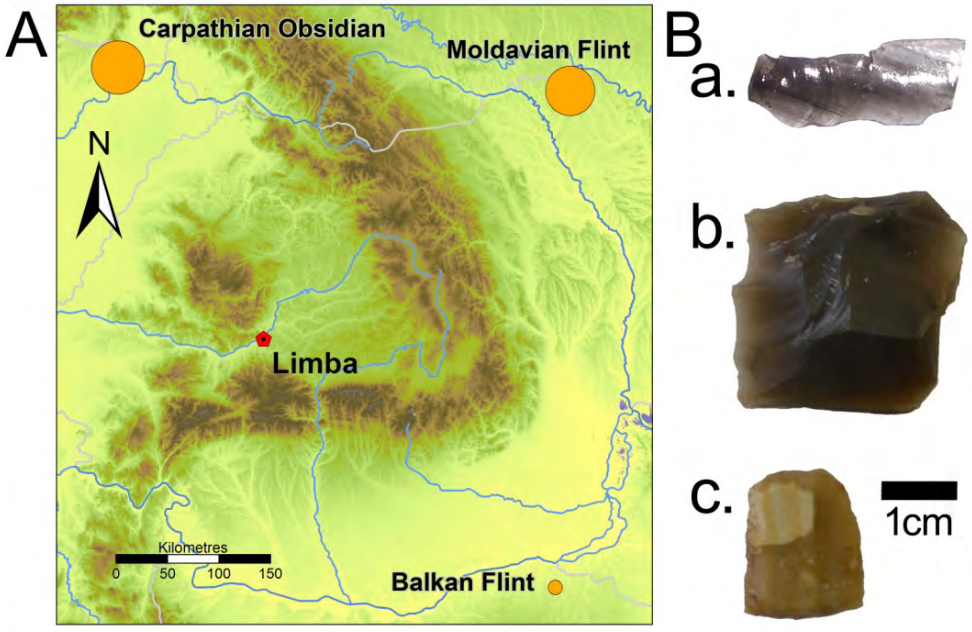

Fig. 1. *A) Location of main sources for knappable material discussed in the text. Circle size is proportionate to the percentage of material from that source; B) Images of lithics made of Carpathian obsidian (a), Moldavian flint (b), and Balkan flint (c).*

THE ATOMIC-SCALE ASPECTS OF TWINNING AND POLYTYPISM IN MINERALS

DANEU, N.* & REČNIK, A.
Department for Nanostructured Materials, Jožef Stefan Institute, Jamova 39, 1000 Ljubljana, Slovenia
* E-mail: nina.daneu@ijs.si

Abstract

Phase transformations in minerals are important indicators of geochemical and thermodynamic changes during crystal growth. Initial stages of phase transformations can be recognized by the formation of thermodynamically or chemically induced planar defects, such as twin, antiphase, or inversion boundaries in the affected crystals. Based on the principles of crystal chemistry, some early scientists suggested that the atomic structure of the twin boundary must be related to the existing polymorphic modification of the major phase. The confirmation of this hypothesis was not possible until the development of modern electron microscopy techniques, which enabled a direct insight into the local structure and chemistry of twin boundaries at the atomic scale. Our studies of twins and other translational defects in minerals have shown that their formation is chemically induced by specific dopants that stabilize the particular polytypic structure. Inherent anisotropy imposed by the chemically induced transformation fault (*e.g.* growth twin) causes exaggerated growth of the crystal parallel to the fault plane as long as geochemical and thermodynamic conditions favour the formation of faulted stacking. These initial growth stages dictated by the growth of the chemically induced fault are clearly reflected in the final morphology of the crystals and can be recognized by the so-called twin-plane re-entrant angles and the additional symmetry elements that can be observed on such crystals. Because of commonly complex geochemical conditions minerals incorporate an assortment of foreign elements that are present during crystal growth, only one of these elements, however is responsible for the faulted stacking (*e.g.* twinning). In order to identify the elements that trigger twinning in minerals we developed new techniques that enable atomic-scale determination of the interfacial crystal chemistry. The investigations of twinning in minerals represents one of the fundamental scientific challenges that offers possibilities for true understanding of the basic building principles of solids and fundamentals of phase transformations in minerals.

Keywords: twinning, phase transformations, sphalerite, spinel, pyrite, bixbyite, perovskite, rutile.

Introduction

In prevalently ionic compounds, like some oxides, chalcogenides and halides, one of the species (often anionic) constitutes close-packed layers of atoms. The layers can then be stacked in either cubic (*ccp*) or hexagonal (*hcp*) sequence, or even some more complex structures can be built by varying the two stackings. A hexagonal sequence is built by stacking the layers in two (out of three) unique positions (*A* and *B*) along the plane normal, coinciding with the hexagonal c-axis. If however, the close-packed layers are stacked in all three positions (*A*, *B* and *C*) the resulting sequence is cubic, and when repeated, identical stacking is observed in four directions coinciding with ⟨111⟩ directions of the cubic structure. {111} planes of *ccp* structures and {0001} planes of their *hcp* analogues are thus aligned parallel with the rudimentary close-packed layers. The rest of the atomic species (*e.g.* cations) occupy the interstitial sites available between any two closed-packed layers of anions. Three basic types of interstitials exist: (i) lower tetrahedral Type-I (at ⅓ of the interlayer distance), (ii) central octahedral (at ½ of the height) and (iii) upper tetrahedral Type-II (at⅔ of the height). While the stacking of the close-packed layers defines the common sub-lattice framework, discrete structures emerge by specific occupancy of the available interstitials. For example, a rock-salt structure is obtained when all octahedral sites in anionic *ccp* sublattice are occupied by cations. Typical representatives of this structure are periclase (MgO), galena (PbS) and halite (NaCl). If however anionic close-packed layers are stacked in an *hcp* sequence, and occupied interstices remain octahedral, we get nickeline, a hexagonal analogue of the rock-salt structure. Typical representatives of this structure are troilite (FeS) and nickeline (NiAs). Another set of correlated structure types is produced if one set of tetrahedral sites is occupied instead of the octahedral ones. This produces sphalerite (*ccp*) and wurtzite (*hcp*) structure types, named after the cubic and hexagonal polymorphs of ZnS. These structures in particular are very prone to polymorphism and other phase transformations between the two (cubic and hexagonal) end-members. For example, zincite (ZnO) crystallizes in wurtzite (*hcp* sub-lattice; Type-I tetrahedral interstices occupied), sphalerite (*ccp* sub-lattice; Type-I tetrahedral interstices occupied), as well as in the rock-salt (*ccp* sub-lattice; octahedral interstices occupied) structure type. The largest variety of anion sub-lattice types are found in moissanite (SiC). It does not occur only in form of simple cubic and hexagonal polymorphs, but it exists in several intermediate repeat sequences, known

as polytypes. In a similar way more complex structures can be built within the common structural sub-lattices. For example, in spinel (AB_2O_4) all three types of interstitials are partially occupied, in perovskite (ABO_3) cation A lies in the anionic sublattice and ¼ of the available octahedral sites are occupied by cations B, and all these structures have polymorphic counterparts or even form polytypes.

Polymorphic phase transitions and twinning in minerals

Each polymorph (or polytype) is stable at different p-T conditions. Quite often however, different polytypes coexist, for example sphalerite *ccp* layers in *hcp* wurtzite, or *hcp* enargite in *ccp* luzonite, *etc*. (PÓSFAI & BUSECK, 1997). This can happen when the minerals pass through the phase transformation temperature so fast, that there is not enough time to completely establish the new equilibrium structure. Another possibility is chemical stabilization of high-temperature polymorphs, so that they can form at much lower temperatures, as long as the particular dopant is available during crystal growth. For example, in HgS the transformation temperature is lowered by the presence of Zn (DICKSON & TUNELL, 1959), whereas in ZnS it is lowered under S-deficient environment (AKIZUKI, 1981). Phase transformations in minerals are therefore important marker of thermodynamic, as well as geochemical conditions during crystal growth. Polytypic sequences are rarely fully evolved and periodic. They may form irregular modular structures or even appear in form of isolated planar faults that have a stacking of a higher-temperature polymorph. As for the polytypes, the cause for the formation of polytypic faults can either be kinetic or thermodynamic. They form as a consequence of mechanical stress, rapid changes of p-T conditions, incorporation of dopant elements, *etc*. While kinetically induced defects can easily be translated through the crystal and even annealed out by suitable thermal treatment, chemically induced faults are thermodynamically stable and can not be moved. Kinetic defects are dislocations, stacking faults (*e.g. hcp* SFs in sphalerite, or *ccp* SFs in zincite) and deformation twins (*e.g.* rutile), while chemically induced faults are growth twins, antiphase and inversion boundaries (REČNIK *et al*., 2001). The most significant difference between the kinetic and thermodynamic defects is that the latter have changed chemistry compared to that of the hosting crystal. The presence of growth twin, antiphase or inversion boundaries is also clearly reflected in crystal morphology (exaggerated growth along the fault planes, the presence of twin-plane re-entrant angles, *etc*.). Therefore they are usually easily distinguished from the kinetic defects.

Chemically induced faults are growth defects that nucleate in the initial stages of crystal growth. They are result of structurally confined 2D chemical reaction between the dopant and the major phase (REČNIK *et al*., 2001). In the nucleation stage, dopant atoms are chemisorbed (react) to specific crystallographic planes of the host in highly ordered manner, controlled by the surface structure. Chemisorption does not take place with any alien species, but only with those, which can form a chemical bond to given structural environment (common sub-lattice framework) in a similar way as the atoms of the hosting structure. Most of the alien atoms do not cause any larger disruption to the structure (they form solid solution), but some however, impose an irreparable fault in the stacking (*e.g. hcp* instead of *ccp*) of otherwise uniform sub-lattice framework. This has a remarkable effect on the next layers that are built in. By introducing a sub-lattice fault, all new layers of the growing host crystal are symmetrically translated by the imposed crystallographic operation. Once such 2D cluster is formed it will persist to grow as long the conditions permit its formation. As the crystals always tend to overgrow defects or inclusions, in the same propensity they try to overgrow the inherent fault. However, because of the imposed symmetry, crystal domains on both sides of the fault are equally successful in this attempt, so instead of overgrowing the fault, they assist its growth. In this way, the dopant atoms that caused the sub-lattice fault will continue to produce the faulted layer (where they are most easily accommodated) while the host crystal is rushing to heal the defect. Thermodynamic stability of the growing 2D structure in most cases is orders of magnitude higher than that of the hosting crystal (REČNIK *et al*., 2012). This has dramatic effects on crystal morphology. In the initial stages of growth, crystals infected with thermodynamically stable faults grow exaggeratedly along the fault plane forming unusual plate-like crystals with distinct tabular morphology (*e.g.* contact twins), if the faults are grown in more equivalent directions the host crystal grows in all these directions (*e.g.* interpenetration twins). In the later stages, when thermodynamic or geochemical conditions change to an extent that the nucleation of the faulted layer is stopped, crystal domains continue to overgrow the inherent fault, which causes development of twin-plane re-entrant angles, characteristic not only for chemically induced twin boundaries, but also other chemically induced faults such as antiphase and inversion boundaries.

In general, there is not much known about the origin of thermodynamic faults. While there is a lot of knowledge about the morphology and crystallography of growth twins, their local structure and chemistry have rarely been assessed quantitatively on the atomic scale. From the recent studies of growth twin, antiphase and inversion boundaries in perovskite (REČNIK *et al.*, 2001), zincite (REČNIK *et al.*, 2001), sphalerite (ŠROT *et. al*., 2003), pyrite (DANEU *et al*., 2005), spinel

(DANEU *et al.*, 2007), bixbyite (KLEEBE *et al.*, 2008) and rutile (DANEU *et al.*, 2007) it is evident that the local structure in most cases is rather trivial, whereas their local chemistry can be more challenging, especially in natural minerals, due to complex geochemical conditions during crystal growth. Out of all foreign elements that can be present near the twin boundary, only one is actually responsible for the formation of faulted stacking. In all cases studied so far, it appears that the local chemistry and structure of these interlayers is closely correlated to the first binary compound that exists between the host phase and the dopant. These 2D phases can never exist stand-alone and can be understood as the preparatory stage of the binary phase formation. They nucleate in those planes of the host phase (preferably close-packed planes, or other high density planes) that most efficiently accommodate the dopant element. As opposed to the pure phase, crystals with these defects more efficiently lower the total free energy (they are thermodynamically more stable than the major phase), which is reflected in exaggerated growth. In systems that are prone to the formation of chemically induced faults, a binary phase (between the major phase and the dopant) would form at elevated temperatures. In binary phase diagrams, where available, these phases are polytypoidic incongruent-melting compounds with modular structures comprising structural elements of both end-phases. Similar structural features as found in these compounds, can be observed in chemically induced faults that nucleate at lower temperatures. Local chemistry is therefore the most important indicator of the origin of growth faults. In the following, few examples of chemically induced twinning in natural minerals are presented.

(111) twins of sphalerite and their relation to zincite

The first systematic nanostructural analysis of growth faults in natural minerals was performed on sphalerite (ZnS) crystals from Trepča in Kosovo (ŠROT *et al.*, 2003). The crystals display characteristic twin-plane re-entrant angles, which indicate the presence of {111} twin boundaries. HRTEM analysis revealed that the local stacking across the twin boundary changes from cubic (*ccp*) to hexagonal (*hcp*). It was shown that the twin boundaries are significantly enriched in oxygen, which triggers local sphalerite-to-wurtzite transformation. The local chemistry and the stacking at the twin boundaries in sphalerite is similar to that of zincite, the stable polymorph of ZnO, which crystallizes in the wurtzite structure. From the structural and compositional point of view, (111) twin plane is nothing but (0001) layer of zincite, coherently intergrown within the sphalerite structure.

In addition to twin boundaries, sphalerite crystals are densely populated by *hcp* stacking faults (SFs) extending in {111} planes. In contrast to twin boundaries, SFs show no change of chemistry, neither they have any effect on the morphology of the crystals. The increased concentration of other elements (Mn, Fe and Cu) in the vicinity of the twin boundary is a consequence of segregation (also a kinetic effect) to the twin boundary during cooling.

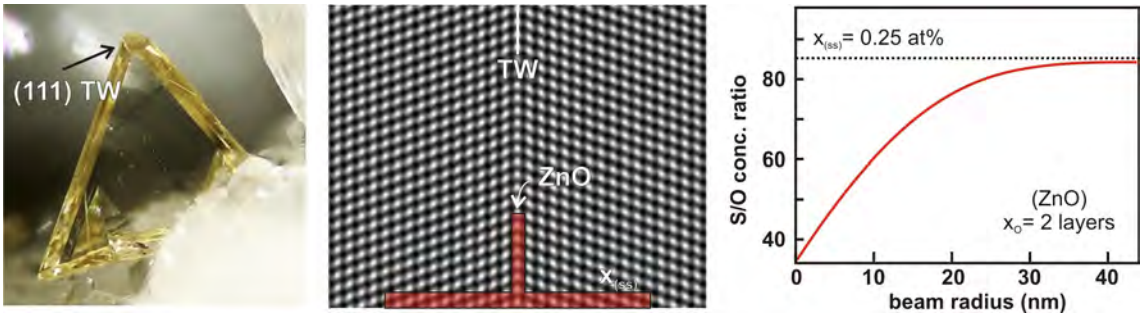

(111) twins of spinel and their relation to chrysoberyl

Another fine example of chemically induced twinning are (111) twins of spinel ($MgAl_2O_4$), after which the spinel-law of twinning received its name. For this study, simple contact twins of spinel from the Mogok metamorphic belt in Burma were used (DANEU *et al.*, 2007). The translational state observed on these twins can be best described by a 180° rotation around [111]-axis in oxygen sub-lattice after the so-called kagome layer of the structure. This operation produces a local *hcp* stacking, which is the basic twin element in an otherwise cubic structure.

To identify the cause of the observed stacking disorder, we used a combination of TEM-based analytical techniques. Results of concentric electron probe (CEP) method (REČNIK *et al.*, 2001) indicated a sharp drop of Mg^{2+} concentration at the twin boundary, implying that

Mg^{2+} ions are not present in the boundary tetrahedral sites. In addition no other impurity element measurable by EDS, showed a corresponding increase. In order to maintain the local charge balance the only candidate to occupy the available tetrahedral interstices was Be^{2+}. The most closely related *hcp* analogue of the *ccp* sublattice of the spinel structure is chrysoberyl ($BeAl_2O_4$). This was an important finding, which indicated that the twin formation in spinel is related to the formation of polytypoidic series that exist between spinel and chrysoberyl, of which taaffeite ($BeMg_3Al_8O_{16}$) is one of the most characteristic representatives. And indeed, *ccp-hcp* modules of the taaffeite structure closely resemble the structural configuration at (111) twin boundaries in spinel, while Be^{2+} ions in taaffeite occupy the tetrahedral sites adjacent to *hcp* layers of the structure. Like all growth twins (chemically induced!), the morphology of spinel crystals reflects the initial exaggerated growth along the twin boundary and a subsequent overgrowth producing characteristic twin-plane re-entrant angles.

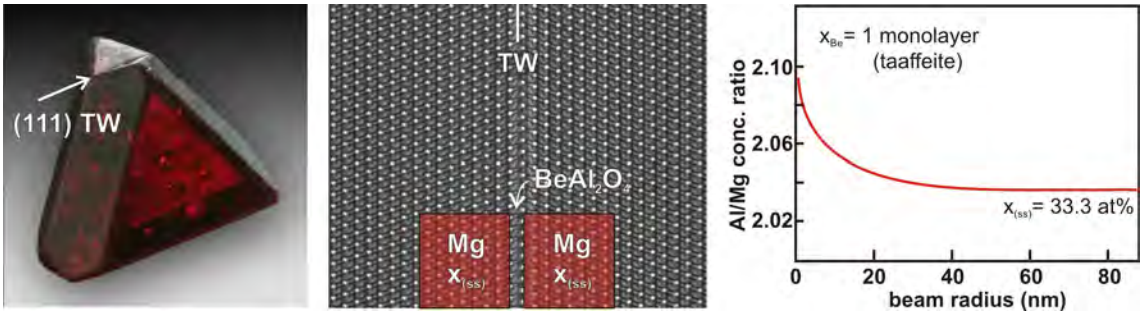

{100} antiphase boundaries in bixbyite and their relation to braunite

And sometimes twins are not twins in spite of all external signs that suggest twinning. Thomas Mountain Range in Utah is famous for splendid crystals of bixbyite ($MnFeO_3$). They occur in rhyolite vugs in a form of black lustrous crystals with marked re-entrant angles at halfways of the cube edges. According to these morphological features, such crystals could be considered {100} twins; however, any crystallographic operation on {100} planes of a centrosymmetric cubic structure such as bixbyite, would produce an untwinned crystal (KLEEBE & LAUTERBACH, 2008).

So, if they are not twins, what they could possibly be? HRTEM study revealed that the crystals are densely intersected by a 3D network of planar faults running along {100} planes of the structure. The highest density of these faults is near the centre of the crystal, where they form ordered lamellas with evident polytypoidic structure, similar to {100} antiphase boundaries reported in synthetic perovskite crystals (REČNIK *et al.* 2001). Chemical analysis showed that faults as well as ordered lamellas are Si-rich, whereas their local structure is closely related to mineral braunite (Mn_7SiO_{12}). Topotaxial intergrowth of (001) braunite layers with {100} planes of bixbyite is the main cause for the apparent bixbyite morphology. A braunite core formed already in the nucleation stage. It caused a 3D exaggerated growth of topotaxial bixbyite crystal along {100} planes. In the final stages of growth the conditions for the formation of intrinsic braunite layers ceased and re-entrant angles developed with bixbyite overgrowth.

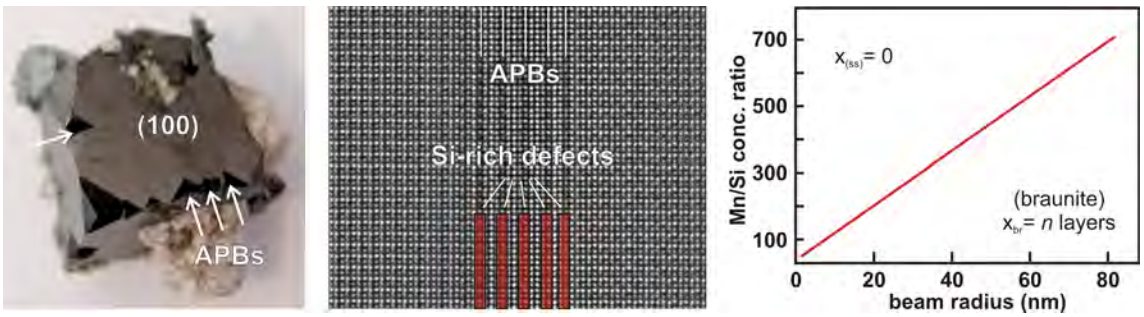

{301} and {101} twins of rutile in relation to ilmenite and corundum

Every now and then the twins can be a result of a whole series of recrystallization processes. This was best demonstrated on {301} and {101} twins of rutile (TiO_2) from Diamantina, Brazil (DANEU *et al.*, 2007). TEM study of (301) rutile twins from this locality revealed that the twin boundary comprises a few nanometers thick Fe-rich lamella with a corundum-type structure. Chemical and structural analysis showed that this internal twin-lamella consists of Al-rich ilmenite ($FeTiO_3$). The orientation relationship between the ilmenite lamella and the epitaxial rutile domains is $(01\bar{1}0)[0001]_I \parallel (301)[010]_R$. Both ilmenite-rutile interfaces are atomically sharp and devoid of misfit dislocations that would compensate for the lattice mismatch between the two structures. The structural mismatch is compensated by incorporation of Al into the ilmenite structure. A detailed HRTEM analysis of the ilmenite lamella revealed goethite-related reflections and presence of nano-twins. This was an important hint to resolve the whole crystallization sequence that led to the formation of these twins. The ilmenite lamella formed during a thermally-induced dehydration process from twinned tivanite-like Fe-Ti-Al oxy-hydroxide precursor. Tivanite (400) planes are mirror twin planes for the common anion sub-lattice and are parallel to the (301) planes of rutile. It is expected that under the inflow of acidic Ti-rich solutions rutile started to grow epitaxially on twinned tivanite-like precursor mineral. This was accompanied by dehydration process, under which an equilibrium boundary was formed between the internal lamella and the epitaxial rutile. In this process, the composition of the lamella reached equilibrium close to the stoichiometry of ilmenite. In order to reduce the lattice mismatch with respect to the epitaxial rutile a sufficient amount of Al^{3+} ions was incorporated into the ilmenite structure to reduce the pertinent unit-cell dimensions.

Our recent study of (101) twin in rutile from the same locality have shown a similar configuration, except that in this case the interface is decorated with precipitates of Ti-rich corundum (Al_2O_3). In this case the orientation relationship between the two phases is identical as in the case of (301) twins, except that the interface is different. The formation of these precipitates is yet unknown, but it seems that the formed in a similar way, from an Al-rich oxy-hydroxide precursor (*e.g.* diaspore), and after dehydration corundum precipitates formed and retracted to equidistant locations along the (101) twin boundary of rutile. The reason why corundum does not form a continuous layer lies in the large lattice mismatch between $\{21\bar{1}0\}$ planes of corundum and {101} planes of rutile.

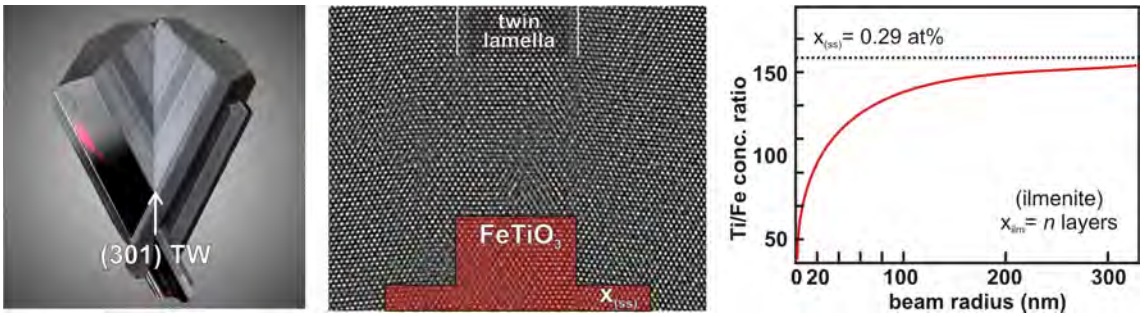

Conclusions

The described analyses show that the formation of transformation faults and intergrown topotaxial structures is always chemically triggered. During their growth, natural minerals are exposed to incomparably more unpredictable thermodynamic conditions and geochemical environments than the minerals synthesized in laboratory. Therefore we can observe the consequences of sequential phase transformations in natural minerals that evidence the dynamics of the geochemical surrounding in which they were formed. In nature we find many examples of transformation faults, polytypic structures and epitaxial overgrowths of minerals and the reasons for their formation are mostly unknown. Based on nanostructural investigations of these planar defects and precipitates in minerals we are able to reconstruct the geochemical conditions in the time of their formation. This knowledge is not only the basis for the explanation of their formation and growth, but is also a rich source of information about regional rock-forming and tectonic processes during their growth.

References

AKIZUKI, M. (1981): Investigation of phase-transition of natural ZnS minerals by high-resolution electron-microscopy. *American Mineralogist*, **66**: 1006–1012.

DANEU, N., REČNIK, A. & DOLENEC, T. (2005): Electron microscopy study of {110} interpenetration twins of pyrite from St. Katarina, NW of Ljubljana. *Proc. of the 7th Multin. Congress on Microscopy* (Portorož, Slovenia): 197–198.

DANEU, N., REČNIK, A. & DOLENEC, T. (2007): Structure and chemistry of (111) twin boundaries in $MgAl_2O_4$ spinel crystals from Mogok. *Physics & Chemistry of Minerals*, **34**: 233–247.

DANEU, N., SCHIMD, H., REČNIK, A. & MADER, W. (2007): Atomic structure and formation mechanism of (301) rutile twins from Diamantina (Brazil). *American Mineralogist*, **92**: 1789–1799.

DICKSON, F.W. & TUNELL, G. (1959): The stability relations of cinnabar and metacinnabar. *American Mineralogist*, **44**: 471–487.

KLEEBE, H.-J. & LAUTERBACH, S. (2008): Exaggerated grain growth in bixbyite via fast diffusion along planar defects. *Crystal Research & Technology*, **43**: 1143–1149.

PÓSFAI, M. & BUSECK, P.R. (1997): Modular structures in sulphides: sphalerite/wurtzite-, pyrite/marcasite-, and pyrrhotite-type minerals. *EMU Notes in Mineralogy*, **1**: 193–235.

REČNIK, A., ČEH, M. & KOLAR, D. (2001): Polytype induced exaggerated grain growth in ceramics. *Journal of the European Ceramic Society*, **21**: 2117–2121.

REČNIK, A., DANEU, N., WATHER, T. & MADER, W. (2001): Structure and chemistry of basal-plane inversion boundaries in antimony oxide-doped zinc oxide. *Journal of the American Ceramic Society*, **84**: 2657–2668.

REČNIK, A., BERNIK, S. & DANEU, N. (2012): Microstructural engineering of ZnO-based varistor ceramics. *Journal of Materials Science*, **47**: 1655–1668.

ŠROT, V., REČNIK, A., SCHEU, C., ŠTURM, S. & MIRTIČ, B. (2003): Stacking faults and twin boundaries in sphalerite crystals from the Trepča mines in Kosovo. *American Mineralogist*, **88**: 1809–1816.

INVESTIGATION OF CLAY MINERALS IN SOILS FORMED UPON LIMESTONES IN THE BÜKK MOUNTAINS, HUNGARY

DOBOS, T.* & KRISTÁLY, F.
Institute of Mineralogy and Geology, University of Miskolc, H-3515 Miskolc-Egyetemváros, Hungary
* E-mail: dobos.ask@gmail.com

This paper reports mineralogical investigation of different kind/type of soils on different limestone formations at the Bükk Mountains. Here we report the investigation of the clay fractions of the acid (5 wt% acetic acid) insoluble residues of the different limestones and soils. One soil sample and one rock sample were gathered from both Három-kő and Létrás-tető hills (peak positions). The former belongs to the Bükkfennsík Limestone Formation, and the latter to the Fehérkő Limestone Formation. After general soil classification, based on the WRB (World Reference Base for Soil Resources), instrumental techniques were applied, which included X-ray powder diffraction (XRPD) and differential thermal analysis.

The bulk soil and limestone samples display totally different XRPD patterns. The Három-kő soil sample dominantly contains nano-crystalline smectite with important quartz and X-ray amorphous phase contribution, with minor albite, while the underlying limestone contains calcite, muscovite-2M_1, minor quartz and important apatite. The Létrás-tető soil sample shows dominant smectite, while the underlying Fehérkő Limestone Formation has important muscovite content nearby the dominant calcite. Neither soil samples contain carbonates, as calcite, or dolomite.

Thermal analyses showed similar type of organic matter in both the soil samples, where the Három-kő soil had much higher organic content. Weight losses of around 60 weight percents are characteristic for the Három-kő soil, while the Létrás-tető soil showed 12–15 weight percent losses during heating up to 1100 °C. The XRPD data of the < 2 μm fraction of soils and limestone residues were compared by the means of oriented clay mineral specimens investigated in air-dried, ethylene-glycol saturated states and after heating to 350°C. The Három-kő soil and limestone samples show no common features. The soil is characterized by almost amorphous smectite (chlorite?) and illite/smectite with poorly crystalline illite (or muscovite) and kaolinite. On the contrary, the limestone is characterized by well-crystallized muscovite-2M_1, with only minor amounts of smectite and kaolinite, where quartz is not present. The Létrás-tető soil is characterized by illite/smectite with high smectite ratio (diffraction peak at *ca*. 12 Å), poorly crystallized kaolinite and minor amount of illite. Minor amount of quartz is also present. The limestone residue sample here is similar to the other limestone. It is again quartz dominated with muscovite-2M_1 and has minor smectite and kaolinite component.

STRUCTURAL STUDY OF A KAOLINITE SINGLE-CRYSTAL USING PED AND DIFFRACTION TOMOGRAPHY

DÓDONY, I.[1]*, PEKKER, P.[2] & CORA, I.[1]
[1] Department of Mineralogy, Eötvös Loránd University, Pázmány Péter sétány 1/C, H-1117 Budapest, Hungary
[2] Institute for Nanotechnology, Bay Zoltán Foundation for Applied Research, H-3515 Miskolc-Egyetemváros, Hungary
* E-mail: dodony@t-online.hu

Kaolinite is an abundant submicrometer-sized "TO"-type dioctahedral sheet silicate [$Al_2Si_2O_5(OH)_4$]. Its building units are the infinite 2D layers of corners shared SiO_4 tetrahedra and edge connected $Al_2O_2(OH)_4$ octahedra. Except of ZVYAGIN's (1960) oblique texture patterns based structure solution, X-ray and neutron diffraction methods were used on powdered samples.

The structure of a kaolinite *single crystal* from Mád (Hungary) was solved using precession electron diffraction (VINCENT & MIDGLEY, 1994; OWN, 2005; AVILOV *et al.*, 2007) and the newly developed technique of electron-diffraction tomography (KOLB *et al.*, 2007, 2008). The data collection was carried out using a Tecnai G^2X transmission electron microscope equipped with a CeB_6 gun operating at 200 kV and a tomography holder with a tilt range up to ±70°. We acquired intensities from 90° large wedge of reciprocal space within 0.8 Å resolution limit using a 4 Mb, 16 bits, Eagle CCD detector.

Structure of kaolinite was determined in the SIR2008 (implemented in the Il Milione package; BURLA *et al.*, 2007) and refined to R1 = 0.227, wR^2 = 0.547 using 236 observed unique reflections in SHELX97 (SHELDRICK, 2008). As a result we described kaolinite in the *C*1 triclinic space group (a = 5.056 Å, b = 9.122 Å, c = 7.250 Å, α = 88.72°, β = 104.18°, γ = 90.25°). Largest deviations are within a ± 0.36 value in the differential Fourier-map.

Authors thank the HAS CRC for financial support through OTKA grant No. 68562.

References

AVILOV, A., KULIGIN, K., NICOLOPOULOS, S., NICKOLSKIY, M., BOULAHYA, K., PORTILLO, J., LEPESHOV, G., SOBOLEV, B., COLLETTE, J.P., MARTIN, N., ROBINS, A.C. & FISCHIONE, P. (2007): Ultramicroscopy, 107: 431–444.

BURLA, M.C., CALIANDRO, R., CAMALLI, M., CARROZZINI, B., CASCARANO, G.L., DE CARO, L., GIACOVAZZO, C., POLIDORI, G., SILIQI, D. & SPAGNA, R. (2007): Journal of Applied Crystallography, 40: 609–613.

KOLB, U., GORELIK, T., KÜBEL, C., OTTEN, M.T. & HUBERT, D. (2007): Ultramicroscopy, 107: 507–513.

KOLB, U., GORELIK, T. & OTTEN, M.T. (2008): Ultramicroscopy, 108: 763–772.

OWN, C.S. (2005): System design and verification of the precession electron diffraction technique. PhD Thesis, Northwestern University, Evanston, Illinois. (http://www.numis.northwestern.edu/Research/Current/precession.shtml)

SHELDRICK, G.M. (2008): Acta Crystallographica, A64: 112–122.

VINCENT, R. & MIDGLEY, P.A. (1994): Ultramicroscopy, 53: 271–282.

ZVYAGIN, B.B. (1960): Kristallografiya, 5: 32–41.

Atom coordinates and isotropic displacement parameters for kaolinite of Mád, Hungary.

Atom	x	y	z	U_{iso}
Si1	0.429	0.930	0.425	0.024
Si2	0.919	0.764	0.449	0.024
Al2	0.714	1.106	0.836	0.027
Al3	0.716	0.770	0.834	0.008
O1	0.544	0.933	0.691	0.001
O2	0.458	1.125	0.953	0.017
O3	0.464	1.222	0.666	0.017
O4	0.620	0.832	0.380	0.013
O5	0.438	1.088	0.393	0.019
O6	0.967	1.256	0.934	0.003
O7	0.899	0.944	0.893	0.068
O8	0.141	0.857	0.369	0.035
O9	1.026	1.118	0.713	0.016

HRTEM STUDY OF TAAFFEITE CRYSTALS FROM MOGOK (MYANMAR)

DREV, S.[1]*, DANEU, N.[1], KYNICKÝ, J.[2] & REČNIK, A.[1]
[1] Department for Nanostructured Materials, Jožef Stefan Institute, Jamova cesta 39, SI-1000 Ljubljana, Slovenia
[2] Ústav geologie a pedologie, Mendelova Univerzita v Brně, Zemědělská 3, CZ-61300 Brno, Czech Republic
* E-mail: sandra.drev@ijs.si

Taaffeite ($BeMg_3Al_8O_{16}$) and musgravite ($BeMg_2Al_6O_{12}$) are members of the rare group of Al-Mg-Be oxide minerals occurring in high-grade metamorphic rocks and their alluvial deposits (SCHMETZER *et al.*, 2005). In most cases taaffeite group of minerals are linked to metamorphic processes. In Mogok (Myanmar), taaffeite crystals are associated with euhedral spinel crystals ($MgAl_2O_4$) in the Mogok marble belt that developed in metamorphic processes along the contact of more or less dolomitic limestones with granitic intrusives, which served as a source of beryllium. Taaffeite group minerals are also found near Stubenberg in Styria (Austria), where they formed as a replacement product of spinel in veins within polymetamorphic dolomitic marbles (BERNHARD *et al.*, 2008). Here, the origin of beryllium could be Be-rich fluids from granites or pegmatites generated during the contact metamorphosis or by mobilization of Be by the fluids formed during the metamorphic processes.

Taaffeite-group minerals comprise basic structural elements that are found in spinel ($MgAl_2O_4$) and chrysoberyl ($BeAl_2O_4$). Spinel (*s.g. Fd* $\bar{3}$ *m*) has *ccp* arrangement of the oxygen sublattice along the ⟨111⟩ directions. In these directions, the structure is composed of alternating kagome (Al) and mixed (Mg and Al) layers, where the Al^{3+} ions occupy the octahedral and Mg^{2+} ions the tetrahedral sites (SICKAFUS *et al.*, 1999). On the other hand, chrysoberyl ($BeAl_2O_4$) has a slightly distorted *hcp* stacking of the oxygen sublattice along the [0001] direction (*s.g. Pbnm*) with Al^{3+} and Be^{2+} ions located in the corresponding octahedral or tetrahedral interstices (TABATA *et al.*, 1974). A recent study of (111) twins of spinel (DANEU *et al.*, 2007) revealed that the stacking across the twin boundary is hexagonal (*hcp*) and Mg^{2+} near the boundary tetrahedral sites are locally replaced by Be^{2+}. This indicates that Be^{2+} in fact causes the hexagonal stacking fault in an otherwise perfect cubic structure. Local structure of (111) twin boundaries in spinel is closely related to chrysoberyl and taaffeite-group of polysomatic minerals and can be understood as an initial stage of taaffeite-type phase transformation. In this view we can understand the alternation of *ccp* and *hcp* sequences at the unit-cell level in these structurally correlated systems.

In the present work, the atomic structure of taaffeite crystals from Mogok was studied by X-ray powder diffraction (XRD), electron diffraction (ED) and high-resolution transmission electron microscopy (HRTEM). XRD analysis confirmed that the sample in fact corresponds to taaffeite ($BeMg_3Al_8O_{16}$). Two slightly different structural models for this compound were reported (MOOR *et al.*, 1981; NUBER & SCHMETZER, 1983). In both models, the stacking sequence of the oxygen sublattice (ABCABA…) along the crystallographic *c*-axis is identical, they differ only in the occupancy of the interstitial sites within mixed layers. In Moor's model, all Al^{3+} ions lie in octahedral positions and all Mg^{2+} ions in tetrahedral positions, whereas in the Nuber's model, the positions of Al^{3+} and Mg^{2+} ions within the mixed layers are switched. At the present state of investigations, we can not confirm the validity of either model from HRTEM images.

References

BERNHARD, F., HAUZENBERGER, C. & WALTER, F. (2008): Canadian Mineralogist, 46: 1195–1205.

DANEU, N., REČNIK, A., YAMAZAKI, T. & DOLENEC, T. (2007): Physics and Chemistry of Minerals, 34: 223–247.

MOOR, R., OBERHOLZER, W.F. & GÜBELIN, E. (1981): Schweizerische Mineralogische und Petrographische Mitteilungen, 61: 13–21.

NUBER, B. & SCHMETZER, K. (1983): Neues Jahrbuch für Mineralogie – Abhandlungen, 146: 393–402.

SCHMETZER, K., KIEFERT, L., BERNHARDT, H.J. & BURFORD, M. (2005): Neues Jahrbuch für Mineralogie – Abhandlungen, 181: 265–270.

SICKAFUS, K.E., WILLIS, J.M. & GRIMES, N.W. (1999): Journal of the American Ceramic Society, 82: 3279–3292.

TABATA, H., ISHII, E. & OKUDA, H. (1974): Journal of Crystal Growth, 24–25: 656–660.

See the figure on the following page.

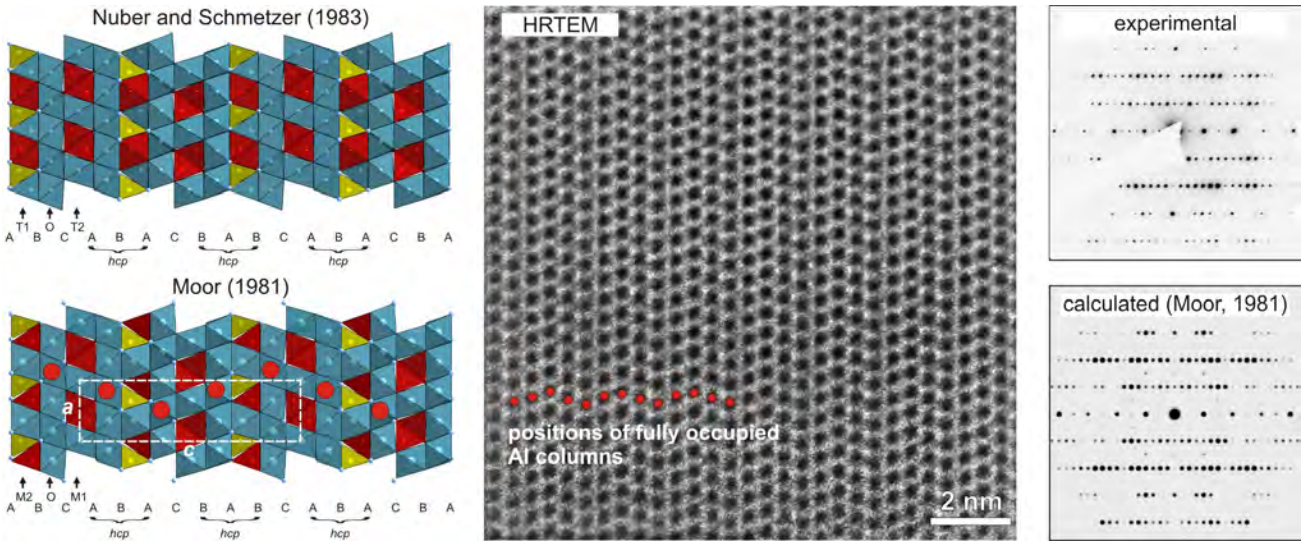
Nuber and Schmetzer (1983)
T1 O T2
A B C A B A C B A B C A B A C B A
hcp hcp hcp
Moor (1981)
a
c
M2 O M1
A B C A B A C B A B C A B A C B A
hcp hcp hcp
HRTEM
positions of fully occupied Al columns
2 nm
experimental
calculated (Moor, 1981)

CORRELATIONS IN Cu- AND Mn-BEARING TOURMALINES FROM BRAZIL AND MOZAMBIQUE

ERTL, A.[1]*, GIESTER, G.[1], TILLMANNS, E.[1], OKRUSCH, M.[2], SCHÜSSLER, U.[2] & BRÄTZ, H.[3]
[1] Institut für Mineralogie und Kristallographie, Universität Wien, Althanstrasse 14, Wien, Austria
[2] Lehrstuhl für Geodynamik und Geomaterialforschung, Institut für Geographie und Geologie, Universität Würzburg, Am Hubland, Würzburg, Germany
[3] GeoZentrum Nordbayern, Universität Erlangen-Nürnberg, Schloßgarten 5a, Erlangen, Germany
* E-mail: andreas.ertl@a1.net

Cu- and Mn-bearing tourmalines from Brazil and Mozambique were characterised chemically (EMPA and LA-ICP-MS) and by single-crystal structure refinement. All these samples are rich in Al, Li and F (fluor-elbaite) and contain significant amounts of CuO (up to ~1.8 wt%) and MnO (up to ~3.5 wt%). MgO and FeO contents are relatively low in the 15 investigated samples (≤0.2 wt%). Single-crystal structure refinements were done on 8 samples.

Tourmaline is a silicate mineral group with a highly complex crystal structure and a large variety of chemical compositions. The general chemical formula of the tourmaline-group minerals is $XY_3Z_6[T_6O_{18}](BO_3)_3V_3W$ (HENRY *et al.*, 2011). Our investigated samples, which were also characterised structurally, show a pronounced positive correlation between the <*Y*-O> distances and the (MnO + CuO) content in this site with $r^2 = 0.84$. There is no significant correlation between the Li content in the *Y* site and the <*Y*-O> distances. The valence states of Mn have not been determined, but we consider it mainly as Mn^{2+}. Another correlation, which is even better, shows a negative correlation between the <*Y*-O> distances and the Al_2O_3 content ($r^2 = 0.94$). In the structurally characterised samples the *T* site is only occupied by Si (<*T*-O> distances of ~1.618 Å). The samples at each locality generally show a strong negative correlation between the *X*-site vacancies and the MnO content ($r^2 \approx 0.9$ for all samples with F<0.9 apfu). The Mn content in these tourmalines is dependent on the availability of Mn, at the formation temperature, as well as on stereochemical constraints. Based on various data ERTL *et al*. (2012) suggest that increasing formation temperatures exist for tourmalines with increasing (Fe^{2+} + Mn^{2+}) contents. Our investigated samples also show evidence for a positive correlation between the Mn content (Fe content is only very low) and the formation temperature, because *X*-site vacancies decrease when the formation temperature increases (HENRY & DUTROW, 1996).

The very weak correlation between MnO and CuO ($r^2 = 0.01$) demonstrates that there is no evidence for a temperature dependent incorporation of Cu into the tourmaline structure. Hence, the Cu content in tourmaline is essentially dependent on the availability of Cu and on stereochemical constraints.

This work was funded by the Austrian Science Fund (FWF) project no. P23012-N19 to AE.

References

ERTL, A., SCHUSTER, R., HUGHES, J.M., LUDWIG, T., MEYER, H.-P., FINGER, F., DYAR, M.D., RUSCHEL, K., ROSSMAN, G.R., KLÖTZLI, U., BRANDSTÄTTER, F., LENGAUER, C.L. & TILLMANNS, E. (2012): European Journal of Mineralogy, 24: in press.

HENRY, D.J. & DUTROW, B.L. (1996): In GREW, E.S. & ANOVITZ, L.M. (Eds.): Boron: Mineralogy, Petrology, and Geochemistry. Reviews in Mineralogy, 33: 503–557.

HENRY, D.J, NOVÁK, M., HAWTHORNE, F.C., ERTL, A., DUTROW, B.L., UHER, P. & PEZZOTTA, F. (2011): American Mineralogist, 96: 895–913.

KOLBECKITE FROM BIXAD, ROMANIA: THE FIRST AUTHENTIC OCCURRENCE IN THE CARPATHIANS

FEHÉR, B.[1]*, SZAKÁLL, S.[2] & ZAJZON, N.[2]
[1] Department of Mineralogy, Herman Ottó Museum, Kossuth u. 13, H-3525 Miskolc, Hungary
[2] Institute of Mineralogy and Geology, University of Miskolc, H-3515 Miskolc-Egyetemváros, Hungary
* E-mail: feherbela@upcmail.hu

Kolbeckite is a rare hydrous scandium phosphate ($ScPO_4 \bullet 2H_2O$) of about 20 occurrences worldwide. Kolbeckite is not mentioned[#] for the Carpathians in the most recent reference work of the Carpathian minerals (SZAKÁLL, 2002). Here we describe the first authentic kolbeckite occurrence from the Carpathian region.

The South Harghita Mountains represent the southernmost part of the Călimani-Gurghiu-Harghita Neogene eruptive chain. Shoshonitic rocks occur in two isolated eruptive bodies in the southernmost part of the Harghita Mountains (SEGHEDI *et al.*, 1987). Kolbeckite was found, extreme rarely, on plagioclase crystals in miarolitic cavities of shoshonite in a quarry at Bixad (Sepsibükszád). The most abundant mineral of these cavities is intermediate plagioclase, forming colourless, stubby prismatic crystals up to 1 mm in length, covering the walls of cavities in close arrangement. Beside plagioclase, well developed diopside, quartz and titanite crystals, up to 0.5 mm in size, can be observed, too. Kolbeckite is present in the surroundings of zircon-containing, anorthite- and diopside-dominant xenoliths.

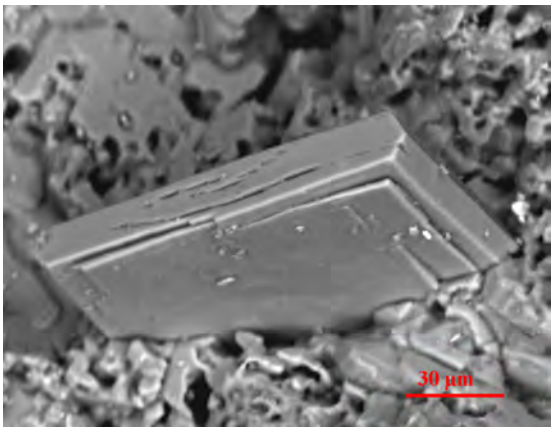

Fig. 1. *Tabular kolbeckite crystal. SEM SE photo.*

Kolbeckite forms colourless, pseudo-orthorhombic tabular single crystals up to 0.1 mm in diameter (Fig. 1). The crystals are never clustered. Kolbeckite has a white streak and vitreous lustre. X-ray powder diffraction pattern was obtained, due to the very limited amount of material available, from a single crystal using Gandolfi camera. On the pattern 45 reflections were identified from which the seven most intensive peaks are [d_{hkl} in Å (I_{obs} %, *hkl*)]: 4.451 (100, 002), 4.795 (89, 110), 6.71 (34, 011), 3.716 (31, 120), 5.10 (26, 020), 2.846 (24, 122) and 2.880 (21, 130). Kolbeckite is monoclinic, space group $P2_1/n$. The obtained cell parameters: a = 5.427(2) Å, b = 10.198(4) Å, c = 8.909(3) Å, β = 90.59(4)°, V = 493.0(2) Å^3, Z = 4. Average of four WDS analyses on the same crystal (in wt%): Sc_2O_3 39.02, P_2O_5 40.35, H_2O (calculated from the stoichiometry) 20.43, Al_2O_3 trace, total 99.80. The empirical formula is analogous with the ideal formula $ScPO_4 \bullet 2H_2O$. The calculated density: 2.370 g/cm^3.

In Bixad kolbeckite should be a relatively low-temperature recrystallisation product of accessory zircon crystals, Sc coming from zircon (or perovskite?), while phosphorous derived from the rock-forming apatite.

References

ANTHONY, J.W., BIDEAUX, R.A., BLADH, K.W. & NICHOLS, M.C. (2000): Handbook of mineralogy. Vol. IV: Arsenates, phosphates, vanadates. Mineral Data Publishing, Tucson, Arizona.

GAINES, R.V., SKINNER, H.C.W., FOORD, E.E., MASON, B. & ROSENZWEIG, A. (1997): Dana's new mineralogy. 8th Edition. John Wiley & Sons, New York, etc.

HEY, M.H., MILTON, C. & DWORNIK, E.J. (1982): Mineralogical Magazine, 46: 493–497.

KRENNER, J. (1929): Centralblatt für Mineralogie, Abt. A, 27–38.

PAPP, G. (2004): History of minerals, rocks and fossil resins discovered in the Carpathian region. Studia Naturalia 15, Hungarian Natural History Museum, Budapest.

SEGHEDI, I., SZAKÁCS, A., UDRESCU, C., STOIAN, M. & GRABARI, G. (1987): Dări de Seamă ale Institutului de Geologie şi Geofizică, 72–73(1): 381–397.

SZAKÁLL, S. (Ed.) (2002): Minerals of the Carpathians. Granit, Prague.

TOKODY, L. (1954): Neues Jahrbuch für Mineralogie – Monatshefte, 204–207.

[#] ***Note:*** Mineralogical textbooks (*e.g.*, GAINES *et al.*, 1997; ANTHONY *et al.*, 2000) give Baia Sprie (Felsőbánya), Romania as locality of kolbeckite on the basis of old references concerning "eggonite" (KRENNER, 1929; TOKODY, 1954; for history of "eggonite" see HEY *et al.*, 1982 and PAPP, 2004). However, this occurrence is rather ambiguous, as the above mentioned papers described "eggonite" as Al phosphate, the old samples are not available any more, and new findings are not exposed.

DACIAN CERAMICS FROM *SARMIZEGETUSA REGIA* ARCHAEOLOGICAL SITE (ROMANIA): AN OPTICAL AND XRPD STUDY

FILIPESCU, R.[1]*, ZAHARIA, L.[1], CRISTESCU, C.[2] & SIMON, V.[3]
[1] Dept. of Geology, Babeş-Bolyai University, Cluj-Napoca, Romania
[2] Faculty of History and Philosophy, Babeş-Bolyai University Cluj-Napoca, Romania
[3] Faculty of Physics & Institute for Interdisciplinary Research in Nano-sciences, Babeş-Bolyai University Cluj-Napoca, Romania
* E-mail: roro_fili@yahoo.com

From a large amount of fine to semifine ceramic fragments found at *Sarmizegetusa Regia*, the former capital of Dacia (Southern Carpathians, Romania), eleven potsherds were studied by means of polarized light optical microscopy (OM) and X-ray powder diffraction (XRPD). These ceramic fragments were recovered from the 7th terrace, located near the sacred zone, and dated towards the end of the Ist century AD.

The shards have a light red color. Microscopically, (Fig. 1) they consist of a red clayey matrix with variable amounts of metamorphic (quartzite, quartz schists, gneiss) lithoclasts, ceramoclasts, as well as crystalloclasts (quartz, feldspar and muscovite). The matrix is mainly microcrystalline *i.e.* anisotropic, but also shows slightly sintered *i.e.* isotropic areas (Fig. 1).

The XRPD pattern shows the presence of quartz and feldspars, the latter of primary but possibly also of secondary (firing) origin. Beside these minerals, there are modified lines of micas and illite and a secondary phase represented by hematite. About 900°C firing temperature was inferred from the thermal changes of primary minerals and the modified XRD patterns.

The fine ceramics does not contain larger clasts which might be assigned to any tempering material. The composition of the lithoclasts and crystalloclasts of the semifine ceramics points to alluvial sands of a metamorphic area used as temper. Indeed, the site's neighbouring area consists of Anteproterozoic crystalline schists (CODARCEA *et al.*, 1968).

Acknowledgements. The study was financed by PN-II-ID-PCE-2011-3-0881 project granted by the Romanian Ministry of Education and Research.

Reference

CODARCEA, D.M., SAVU, H., PAVELESCU, M., STANCU, I. & LUPU, D. (1968): Geological map of Romania, 1:200,000, Orăştie Sheet, Bucharest.

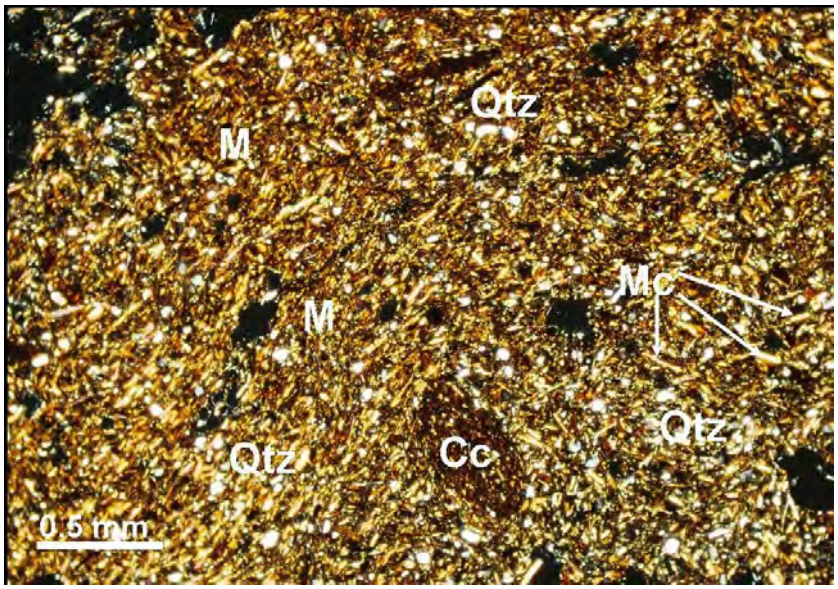

Fig.1. *Polarized light microphotograph of the Sarmizegetusa fine ceramics, composed of an anisotropic matrix (M), quartz (Qtz), micas (Mc) and ceramoclasts (Cc). P+.*

NANO- AND MICROTESTING OF HISTORICAL NOBLE METAL THREADS

GHERDÁN, K.[1]*, WEISZBURG, T.G.[1], JÁRÓ, M.[2], RATTER, K.[1], ZAJZON, N.[3], BENDŐ, Zs.[1], VÁCZI, T.[1], TAKÁCS, Á.[1], VARGA, G.[1] & SZAKMÁNY, Gy.[1]
[1] Eötvös Loránd University, Pázmány Péter sétány 1/C, H-1117 Budapest, Hungary
[2] Hungarian National Museum, Múzeum körút 14–16, H-1088, Budapest, Hungary
[3] Institute of Mineralogy and Geology, University of Miskolc, H-3515 Miskolc-Egyetemváros, Hungary
* E-mail: gherdankata@hotmail.com

Besides wearing gold jewels man has woven noble metal threads into textiles and used them for embroidering his clothes for thousands of years. The first written record on the use of golden metal threads comes, as far as we know, from the Old Testament (Exod.39:2–3). Obtaining information on the manufacturing technique of textile decorating metal threads can help us to date and define the provenance of textiles and provides data also on the history of technology (JÁRÓ, 2010).

Solid gold (or gold looking) metal threads are basically of two morphological types (strips and wires). Both types were applied "bare" or wound around a fibrous core, in most cases silk yarn. In the beginning they were made of pure gold or gold alloys, but later on gilt silver, gilt-silvered copper and other metal combinations were also used (JÁRÓ, 1990). In order to reconstruct the manufacturing techniques (e.g., the way of gilding) of these composite threads, it is important to determine their fine texture and the related chemical composition. However, due to the limited dimensions of the threads themselves (STRIPS: width 150–1500 μm, thickness 7–40 μm; WIRES: diameter 70–500 μm, typically) and to the extreme thinness of the coatings (dominantly 10–300 nm), it is difficult to prepare a proper cross-section by traditional cutting and polishing, while in most cases simple surface analysis is not sufficient (e.g., ENGUITA *et al.*, 2002; HACKE *et al.*, 2004).

We prepared cross-sections of a dozen of 14^{th}–17^{th} century gilt silver threads by focused ion beam (FIB) milling. These cross-sections, as well as the surface of the threads, were studied by a combination of several techniques (high-resolution SEM, EPMA, EBSD, micro-Raman). Nanotexture and nanoscale chemical composition of the silver base metal, morphology of the surface gold coating, geometry of the gold/silver interface, as well as the corrosion features of the threads were examined.

The *silver base metal* of the examined metal threads contains copper both in solid solution and in dispersed particles. Micrometer and sub-micrometer sized solid inclusions inherited from the silver base metal preparation could also be identified. These observations help the reconstruction of the original metallurgical processes.

The thickness of the *gold coating*s was directly measurable (maximum thickness: 395 ± 5 nm). Finger-like intrusions of gold into the silver base metal are characteristic for the drawn wires, while in samples where subsequent manufacturing had a strong vertical component (post gilding hammering, rolling) smooth or wavy gold/silver boundary line can be seen.

At the *gold/silver interface* no enrichment of elements indicating special gilding techniques was found (Cu: use of a copper-based soldering material, Hg: fire gilding).

Most of the samples are affected by *corrosion*. Corrosion progressed along the grain boundaries and resulted in depletion of copper and formation of pores. Inside the pores corrosion products (silver chloride, silver sulphide) could deposit.

Our data indicates that the examined historical metal threads were presumably gilt by welding (not by fire gilding or soldering). The phenomenon that strips are of elevated copper content compared to drawn wires might reflect intentional technological choice: the use of copper-enriched silver base metal rather than copper-based soldering material (see also JÁRÓ, 2010).

The strong nano- and microscale textural inhomogeneity demonstrated here shows FIB/SEM as an inevitable, routinely used technique when characterizing historical metal threads and their manufacturing techniques.

The European Union and the European Social Fund have provided financial support to the project under the grant agreements no. TÁMOP 4.2.1./B-09/KMR-2010-0003 and TÁMOP-4.2.1.B-10/2/KONV-2010-0001.

References

ENGUITA, O., CLIMENT-FONT, A., GARCÍA, G., MONTERO, I., FEDI, M.E., CHAIRI, M. & LUCARELLI, F. (2002): Nuclear Instruments and Methods, B189: 328–333.

HACKE, A., CARR, C.M. & BROWN, A. (2004): Proceedings of Metal, 415–426.

JÁRÓ, M. (1990): Gold Bulletin, 23(2): 40–57.

JÁRÓ, M. (2010): Fémfonalak az Esterházy-gyűjtemény textíliáin. In: PÁSZTOR, E. (Ed.): Az Esterházy-kincstár textíliái [Textiles of the Esterházy collection], Iparművészeti Múzeum: 56–66.

GEOCHEMICAL ASPECTS ON THE HIGH-TEMPERATURE SKARNS FROM ORAVIȚA (ROMANIA)

GHINEȚ, C.[1]*, MARINCEA, Șt.[1], BILAL, E.[2] & IANCU, A.M.[1]
[1] Geological Institute of Romania, 1 Caransebes Str., RO-012271, Bucharest, Romania
[2] Centre SPIN, Ecole Nationale Supérieure des Mines de Saint-Etienne, 158, Cours Fauriel, F-42023 Saint-Etienne Cedex 2, France
* E-mail: ghinet.cristina@yahoo.com

Beside the similar skarns from Cornet Hill, Măgureaua Vaței (Cerboaia Valley) and Ciclova (Țiganilor Brook), the Oravița–Crișenilor Brook skarn is one of the very few occurrences of high-temperature skarns in the world. It occurs at the very contact between a dioritic body of Upper Cretaceous age and carbonaceous sequences of Mesozoic age. The presence of a calcareous protolith favored the formation of the high-temperature calcium-silicate mineral species.

The studied skarns are dominated by the presence of gehlenite (up to 98% from the volume of the rock) associated with monticellite, grandites, ellestadite-(OH) and scarce spurrite. The late-stage metasomatic replacement of gehlenite by vesuvianite and clintonite is common as a result of late hydrothermal processes, as well as its replacement by some OH-silicate phases as hibschite, thomsonite, 11 Å tobermorite and allophane due to the late hydrothermal and weathering processes.

The chemical components of the system within which the pyrometasomatic processes took place are very numerous. In this case, according to the mineral species and the major elements analyses, they can be limited to the Si–Ca–Al, Si–Ca–Mg and Si–Ca–Fe geochemical systems. As it was expected, the inner skarn zone is described by the quartz-plagioclase-clinopyroxene system, characterized by the values of Al_2O_3 and TiO_2 in good agreement with the values of the same elements in the magmatic intrusion. The outer skarn zone can be assumed to a geochemically Al-poor and Si- and Mg-rich system. The extensive development of the garnet-vesuvianite skarn indicates an open thermodynamic system marked by a series of complex post-magmatic processes, which further leads to the formation of the silicate minerals with a more complex structure (e.g., clintonite and clinochlore).

MINERALOGY OF DIAMONDIFEROUS PALEOPLACER IN THE TIMAN, RUSSIA

GRAKOVA, O.V.
Institute of Geology, Komi Science Centre, Ural Branch of the Russian Academy of Sciences, Syktyvkar, Republic of Komi, Russia
E-mail: ovgrakova@geo.komisc.ru

Diamond-bearing terrigenous rocks in the north-east borderland of the East-European platform are located in the Timan ridge. Diamonds have been established in the Pizhma series of the mid-Devonian in the Middle Timan. The Pizhma series includes the polymineral diamondiferous paleoplacer "Ichet'yu" being the largest in the Timan. The series is made of brownish-grey quartz sandstones interlaid by gritstones and greenish-grey clays. The thickness of the series within the paleoplacer is 30 m. Its productive bed is represented by quartz gritstones and pebbly conglomerates. In spite of the long mineralogical study of this stratigraphical subdivision, there is still no answer to two important questions: 1 – whether the productive formations are sedimentary rocks; 2 – if the productive deposits of the Pizhma series are secondary accumulation, as it was traditionally thought, where is the source rock of Timanian diamonds?

Detailed lithological-stratigraphical, mineralogical, and geochemical investigations can help to answer the questions. The mineral composition of the heavy fraction consists of garnet, zircon, rutile, ilmenite, leucoxene, anatase, brookite, monazite, xenotime, ilmenorutile, columbite, chromite, tourmaline, staurolite, monoclinic pyroxene, and amphibole. Based on mineralogical description of the accessory minerals (KATELYA, 2007) one can conclude that most of them are allothigenous. This conclusion confirms the traditional opinion which regards the Ichet'yu diamond-bearing rocks, as sedimentary formations, in contrast to new ideas about their tuffisite genesis. The heavy fraction is rich in different minerals, indicating mixed provenance. Pyroxene and amphibole possess weak roundness in respect to transportation, thus the paleoplacer Ichet'yu is relatively close to a mafic source area, a possible provenance of diamonds. Taking into account the fact that terrigenous material came to the paleoplacer from the south-west, it is likely that buried massifs of diamond-bearing rocks are located in the Chetlass Kamen.

Reference

KATELYA (GRAKOVA), O.V. (2007): Minerals of diamond-bearing rock of the Pizhma series of the Middle Timan. The Syktyvkar mineralogical collection. Syktyvkar, № 35, p. 81–88. (Institute of Geology, Komi Science Centre, Ural Branch of the Russian Academy of Sciences. V. 122).

ZIRCON – "FINGER PRINTS" FOR SOURCE ROCKS: A CASE STUDY OF PALEOGENE VOLCANICS IN SW BULGARIA

GROZDEV, V.[1]*, PEYTCHEVA, I.[1], GEORGIEV, S.[1] & VON QUADT, A.[2]
[1] Geological Institute, Bulgarian Academy of Sciences, BG-1113 Sofia, Bulgaria
[2] Eidgenössische Technische Hochschule (ETH), Zurich, Switzerland
* E-mail: val.grozdev@abv.bg

CL imaging and LA-ICP-MS investigation of the zircon population in magmatic rocks provide geochronological and geochemical information about the age of the source rocks and their magmatic, metamorphic or sedimentary origin – the geodynamic setting of magma generation, and finally, the possible composition of the magmatic rock. We applied these techniques to constrain the time and source of the Tsarvaritsa body – a Paleogene volcanic rock with trachyrhyodacitic composition and characteristic coarse sanidine phenocrysts (up to 5 cm). This volcanic rock variety is dominant in the Ruen magmatic zone (MILOVANOV *et al.,* 2007). It crops out in SW Bulgaria with 5–10 km width and more than 50 km in length, striking 320° NW. The trachyrhyodacites have average SiO_2-content of 68.8 wt%, and total alkalis (Na_2O + K_2O) about 8.3 wt%. The K_2O prevails over Na_2O content and the rocks plot in the field of the high-K calc-alkaline magmatic series on the SiO_2 vs. K_2O diagram. The ORG-normalized patterns are characteristic for post-orogenic granitoids, and the REE-normalized values shows similarity with rocks formed in the continental crust.

The studied zircon population (30 grains) consists of mainly inherited old cores with magmatic overgrowths (15 grains), and one third of the population (9 grains) is magmatic Paleogene zircon crystal with fine magmatic oscillatory zoning. Only five of the zircons are xenocrysts (without Paleogene overgrows). LA-ICP-MS zircon dating defines an age of 32.01 ± 0.50 Ma for the magmatic zones and autocrystic grains. The inherited zircon cores and xenocrysts reveal ages in the range of 250–280 Ma (Lower Triassic-Permian) and 400–460 Ma (Lower Devonian-Ordovician).

The common crystallographic forms of the Paleogene zircons are S3, S4, S8, S9 type (according to the typological classification of PUPIN, 1980) with predominance of the {101} bipyramid over {211} and the {110} prism over {100}, respectively. The inherited zircons with 250–280 Ma age have predominantly {101} and {100} forms - types P1, P2, and for the 400–460 Ma old zircons the characteristic morphological types are L1, S1, S6 with bipyramid {211} and prism {110}.

Trace and REE elements were analyzed in three zircon groups: i) in the Paleogene zircons (32 Ma); ii) in the zircons with 250–280 Ma age; iii) and in the 400–460 Ma old zircons. The measured Zr/Hf ratio in all zircon varieties ranges from 36 to 40. The average Y content is 860 ppm (i), 670 ppm (ii), and 2100 ppm (iii), respectively. The Th/U ratio is > 0.4 in the three zircon subgroups. The REE-chondrite normalized patterns of the zircons with 32 Ma and 250–280 Ma age, are very similar with weak Eu-anomaly. The 400–460 Ma old zircons have one order higher HREE (from Gd to Lu) content and a deep Eu-anomaly.

The trace elements and REE content of the Paleogene and old cores/xenocrysts zircons indicate igneous origin of the source rocks on the base of Th/U ratio ≥ 0.4 (HOSKIN & SCHALTEGGER, 2003), as well as Ce-content less than 50 ppm (GRIFFIN *et al.,* 2002). Their Zr/Hf ratio (in the three zircon variety) is typical for crustal zircons. The Eu-anomaly in the REE-normalized pattern in all zircon types shows that during the formation of Paleogene and Upper Permian rocks the plagioclase was involved in the melt, while for the Lower Devonian rocks (400–460 Ma) the plagioclase was probably a stable phase. Moreover, based on the zircon morphology of the (400–460 Ma) old grains we may relate them to the granitoids of mainly crustal origin (PUPIN, 1980).

Acknowledgements. This research is made in the frame of running SCOPES IZ73Z0-128089 project of the Swiss National Fund.

References

GRIFFIN, W.L., WANG, Y., JACKSON, S.E., PEARSON, N.J., O'REILLY, S.Y., XU, X. & ZHOU, X. (2002): Lithos, 61: 237–269.

HOSKIN, P.W.O. & SCHALTEGGER, U. (2003): In: HANCHAR, J.M. & HOSKIN, P.W.O. (Eds.): Zircon. Reviews in Mineralogy & Geochemistry, 53: 27–62.

MILOVANOV, P. *et al.* (2007): Explanatory Note of the Geological Map of Bulgaria in Scale 1:50 000 (Map Sheet Kriva palanka – Kyustendil). Sofia, 57–58.

PUPIN, J. (1980): Contributions to Mineralogy and Petrology, 73: 207–220.

ENVIRONMENTAL RISK ASSESSMENT OF THE ABANDONED ASBESTOS MINE AT DOBŠINÁ, SLOVAKIA: A MINERALOGICAL APPROACH

GROZDICS, T.[1]*, TÓTH, E.[2] & WEISZBURG, T.G.[1]
[1] Department of Mineralogy, Eötvös Loránd University, Pázmány Péter sétány 1/C, H-1117 Budapest, Hungary
[2] Eötvös Museum of Natural History, Eötvös Loránd University, Pázmány Péter sétány 1/C, H-1117 Budapest, Hungary
* E-mail: tibor.grozdics@gmail.com

The Dobšiná chrysotile asbestos mine is located in the Spiš-Gemer Portion of the Slovak Ore Mountains, where chrysotile asbestos formed in the cracks of a small serpentinised basic-ultra basic magmatite body. The abandoned open-pit mine is about hundred meters to the north from the township Dobšiná. Due to the mining activity, serpentinites and serpentinite debris (waste dumps) crop out in an area of approximately 0.2 km^2. The former processing plant is situated in the eastern side of the township. The mine and the plant were formally opened in 1927. The asbestos mine closed in 1998, with no land rehabilitation. The surroundings of the plant are neglected, but seemingly contain no heaps of debris or process dust.

Asbestos fibres were extracted from the excavated serpentinite in the processing plant: the rock was first crushed and ground, the debris was separated according to grain size on a moving sieve-series, then the fibres were sucked up by air from the sieves. The residual "rock flour" was deposited in the mining area. The deposited serpentinite weighs approximately three million tons, and has roughly 2% residual asbestos content. PV-panels have been set up on part of the former mine area, and there are some plans for the utilization of the waste material, too: production of silica is in the experimental phase, and there was a proposal to use the waste material for CO_2 capture. The oldest waste heap, on the eastern edge of the mine, has been taken back by nature without human interference: a thin layer of soil developed, and a young forest grew up in the last few decades.

Currently, the mine area is the only possible source of asbestos, it may contaminate both air and runoff water. The present study is aimed at checking these possibilities, especially as the township is in the closest vicinity of the mine. Raw (original asbestos-content), ungraded (variable grain size) loose debris, and ground waste material are the major source of asbestos fibres, they are piled up on a stepwise slope with ca. 6–7 levels. We tried to trace the dissemination routes of the fibres.

The most common spreading track of asbestos fibres is the transportation by rainwater. Rainwater flowing down from the hilltop erodes asbestos fibres from the lose serpentinite debris and the rock flour, and transports them downwards, in the direction of the township. Between the levels, water created small channels on the slopes. At the end of the channels, when the surface becomes horizontal again, the rainwater slows down and deposits almost exclusively the fibres, creating a few millimetres thick asbestos mat that cracks like mud upon drying. At the lowermost part of the mine, water is collected in a little pond with overflowing possibility, in order to avoid major erosion of the debris. Further on, overflowing water is directed into a creek that already runs in an open concrete channel in the settlement centre.

At a lower level of the mine, blocks of a serpentinite clast-rich breccia were found, which probably formed at the tectonic emplacement of the serpentinite body. These ungraded, matrix-supported breccia blocks have sometimes fine-grained multi-layered crusts, consisting of mm-sized serpentinite clasts embedded in an asbestos matrix. These crusts are interpreted as the petrified varieties of the asbestos mats forming recently at the hillfoot, implying that the current sedimentation pattern (asbestos concentrating effect of water) occurred in the past, too.

Samples were taken from the rock flour (processed serpentinite debris with residual asbestos content), the unprocessed serpentinite debris containing lose bunches of asbestos, the recent asbestos mat, accumulating at the foot of the slopes and the petrified asbestos mat. Samples were first studied under the stereomicroscope, followed by SEM+EDX analysis and X-ray powder diffraction.

The recent mat consists in large part of asbestos fibres and a subordinate amount of clay minerals (chlorite, illite, talc) and quartz. It is practically free of serpentinite clasts. The petrified version is crack-free, hosts a lot of serpentinite debris and is subordinately cemented by calcite. Asbestos fibres are well bound both in the recent and the petrified mat, with low probability of the fibres becoming airborne. Therefore these natural asbestos concentrates have a low potential to contaminate the air with asbestos fibres. The lose bunches of asbestos on the surface can be a potential source of airborne fibres, air sampling is in progress to test this possibility. Overflow water samples are also under study, to check if asbestos fibres escape the mine area with the runoff waters.

FOCUSED ION BEAM STUDY ON MELT AND FLUID INCLUSIONS FROM KERIMASI VOLCANO, TANZANIA

GUZMICS, T.*, BERKESI, M. & SZABÓ, Cs.
Lithosphere Fluid Research Lab, Department of Petrology and Geochemistry, Institute of Geography and Earth Sciences, Eötvös L. University; Pázmány P. sétány 1/C, H-1117 Budapest, Hungary
* E-mail: tibor.guzmics@gmail.com

In this study we demonstrate applicability of focused ion beam-scanning electron microscopic (FIB-SEM) technique in melt and fluid inclusion research (BERKESI *et al.*, 2012; GUZMICS *et al.*, 2012). The samples studied are calciocarbonatite and pyroxene-nephelinite (afrikandite) from Kerimasi volcano, Tanzania. The rock-forming phases are abundant in primary melt and fluid inclusions. Our stepwise exposure technique (Fig. 1) allowed us to calculate the actual volume proportions of daughter phases in both melt and fluid phases inside the inclusions. This can uniquely help in determination of composition of bulk fluid system coexisted with the melts by combining our FIB-SEM results with that from Raman analyses.

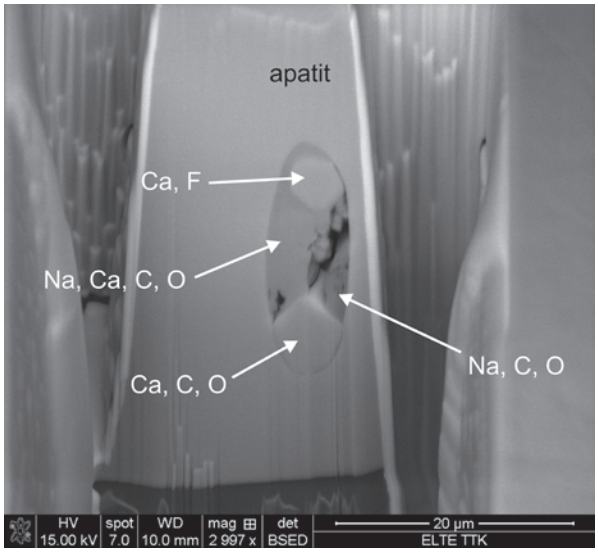

Fig. 1. *Focused-ion-beam-exposed carbonate melt inclusion in apatite from Kerimasi calciocarbonatite. Backscattered electron image.*

The FIB-SEM study shows presence of daughter phases in the carbonate melt and coexisted fluid inclusions, such as $(Ba,Sr)SO_4$, $NaHCO_3$, CaF_2, $(Na_2,Ca)(CO_3)$, Na_2SO_4 and NaCl. This suggests that the fluid, coexisted with the melt(s), was mainly consisting of components of Na, Cl, C, O, S and H. In contrast to previous fluid inclusion studies (e.g., BÜHN *et al.* 2003), our work suggests that fluids, derived from carbonate-rich igneous systems, are not capable in carrying rare earth and high field strength elements in a comparison with melts, but play important role in precipitation of late stage alkaline-rich phases, such as nahcolite, alkaline carbonates and alkali sulphates. Our study additionally demonstrates that FIB-SEM technique is powerful in studying daughter phases that are highly sensitive (e.g. use conventional polishing) and/or easily can alter due to humidity of air.

References

BERKESI, M., GUZMICS, T., SZABÓ, Cs., DUBESSY, J., BODNAR, R.J., HIDAS, K. & RATTER, K. (2012): Earth and Planetary Science Letters, in press: EPSL-D-11-01099.

BÜHN, B., SCHNEIDER, J., DULSKI, P. & RANKIN, A.H. (2003): Geochimica et Cosmochimica Acta, 67: 4577–4595.

GUZMICS, T., MITCHELL, R.H., SZABÓ, Cs., BERKESI, M., MILKE, R. & RATTER, K. (2012): Contributions to Mineralogy and Petrology, in press: DOI 10.1007/s00410-012-0728-6.

CHEMICAL CHARACTERISATION AND XRD STUDY OF ZIRCONOLITE FROM HÅKESTAD ALKALINE PEGMATITE, LARVIK PLUTONIC COMPLEX, SOUTH NORWAY

HAIFLER, J.* & ŠKODA, R.
Department of Geological Sciences, Masaryk University, Kotlářská 267/2, Brno, Czech Republic
* E-mail: haifler.j@mail.muni.cz

Zirconolite, ideally $CaZrTi_2O_7$, is a mineral that has been in focus in the past several decades due to its property to incorporate large amounts of actinides and lanthanides into its structure and due to its long-term chemical durability in the geological environment. Because of these properties, the doped synthetic phase analogous to zirconolite is one of the ingredients of SYNROC ceramics designed for the immobilization of the components of high-level nuclear waste. Depending on the content of radioactive elements and the geological age, zirconolite often undergo metamictization, transition from crystalline to partially or completely amorphous state. In the previous works, minerals with composition close to $CaZrTi_2O_7$ were called zirconolite, polymignite or zirkelite. Currently such polytypoids with fluorite type structure should be called zirconolite-2*M*, -3*T* or -3*O* depending on their symmetry. Zirkelite should be the cubic mineral with formula $(Ti,Ca,Zr)O_{2-x}$. However, the relationship between zirconolite polytypoids and zirkelite is not well understood yet.

We examined zirconolite from alkaline pegmatite in Håkestad quarry, Larvik plutonic complex in Norway. Zirconolite there forms euhedral black lathy crystals about 3 cm long with striated prismatic and pinacoidal faces. Associating minerals are mainly albite, K-feldspar, biotite, magnetite, britholite, zircon, pyrochlore, and nepheline. EPMA analysis gives analytical totals of 95.2 to 96.35 wt% for fresh parts. Mineral formula and Fe^{2+}/Fe^{3+} ratio was calculated on the basis of 4 cations and 7 anions, so in result near all the Fe seems to be in the ferrous form (about 7.3–7.8 wt% FeO against 0–0.9 wt% Fe_2O_3). The zirconolite is enriched in Y+REE, Nb, Ta and Fe and the resulting formula is as follows: $(Ca_{0.53–0.55}REE^{3+}_{0.33–0.35}Th_{0.07–0.08}U_{0.02–0.03})(Zr_{0.93–0.98})(Ti_{1.06–1.13}Nb_{0.35–0.40}Ta_{0.02}Me^{2+}_{0.47–0.52}Me^{3+}_{0.01–0.07})(O_{6.94–6.95}F_{0.05–0.13})$, where REE^{3+} includes Ce, Nd, Y, La dominating over Pr, Sm, Gd, Dy, Er, Yb; Me^{2+} includes most of Fe dominating over Mn, Mg and Me^{3+} includes small amounts of Fe^{3+} and Al. The reliable determination of the substitution vectors is complicated by very homogenous chemical composition, but the positive correlation of the Me^{2+} vs. Me^{5+}, Me^{2+} vs. REE^{3+} and Me^{5+} vs. REE could indicate substitution involving $REEZrMe^{5+}Me^{2+}O_7$ end-member. Zirconolite significantly enriched in $REEZrMe^{5+}Me^{2+}O_7$ molecule is described by DELLA VENTURA *et al.* (2000).

Some narrow zones along the rim or the cracks within the crystal were altered by penetrating hydrothermal fluid that significantly affected the chemical composition of these zones. The most distinct changes are the enrichment of SiO_2 (from nearly Si-free fresh parts increased to about 5–6 wt% SiO_2 in altered region), Al_2O_3 (increased from 0.14 to 0.27 wt%), WO_3 (increased from nearly W-free to 0.3–0.4 wt%), F (increased from 0.3 to 0.5 wt%) and the content of actinides and lanthanides is also relatively slightly higher in altered parts. The hydratation of the mineral is also probable. On the other hand there is a great loss of Fe (decreased from about 7.6 wt% FeO to about 1 wt%), quite distinct loss of Ca (decreased from 7 to 4 wt% CaO), Ti (decreased from 20.5 to 18 wt% TiO_2), Zr (decreased from 28 to 26.5 wt% ZrO_2), and lower disparities in Pb, Mg and Mn content. This behaviour during alteration is in agreement with published data (BULAKH *et al.*, 1998). The content of U, Th and Y+REE seems not to be significantly affected by the alteration.

The radiation dose the mineral have suffered calculated from the contents of ThO_2 and UO_2 assuming the geological age to be 295 Ma is about 2.0 to 2.8 • 10^{16} α decays per mg, which is one order more than the transition from crystalline to metamict zirconolite is usually occurred (LUMPKIN *et al.*, 1997, 1998). XRD study confirms its metamict state. The annealing of the zirconolite powder under an inert atmosphere to 800°C caused recrystallization to a phase with the cubic space group *Fm*3*m* and with the cell parameter a_0 = 5.104(3) Å that is close to the cubic ZrO_2 , tazheranite, ($CaTiZr_2O_8$) or zirkelite. This result is very similar to that which was gained by BULAKH *et al.* (1998), but their specimen was described as zirkelite because of its cubic morphology. During heating to 900°C another unidentified phase appeared.

References

BULAKH, A.G., NESTEROV, A.R., WILLIAMS C.T. & ANISIMOV, I.S. (1998): Mineralogical Magazine, 62: 837–846.

DELLA VENTURA, G., BELLATRECCIA, F., & WILLIAMS, C.T. (2000): Canadian Mineralogist, 38: 57–65.

LUMPKIN, G.R., SMITH, K.L. & GIERÉ, R. (1997): Micron, 28(1): 57–68.

LUMPKIN, G.R., SMITH, K.L., BLACKFORD, M.G., GIERÉ, R. & WILLIAMS, C.T (1998): Materials Research Society Symposium Proceedings, 506: 215–222.

UPPER CRETACEOUS–PALEOGENE DACITIC DYKES FROM IARA VALLEY (NORTH APUSENI MOUNTAINS, ROMANIA)

HAR, N., GRIGORAŞ, R.* & ZAHARIA, L.
Department of Geology, Babeş-Bolyai University, M. Kogălniceanu Street 1, Cluj-Napoca, Romania
* E-mail: albanu_81@yahoo.com

Upper Cretaceous–Paleogene magmatic rocks on the Romanian territory are located in two distinctive areas as the ophiolitic suture of the Apuseni Mountains: in Banat and in northern Apuseni Mountains. In the northern part of the Apuseni Mts., calc-alkaline plutonic and subvolcanic bodies, as well as volcanics, occur in different areas, as Bihor Mts., Vlădeasa Mts., Gilău Mts., Mezeş Mts., Chioarului Valley, etc. (ŞTEFAN *et al.*, 1988, 1992). In Apuseni Mts., the magmatic activity was the result of westward subduction of the oceanic lithospheric plate from the western Tethys Basin beneath Preapulian Craton during Mesozoic time, into an active continental margin tectonic setting (SĂNDULESCU, 1984; HAR, 2001).

The studied intrusive magmatic bodies mostly dacites, occurring as dykes up to 5–6 m in width located in the Iara Valley (Gilău Mts.). Under the microscope they show a porphyritic texture with microgranular groundmass. Mineralogically, they consist of quartz, plagioclase feldspar, biotite and hornblende as primary minerals. They are intensively altered (except quartz) and secondary phases as chlorite, sericite, epidote and clay minerals are present in secondary assemblages replacing the primary minerals.

Seven samples of volcanics were analyzed for major, trace and rare earth elements. Silica (SiO_2) content ranges from 53.1–64.9 wt%, the most weathered sample having the lowest value. An intense hydrothermal alteration resulted very elevated LOI values (1.80–8.48 wt%). The MgO content is low and varies between 1.64–4.60 wt%, while the Al_2O_3 content ranges from 14.66–16.28 wt%. According to the total-alkali vs. SiO_2 classification, six of the analyzed samples are dacite while one is trachyandesite. The trachyandesite composition could be either the result of fractional crystallization trend or of the alteration processes. The calculated AFM parameters show a typical calc-alkaline trend of the magmatic rocks from Iara Valley (Fig. 1a).

A chondrite-normalized trace elements diagram (Fig. 1b) shows a negative Nb anomaly relatively to the U and La, a feature of subduction-related magmas. A similar tectonic setting is indicated by the enrichment of the large ions lithophile (Rb, Ba, Sr), while Th/Hf and Ta/Hf values are typical for active continental margins. Chondrite-normalized REE patterns of the analyzed samples are very similar, with enrichment of the LREE as compared with HREE, suggesting that magmas proceeded from a primary source affected by a low degree of partial melting.

References

HAR, N. (2001): Andezite bazaltice alpine din Munţii Apuseni, Cluj-Napoca, 214 p.

IRVINE, T.N. & BARAGAR, W.R.A. (1971): Canadian Journal of Earth Sciences, 8: 523–548.

SĂNDULESCU, M. (1984): Geotectonica României, Bucharest, 336 p.

ŞTEFAN, A., LAZĂR, C., BERBELEAN, I. & UDUBAŞA, Gh. (1988): Dări de Seamă ale Institutului de Geologie şi Geofizică., 72–73(2): 195–213.

ŞTEFAN, A., ROŞU, E., ANDĂR, A., ROBU, L., ROBU, N., BRATOSIN, I., GRABANI, G., STOIAN, M. & VĂJDEA, E. (1992): Romanian Journal of Petrology, 75: 97–115.

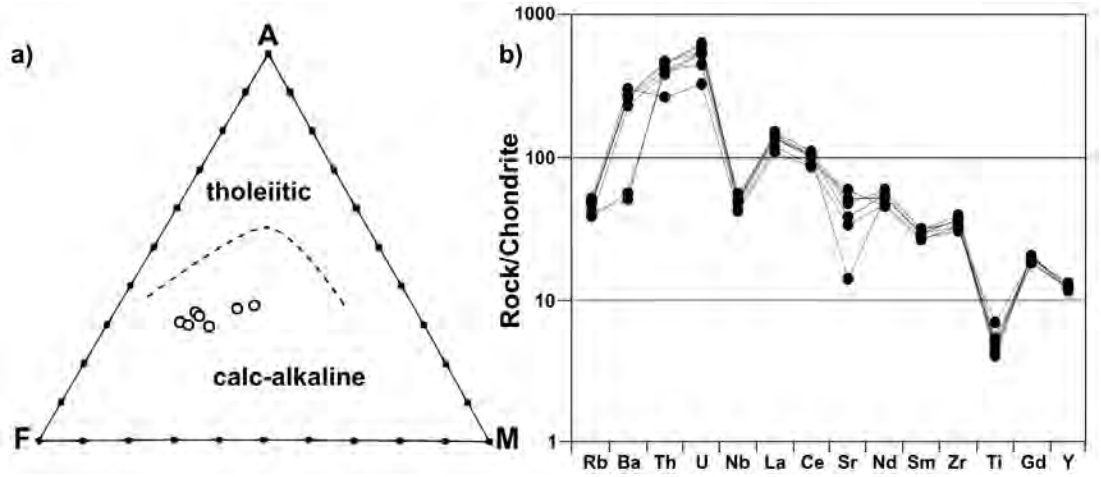

Fig. 1. a) *Calc-alkaline features in AFM diagrams (IRVINE & BARAGAR, 1971) and* ***b)*** *Chondrite-normalized trace elements diagram of the dacitic dykes from Iara Valley.*

ABANDONED CHRYSOTILE ASBESTOS MINES IN SERBIA: AN ENVIRONMENTAL MINERALOGICAL STUDY

HARGITAI, A.[1]*, TÓTH, E.[2], VASKOVIĆ, N.[3], MILOŠEVIĆ, M.[4] & WEISZBURG, T.G.[1]
[1] Department of Mineralogy, Eötvös Loránd University, Pázmány Péter sétány 1/C, H-1117 Budapest, Hungary
[2] Eötvös Museum of Natural History, Eötvös Loránd University, Pázmány Péter sétány 1/C, H-1117 Budapest, Hungary
[3] Dept. of Petrology and Geochemistry, Faculty of Mining and Geology, Belgrade Univ., Djusina 7, Belgrade, Serbia
[4] Department of Mineralogy and Crystallography, Faculty of Mining and Geology, Belgrade University, Djusina 7, Belgrade, Serbia
* E-mail: anna.hargitai@gmail.com

Asbestos is an industrial term for a group of silicate minerals, and as such, asbestos is a component of the natural environment. In addition, mankind has been using asbestos minerals for a few thousand years as industrial raw materials. Since the end of the 19th century, it has been inserted in large quantities into our built environment. As the health risks associated with the inhalation of asbestos fibres became evident in the second half of the 20th century, all asbestos types (chrysotile and five amphiboles) were classified as carcinogenic. Most developed countries have banned the use of asbestos and continue to remove them from the built environment.

Recently, natural asbestos outcrops draw increasing attention due to the potential health risks associated with them. The risk is primarily manifested in that fibres may become airborne and inhalable. Large-surface and disturbed outcrops, such as abandoned and non-rehabilitated asbestos mines, have the highest air contamination risk. Two such mines have been selected for study: Korlaće and Stragari in Serbia. Both mines produced the least dangerous chrysotile asbestos by open-cast mining. Asbestos extraction was performed near the mines, and the processed serpentinite debris was deposited in huge piles (waste dumps) in the mining area, still having a few percents residual asbestos content.

In Korlaće, classic cross-fibre chrysotile was mined, while in Stragari the leather asbestos variety was mined and in subordinate amount, dark green splintery antigorite is present, too. We sampled the asbestos types, the waste material and the air (MCE filters were used for phase contrast microscopy (PCM) and gold filters for comparative SEM+EDX studies).

At Korlaće, on the waste dumps, 0.4 fibre/dm^3 concentration (PCM; Hungarian background permissible limit: 1 fibre/dm^3) was measured during dry, windy weather. Dust formation was found to be insignificant. Potential air contamination may arise if the spoil material is disturbed (by move or re-use). This process is being tested by lab experiments. On the comparative gold filter sample, gypsum particles in the asbestos size range were detected, and a bunch of blue asbestos (riebeckite) was found, too, probably originating from corrugated asbestos cement roofing. According to our results, the host rock contains all the three serpentine varieties, namely chrysotile, antigorite and lizardite, and constant iron content is typical of them (0.05–0.1 *a.p.f.u.*).

The former processing plant is located in the mine area, and towards the end of its operation, it was not cleaned regularly, so that the finest-grain dust accumulated in vast quantities inside the plant buildings. This dust is composed of serpentinite fragments and a few percents of asbestos fibres, "indoor" air sampling (MCE filter, phase contrast microscopy) yielded 14 fibre/dm^3 concentration (above the Hungarian asbestos removal efficiency limit, 10 fibre/dm^3). When dismantling the building, this dust needs to be collected first, in order to avoid large-scale asbestos fibre release into the air. Fibre release from unprocessed serpentinite blocks is not probable in large quantities, as the outcrop of fresh chrysotile veins is negligible in the mine yard.

In Stragari, the mine yards are dominantly covered with serpentinite debris, while the fine-grained processed waste material is deposited in huge piles, closer to the village, along the way. The ground waste material is still used by local potters as temper in jars and bricks. The processing plants are now largely dismantled and do not contain fine-grained serpentinite dust any more. The factory where asbestos paper and asbestos plate were once manufactured, was last used for the production of recycled paper, therefore its surroundings are clear of asbestos, too. Approximately 1 km to the north-east of the mine, a reservoir basin of 400 m diameter hosts the production sludge of asbestos paper and plate production. In the past 30 years, since not in use, soil formation has started on the surface, and the area is partly covered with trees and shrubs. According to the mine manager, plans are already outlined for the utilisation of the waste material for silica gel production.

Fibres of the Stragari leather asbestos cling strongly together, therefore have a low potential to become airborne, even in the case of the processed material. The green, macroscopically splintery antigorite weathers to asbestos-sized fibres, too, therefore may present additional health risk. PCM of air samples (sampling in dry, windy weather) yielded low airborne fibre concentrations: 0.3–1 fibre/dm^3 at the waste piles and 0.5 fibre/dm^3 in the mine yard. At this site, the application of TEM for air filter analysis is suggested, for the proper discrimination between antigorite and chrysotile fibres, both having some iron content (0.06–0.09 *a.p.f.u.*).

Nb, Ta, Ti, REE(Y), Zr, Sn, Th, U OXIDES FROM GRADISTEA DE MUNTE RARE ELEMENT MINERALS OCCURRENCE, SEBES MTS., ROMANIA

HIRTOPANU, P.[1]*, ANDERSEN, J.C.[2], FAIRHURST, R.J.[2], LUDUSAN, N.[3] & JAKAB, Gy.[4]
[1] University of Bucharest, Romania; [2] University of Exeter, Camborne School of Mine, UK; [3] 1 Decembrie 1918 University, Alba Iulia, Romania; [4] I.G. Mineral, Gheorgheni, Romania; * E-mail: paulinahirtopanu@hotmail.com

The Gradistea de Munte (GM) rare element minerals occurrence is situated in the north of the Sebes Mts., Southern Carpathians, in the upper course of the Orastie River. Geologically-structurally the GM area consists of the amphibolite facies rocks of the Upper Proterozoic Sebes-Lotru Series of the Getic Crystalline. The most important host rock of the mineralization is a quartz-microcline-albite gneiss/"granite". Sometimes the rocks being formed only from microcline, albite, some phlogopite/biotite and accessory rare minerals, quartz is missing. Cyrtolite/zircon and magnetite are always present as ore/mineral components of the rock. The rare earth element mineralization is represented by carbonates, oxides, silicates and phosphates, in veinletes and nests of mm to cm size grains. The REE oxides in GM belong to 7 groups: **pyrochlore, fergusonite, columbite, "ilmeno-struverite", baddeleyite**, **cassiterite** and **thorianite-uraninite**. **1. Pyrochlore group** has 3 subgroups**. A. Pyrochlore subgroup** with the major B-site cations (Nb + Ta) > Ti and Nb > Ta, comprises **pyrochlore, yttropyrochlore-(Y), uranpyrochlore, plumbopyrochlore** and **thoriopyrochlore**, defined by the cations residing in A-site. The GM **pyrochlore** has (Ca,Fe,U,Th) > 20% in A-site, $Nb_2O_5 \approx 50\%$ and $Ta_2O_5 \approx 2–10\%$. **Yttropyrochlore-(Y)** contains beside dominant Y (≈ 15–20 wt% Y_2O_3) in A site some oxides of Ce, Nd, Dy, Gd, Yb≈(10 wt%). The Nb_2O_5 content varies between 40–50 and Ta_2O_5 between 1–2 wt%. It always contains some UO_2 and ThO_2, thus metamictisation being very common. In addition, yttropyrochlore-(Y) has some SiO_2 content, common in metamictic and late stage hydrated pyrochlores. Yttropyrochlore-(Y) is the best widespread term of pyrochlore. **Plumbopyrochlore** has (Pb,Ca,U) > 20% in A site, Nb_2O_5 = 46.5 and Ta_2O_5 = 18.5 wt%. **Uranpyroclore** has UO_2 dominance in A site (= 13–25%) with some $Ln_2O_3 \approx 4$, Ca + Ba ≈ 10, Y_2O_3 = 1.5–6 and ThO_2 = 2 wt%. Its Nb_2O_5 content varies between 30–50 and Ta_2O_5 between 10–15 wt%. It is omnipresent as few mm to cm size grains in all types of rocks/ores from GM. In transmitted light it is light red, yellow orange, red. It contains some ZrO_2 (≈ 2 wt%), being associated with cyrtolite. Like yttropyrochlore, it has high SiO_2 content (7–10 wt%). The GM **thoriopyrochlore** is Th dominant with some Y, and Fe in A site. The ThO_2 content is very high, around 40 %wt. It contains OH and clorine≈(0.6 wt%) in *Y* site. It is associated with thorite and thorogummite. **B**. **Microlite subgroup** ($Ta_B \geq Nb_B$, Nb + Ta > 2Ti) comprise the **uranmicrolite,** with $Nb_2O_5 \approx 30$, $Ta_2O_5 \approx 48.5$, $UO_2 \approx 14.6$ wt%, **thormicrolite** with $Nb_2O_5 \approx 19$, $Ta_2O_5 \approx 25$, $ThO_2 \approx 48$ wt%, and **yttromicrolite** with $Nb_2O_5 \approx 22$, $Ta_2O_3 \approx 25$ wt%, having U, Th, respectively Y in A site > 20%. **C**. **Betafite subgroup,** $B = 2Ti_B \geq (Nb + Ta)_B$, in GM is represented by the occurrence of **betafite** (U > 20% in A site) and **yttrobetafite-(Y)** (Y > 20% in A site). The last one occurs as big grains of up to 1 cm. The chemical composition of yttrobetafite-(Y) varies: TiO_2 = 27–30, Y_2O_3 = 15–22, Nb_2O_5 = 22–27, Ta_2O_5 = 7–19, ThO_2 = 5–10, UO_2 = 4–6 wt%. Some yttrobetafite-(Y) grains have a very Ta-rich composition: Ta_2O_5 = 31.2, Y_2O_3 = 28.8, TiO_2 = 36.0 wt% and they do not contain Nb_2O_5. Compositional zoning was visible from yttrobetafite-(Y) inside to **Ta-yttrobetafite-(Y)** outside in a grain. **2**. The **fergusonite group** contains the **fergusonite-(Y)** with Nb_2O_5 = 45–58, Y_2O_3 = 25–35, $Yb_2O_3 + Gd_2O_3 + Dy_2O_3 \approx 4.5$ wt% and very little Ta_2O_5, with maximum 5 wt% UO_2 and ThO_2 content. The grains of fergusonite-(Y) are zoned with **formanite-(Y),** which has Y_2O_3 = 34.6, Ta_2O_5 = 48.2 wt% and little CaO, FeO and ThO_2. Another grain has Y_2O_3 = 36.15, Ta_2O_3 = 45.72, Ce_2O_3 = 5.17 and CaO = 4.43 wt% composition. The same grain could be built up from many phases, corresponding to yttropyrochlore-(Y), yttromicrolite-(Y), formanite-(Y) showing the Ta increase. **3. Ferrocolumbite** has: FeO = 16.2, MnO = 3.03, Nb_2O_5 = 72.8, Ta_2O_5 = 4.2, TiO_2 = 3.5 wt% and **manganocolumbite** has Nb_2O_5 = 76.28, MnO = 10.93, FeO = 0.44, TiO_2 = 0.8 wt%. Some grains have high UO_2 content of up to 8.4 wt%. The composition of some grains are (Y_2O_3 + FeO + MnO) > 20 wt%, high Nb_2O_5 (> 65 wt%) some Ta_2O_5 and no TiO_2 which could belong to **yttrocolumbite. 4**. **"Ilmenorutile"** has: TiO_2 = 49.5–52.5, Nb_2O_5 = 21.8–26.5, Ta_2O_5 = 7.7–13.31, FeO = 9.4–12.03 wt%, showing a solid solution with **"struverite"**. **5**. **Baddeleyite** appears to be one of the oldest minerals, older than cyrtolite and its presence indicates that the first mineralized solutions were subsaturated in silica. Its composition shows only ZrO_2 with some ThO_2 and very little HfO_2. **6. Cassiterite** appears as big cm grains in hydrothermal veinlets and has little U, Th and Fe in its composition. **7**. **Uraninite** and **thorianite,** usually form solid solutions with the composition UO_2 = 49.1, ThO_2 = 48.0 wt%. Separately, uraninite has composition: $UO_2 \approx 96.6$ wt% with little ThO_2, Y_2O_3, PbO, FeO, and thorianite has ThO_2 = 96.3, PbO = 3.27, FeO = 0.23, SiO_2 = 0.16 wt%. Generally, the content of Nb + Ta in all rare minerals is higher than that of Y + REE, and the Y content is much higher than Ce. Also, the Th content is much higher than U. The zirconium has the highest content.

BARIUM MINERALIZATION WITHIN THE TULGHEŞ GROUP, EAST CARPATHIANS, ROMANIA

HIRTOPANU, P.[1]*, SCOTT, P.W.[2], ANDERSEN, J.C.[2], FAIRHURST, R.J.[2], CHUKANOV, N.V.[3], JAKAB, Gy.[4] & PETRESCU, L.[1]

[1] University of Bucharest, Romania; [2] University of Exeter, Camborne School of Mine, UK; [3] Institute of Problems of Chemical Physics, Russia; [4] I.G. Mineral, Gheorgheni, Romania; * E-mail: paulinahirtopanu@hotmail.com

A Ba mineralization, less known than the Mn and sulphide ones, also is situated in the Cambrian Tulgheş Group (TG) extending over more than 200 km. The Mn belt is situated at the bottom and the sulphide belt on the top of TG. The Ba mineralization is present in the whole TG together with both Mn and sulphide belts. It has a large development of about 10 km at the crossing of two belts Holdita-Paraul and Caselor-Brosteni-Borca, with the same orientation (NW-SE), like the Mn and sulphide ores. The mineralogy of TG is simple and uniform being made up generally of five major minerals in variable proportions: quartz, muscovite albite, chlorite, Ca-Mg-Fe-carbonates (± graphite ± titanite ± rutile ± stilpnomelane ± ilmenite ± magnetite ± pyrite). Its huge thickness is due to its developmental history in a narrow deep, active subduction zone. The rocks of TG are metamorphosed under greenschist facies and display a pronounced schistosity, having some similarities with that of burial metamorphism. During metamorphism, the wall rocks were tidily folded and microsheared. VODA & VODA (1980) have described the Holdita-Brosteni syngenetic barite ore deposit, as conformable beds within the metamorphic formation of the black quartzites of the TG. The lithostratigraphical sequence with Ba mineralization of about 80–120 m comprises on the bottom, a lens of Mn ore and on the top, a barite lens banded by sulphide ore. The **barite** ore contains **Ba-feldspars** (celsian, hyalophane), **cymrite, barytocalcite, benstonite**, **aragonite, witherite**, phlogopite, sericite, diverse carbonates and quartz. Pyrite, and other sulphides, including sphalerite, bornite, galena, chalcopyrite, tetrahedrite-tennantite also occur. **Alabandite,** sometimes associated with **pyrochroite** also occurs in the Mn belt, in reduced tephroite parageneses. The Mn belt also contains other Ba minerals, including celsian, hyalophane, barite and cymrite as accessory minerals. This indicates a genetic link between the Ba and Mn mineralization, which is suggested to have formed by the same submarine hydrothermal process on the Cambrian sea floor. The lenses of Mn-carbonate-silicate ore are closely interbedded with barite ore. This close interbedding of barite, Mn and sulphide ores demonstrates their common origin and evolution. Barite is the main barium mineral (more than 70%) of these deposits, having isometric grains of 0.5 mm diameter and more, forming compact, grainy aggregates from several cm to 4 m. In the Holdita deposit, the late barite replaces the earlier Ba-feldspars. The Holdita barite contains: BaO = 65–77%, SO_3 = 33–19%, and SrO = 3–4%. There is some isomorphism with celestine. The hydrothermal activity (like springs) began on the Cambrian seafloor, where the Mn ores were deposited and mixed with little barium mineralization in the distal zones. In the southern area, the barium is predominant, where it is mixed with some Mn and sulphide mineralization. The Ba-feldspars occur in crystals ranging from a few mm to 1 cm and even larger, forming thin layers interbedded with other enriched layers of barite, apatite, sulphides (mostly pyrite, but also alabandite, chalcopyrite occur). Celsian is the predominant Ba-feldspar. Hyalophane is very rare. The primary substitution is between BaAl and KSi series ($KAlSi_3O_8$–$BaAl_2Si_2O_8$) seems to be continuous. However exsolutions of hyalophane in celsian in the same grain shows a compositional gap between the two minerals on the BSE images from Holdita deposit. The celsian contains over 90% $BaAl_2Si_2O_8$ component (Cn), whereas hyalophane contains under 30% Cn, consistent with the presence of a substantial compositional gap. The Ba feldspars are replaced by barite and by cymrite plates (HIRTOPANU *et al.*, 2008). The relics of celsian in cymrite may have escaped the reaction because locally P_{H2O} may have been lower than P_{fluid}, and when P_{H2O} was higher than P_{fluid}, celsian did not form. The real situation could be more complex kinetically, *e.g.* the substitution process could be not completed because its speed was too low, or because the activity of H_2O decreased. The coexistence and phase relations between celsian and cymrite are of great petrological interest being a natural example of the experimentally established reaction curve, celsian + H_2O = cymrite (ESSENE, 1967). The lineally developed Ba, Mn and sulphide mineralization belts evolved in a subduction zone of the Cambrian sea floor, in a narrow active paleotrench area. The hydrothermal submarine activity began with Mn ore with little Ba in the North and more Ba and little Mn in the South. Later, in the upper Cambrian, the sea floor was subducted towards the East and sulphides were deposited at some distance from, and over the Mn ore containing body.

References

ESSENE, E.J. (1967): American Mineralogist, 52: 1885–1890.

HIRTOPANU, P., ANDERSEN, J.C., CHUKANOV, N. & PETRESCU, L. (2008): Romanian Journal of Mineral Deposits / Romanian Journal of Mineralogy, 83: 58–61.

VODA, A. & VODA, D. (1980): Dări de Seamă ale Institutului de Geologie şi Geofizică, 67(2): 233–246.

BRONZE AGE CERAMICS AND SLAG FROM THE LĂPUŞ NECROPOLIS (NW ROMANIA)

HOECK, V.[1]*, IONESCU, C.[2], METZNER-NEBELSICK, C.[3], NEBELSICK, L.D.[4] & KACSÓ, C.[5]
[1] Dept. of Geography and Geology, Salzburg University, 34 Hellbrunner Str., A-5020 Salzburg, Austria
[2] Dept. of Geology, Babeş-Bolyai University, 1, Kogălniceanu Str., RO-400084 Cluj-Napoca, Romania
[3] Ludwig Maximilian University, Munich, Germany
[4] Cardinal Stefan Wyszynski University, Warsaw, Poland
[5] County Museum, Baia Mare, Romania
* E-mail: volker.hoeck@sbg.ac.at

The Bronze Age (13^{th}–12^{th} century BC) necropolis and cult area from Lăpuş is situated in NW Romania. Large amounts of potshards as well as scattered slag pieces were found in a multi-phased cult building in the center of the necropolis as well as in burial mounds. The ceramic shards are interpreted as intentionally destroyed vessels during funerary celebrations as an act of ritual violence. The potshards display a large range of colours (from creamy, orange or red, to grey or black) and fabrics (from coarse to semifine, rarer fine). Signs of burning, such as cracked black surface, partial melting and deformed shape, are not uncommon. For comparison and provenance study, samples of soil and daub, ceramics and slag were mineralogically and chemically analyzed by optical microscopy, electron microprobe (EMPA) and ICP-MS.

Here we will focus on the chemical similarities and differences among these categories, i.e. "clay" (including soil and daub), slag and ceramics. Questions which should be addressed by chemical investigation include the relation between ceramics and slag: is the slag over-fired ceramics or clay, or a completely different material? Is the local soil ("clay") the raw material for the ceramics?

Variation diagrams among several major element oxides and SiO_2, on a LOI-free basis, show a wide range of SiO_2 for the whole data set, from 60–82 wt%, suggesting a continuous transition from ceramics (60–77 wt%) over slag (71–76 wt%) to clays (74–82 wt%). The increasing SiO_2 is combined with a continuous decrease of Al_2O_3 and Fe_2O_3, and some increase of Na_2O. On the first sight this would suggest a genetic relationship among clay, slag and ceramics. The similarity of REE and some spider diagrams point in the same direction.

However, the distribution of other major and trace elements shows clear differences. For example, TiO_2 displays a weak negative correlation with increasing SiO_2 for ceramics and slag but significant higher contents for clays. Equally, trace elements such as Zr, Hf and Yb are substantially higher in the clay group compared with the others. The SiO_2 content of the slag on the other hand is lower than in the clays and in the same range as in the ceramics. The MgO is slightly higher at a given SiO_2, the K_2O and CaO increase significantly. Additionally, Zr and Hf are higher in slag than in ceramics. The clays finally are relatively low in SiO_2 but rich in Al_2O_3 and Fe_2O_3. MgO, K_2O and CaO are relatively depleted compared to the slag. On the other hand, the ceramics are enriched in transition elements such as V and Sc, relative to slag and clays. In terms of mineralogy, the difference between ceramics and slag can be explained by a higher content of Ca-rich and K-rich feldspars in the latter, while the former are dominated by illitic clay. Chemically, this difference is expressed by higher K_2O/Al_2O_3 ratios and CaO/Al_2O_3 ratios in the slag, compared with the ceramics.

Despite some undisputable similarities in the chemistry of all three groups, the compositional difference excludes a genetic relation among them. For example, mixing of the clays with the raw material of ceramics and slag is not feasible. Also the source material of ceramics and slag is significantly different ad characterized by an increase of feldspar content in the slag raw material. Summarizing, the clay found at the site was neither used for manufacturing the ceramics nor for the items which became later on slag. Both were manufactured from different materials, most likely at some other places but in the same area.

Acknowledgements. The study was supported by DFG Program granted to C.M.-N. and ID-2241/2008 and PN-II-ID-PCE-2011-3-0881 projects, granted to C.I. (Romanian Ministry of Education and Research).

PETROGRAPHIC CHARACTERISTICS OF THE MAGMATIC ROCKS OF DILJ MT. (SOUTHERN PART OF THE PANNONIAN BASIN, CROATIA)

HORVAT, M.* & SLOVENEC, Da.
Croatian Geological Survey, Department of Geology, Sachsova 2, 10 000 Zagreb, Croatia
* E-mail: mhorvat@hgi-cgs.hr

Dilj Mt. (Croatia) is situated in the southernmost part of the Pannonian Basin. During the 20th century several researchers worked in this area (e.g. KOCH, 1917; ŠPARICA & CRNKO, 1973 and MALEZ & TAKŠIĆ, 1977). According to the Basic Geological Map 1:100 000 (ŠPARICA, 1986) albite rhyolites and metaandesites occur as an elongated, partially disintegrated body, with tectonic and/or covered contact with Middle and Upper Miocene and Early Pliocene sedimentary deposits. PAMIĆ & ŠPARICA (1988) presented a petrological study of volcanic rocks from the area assuming their Badenian age. BELAK *et al.* (1991) described the appearance of Badenian rhyolitic volcanoclastic rocks from middle parts of Dilj Mt. Detailed geological mapping in 1:50 000 scale on Dilj Mt., beside acid and intermediate volcanic rocks, revealed basic varieties of magmatic rocks.

This work presents basic results regarding magmatic rocks of Dilj Mt. in general. The most frequent igneous rocks on Dilj Mt. are acid volcanic rocks while the basic rocks present sporadically. HORVAT *et al.* (2011) gave preliminary petrographical and geochemical report about the acid volcanism. Basic magmatic rocks are represented by volcanic rocks and vein or dyke (?) of hypabyssal rocks. The contact between the basic hypabyssal and acid volcanic rocks is sharp and does not show chilled ("frozen") margins. Basalt fragments are detected with fragments of Upper Cretaceous bioclastic limestones (Scaglia type) in tectonic breccias. Furthermore, field investigations have not confirmed an active igneous contact of acid and intermediate volcanites with surrounding Badenian sediments. All of the above, as well as finding of centimetre to decimetre pebbles of acid volcanites within the Badenian and Sarmatian deposits (KOVAČIĆ *et al.*, 2011) suggest that the studied magmatic rocks of Dilj Mt. are most probably older than Badenian.

Acid and intermediate volcanic rocks, rhyolites and andesites, are light green to green-gray in colour. They are microcrystalline with aphyric to porphyritic texture. The structure is homogeneous or vesicular. The main composition is uniform and consists of: quartz + albite and/or peristerite + K-feldspar ± pyroxene + secondary minerals (chlorite, epidote, illite, calcite). Feldspars occur as phenocrysts (up to 2.5 mm) and as groundmass microlites (0.1 to 0.4 mm). They are affected by sericitization and chloritization. The groundmass is cryptocrystalline, holocrystalline or hypocrystalline. Microlites are sometimes radially arranged. Polymorphic modifications of SiO_2 filled up vesicles.

Mafic magmatic rocks are basalts and microgabbros (dolerites). Basalts have relict-ophitic and arborescent textures and homogeneous structure. Prismatic plagioclase grains are uniform in size (0.7 mm). The groundmass is a mixture of very fine-grained mineral crystals (pyroxene (?), chlorite and epidote) and volcanic glass. Cracks are filled with calcite. Microgabbro has a grained texture and homogeneous structure. The main mineral constituents are coarse grained prismatic basic (?) plagioclase grains moderately sericitized and chloritized and affected by albitization along the edges. Among them there are relatively large (1.1 to 1.9 mm) hypidiomorphic primary (?) amphiboles represented by pale green chloritized hornblende.

The investigated rocks with the SiO_2 content ranging from 73.32 to 76.62 wt.% and from 55.46 to 63.29 wt.%, according to PEACOCK (1931) and WINCHESTER & FLOYD (1977), are classified as middle- to high-Si rhyolites to rhyodacites and trachyandesites, respectively. However, according to the relationship of Nb/Y vs. $Zr/TiO_2 \times 0.0001$ some samples are classified as subalkalic basalts, while the hypabyssal samples in the TAS diagram for plutonic rocks (WILSON, 1989) are positioned in the gabbro field.

References

BELAK, M., SARKOTIĆ-ŠLAT, M. & PAVELIĆ, D. (1991): Geološki vjesnik, 44: 151–159.
HORVAT, M., SLOVENEC, Da. & SLOVENEC, Dr. (2011): The 4th International Workshop on the Neogene from the Central and South-eastern Europe, Banská Bystrica, Slovak Republic, 16–17.
KOCH, F. (1917): A Magyar Királyi Földtani Intézet Évi Jelentése az 1916. évről, 702–710.
KOVAČIĆ, M., HORVAT, M., PIKIJA, M. & SLOVENEC, Da. (2011): Geologia Croatica, 64(2): 121–132.
MALEZ, M. & TAKŠIĆ, A. (1977): Tla Slavonije i Baranje, 235–256.
PAMIĆ, J. & ŠPARICA, M. (1988): Bulletin de Academie Serbe des Sciences et des Arts, 28: 47–56.
PEACOCK, M.A. (1931): Journal of Geology, 39: 54–67.
ŠPARICA, M. (1986): Osnovna geološka karta 1:100 000, list Slavonski Brod. Inst. za geol. istraž., Zagreb, Inst. za geol., Sarajevo, Sav. geol. zavod, Beograd.
ŠPARICA, M. & CRNKO, J. (1973): Geološki vjesnik, 26: 83–92.
WILSON, M. (1989): Igneous petrogenesis. Unwin Hyman, London, 465 p.
WINCHESTER, J.A. & FLOYD, P.A. (1977): Chemical Geology, 20: 325–343.

THE MORPHOLOGY OF CRYSTALLINE PHOSPHOGYPSUM FROM ROMANIA

IANCU (CARAVETEANU), A.M.*, DUMITRAS, D.G., MARINCEA, Şt., ANASON, A.M. & GHINEŢ C.
Department of Mineralogy, Geological Institute of Romania, 1 Caransebeş Str., RO-012271 Bucharest, Romania
* E-mail: aurash83@yahoo.com

Phosphogypsum is a secondary technogenic product of the acid phosphate fertilizer industry, derived from phosphate rock during the production of phosphoric acid. Phosphate rock mainly composed of apatite, originating from Morocco, Russia, Syria, Jordan and India, is treated with concentrated sulfuric acid (96%), after fine crushing to supra colloidal size and passing into an aqueous solution of phosphoric acid. The solution is recirculated to produce gypsum, phosphoric and hydrofluoric acid.

Scanning electron microscopy was performed on samples taken from the deposits of Turnu Măgurele, Valea Călugarească, Năvodari and Bacău. The analysis resulted in the definition of four morphological types of phosphogypsum. All of the analyzed samples of the first morphological type have compositions close to stoichiometry. The gypsum crystals are prismatic to acicular, showing perfect cleavage after [001]. Individual crystals have lengths ranging from 10 to 120 μm (Fig. 1). The phosphogypsum crystals of the second morphological group are grouped in polycrystalline, weakly cohesive aggregates. A morphological feature of this type consists of the homogeneous crystal size. Crystal morphology of this group is relatively large and tends to form aggregates of accretion, with randomly oriented and interlocking crystals. The crystal size varies from 100 μm to 1 mm (Fig. 2). The third morphological group of phosphogypsum is dominated by the presence of crystalline aggregates that are similar to the "sand roses". The largest dimension of the aggregates reaches 1 mm (Fig. 3). The fourth morphological group of phosphogypsum is common at the lower levels of all stockpiles and consists of a series of crystalline, cauliflower-like aggregates. These are practically similar to those of the third group, but the crystalline forms of gypsum are difficult to distinguish (Fig. 4).

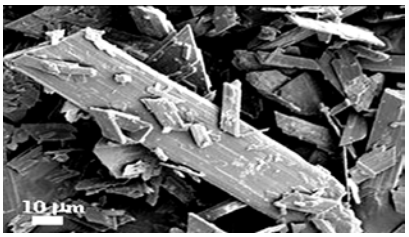

Fig. 1. Type I

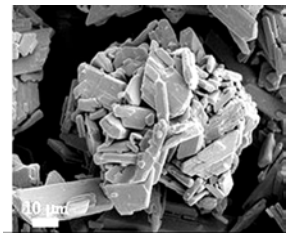

Fig. 2. Type II

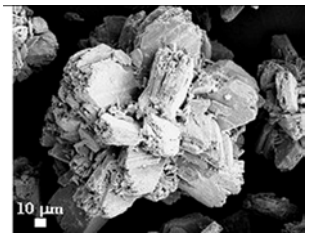

Fig. 3. Type III

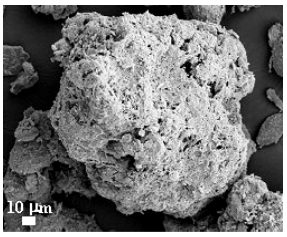

Fig. 4. Type IV

UPPER CRETACEOUS CONTACT METAMORPHISM AND RELATED MINERALIZATION IN ROMANIA

ILINCA, G.
Department of Mineralogy, University of Bucharest, Bd. N. Balcescu 1, RO-010041 Bucharest, Romania
E-mail: ilinca@geo.edu.ro

The purpose of this plenary lecture is to give a general view over the contact phenomena and mineralization related to the Banatitic Magmatic and Metallogenic Belt (BMMB – see history of the term in BERZA *et al.* 1998) which represents a series of discontinuous magmatic and metallogenic occurrences of Upper Cretaceous age, which are discordant in respect to mid-Cretaceous nappe structures (CIOFLICA & VLAD, 1973; CIOBANU *et al.*, 2002.) The subvolcanic/plutonic rocks belonging to the BMMB are known under the collective name of "banatites", a term coined by VON COTTA (1864) who described a suite of cogenetic magmatic rocks occurring as either shallow intrusions or subvolcanic bodies, younger than Jurassic and Cretaceous sedimentary formations. Ever since this first description, the name "banatites" has reflected their *locus tipicus*, that is, Banat and Timok region, covering parts of the south-western Romania and north-eastern Serbia.

During the last few decades, the BMMB has drawn considerable interest in petrology, age, structural-tectonic significance and in the contained skarn, porphyry-copper and hydrothermal ore deposits, with a vast amount of literature published to date. Owing to the space constraints, only selected citations were therefore included in this abstract.

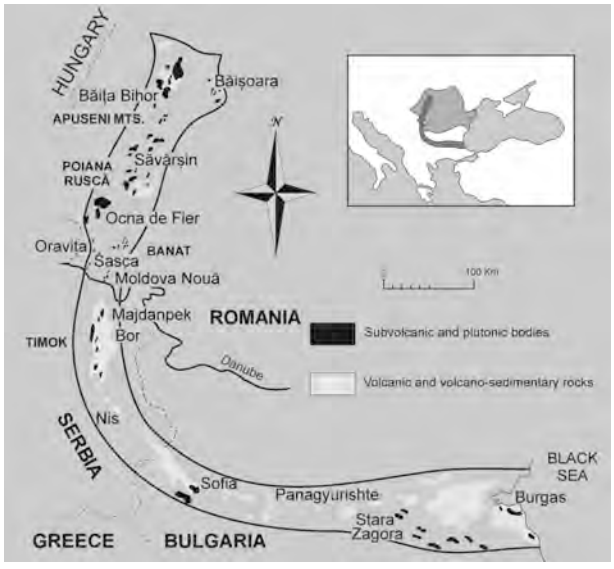

Fig. 1. *The extension of the Banatitic Magmatic and Metallogenic Belt over Romania, Eastern Serbia and Bulgaria (with dark gray in the inset and with heavy outline in the map). Simplified after CIOFLICA & VLAD (1973).*

Regional extension and geodynamic setting of the BMMB

The BMMB is exposed over approximately 900 km in length and around 30 to 70 km in width. It has a north-east to south-west trend over Apuseni Mts. and Southern Carpathians, it aligns to a north-south direction over eastern Serbia (Timok and Ridanji-Krepoljin zones), and bends widely to the east, through the Srednogorie area, reaching the shores of the Black Sea (Fig. 1). The northern most occurrences of the BMMB in Romania are in Apuseni Mountains where banatites are found both as volcanics in Late Cretaceous Gosau-type basins (*e.g.*, Vlădeasa, Cornițel-Borod, Gilău-Iara, Sălciua-Ocoliş, Vidra, Găina, Roşia) and as dyke swarms or major intrusions, cross-cutting these volcanics or any older formations or tectonic planes (*e.g.*, Gilău, Budureasa, Pietroasa, Băişoara, Valea Seacă, Băița Bihor, Brusturi, Căzăneşti, Măgureaua Vaței).

South of Mureş Valley, in the Romanian South Carpathians, Late Cretaceous volcanic and plutonic rocks are found in the upper (Supragetic/Getic) and only as tuffs in the lower (Danubian) stacks of basement nappes. BMMB outcrops in the Supragetic/Getic nappes largely consist of dioritic and granodioritic plutons crossed by dyke swarms of andesites, dacites, rhyolites, lamprophyre, as at Hăuzeşti, Tincova and Ruschița and further south at Bocşa, Ocna de Fier-Dognecea, Surduc, Oravița-Ciclova, Sasca Montană, Moldova Nouă which intersect Upper Paleozoic – Mesozoic covers and underlying crystalline formations of both Getic and Supragetic nappes (BERZA *et al.*, 1998). Eastward of the Bocşa-Moldova Nouă lineament of plutons and of the Late-Carboniferous to Early Cretaceous cover formations, dyke swarms of banatitic rocks are known in the crystalline (metamorphic and granitic) basement of the Getic Nappe or in Late Cretaceous Gosau-type deposits (at Şopot) and were grouped by RUSSO-SĂNDULESCU & BERZA (1979) in the Hypabyssal Banatite Zone (HBZ).

In the Supragetic/Getic nappe stack, banatitic volcanics occur on both the northern and southern slopes of Poiana Ruscă Mountains, as well as in the west (Nădrag Basin), in the center (Rusca Montană Basin) and in the east of the massif (Hațeg Basin), associated with Maastrictian continental sediments in volcano-sedimentary formations.

Attempts were made to ascribe such apparently randomly distributed occurrences to several alignments or magmatic trends, with NE-SW orientation (*e.g.*, CIOFLICA & VLAD, 1980), but geophysics show a different

trend of larger plutons from beneath (ANDREI *et al.*, 1989).

Numerous models have been published in the last decades to explain the formation and the geodynamic significance of the BMMB. *Subduction models* have used the two major ocean sutures within the Carpathian-Balkan orogen: the Vardar Ocean with its Mureş Zone (and Transylvanian?) extension, and the Severin Ocean with remnants preserved in Măgura, Ceahlău, Severin and Trojan nappes. Both the dominant calc-alkaline geochemical trend of the igneous rocks and the metallogenic features of the associated ore deposits were extensively used supporting the subduction models. However, major disagreement exists among these models, especially in what concerns the direction and timing of subduction.

Comprehensive overviews of such subduction related models are given by BERZA *et al.* (1998), CIOBANU *et al.* (2002) and ZIMMERMANN *et al.* (2008) and will be summarized during the lecture.

Authors such as POPOV *et al.* (2000), BERZA *et al.* (1998) and NEUBAUER (2002) have considered that the banatitic magmas where generated in an *extensional regime* during Late Cretaceous – documented by Gosau-type basins – caused by orogenic collapse affecting the upper crust. Mantle delamination due to slab break-off in the Late Cretaceous has followed the Jurassic and Lower Cretaceous northwards directed subduction Vardar Ocean.

Slab-rollback models postulate that in the Late Cretaceous, the subducting Vardar oceanic slab began to roll back and steepened, thus leading to extension in the upper crustal block and favouring the access of melts to high crustal levels, ultimately leading to volcanism. The slab-tear model (NEUBAUER, 2002, NEUBAUER *et al.*, 2003) predicts that in a post-subduction, post-collisional regime, the subducting slab breaks from its continental counterpart and initiates asthenospheric upwelling into the slab window created as the tectonic units separate.

Based on the paleomagnetic data from the Carpathian and Pannonian areas, PANAIOTU *et al.* (2005) suggested a two-step rotation model, to explain the up to 90° declinations measured on banatites in the Apuseni Mountains and in the Southern Carpathians. The Late Cretaceous paleoaltitude calculated for banatites by PANAIOTU *et al.* (2005) is 24°N ± 4°. At the time of their emplacement, the banatites of the BMMB had an east-west spatial trend, and continued to the east with the alignments of the Western and Eastern Pontides (Fig. 2).

Petrology and geochronological summary of the banatites

The BMMB is characterized by an extreme petrographic diversity, and many of the individual outcropping massifs encompass a significant part of this variety. Thus, a detailed petrographic inventory of each banatite occurrence in the Romanian part of BMMB would be far beyond the scope of this lecture.

Effusive banatites encompass a wide range of compositions from rhyolites (Vlădeasa), to alkali basalts (Poiana Ruscă Mountains), but medium and high-K andesites and dacites prevail in all volcanic complexes of the Romanian portion of the BMMB. Intrusive banatites range from gabbros to leucogranites, but the most widespread are (quartz) diorites, granodiorites and (quartz) monzodiorites (BERZA *et al.*, 1998, POPOV *et al.*, 2000). Numerous satellite dykes contain basalts, andesites, dacites, rhyolites and relatively diverse lamprophyres. A general characteristic of banatitic intrusions is the large quantity of the mafic microgranular enclaves, frequently porphyric and incorporating crystals from the host, thus testifying for magma mingling.

A compilation of radiometric dating for banatites was published by CIOBANU *et al.* (2002), pointing to K-Ar age spans between 49.5–77 Ma in Apuseni Mountains, 47.2–110 Ma in Poiana Ruscă Mountains, 67–89 Ma in Banat, 38–93 Ma in Serbia and 67–94 Ma in Bulgaria, respectively. Maximum of K-Ar age frequencies occur in the 65–95 Ma interval (Turonian–Maastrichtian), a shorter time span, confirmed by recent Ar-Ar, U-Pb and Re-Os dating (*e.g.*, POLLER *et al.* 2001; VON QUADT *et al.*, 2001).

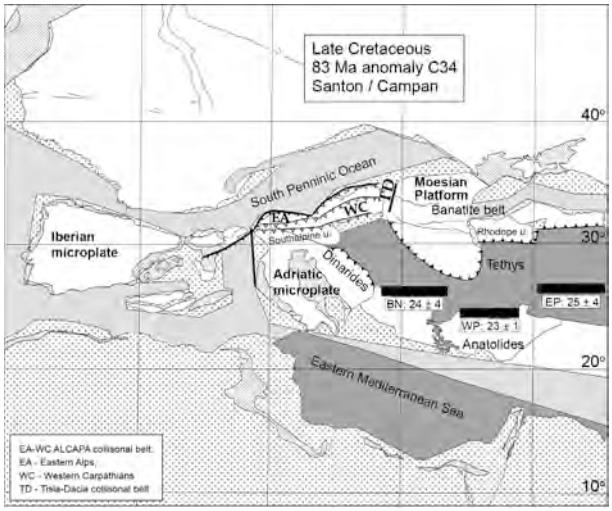

Fig. 2. *The position of banatites (BN), western Pontides (WP) and eastern Pontides (EP) on the basis of paleomagnetic data, compared with the paleogeographic reconstructions of NEUBAUER et al. (2003); (after PANAIOTU et al., 2005).*

Re-Os ages published by ZIMMERMAN *et al.* (2008) for 50 banatite (molybdenite bearing) samples, from throughout the BMMB (Romania, Serbia, Bulgaria), indicate 20 My time interval, *i.e.*, 72.2–92.4 Ma, in good agreement with the zircon U-Pb ages and overlapping with median zone of the much more scattered

K-Ar or Rb-Sr data. The Re-Os ages measured on molybdenite bearing samples by ZIMMERMANN *et al.* (2008) for various segments of the BMMB, distribute as follows: Apuseni Mountains (Băiţa Bihor): 78.7–80.6 Ma; Poiana Ruscă (Calova, Valea Căprişoara, Tincova): 72.2–76.6 Ma; Banat (Ocna de Fier, Bocşa, Oraviţa, Ciclova, Moldova Nouă): 72.4–82.7 Ma; Timok (Majdanpek, Crni Vrh, Veliki Krivelj, Bor): 80.7–87.9; Panagyurishte (Elatsite, Chelopech, Medet, Assarel, Vlaykov Vruh-Elshitsa): 86.8–92.4 Ma.

Contact metamorphism related to BMMB

The main effect of the banatitic emplacement was the thermal and metasomatic transformation of the surrounding rocks. Often, the metasomatic processes had an endomorphous character, affecting to different degrees the intrusive bodies themselves. In the majority of igneous occurrences in the BMMB, the contact metamorphism extended over the pre-intrusion host formations, including crystalline schists, detrital sedimentary and carbonate rocks, leading to the formation of structurally and mineralogically complex contact aureoles.

Isochemical transformations include recrystallization, prograde reactions without major implication of fluid phases, combinations of both, and subordinately, irreversible devolatilization (pyrolysis). The later process is often responsible for the discoloration of recrystallized carbonate rocks in the close vicinity of magmatic sources (*e.g.*, Dognecea – VLAD, 1974), followed by the removal of organic carbon traces.

Recrystallization products are widespread within the contact aureoles, especially in areas where pure carbonate rocks prevail: calcitic or dolomitic marbles, often zoned, with rougher textures in the vicinity of the magmatic bodies (VLAD, 1974; IONESCU, 1996b). Carbonate rocks with silicate alloclasts, argillaceous or arenaceous limestones, marls, detrital rocks or crystalline schists are also transformed under the heat flow and may result in "hardening", "hornfelsing", "softening" of the rocks – as named by various authors, or in textural transformations leading to obliteration of initial stratification or schistosity. Recrystallization commonly resulted in micro- or mesoblastic calcic or dolomitic marbles and relatively homogeneous, medium-grained calc-silicate hornfels with grossular + calcite or diopside + calcite. Siliceous and aluminous hornfels with biotite- or quartz-dominant assemblages or with andalusite + cordierite ± corundum and actinolite + chlorite + epidote ± zoisite are also present, yet at least in part, their mineralogical composition might point as well to superposed hydrothermal alteration.

Prograde reaction products are much more diversified and reflect the complex nature of the premetamorphic rocks. Various criteria have been used to classify hornfels: (1) texture or overall macroscopic appearance; (2) mineralogical composition; (3) chemical composition; (4) metamorphic "facies" or the nature of premetamorphic rock. In some cases, the prograde reactions are weak and only singular metamorphic mineral phases are identified against an unchanged background (*e.g.*, "biotite in gneisses", "cordierite in porphyritic rocks", "andalusite in biotite-bearing gneisses"). Sometimes, the thermal effects are inferred from *the loss* of certain mineral phases from the initial paragenesis (*e.g.*, loss of biotite from thermally affected gneisses).

The most typical products of *allochemical transformations* in the contact aureoles of banatites are skarns and hydrothermal alterations. Cases of large scale Ca ⇔ Mg transfer reactions resulting in dolomitization of limestones (*e.g.*, Ocna de Fier-Dognecea – VLAD, 1974) or in dedolomitization (*e.g.*, Antoniu metasomatic body, Băiţa Bihor – CIOFLICA *et al.*, 1992) have also been recorded.

Skarns have also been classified or referred to according to a multitude of criteria: (1) dominant chemical character ("calcic skarns", "magnesian skarns"); (2) mineralogical composition (skarns with various Ca, Mg, Al silicates); (3) the nature of the carbonate paleosome ("skarns formed on limestones", "skarns formed on dolostones"; (4) the passive or active role of the paleosome *vs.* the mineralizing fluids ("exoskarns", "endoskarns", "periskarns"); (5) position with regard to the magmatic contact ("proximal skarns", "distal skarns"); (6) evolution stage of magmatic bodies ("magmatic skarns", "post-magmatic skarns"); (7) thermal character of fluids ("pyro-metasomatites", "hydrometasomatites", "pseudo skarns").

Calcic skarns prevail in all banatite occurrences located nearby carbonate sedimentary formations. Subordinately, in several massifs from Bihor and Banat, magnesian skarns occur, with assemblages including forsterite + chondrodite + diopside ± phlogopite (clinochlore) + tremolite. At Băiţa Bihor, Budureasa, Pietroasa, Cacova Ierii, Ocna de Fier, skarns contain endogenous borates, such as ludwigite, kotoite, suanite or szaibélyite (*e.g.*, IONESCU, 1996a,b; MARINCEA, 2006). Other chemical types may also be present, such as Mn-rich skarns at Dognecea (*e.g.*, VLAD, 1974). Skarns unusually rich in aluminum occur in Valea Ţiganilor, Ciclova and at Sasca Montană. The main Al-rich phase is vesuvianite which forms monomineralic concentrations, with crystals reaching up to 5–10 cm. Commonly, vesuvianite replaces diopside, wollastonite and garnet and points rather to a significant Al-mobility towards the late phases of metamorphism than to an Al-rich host rock.

Exoskarns are predominant in the banatitic contact aureoles, but well developed endoskarn assemblages have also been described. At Ciclova, the outer parts of a monzodiorite body have been transformed in endoskarns with grossular + vesuvianite + Fe-diopside + phlogopite, locally accompanied by periskarns with Fe-augite + orthoclase + titanite + grossular (CIOFLICA *et al.*, 1980). At Surduc, MARINCEA & RUSSO-SĂNDULESCU (1996) described calcic endoskarns with prehnite + andradite + Ca-rich plagioclase + diopside, formed on bodies of basic magmatites of the Coniacian – Maastrichtian cycle.

High-temperature skarn assemblages with spurrite-tilleyite-gehlenite, or diopside-gehlenite occur at Cornet Hill-Măgureaua Vaței, Apuseni Mountains (MARINCEA *et al.,* 2001; PASCAL *et al.,* 2001) and Ogaşul Crişenilor-Oravița (CONSTANTINESCU *et al.*, 1988b; KATONA *et al.,* 2003) where they are related to quartz monzonite-monzodiorites, or diorite-gabbros.

Skarns related to BMMB in Romanian have been examined and classified also with respect to regional structural relationships with surrounding rocks. Three main types have been distinguished (CIOFLICA & VLAD, 1973; VLAD, 1997), (1) the Băița Bihor type, (2) the Ocna de Fier type and (3) the Moldova Nouă type.

- The *Băița Bihor type* skarns may develop along magmatic-sedimentary contacts, but more often they form distal bodies along fractures or thrust planes, or highly brecciated metasomatic columns.

- The *Ocna de Fier type* skarns are controlled by the contact of the Ocna de Fier-Dognecea pluton with carbonate rocks and form discontinuous bands, irregular- or tabular-shaped bodies and metasomatic veins. A relatively homogeneous carbonate paleosome favoured diffusion, rather than infiltrative exchange as the major metasomatic process involved. Metasomatic asymmetrical zoning is obvious: an inner zone with andradite-dominant assemblages, locally rimmed by wollastonitites and an outer zone with pyroxenic skarns – diopside at Ocna de Fier and Mn-hedenbergite at Dognecea (VLAD, 1974).

- The *Moldova Nouă type* skarns develop at Moldova Nouă, Sasca Montană and partially at Oravița-Ciclova, where they are controlled mainly by contact zones between subvolcanic bodies and carbonate rocks. They occur commonly as lenses with branching apophyses in the vicinity of igneous apices. Skarns of this type display no striking mineral zoning.

A continuum between skarns and hydrothermal alterations is specific to all skarns occurrences in BMMB, but the effects of hydro-metasomatism are usually extended beyond the limits of skarn zones.

Hydrothermal retrograde reactions affecting garnets and vesuvianite, commonly result in epidote + chlorite ± carbonates, quartz whereas pyroxenes breakdown to form tremolite - actinolite + serpentine + talc. High temperature hydrothermal assemblages with tourmaline + quartz ± orthoclase, magnetite were described in relation to porphyritic granodiorite intrusions from Oravița and from Sasca Montană (CONSTANTINESCU, 1980).

More abundant are the hydrothermal assemblages containing a) K-feldspar + biotite ± quartz, muscovite (potassic alteration), b) epidote + actinolite + chlorite + quartz + calcite (propylitic alteration), and c) illite + quartz ± chlorite, calcite, pyrite (phyllic alteration) which are frequently related to ore deposits. Rich epithermal alteration with zeolites (laumontite, stilbite, thomsonite, chabazite, etc.), gypsum, anhydrite, and cryptocrystalline silica are also present.

Types of mineral deposits in the BMMB

The studies of VON COTTA (1864) upon the Fe-Cu-Pb-Zn skarn deposits of Dognecea, Ocna de Fier and other mines in Banat are the first widely cited papers to define a class of "contact-deposits" found at the contact of igneous intrusions and limestones. Since then, more than 50 mineral deposits have been discovered, and pending of a given historical epoch, they were of some economic interest. The mineralization related to the BMMB is represented mainly by porphyry copper, massive sulphide, skarn and vein (epithermal and mesothermal) deposits (BERZA *et al.,* 1998).

Copper metallogeny is predominant and distinguishes the BMMB in the context of the larger Alpine-Balkan-Carpathian-Dinarides belt (CIOBANU *et al.*, 2002). Copper ores are commonly associated with Pb-Zn, Au-Ag, and subordinately with Mo, Bi, W, Fe, Co, Ni and B. Mineral deposits within the BMMB are strongly differentiated with respect to host rock types and depth of magma emplacement. Shallower hypabyssal bodies are hosts for porphyry copper ores with Cu ± Au, Ag, Mo: *e.g.*, Moldova Nouă, Majdanpek, Cerovo, Veliki Krivelj, Bor (Timok Massif, Serbia), Elatsite, Chelopech, Assarel (Panagyurishte district, Bulgaria). High-sulphidation epithermal deposits are sometimes spatially associated with larger porphyry copper systems (*e.g.*, at Bor and Majdanpek – CIOBANU *et al.*, 2002). Subeconomic porphyry copper (± Mo) accumulations are also present at Oravița, but hydrothermal alteration is far less pervasive than at Moldova Nouă. Large shallow porphyry-style systems with pyrite halos (and/or skarn halos) extend only south of Poiana Ruscă but they lack economic mineralization: *e.g.,* Tincova-Ruschița, Șopot-Teregova-Lăpuşnicel areas.

Copper and base metal skarn deposits form the most widespread metal accumulations across the BMMB. Some occurrences are set apart by prominent Fe metallogeny (*e.g.*, Ocna de Fier, Maşca Băişoara). Ocna de Fier is considered typical for fluid plume mineralization in a proximal skarn setting (COOK & CIOBANU, 2001). Forsterite skarns host a magnetite-chalcopyrite-bornite mineralization which represents the inner Cu-Fe core of the deposit (COOK & CIOBANU, 2001). Scheelite forms significant concentrations in the Cu-Mo mineralization of Băița Bihor and Oravița. Bismuth sulphosalts are minor but ubiquitous components of many skarn deposits. Extremely rich and diverse bismuth sulphosalt assemblages have been described at Băița Bihor, Valea Seacă, Ocna de Fier and Oravița-Ciclova.

Regional zoning of skarn deposits in correlation with Upper Cretaceous subduction settings was summarized by VLAD (in BERZA *et al.* 1998; VLAD & BERZA 2003) who distinguished two major metallogenic segments within the BMMB (Apuseni Mountains and Southern Carpathians), each one still amenable of division into further units (sub-belts, zones and districts). Local zoning is well expressed for numerous ore environments in the BMMB. At Băița Bihor, the areas clos-

est to the magmatic sources are enriched in molybdenite. Towards the external zones, Mo-rich ores grade into Mo-W-Bi-Te (in calcic skarns) or Cu-W-Bi (in magnesian skarns), Pb-Zn (in magnesian skarns and sedimentary schists) and finally into boron mineralization overlapping dedolomitization zones. At Dognecea-Ocna de Fier, CIOBANU & COOK (2000) described a Cu-Fe → Fe → Pb -Zn metal zoning around a single granodiorite core in the deepest part of the deposit.

The polyascendant character of skarn deposits in the BMMB has either been asserted (*e.g.*, POPESCU & CONSTANTINESCU, 1977; CIOFLICA & VLAD, 1981) or argued against (ILINCA, 1998). Extensive sampling and detailed investigation of ore paragenesis over numerous skarn deposits in the BMMB, plead for coeval and isochronous mineralization, most probably formed from the differentiation of a single fluid. Moreover, apart from several cases of prominent metallogeny (*e.g.*, Fe at Ocna de Fier), the overall paragenetic sequence for virtually all mineral deposits in the BMMB is roughly the same, both as mineral phases and deposition sequence. ILINCA (1998) separated the following ore deposition sequences:

- Stage 1 ("siderophile" – Fe ± Co, Ni, As, Mn) – iron oxides and sulphides, Co, Ni, Fe arsenides and sulpharsenides, with subordinate Fe-Mn calcic silicates. The stage signifies the highest deposition temperatures and a continuous decrease of oxygen fugacity (*e.g.*, hematite → magnetite, magnesioferrite) *vs.* increase of sulphur fugacity (pyrrhotite → pyrite). At Băiţa Bihor, Ocna de Fier, Oraviţa, Ciclova and Sasca Montană, early iron sulphides are accompanied by nickeline, rammelsbergite, cobaltite, gersdorffite (ILINCA, 1998), Co-pentlandite (COOK & CIOBANU, 2001), linnaeite, bravoite, siegenite, millerite.

- Stage 2 (Pb, Zn ± Ag, Bi, Fe) – forms the bulk of the mineralization in numerous occurrences across the BMMB. The stage is represented by galena (with up to 10 mol% matildite) and sphalerite usually with 14–15 mol% FeS). Invariably, the direct contact between galena and siderophiles, shows the late character of the Pb-Zn phases.

- Stage 3 (Pb, Bi ± Ag, Sb, Te, Cu) – contains Pb-(Ag)/Bi sulphosalts (lillianite homologues (heyrovskýite, lillianite, vikingite), cosalite, cannizzarite, galenobismutite. Some Pb-Bi sulphosalts are formed on older galena, most probably belonging to the previous stage. Stage 3 members often substitute siderophile sulphides likely to belong to stage 1. The same stage witnesses the deposition of Bi (±Pb) tellurides: joséite-A, joséite-B, protojoséite, and rarely native bismuth. Cosalite represents a late deposition within this stage. It contains small amounts of Cu and replaces heyrovskýite, lillianite and cannizzarite. In Sasca Montană and Moldova Nouă, stage 3 assemblages are mostly represented by Sb (±As) sulphosalts: geocronite, boulangerite and zinkenite, often formed on older galena.

- Stage 4 ("copper metasomatosis" (CM) – Cu, Bi ± Pb, Ag, Fe, Sb, Te, As, Zn, Au, Mo, W) – is distinguished by an increase of Cu content in sulphides and sulphosalts. Massive deposition of chalcopyrite, cubanite and bornite takes place in this stage. Fahlore minerals (tetrahedrite-tennantite, enargite, luzonite) occur also now, most frequently on Fe, Zn, Sb, As phases of earlier stages. At Băiţa Bihor, Oraviţa and Ciclova, chalcopyrite and cubanite are often pseudomorphs after pyrite and replace Co and Fe sulpharsenides. "Chalcopyrite disease" phenomena, *i.e.* chalcopyrite (± bornite, mackinawite) blebs in sphalerite are widespread and represent yet another facet of CM. Bi-sulphosalts are particularly sensitive to CM transformations. First Bi phases show an increased Bi_2S_3/PbS ratio compared to previous stages and grade towards decreasing Bi/Cu. Such minerals form directly or by replacing older Pb-Bi sulphosalts (especially cannizzarite and galenobismutite): proudite, lillianite (with up to 2.9 at% Cu), felbertalite, (high Cu) cosalite, cuproneyite, junoite. The sequence continues with nuffieldite and massive deposition of bismuthinite derivatives, covering the entire range between bismuthinite and aikinite. In antimony-dominated assemblages, bournonite is formed. The highest Cu contents are embodied by makovickyite-cupromakovickyite, paděraite, hodrushite and kupčíkite and finally by pure Cu-Bi sulphosalts such as emplectite and wittichenite.

References

ANDREI, J., CRISTESCU, T., CALOTĂ, C. *et al.* (1989) Revue Roumanie de Géologie, Géophisique et Géographie, Série de Géophisique, 33: 79–85.

BERZA, T., CONSTANTINESCU, E. & VLAD, Ş.N. (1998): Resource Geology, 48: 291–306.

CIOBANU, C.L. & COOK, N.J. (2000): European Journal of Mineralogy, 12: 899–917.

CIOBANU, C.L., COOK, N.J. & STEIN, H. (2002): Mineralium Deposita, 37: 541–567.

CIOFLICA, G. & VLAD, Ş.N. (1973): Revue Roumanie de Géologie, Géophisique et Géographie, Série de Géologie, 17: 217–214.

CIOFLICA, G. & VLAD, Ş.N. (1980): European Copper Deposits, Belgrade, 67–71.

CIOFLICA, G. & VLAD, Ş.N. (1981): Analele Universitatii Bucuresti, 30: 3–17.

CIOFLICA, G., JUDE, R. & LUPULESCU, M. (1992): Romanian Journal of Mineralogy, 76: 1–16.

CONSTANTINESCU, E. (1980): Mineralogy and genesis of the skarn deposit at Sasca Montană. Ed. Acad. Rep. Soc. România, Bucharest, 158 p. (in Romanian).

CONSTANTINESCU, E., ILINCA, Gh. & ILINCA, A. (1988b): Dări de Seamă ale Institutului de Geologie şi Geofizică, 72–73(2): 27–45.

COOK, N.J. & CIOBANU, C.L. (2001): Mineralogical Magazine, 65: 351–372.

ILINCA, G. (1998): PhD Thesis, University of Bucharest, Romania, 356 p. (in Romanian).

IONESCU, C. (1996a): Ph.D. Thesis, Babeş-Bolyai University, Cluj-Napoca, 180 p. (in Romanian).

IONESCU, C. (1996b): Studia Universitatis Babeş-Bolyai, Geologia, 41: 127–135.

KATONA, I., PASCAL, M.-L., FONTEILLES, M. & VERKAEREN, J. (2003): Canadian Mineralogist, 41: 1255–1270.

MARINCEA, Şt. (2006): Neues Jahrbuch für Mineralogie – Abhandlungen, 182: 183–192.

MARINCEA, Şt. & RUSSO-SĂNDULESCU, D. (1996): Romanian Journal of Mineralogy, 77: 55–71.

MARINCEA, Şt., BILAL, E., VERKAEREN, J., PASCAL M.-L. & FONTEILLES, M. (2001): Canadian Mineralogist, 39: 1435–1453.

NEUBAUER, F. (2002): Geological Society (London) Special Publication, 204: 81–102.

NEUBAUER, F., HEINRICH, C. & GEODE WORKING GROUP (2003): In: Mineral Exploration and sustainable development. MillPress, Rotterdam, 1133–1136.

PANAIOTU, C.G., PANAIOTU, E.C. & NEDELCU, A. (2005): Rev. Pol. St. Sci - 2005, 8 p.

PASCAL, M.-L., FONTEILLES, M., VERKAEREN, J., PIRET, R. & MARINCEA, Şt. (2001): Canadian Mineralogist, 39: 1405–1434.

POLLER, U., UHER, P., JANÁK, M., PLASIENKA, D. & KOHUT, M. (2001): Geologica Carpathica, 52: 41–47.

POPESCU, Gh. & CONSTANTINESCU, E. (1977): Analele Universitatii Bucuresti, 26: 45–58.

POPOV, P.N., BERZA, T. & GRUBIĆ, A. (2000): ABCD–GEODE workshop, Borovets, Bulgaria, 69–70.

RUSSO-SĂNDULESCU, D. & BERZA, T. (1979): Revue Roumanie de Géologie, Géophisique et Géographie, Série de Géologie, 23: 149–158.

VLAD, Ş.N. (1974): The mineralogy and genesis of the skarns at Dognecea. Ed. Acad. Rep. Soc. România, Bucharest, 119 p. (in Romanian).

VLAD, Ş.N. (1997): Mineralium Deposita, 32: 446–471.

VLAD, Ş.N., & BERZA; T. (2003): Studia Universitatis Babeş-Bolyai, Geologia, 48: 113–122.

VON COTTA, B. (1864): Erzlagerstätten im Banat und in Serbien. Braumüller, Wien, 108 p.

VON QUADT, A., PEYTCHEVA, I. & CVETKOVIC, V. (2003): In: Mineral Exploration and Sustainable Development, MillPress, Rotterdam, 1: 407–410.

ZIMMERMANN, A., STEIN, H., HANNAH, J., KOŽELJ, D., BOGDANOV, K. & BERZA, T. (2008): Mineralium Deposita, 43: 1–21.

THE "BLACK CERAMICS OF MARGINEA" (ROMANIA): A MODERN ANALOGUE OF ANCIENT CERAMICS?

IONESCU, C.[1]*, HOECK, V.[2] & SIMON, V.[3]
[1] Dept. of Geology, Babeş-Bolyai University, 1, Kogălniceanu Str., RO-400084 Cluj-Napoca, Romania
[2] Dept. of Geography and Geology, Salzburg University, 34 Hellbrunner Str., A-5020 Salzburg, Austria
[3] Faculty of Physics & Institute for Interdisciplinary Research in Nano-sciences, Babeş-Bolyai University, Cluj-Napoca, Romania
* E-mail: corina.ionescu@ubbcluj.ro

The so-called "Marginea ceramics" is one of the most famous modern black ceramics in Romania. The raw material is a Miocene illite-rich clay, no temper is additionally used. The clay consists of illite, muscovite, feldspar, quartz, chlorite/kaolinite, Fe oxi-hydroxides and carbonate. Recalculated on a dry basis, the clay has ~59 wt% SiO_2, ~8.4 wt% CaO, ~17 wt% Al_2O_3, and ~3 wt% MgO. This chemistry fits very well to that of the black ceramics, given below. The firing takes place in quite primitive ovens, using wood fuel, with no temperature control.

The study focused on the changes occurring in the fired ceramics, compared with the raw material. It involved polarized light optical microscopy, X-ray powder diffraction (XRPD), electron microprobe analysis (EMPA), scanning electron microscopy (SEM) and ICP-MS.

The ceramics show magnetic properties strong enough to keep a small magnet on the pot walls. On broken surfaces the wall of the black pots consist of light to dark grey fine layered core covered by thin black layers on both sides. The SEM and the backscattered electron (BSE) images revealed a ceramic body composed of a very fine network of glassy material connecting relics of untransformed primary minerals and newly-formed phases (Figs. 1a,b). Scarce quartz, K-feldspar and plagioclase grains, some muscovite, biotite flakes and Fe-rich grains are embedded in a matrix of glass, illite, muscovite ± chlorite/kaolinite. Pyroxene and a part of feldspar together with magnetite are obviously firing phases. The black outer layer is more compact and shows a higher content of Ca-rich plagioclase and Fe-rich phase. X-ray powder diffraction indicates the presence of magnetite and possibly maghemite in the fired ceramics body, and in particular in the outer layer. These two minerals are responsible for the black colour (IONESCU *et al.*, 2011).

Recalculated on LOI-free basis, the ceramic chemistry shows only little variation and no distinct trends: SiO_2 ranges from 58 to 60 wt%, CaO from 8.1 to 8.8 wt% and MgO is around 3 wt%. A precise comparison of the ceramics with the clayey raw material is feasible and can solve some problems regarding mineral changes during firing. The results can be applied for compositional and technological studies on ancient black ceramics.

The study was financed by ID-2241/2008 and PN-II-ID-PCE-2011-3-0881 projects, granted to CI (Romanian Ministry of Education and Research).

Reference

IONESCU, C., HOECK, V. & SIMON, V. (2011): Studia Universitatis Babeş-Bolyai, Physica, 56(2): 69–78.

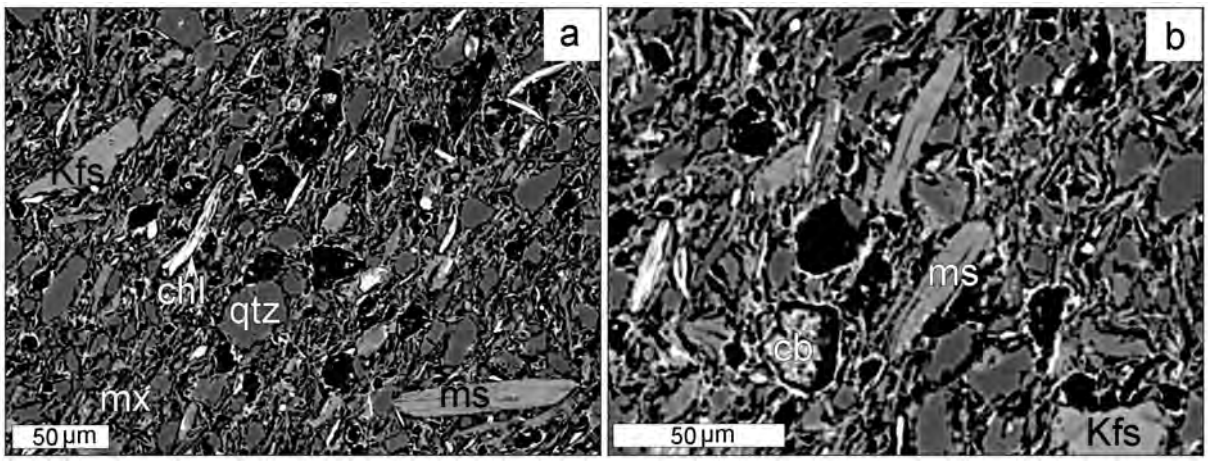

Fig. 1. *BSE images of the ceramic body, with a fine network of partially melted clayey matrix (mx) embedding quartz (qtz), muscovite (ms), K-feldspar (Kfs), chlorite (chl) and carbonate (cb). The black parts are pores.*

IMPLICATIONS FOR THE PETROGENESIS OF THE BASALTIC ROCKS ERUPTED FROM THE MONOGENETIC KISSOMLYÓ VOLCANIC CENTRE, WESTERN PANNONIAN BASIN, HUNGARY

JANKOVICS, M.É.[1]*, HARANGI, Sz.[1], KISS, B.[1] & NTAFLOS, T.[2]
[1] Volcanology Group, Department of Petrology and Geochemistry, Eötvös Loránd University, Pázmány Péter sétány 1/C, H-1117 Budapest, Hungary
[2] Department of Lithospheric Research, University of Vienna, Althanstrasse 14, Vienna, Austria
* E-mail: jeva182@gmail.com

The Kissomlyó volcanic centre is located in the Little Hungarian Plain Volcanic Field (Western Pannonian Basin, Hungary) that is one of the post-extensional monogenetic alkaline basaltic volcanic fields in the Carpathian-Pannonian Region. This eruptive centre is a complex monogenetic volcano that consists of different eruptive units. First, phreatomagmatic explosions built up a tuff ring in a terrestrial setting which was followed by the cessation of the volcanism and the formation of lacustrine sediments in a crater lake. However, later the volcanic activity rejuvenated: subaqueous lava flow emplaced within the crater resulted in the formation of pillow lava that intruded into the lacustrine sediments. The time gap between the tuff ring formation and the emplacement of the lava flow is estimated to be a few thousand years (MARTIN & NÉMETH, 2005). Afterwards, subaerial intracrater lava flows took place represented by columnar jointed basalt. In addition, on the top of the volcanic edifice a spatter cone (Királykő) can be found. The $^{40}Ar/^{39}Ar$ age of the subaerial lava flow unit is 4.63 Ma (WIJBRANS *et al.,* 2007). The complex volcanological feature and the rejuvenation of volcanic activity in the same place imply that this monogenetic volcano can be characterized by a complex evolution.

To reveal the magma evolution processes and whether there is significant compositional variability through the succession we carried out stratigraphically controlled sampling, i.e., collected rock samples from the different eruptive units (pyroclastics, pillow lava, columnar jointed basalt, lava spatter). The samples have porphyritic textures containing abundant glomerocrysts of clinopyroxenes, olivines and clinopyroxenes +olivines. The pheno- and microphenocrysts are olivine (with chromian spinel inclusions), clinopyroxene and plagioclase. The groundmass consists of microlitic plagioclase, olivine, clinopyroxene, Fe-Ti-oxides, apatite and some glass. The texture of the columnar jointed lava is much coarser-grained than that of the juvenile basalt fragments of the pyroclastics concerning their phenocrysts (up to 1.2 mm) as well as their groundmass.

Whole-rock major and trace element analyses were performed on samples from each eruptive unit. Based on their total alkalis relative to silica contents the samples are basalts, trachybasalts and basanites. They have Mg#s (54–65), Ni (99–140 ppm) and Cr contents (144–263 ppm) characteristically lower than those of the basaltic rocks from the other volcanic centres in the Little Hungarian Plain Volcanic Field. These together with the abundance of clinopyroxene phenocrysts (which are also rare in this region) suggest that the magma that erupted from the Kissomlyó volcano was more fractionated than those of the other eruptive centres in this region. Concerning the whole-rock major and trace element concentrations of the samples from the distinct eruptive units they do not show significant compositional differences. The compositions of the studied sideromelan glass shards in the pyroclastics can be originated from the whole-rock compositions by magma fractionation.

Textural and chemical investigations of the rock-forming minerals were carried out on selected samples from the pyroclastic unit and from the columnar jointed basalt representing the magmatism before and after the quiescence period. In all samples most of the olivine phenocrysts show normal zoning, however, in the juvenile basalt fragments of the pyroclastics reversely zoned olivines can be also found. These Fo-poor cores do not fit in the trend formed by the dominant olivine compositions (in the plots of CaO, NiO and MnO vs. Fo) suggesting possible open-system processes. Additionally, exotic olivine crystals with completely different compositions also occur. Chromian spinel inclusions found in olivines (and in a few clinopyroxene phenocrysts as well) have diverse compositions, but the majority of them are characterized by Cr#s varying from 45 to 55. Exotic spinel inclusions with distinct compositions can be found in phenocrystic olivines as well as in exotic olivines. Clinopyroxene phenocrysts show sector zoning and usually surround olivine phenocrysts indicating that they crystallized after the olivines. Based on clinopyroxene-melt thermobarometry (PUTIRKA *et al.,* 1996) the studied clinopyroxenes could have crystallized in a melt accumulation zone at the crust-mantle boundary.

References

MARTIN, U. & NÉMETH, K. (2005): Journal of Volcanology and Geothermal Research, 147: 342–356.
PUTIRKA, K., JOHNSON, M., KINZLER, R. & WALKER, D. (1996): Contributions to Mineralogy and Petrology, 123: 92–108.
WIJBRANS, J., NÉMETH, K., MARTIN, U. & BALOGH, K. (2007): Journal of Volcanology and Geothermal Research, 164: 193–204.

THE OCCURRENCE AND DISTRIBUTION FEATURES OF BISMUTH IN NEOGENE VOLCANITES OF SLOVAKIAN AND UKRAINIAN CARPATHIANS

JELEŇ, S.[1]*, PONOMARENKO, O.[2], MIKUŠ, T.[1], SKAKUN, L.[3], BONDARENKO, S.[2], GRINCHENKO, O.[4] & PRŠEK, J.[5]

[1] Geological Institute of Slovak Academy of Sciences, Ďumbierska 1, 974 11 Banská Bystrica, Slovakia

[2] Institute of Geochemistry, Mineralogy and Ore Formation, NAS of Ukraine, Palladina av. 34, 03680 Kiev-142, Ukraine

[3] Geological Faculty of Ivan Franko National University of L'viv, Hrushevskogo str. 4, 79005 L'viv, Ukraine

[4] Geological Faculty of Kiev National Taras Shevchenko University, Str. Vasyl'kivska 90, 03022 Kiev, Ukraine

[5] Department of Economic Geology, Faculty of Geology, Geophysics and Environmental Protection, AGH – University of Science and Technology, al. Mickiewicza 30, 30-059 Kraków, Poland

* E-mail: jelen@savbb.sk

General review of regional mineralogical-geochemical data on bismuth of neovolcanites of the Ukrainian and Slovakian Carpathians show some features of its distribution and typical mineralogical forms of its occurrence. As a whole regional geochemistry bismuth is characterized by its ununiform distribution, from wide dispersion in sedimentary and volcanic rocks to high concentration found in products of metasomatic alteration of these volcanites.

Two stages of bismuth mineralization, which are closely coeval with hydrothermal activity associated with Miocene (Sarmatian) and Pliocene volcanic stages, are established. Mineralization of the first stage is mostly occurred in internal zone of Inner Carpathian volcanic belt (Beregove, Prešov, Middle Slovakian focus structures), and the second one is found confined to the external zone, namely Vyghorlat-Ghutin ridge. Each stage is characterised by the set of bismuth minerals and different intensity of mineralization processes.

Hydrothermal deposits of Sarmatian age (Beregove and Banská Štiavnica-Hodruša ore fields) might be related to epithermal-copper-porphyric and epithermal precious- and base-metal vein type. Sulphosalts association of Ag-Cu-Bi system is localized in copper ores, at sites of superposition of quartz-chalcopyrite mineralization on much earlier galena-bearing aggregates. It is formed from neutral solutions that is manifested by the stability of adularia-carbonate-sericite association. Reactional nature of Ag-Cu-Bi-S sulphosalts is proved by wide development of symplectites (KOVALENKER *et al.,* 1993). The composition of sulphosalts naturally changes with increasement of chalcopyrite contents in aggregates, forming sequence: (1) matildite-galena solid solution that replaces galena; (2) minerals ranging in composition from ourayite-mummeite to gustavite-lillianite series; (3) sulphosalt series from Ag-Cu-Bi-Pb (pavonite homologues) to Cu-Bi and Cu-Bi-Pb (cuprobismutite homologues) and emplectite as well as bismuthinite derivatives in Banská Štiavnica (JELEŇ *et al.,* 2009) and gladite-krupkaite in Beregove. Bismuthinite was found only in massive chalcopyrite aggregates (Beregove, Hodruša-Hámre). Gold occurs in association with chalcopyrite that is caused (in ore bodies of Beregove) by formation of Ag-Cu sulphosalts in front of distribution of solutions of Cu-Au stage, with gold being found in rear part.

Volcanic formations of Pliocene age of the Vyghorlat-Ghutin ridge are represented by the chains of late Pannonian-Levantian volcanic centres, which form complex polygene domal-focus structures (Vyghorlat, Latovka, Borzhava, Ghutin). Hydrothermal systems of this age form fields of metasomatic rocks related to argillaceous and greisen types. The most wide area of these rock distribution are known in Perechin, Dubrinichi, Kibliary, Ilkovtsy, tract Podulki, river Syniak, tract Smerekov Kamin', mountains Dehmaniv and Tolsty Verh (in Ukraine) and in Poruba pod Vihorlatom and Remetské Hámre (in Slovakia). Metasomatic rocks show the development of Bi-Te-S-Se mineral associations. The tellurium content may reach 4 wt%, that is found in some pseudo-breccias.

Tellurides and sulphotellurides show the presence of groups with different values of Bi/(Te + Se + S) ratios, 2:2, 2:3, 3:2, 4:3 and 8:5. Bismuth-bearing associations include following minerals: native bismuth, hedleyite (Bi_7Te_3), tsumoite (BiTe), pilsenite (Bi_4Te_3), joséite-A (Bi_4TeS_2), joséite-B (Bi_4Te_2S), tetradymite (Bi_2Te_2S), phase on structure to Bi_2Te and Bi_3Te_2 (MELNIKOV *et al.,* 2009), telluronevskite (Bi_3TeSe_2), vihorlatite [$Bi_{8+x}(Se, Te, S)_{11-x}$], ikunolite ($Bi_4S_3$). Secondary bismuth minerals are represented by montanite and some other oxides. Some phases of tellurides need more detailed investigation to be properly established. It is also found, that selenium essentially increases in mineralization processes in Slovakian area of the Vyghorlat-Ghutin zone (MELNIKOV *et al.,* 2009).

References

JELEŇ, S., MIKUŠ, T. & PRŠEK, J. (2009): Mineralogical Review, 59(2): 64–76.

KOVALENKER, V., JELEŇ, S. & SANDOMIRSKAYA, S. (1993): Geologica Carpathica, 44(6): 409–419.

MELNIKOV, V., JELEŇ, S., BONDARENKO, S., BALINTOVÁ, T., OZDÍN, D. & GRINCHENKO, A. (2009): Mineralogichesky Zhurnal, 31(4): 38–48.

PROJECTS FOR THE EXTRACTION OF PYRITE IN ALBANIA AND KOSOVO

KASTRATI, S.*, GRIECO, G. & PEDROTTI, M.
Dipartimento di Scienze della Terra "A. Desio", Università degli Studi di Milano, Via Botticelli, 23, Milano, Italy
* E-mail: shpetim.kastrati@unimi.it

Pyrite (FeS_2) is an iron sulfide and one of the most ubiquitous minerals of earth crust. It is found in igneous, metamorphic and sedimentary rocks and crystallizes at both high and low temperatures.

Pyrite was widely used in the past for the production of sulfuric acid, but due to environmental pollution nowadays this use is limited to China and pyrite lost its value as an industrial mineral. In the last decade anyway new industrial applications of pyrite have opened new markets for this mineral. Such applications comprise: stainless steel production (60% of total pyrite market), abrasives (15%), dyes, pigments for glass (20%), brakes (3%), rechargeable batteries (2%). These new applications need small amounts of pyrite but require very demanding quality parameters.

The present work deals with projects for the extraction of pyrite in Albania and Kosovo for these new industrial applications.

For the projects three different ways to recover pyrite were considered: a) as a by-product of pyrite-bearing active mines (Trepça, Kosovo; Fusharrez, Albania); b) re-opening of abandoned pyrite mines used in past for sulfuric acid production (Spaç, Albania); c) exploitation of a new pyrite deposit (Lunik, Albania).

Pyrite is an important sulfide phase in the active lead and zinc Trepça Mine, Kosovo. Trepça Belt belongs to the Kosovo sector of the Serbo-Kosovo-Macedonian-Rhodope Metallogenic belt of Oligocene-Miocene age, which includes base and precious-metal districts in Kosovo, southern and western Serbia, variscan structures marginal to the Serbo-Kosovo-Macedonia, northern Greece and southern Bulgaria (HEINRICH & NEUBAUER, 2002). At Stanterg (Trepça mine), massive sulfide ore of economic importance forms continuous, columnar shaped ore bodies of carbonate replacement type (skarn) related to the emplacement of tertiary magmas (granodiorite and dacite-andesite). These are located along the carbonate-schist contact and dip parallel to the plunge of the anticline. The ore bodies extend along a strike length of 1200 m, and have been explored to a depth of 925 m below the surface (11 levels). Pyrite can be also recovered from tailing dumps.

In northern Albania, pyrite can be recovered within the Mirdita ophiolite belt, in similar geological settings, as a by-product and from the tailings of the copper Fusharrez mine and from the abandoned pyrite Spaç mine.

Mirdita is located in the Jurassic age Mirdita-Pindos ophiolite belt of Albania-Greece that ranges from ultramafic to mafic rocks with a number of andesitic and felsic volcanic domes in the central portion. The volcanic rocks are overlain by a sedimentary melange (BECCALUVA *et al*., 1994).

Finally, in eastern Albania the never exploited pyrite Lunik deposit is placed inside volcanic rocks. It was formed under water together with pillow basalts and at low temperature hydrothermal conditions.

Basalt rocks of Lunik are placed over gabbro through gabbrodiabase or over the ultramafic sequence of the western ophiolites through ocean metamorphics (metabasalt), and covered normally by the Upper-Middle Jurassic siliceous radiolarite, or transgressively by heterogeneous ophiolitic melange of Upper Jurassic (Tithonian). Volcanites of this series in many sectors underwent low grade metamorphism from zeolite to greenschist facies and were affected by low temperature hydrothermal alteration that was responsible for the precipitation of pyrite.

The demanding quality parameters for the new industrial applications concern grain size (90% between 10-50 mm), S content (48 ± 2 wt%) and Fe (above 44 wt%). These conditions are satisfied at Fusharrez, Spaç, and Trepça rock pyrite, while at Lunik are not.

Flotated pyrite, due to its fine grain size (< 0.075 mm), can be used only for the glass industry. Trepça tailings do not satisfy chemical quality parameters, while at Fusharrez tailings reach the values for glass industry.

References

BECCALUVA, L., COLTORTI, M., PREMTI, I., SACCANI, E., SIENA, F. & ZEDA, D. (1994): Ofioliti, 19(1): 77–96.

HEINRICH, C.A. & NEUBAUER, F. (2002): Mineralium Deposita, 37: 533–540.

MORPHOLOGY AND TEXTURE OF ZIRCONS AND THEIR INCLUSIONS OCCURRING IN GRANITOID ROCKS OF THE MECSEK MTS., HUNGARY

KIS, A.[1]*, KLÖTZLI, U.[2], KOLLER, F.[2] & BUDA, Gy.[1]
[1] Department of Mineralogy, Eötvös Loránd University, Pázmány Péter sétány 1/C, H-1117 Budapest, Hungary
[2] Department of Lithospheric Researches, University of Vienna, Althanstraße 14, A-1090 Vienna, Austria
* E-mail: annamari.kis@gmail.com

Major outcrops of Variscan plutonic rocks are found in South Hungary in the Mecsek Mountains. Four major rock-types can be distinguished: microcline megacryst-bearing granitoids (quartz monzonite), mafic enclaves (melasyenite, melamonzonite) in granitoids, hybrid rocks (quartz syenite) in the zone between granitoids and enclaves, and microgranite (dikes). This granitoid is mainly I-type. Rock forming minerals are microcline, plagioclase with "spike" zonation, biotite (Mg-rich), hornblende (Mg-rich) and quartz. Accessory minerals are allanite, zircon, apatite, titanite, pyrite, chalcopyrite in all rock-types. In the mafic enclaves, small amount of chromite can be found, too.

We studied the morphology of zircons of the microcline megacryst-bearing granitoids, mafic enclaves and hybrid rocks using Pupin-diagram. Three zircon types have been distinguished: 1. "normal" calc-alkaline magmatic zircon (S_{24}, S_{25}) in biotite, amphiboles and feldspar, 2. flat prismatic zircon (AB_5) (that had been earlier considered as S_4) in biotite 3. elongated, prismatic zircon (P_5) in feldspar and quartz.

Detailed internal textures of zircons had been studied by cathodoluminescence and backscattered electron imaging methods. Four zircons texture-types (primary textures and secondary texture) were distinguished: The primary textures are 1. grown zoning (possibly oscillatory zoning), 2. normal magmatic zoning with xenocrystic core, both occur in the three rock types, 3. sector zoning (that had not been earlier considered) in hybrid rock. The secondary texture is convolute zoning also occurring in the three rock types. Modifications of magmatic zircon during late and post-magmatic cooling or metamorphism tends to result in a disruption of grown zoning.

Different inclusions have been found in zircons: apatite, feldspar, biotite, quartz, chlorite, thorite/uranothorite. We distinguished multiphase (K-feldspar, albite, quartz) and single phase inclusions in zircons. This indicating that zircon crystallized continuously during the solidification of granitoid magma. The multi phase inclusions crystallized latter at a lower temperature from the Si-rich granite melt.

These morphological and textural investigations are important before applying the U-Pb, Th-Pb geochronology of zircon using LA-ICP-MS techniques in order to select the different generations of zircons and exclude metamictization and other secondary alterations by the picking of entire zircons without cracks. By these methods we can determine the origin and age of the crystallization of different rock-types and probably age of K-metasomatism e.g. mafic enclaves can be restitic in origin (ages of granitoids and enclaves are different), or "in situ" unmixing of felsic and mafic magma (same crystallization age). Xenolithic origin is not possibly because of the morphology and very similar composition of the enclaves.

This study supported by HRF (OTKA), No. 67787.

Au-PORHYRY SYSTEMS AND THEIR OUSTANDING FLUID PROPERTIES – EXAMPLE FROM THE BIELY VRCH DEPOSIT, SLOVAKIA

KODĚRA, P.[1]*, HEINRICH, C.A.[2], WÄLLE, M.[2] & FALLICK, A.E.[3]
[1] Department of Geology of Mineral Deposits, Faculty of Natural Sciences, Comenius University, Bratislava, Slovakia
[2] Dept. of Earth Sciences, ETH Zurich, Switzerland; [3] Scottish Universities Environmental Research Centre, Glasgow, UK; * E-mail: peter.kodera@gmail.com

Au porphyries are a relatively new type of porphyry deposit of increasing importance. Common properties of these systems are significantly lower Cu content (< 0.25%) than Cu-Au porphyries, low amounts of sulphides and enrichment in magnetite. They are thought to originate at shallow depths (< 1 km) from magmatic fluids affected by decompression (MUNTEAN & EINAUDI, 2001). EMED Mining Ltd. recently discovered a typical Au-porphyry mineralisation at six localities in the Neogene Javorie stratovolcano, forming a new Au-porphyry province. The Biely Vrch deposit is centred on a diorite to andesite porphyry stock, emplaced into andesitic volcanic host rocks. Stockwork of quartz veinlets mark the area of economic Au mineralisation. Alteration is dominated by intermediate argillic (IA) that variably overprints earlier K-silicate at shallow and Ca-Na silicate alteration at deeper levels. Propylitisation forms an outer alteration zone. Ledges of advanced argillic (AA) alteration are the youngest alteration type. Several generations of veinlets are dominated by quartz. Veinlets are often banded with botryoidal textures. Gold grains of several generations are of high fineness and occur in altered rock next to the quartz veinlets (KODĚRA *et al.,* 2010).

Vapour inclusions dominate (> 95% of inclusions) in all generations of vein quartz. Especially A-type quartz veinlets also host inclusions with a green anisotropic solid and variable proportions of vapour, but no aqueous liquid, interpreted as inclusions of hydrous salt melt and vapour. Microthermometry showed quick melting of the solid in the range 320–380°C, but total homogenisation (Th) was never reached prior to 900°C, indicative of heterogeneous trapping and/or post-entrapment modification due to α- to β-quartz transition. Rarer, vapour-free, salt melt inclusions with tiny opaque grains and trails or clusters of opaque sulphides (sulphide melts in origin?) are also sometimes associated. LA ICPMS microanalysis showed that vapour as well as salt melt bearing inclusions contain major elements Fe-K-Na-Cl in relatively stable proportions ($FeCl_2$ > KCl > NaCl) with charge balance between major cations and Cl ranging from 0.5 to 1.6 (median 1.1). Due to very high Fe-K content and high total salinity, crystallising salts incorporated all available water forming hydrous salt melts in addition to a much bigger volume of vapour. Low-density vapour, accompanied by extreme "brines", resulted from fluid heterogeneisation at very low pressures (deduced from phase relations in the NaCl–H_2O system). Shallow emplacement of the parental intrusion is also suggested by rapid supersaturation of SiO_2 in fluids inferred from banded veinlets, likely resulting from rapid fluid decompression. Most of the inclusion assemblages had similar or even lower Cu/Au ratio as it is the average ratio of the deposit (0.023 wt% Cu/ppm Au; HANES *et al.,* 2010), except of a sample of a quartz xenolith showing significantly higher ratios in inclusions. This indicates that deeper and/or earlier fluids had significantly higher Cu content than shallow/earlier fluids. Gold is preferentially concentrated in vapour (in respect to total salinity of inclusions). Most of Au precipitated from vapour together with secondary feldspar and Fe-oxides but without abundant sulphides, due to the effective stripping of the stabilising hydration sphere of gold complexes in a high-T but low-P subvolcanic fumarole environment (WILLIAMS-JONES & HEINRICH, 2005). Cu and Ag do not show preferential concentration except of the quartz xenolith sample. Rare liquid-rich inclusions are mostly secondary, trapped from late fluids (~0–5 wt% NaCl eq., Th 230–260°C).

Oxygen isotope data from vein quartz and magnetite showed very little variation from surface down to ~700 m, indicating isotopically homogenous, purely magmatic fluid source. Both minerals were in equilibrium with the fluid at ~672°C. Missing thermal gradient of magmatic fluids is consistent with decompression in shallow depth. Fluids in equilibrium with illite-smectite from the IA alteration also contained a significant meteoric component. Several generations of gold point to significant remobilisation of gold in the system by later aqueous fluids in the clay mineral stability field, composed of mixture of magmatic and meteoric fluids. Isotopic composition of fluids in equilibrium with minerals from the AA alteration indicate subsequent mixing of magmatic and meteoric fluids upon cooling. A temperature of crystallization of coarse-grained alunite 294°C was calculated based on isotope fractionation between SO_4 and OH groups in alunite. Sulphur isotope data for alunite ($\delta^{34}S$ 10.6 to 15.6‰) are suggestive of a magmatic-hydrothermal origin.

Support by APVV grant 0537-10, VEGA grant 1/0311/08 and EMED Mining, Ltd. is acknowledged.

References

HANES, R., BAKOS, F., FUCHS, P., ŽITŇAN, P. & KONEČNÝ, V. (2010): Mineralia Slov., 42: 15–32.
KODĚRA, P., LEXA, J., BIROŇ, A. & ŽITŇAN, J. (2010): Mineralia Slovaca, 42: 33–56.
MUNTEAN, J.L. & EINAUDI, M.T. (2001): Economic Geology, 96: 743–772.
WILLIAMS-JONES, A.E. & HEINRICH, C.A. (2005): Economic Geology, 100: 1287–1312.

GEOCHEMISTRY OF THE NANNA PEGMATITE, NARSAARSUUP QUAAVA, SOUTH GREENLAND

KOLLER, F.[1]*, MEISEL, T.[2], PETERSEN, O.V.[3] & NIEDERMAYR, G.[4]
[1] Department of Lithospheric Research, University of Vienna, Altanstraße 14, A-1090 Vienna, Austria
[2] Department of General and Analytical Chemistry, University of Leoben, Austria
[3] Geological Museum Copenhagen, Denmark
[4] Natural History Museum of Vienna, Burgring 7, A-1010 Vienna, Austria
* E-mail: friedrich.koller@univie.ac.at

The Nanna pegmatite is located near Narssârssuk on a plateau between the Igaliko and the Tunugdliarfik fiord. The Nanna pegmatite is a small lens-shaped body in the border zone of the huge Igaliko nepheline syenite complex. The pegmatite forms a lens like body and is surrounded by a ~20 cm wide leashing zone in the nepheline syenite. The pegmatite is less than 10 m long and slightly more than 50 cm wide, towards the north it ends fairly abruptly, towards the south it is thinning more gradually. The dipping is about 45° to the east.

The pegmatite is zoned with a fine grained border zone, definitely best developed in the visible top part. In the top part of the pegmatite this border zone is up to 10 cm wide and is dominated by aegirine and catapleiite and minor feldspar.

The central and main part of the pegmatite consists of sodalite (variety hackmanite), natrolite, some analcime, platy crystals of feldspar, some aegirine prisms, needle shaped astrophyllite, and onion-shell-like aggregates of curved catapleiite crystals. Other minerals identified, mainly from the core zone, are calcio-ancylite, fluorite, galena, gibbsite, leucophane, micheelsenite, polylithionite, todorokite and widespread the rare mineral nafertisite (PETERSEN *et al.*, 1999).

Most of the main elements in relation to the nepheline syenite are depleted, only Na and P are enriched up to 2 times, Mn more than 10 times. Very high enrichment of all volatile elements can be found in the pegmatite like F, Cl, S, CO_2 and H_2O with enrichment factors up to 10. Also Li is 10 times enriched in both, the border and core zones. Be increase from few ppm in the nepheline syenite up to 370 ppm Be in the core area and is mainly incorporated in the hackmanite. Further, the incompatible elements (Y, Nb, Ta, Zr, Hf, Th, and the REE) are also highly enriched in the pegmatite with varying factors up to 300. Especially the border zone contains up to 18 wt% trace elements, the core area only 4.6 wt%. The LREE elements are in the core zone ~100 times enriched, in the border zone up to 160 times. In contrast the HREE are less enriched, up to 20 times in the core zone, but generally higher in the rim zone. They are incorporated into the rare minerals.

The leashing zone in the surrounding nepheline syenite shows only a moderate increase of the volatile elements and almost no enrichment in the incompatible elements.

Reference

PETERSEN, O.V., JOHNSEN, O., CHRISTIANSEN, C.C., ROBINSON, G.W. & NIEDERMAYR, G. (1999): Neues Jahrbuch für Mineralogie – Monatshefte, 1999: 303–310.

THE DEMANTOID GARNETS OF THE GREEN DRAGON MINE (TUBUSSI, ERONGO REGION, NAMIBIA)

KOLLER, F.[1]*, NIEDERMAYR, G.[2], PINTÉR, Zs.[3] & SZABÓ, Cs.[3]
[1] Department of Lithospheric Research, University of Vienna, Altanstraße 14, A-1090 Vienna, Austria
[2] Natural History Museum of Vienna, Burgring 7, A-1010 Vienna, Austria
[3] Lithosphere Fluid Research Lab, Department of Petrology and Geochemistry, Eötvös Loránd University, Pázmány Péter sétány 1/C, H-1117 Budapest, Hungary
* E-mail: friedrich.koller@univie.ac.at

Demantoid garnets are known from the forelands of the Erongo Mountains in Namibia since mid of 1990's, but it is worth to note that also a Sn-bearing andradite has been reported approximately 70 years earlier from farm Davib Ost 61. The demantoid garnets of the Green Dragon Mine near Tubussis are bound to a neoproterozoic metasedimentary sequence consisting of schists, amphibolites, calc-silicate rocks and marbles part of the Damara Orogen. In Cretaceous time this sequence was intruded by granitic rocks of the Erongo Complex (MILLER, 2008). The granitic dikes are exposed also in the Green Dragon Mine and it is not unlikely to assume that these granitic rocks might at least in part have given rise to a contact metamorphism of the marbles resulting in the formation of calc-silicate rocks and even andradite garnet, too. Therefore, demantoid garnets can be found in the marbles, as well as in the calc-silicate rocks along the contact to the granitic veins and plugs.

In the calc-silicate rocks a zone with up to 1–2 cm large green garnet crystals in a calcite matrix together with quartz and minor silicates is common. These green garnets are close to an andradite end-member composition with low Ti, Cr, Mn and Mg content. The rim of these garnet shows a complex zoning with anisotropic zone formed by increasing grossular component (up 40 mol%) and Ti contents up to 1.6 wt% TiO_2. Few crystals show a wider variation with a complex zoning ranging from pure andradite to almost pure grossular. Diopside (X_{Mg} = 0.92–0.95), wollastonite, quartz, calcite and sphalerite were found as inclusions. Sometimes they also form vein type pockets with perfect crystals of high gem quality and perfect shape, they occur together with quartz and prehnite. In the marble and massive calc-silicate rock a more brownish garnet with an almost pure grossular end-member is common.

Several generations of fluid inclusions can be recognized in the garnet. All fluid inclusion generations have secondary origin as the fluids are trapped along healed fractures. Based on the shapes, three different "age" generations can be distinguished. The oldest generation fluid inclusions could be seen in 30–60 micrometer sizes. They always contain a vapour bubble, a liquid phase and several solid phases. The "middle" generation fluid inclusions have 20–70 micrometer size; they show irregular ratty shape with a vapour and a liquid phase, rarely also solid phase. The "youngest" generation fluid inclusions occur in small size (10–50 micrometer). They are always characterized by dark color, and two fluid phases as vapour and liquid.

Microthermometric measurements were carried out in the "oldest" generation fluid inclusions. The liquid phase could be H_2O–$CaCl_2$ system (first melting point is around -45°C). The other (two) fluid inclusion generations show the same microthermometric nature and results as the older generation one, therefore they can be the same salty H_2O system. The last melting point of the fluid inclusions suggests low salinity: 6–8% in $CaCl_2$–H_2O system (in Na-equivalent salinity: 10–13%, after ROEDDER, 1984). Raman spectroscopy, used at room temperature, indicates the presence of CH_4 in vapour phase.

References

MILLER, R.M.G. (2008): The geology of Namibia. Geological Survey of Namibia, Windhoek.

ROEDDER, E. (1984): Fluid inclusions. Reviews in Mineralogy, 12: 1–646.

MINERALOGICAL AND GEOCHEMICAL STUDY OF ALTERATION HALOES IN BASALTS OF THE BAKONY–BALATON HIGHLAND VOLCANIC FIELD, HUNGARY

KÓNYA, P.[1]*, SZAKÁLL, S.[2] & BARTHA, A.[1]
[1] Geological Institute of Hungary; Stefánia út 14, H-1143 Budapest, Hungary
[2] Institute of Mineralogy and Geology, University of Miskolc; H-3515 Miskolc-Egyetemváros, Hungary
* E-mail: peter.konya.zeo@gmail.com

Alteration haloes occurring around the cavities in basalt of the Bakony–Balaton Highland Volcanic Field (BBHVF) are 0.5 to 3 centimetres wide, having light or dark gray, rarely greenish brown colour. The rims have always a larger grain size than basalt matrix indicating this similar to the pegmatite stage (pseudo-pegmatite texture).

Minerals, chemical composition and paragenesis of the alteration halo are less studied in basalts. The haloes have not been mentioned before from BBHVF. However, our recent studies found alteration haloes in 365 samples. Based on appearance and grain size of rims, these were classified to three groups. Group 1: grey, fine-grained, massive alteration haloes with green olivine phenocrysts and rare cavities filled with phillipsite. Group 2: grey, coarse-grained, massive haloes with pyroxene, feldspar and opaque crystals in matrix. Group 3: greenish grey fine- and coarse-grained alteration haloes with olivine, pyroxene, feldspar and opaque crystals in matrix (Fig. 1). 15 of these rims were characterized in detail by XRD, thin section and ICP-MS methods.

One part of the minerals of alteration haloes equal to the basalt matrix: apatite, biotite, K-feldspar, magnetite, nepheline, olivine, pyroxene and plagioclase. The other part of minerals consists of hydrothermal phases: zeolites (analcime, chabazite, phillipsite) and clay minerals (chlorite, illite, illite/smectite mixed layer minerals and smectite).

Chondrite-normalized rare earth elements are very similar to the other alkaline basalts in Carpathian-Pannonian Region (SEGHEDI *et al.*, 2004). Basalts and alteration haloes of BBHVF show enrichment in LREE and depletion in HREE, with a negative Eu anomaly.

The main mineralogical components (apatite, pyroxene, K-feldspar, plagioclase, olivine, phillipsite and smectite) of alteration haloes can observed in the most of the rims. Consequently the crystallization and then alteration were very similar in the haloes. Occurrence of high temperature (miarolitic) minerals was followed by alteration of these minerals at low temperature. Coloured phases altered to smectite, and colourless phases (e.g. nepheline) altered to zeolites by hydrothermal fluids. Differences in the quantity of hydrothermal minerals show the distinct degree of alteration.

Reference

SEGHEDI, I., DOWNES, H., SZAKÁCS, A., MASON, P.R.D., THIRLWALL, M.F., ROŞU, E., PÉCSKAY, Z., MÁRTON, E. & PANAIOTU, C. (2004): Lithos, 72(3-4): 117–146.

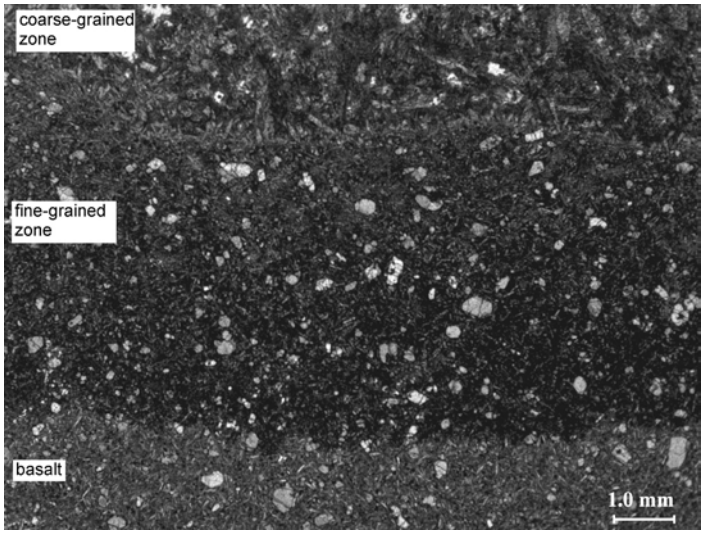

Fig. 1. *Fine- and coarse-grained alteration halo.*

BENTONITE OCCURRENCES IN THE BUDATÉTÉNY–SÓSKÚT REGION (CENTRAL HUNGARY)

KOVÁCS-PÁLFFY, P.[1]*, KÓNYA, P.[1], FÖLDVÁRI, M.[1], THAMÓ-BOZSÓ, E.[1], SZEGŐ, É.[1], ZELENKA, T.[2] & PÉCSKAY, Z.[3]
[1] Geological Institute of Hungary; Stefánia út 14, H-1143 Budapest, Hungary
[2] Institute of Mineralogy and Geology, University of Miskolc; H-3515 Miskolc-Egyetemváros, Hungary
[3] Institute of Nuclear Research of the Hungarian Academy of Sciences, Bem tér 18c, H-4026 Debrecen, Hungary
* E-mail: kovacs@mafi.hu

The investigated area is situated on a calcareous plateau in south-west from the center of Budapest. The bentonite occurrences are intercalated in Sarmatian limestones of the Tinnye Formation. There are 1–6 bentonite strata with thickness of 0.1–0.8 m. They were produced by the hydrodiagenetic alteration of rhyolitic-dacitic tuffs (Galgavölgy Rhyolite Tuff) based on their stratigraphical position, mineral composition, and total silica vs. alkali content (Fig. 1).

According to the XRD and thermal analysis, the montmorillonite content of the bentonite samples is between 58–96 wt%. The other mineralogical components of the samples are biotite, quartz, zircon and apatite. These bentonites are characterized by the absence of cristobalite.

The predominant exchangeable cation is Ca^{2+}, and subordinately Na^{+}. The cation exchange capacity (meqv/100g) of the samples are the follows: Ca^{2+} (0.57–0.75), Mg^{2+} (0.12–0.24), Na^{+} (0.02–0.33) (Budatétény) and Ca^{2+} (0.90–0.95), Mg^{2+} (0.06), Na^{+} (0.05–0.07) (Sóskút).

The swelling capacity ranges from 6.6 to 14.0 (natural) and from 14 to 29 (activated, ml/2g).

According to the K/Ar dating on biotite crystals, the age of these bentonites is between 11.7 (Sóskút) and 13.2 (Budatétény) Ma.

Frequently a Sarmatian Foraminifera association of *Elphidium* (*E. macellum, E. aculeatum*) and *Cibicidoides lobatulus* is present in the samples.

The bentonite and the limestone in this region was mined underground at Budatétény (Endre Gallery) and Nagytétény between 1934 and 1965. The main product was limestone blocs, which were used in construction. The bentonite was used predominantly to purify mineral oils and bond foundry sands, and it was exported as activated bentonite to Germany (former East Germany), Poland and former Czechoslovakia.

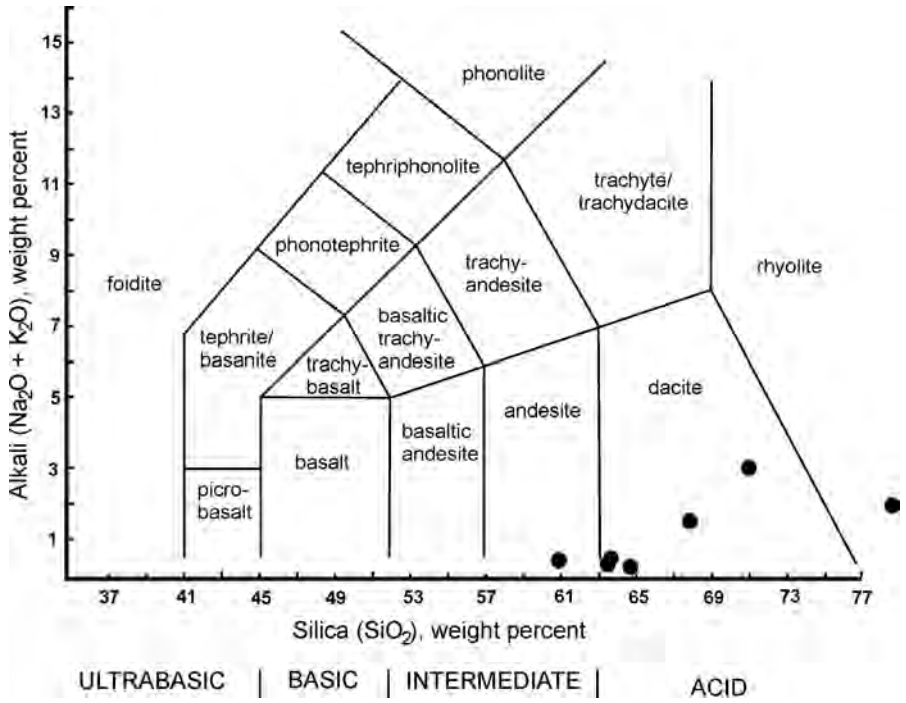

Fig. 1. *Total silica vs. alkali diagram of the studied bentonites.*

GEIGERITE, A NEW MEMBER OF THE KRAUTITE-VILLYAELLENITE PARAGENESIS FROM SĂCĂRÂMB (SOUTHERN APUSENI MTS., ROMANIA)

KRISTÁLY, F.[1]*, GÁL, Á.[2], SZAKÁCS, A.[3] & SZAKÁLL, S.[1]
[1] Institute of Mineralogy and Geology, University of Miskolc, H-3515 Miskolc-Egyetemváros, Hungary
[2] Department of Geology, Babeş-Bolyai University, Kogalniceanu 1, RO-400084 Cluj-Napoca, Romania
[3] Dept. of Environmental Sciences, Sapientia University, Matei Corvin str. 4, RO-400112 Cluj-Napoca, Romania
* E-mail: askkf@uni-miskolc.hu

The Săcărâmb (formerly Nagyág) low-sulphidation epithermal deposit is located in the southern termination of the "Gold Quadrilateral" of the Apuseni Mts., Romania. The deposit is hosted by amphibole andesites containing plagioclase, biotite, quartz and sparse resorbed pyroxene. Besides common sulphides and tellurides, Mn-minerals are unusually common and diverse. As-bearing sulphosalts, As-sulphides and native As are common in several segments of the deposit, too. Arsenates were observed in the late stage hydrothermal products related to the presence of As. Săcărâmb is the type locality of krautite, $MnAsO_3(OH)_2 \cdot H_2O$ (FONTAN *et al.*, 1975). Villyaellenite, $Mn_5(AsO_3OH)_2(AsO_4)_2 \cdot 4H_2O$ was also reported from krautite-bearing hydrothermal samples (GHERGARI *et al.*, 1994), accompanied by arsenolite and native arsenic. The current study adds a new member, geigerite, $Mn_5(AsO_3OH)_2(AsO_4)_2 \cdot 10H_2O$, to that paragenesis.

Geigerite, described for the first time from Romania, was found in samples from the Bernad adit. The material studied is a breccia-like brown to pink aggregate, with several millimetre sized groups of minute lamellar crystals. The aggregates are grown on a silky, fibrous to earthy material. Crystals of dark pink, pale pink to colourless and light blue colours were observed. Subspecimens, individual crystals for X-ray powder diffractometry (XRD), scanning electron microscopy (SEM) and energy dispersive spectrometry (EDS) were carefully prepared under stereomicroscope. XRD investigations were performed on ~1 mg samples with "zero-background" sample holder on a Bruker D8 Advance diffractometer (Cu*K*α, 40 kV and 40 mA). SEM and EDS investigations were carried out on polished specimens on a Hitachi S-8400 microscope equipped by Bruker X-flash EDS detector.

The silky material supporting the arsenate crystals proved to be amorphous by XRD (with a low quartz content), and was found to be a mixture of SiO_2 and Mn-arsenates by SEM and EDS. The dark pink crystals are krautite aggregates, with the main observed XRD peaks (d Å/hkl) at 7.980/020 and 100, 7.137/110, 5.643/120, 3.992/040 and 200, 3.863/210 and 3.187/230 and $\bar{1}12$. The pale pink crystals are mixtures of krautite and villyaellenite, presenting the peaks at 8.991/200, 8.280/110, 6.474/$\bar{1}11$, 6.168/111, 4.658/020 and $\bar{3}11$, 4.494/400 and $\bar{2}02$, 3.275/$\bar{5}11$, 3.235/420 and $\bar{2}22$ and 3.079/222 for villyaellenite. SEM observations reveal zoned Ca-substitution in the euhedral crystals, from 1 to 4 wt% (by oxides) according to EDS. For geigerite the main XRD peaks are 10.472/010, 7.836/100, 3.486/030 and 2.789/230. Traces of villyaellenite are also present. EDS measurements indicated the presence of calcium in <0.5 wt% (by oxides) as well as the variation of the As content.

The (Ca + Mn)/As (in atomic weight percents, without H) ratio of measured data is clustered around 0.75 (± 0.02) for the dark pink crystals, while this ratio for krautite is 0.73. For the blue crystals a value of 0.93 (± 0.03) is obtained, while geigerite is of value 0.92. Villyaellenite was detected as solid-solution with krautite. The silky mass supporting the crystals gave 0.69 (± 0.06) values (with no Ca content), which is not appropriate for any Mn-arsenate.

Based on the position of differently colored crystal groups relative to the silky matrix, a crystallization sequence of krautite to krautite-villyaellenite to geigerite is suggested. Geigerite, being the latest, the most hydrated phase, is rich in fluid inclusions, too. The high water/fluid content decreased the reliability of the EDS measurements.

References

FONTAN, F., ORLIAC, M. & PERMINGEAT, F. (1975): Bulletin de la Société française de Minéralogie et de Cristallographie, 98: 78–84.

GHERGARI, L., FORRAY, F., GÁL, Á. & FĂRCAŞ, T. (1994): Studia Universitatis Babeş-Bolyai, Geologia, 39: 127–140.

MINERALOGY OF WEATHERING PRODUCTS OF MINE WASTES AT SELECTED DEPOSITS IN SLOVAKIA

KUČEROVÁ, G.[1]*, LALINSKÁ-VOLEKOVÁ, B.[1], CHOVAN, M.[1], MAJZLAN, J.[2], GÖTTLICHER, J.[3] & STEININGER, R.[3]

[1] Department of Mineralogy and Petrology, Faculty of Natural Science, Comenius University, Mlynská dolina G, 842 15 Bratislava, Slovakia

[2] Institute of Geoscience, Friedrich-Schiller University, Burgweg 11, 07749 Jena, Germany

[3] Institute for Synchrotron Radiation, Karlsruhe Institute for Technology, Hermann-von-Helmholtz-Platz 1, 76344 Eggenstein-Leopoldshafen, Germany

* E-mail: kucerovag@fns.uniba.sk

In this study, we have investigated secondary minerals forming in the environment of mine tailings at the localities Slovinky, Rudňany-Markušovce and Čučma. Siderite-barite-sulphide deposit Rudňany and siderite-sulphide deposit Slovinky were intensively mined for Cu and Fe ores. Sulphide minerals include mainly chalcopyrite, tetrahedrite, pyrite and arsenopyrite. Sulphides at Sb-Au deposit Čučma are represented mainly by stibnite, pyrite and arsenopyrite.

Samples were collected from mine tailing impoundments from several boreholes and dug wells. Samples were separated into light and heavy fraction by panning in water or in ethanol. Several greenish and reddish grains were separated from all tailing material with binocular loupe from locality Slovinky. Selected heavy-grain concentrates were prepared for further study in the form of standard thin and polished grain mounts, for inspection in transmitted and reflected polarized light, respectively. Chemical composition of the individual grains and oxidation rims were determined with a Cameca SX100 electron microprobe (ŠGÚDŠ, Bratislava) in wavelength dispersive mode under the operation conditions of 15 kV, 20 nA. Samples of interest were later prepared for μ-X-ray diffraction experiments. The μ-XRD data were collected at the beamline of the Synchrotron Radiation Laboratory for Environment Studies (SUL-X, Angströmquelle, Karlsruhe, Germany) in the synchrotron radiation source ANKA. All the μ-XRD patterns were preliminary evaluated by the DIFRAC^{plus}EVA software using PDF4 database. The 1D XRD patterns were then used for the Rietveld refinement with the programs GSAS and TOPAS.

The most common sulphides in flotation wastes at Markušovce and Slovinky are pyrite and chalcopyrite, tetrahedrite occurs rarely. At Čučma, pyrite is the most abundant sulphide; arsenopyrite and stibnite are less common. Primary oxides in tailing impoundments are represented by hematite (Markušovce), and valentinite (Čučma). Oxidation products can be divided into two groups: oxidation rims on primary sulphides and individual grains of secondary oxides. Oxidation rims on pyrite grains are composed of Fe oxides/hydroxides with enhanced amounts of elements such as Mg, Mn, Ca, Si, As, Cu and Sb. These oxides were mostly identified as a mixture of poorly crystalline goethite with amorphous Fe oxy-hydroxides. Rims on chalcopyrite grains are depleted in Cu, compared to primary sulphide and conversely enriched in As, Sb and Ca (Slovinky). Rims on arsenopyrite grains are often depleted in As compared to primary arsenopyrite and enriched in Ca, Si, Cu, Pb (Slovinky, Markušovce) and Sb (Čučma).

Goethite is the most frequent secondary mineral at all studied sites, hematite is also common. Goethite grains from Markušovce and Slovinky are often enriched in Cu (up to 1.29 at%), Si (2.91 at%), Mg (2.1 at%), Mn (2.14 at%), Sb (0.38 at%) and As (0.46 at%). Cell parameter *a* is in the range from 4.5599(7) Å to 4.69(9) Å, *b* from 9.88(2) Å to 10.02(2) Å and *c* from 3.00(10) Å to 3.056(9) Å, cell volume is in the range from 136.46 Å^3 to 141.25 Å^3. A significant positive correlation was observed between cell parameter *b* and Cu content (R = 0.94), which can indicate substitution of Cu for Fe in the structure of goethite. Goethite grains from Čučma have following cell parameters: *a* is in the range from 4.55(8) Å to 4.7(2) Å, *b* from 9.9(4) Å to 10.05(1) Å, *c* from 2.98(4) Å to 3.06(4) Å and cell volume is in the range from 136.6(4) Å^3 to 140.4(2) Å^3. Differences in cell parameters are caused probably by enhanced amounts of elements such as Sb, As, Cu, from which at least a part is probably incorporated directly into the structure of the mineral. At Slovinky, secondary Cu minerals occur also frequently and were identified as cuprite, malachite and azurite, or their mixture. Secondary mineral covellite was observed in few samples at Slovinky and Markušovce. Products of tetrahedrite oxidation (Markušovce, Slovinky) are represented by Fe oxy-hydroxides with remains of Cu, Sb, As, Hg and S (from primary ore), and enhanced amounts of Ca and Mg (adsorbed from pore solutions). At Čučma, where the content of Sb is high in the tailing impoundment minerals from roméite group (pyrochlore supergroup) and tripuhyite were also identified.

Acknowledgement. This study was supported by the Slovak Research and Development Agency under the contract No. APVV-0663-10 and APVV-VMSP-P-0115-09.

CRYSTAL STRUCTURE STUDY OF JACUTINGAITE (Pt_2HgSe_3) AND TISCHENDORFITE ($Pd_8Hg_3Se_9$)

LAUFEK, F.[1]*, VYMAZALOVÁ, A.[1], DRÁBEK, M.[1] & DRAHOKOUPIL, J.[2]
[1] Czech Geological Survey, Geologická 6, 152 00 Praha 5, Czech Republic
[2] Institute of Physics AS CR v.v.i., Na Slovance 2, 182 21, Praha 8, Czech Republic
* E-mail: frantisek.laufek@geology.cz

Two naturally occurring phases Pt_2HgSe_3 and $Pd_8Hg_3Se_9$ were synthesised and structurally characterized. Recently, Pt_2HgSe_3 phase was discovered in hematite-rich auriferous veins, known as jacutinga, from Cauê iron-ore deposit (Itabira district, Minas Gerais, Brazil) (CABRAL *et al.*, 2008). This Pt-Hg selenide was observed in one polished section as a grain with size of 50 μm and occurs on an aggregate of atheneite, potarite and hematite. $Pd_8Hg_3Se_9$ phase is known from Tilkerode (Harz, Germany) as a mineral tischendorfite (STANLEY *et al.*, 2002). Crystal structures of these phases have not been hitherto known.

Because of extremely low amount of natural samples and difficulties connected with their isolation, the two above-mentioned phases were synthesized from elements by conventional solid-state reactions using silica glass tube technique. All attempts to prepare single crystals suitable for single-crystal examinations failed; hence the crystal structures of Pt_2HgSe_3 and $Pd_8Hg_3Se_9$ were determined from powder X-ray diffraction data. The programs EXPO2004 and SuperFlip were used for structure determinations; subsequent Rietveld refinements were performed width FullProf program.

Pt_2HgSe_3 phase, which was recently described as a new mineral jacutingaite (VYMAZALOVÁ *et al.*, 2012), crystallizes in space group $P\bar{3}m1$, (a = 7.34 Å, c = 5.29 Å, V = 247 Å^3) and Z = 2. Its crystal structure is composed of layers of [$PtSe_6$] octahedra and [$PtSe_4$] squares running parallel to (001) planes. The Se atoms are arranged in layers perpendicular to the **c**-axis forming the *Kagomé*-nets. The Hg atoms are located in voids, defined by Se atoms, between these layers. Jacutingaite is structurally related to the sudovikovite, $PtSe_2$.

The tischendorfite crystal structure shows *Pmmn* symmetry (a = 7.18 Å, b = 16.80 Å, c = 6.48 Å, Z = 2). Its crystal structure has two Hg sites, three Pd sites, and four Se sites and can be described as a three-dimensional framework.

References

CABRAL, A.R., GALBIATTI F.H., KWITKO-RIBERIO, R. & LEHMANN, B. (2008): Terra Nova, 20: 32–37.

STANLEY, C.J., CRIDDLE, A.J., FÖRSTER, H.J. & ROBERTS, A.C. (2002): Canadian Mineralogist, 40: 739–745.

VYMAZALOVÁ, A., LAUFEK, F., DRÁBEK, M., CABRAL, A.R., HALODA, J., SIDORINOVÁ, T. & LEHMANN, B. (2012): Canadian Mineralogist, 50: in press.

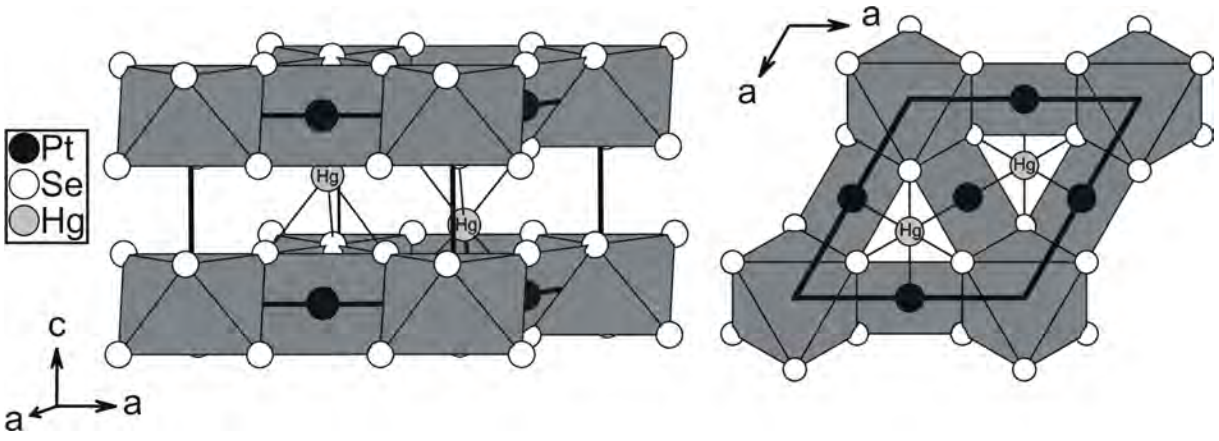

Fig.1. *Polyhedral depiction of the jacutingaite (Pt_2HgSe_3) crystal structure. [$PtSe_6$] octahedra and [$PtSe_4$] squares are emphasised (adapted from VYMAZALOVÁ et al., 2012).*

FORMATION MECHANISM OF α-QUARTZ FROM OPAL-A BY HYDROTHERMAL SYNTHESIS

LENART, A.[1]*, BRAČKO, I.[2], PLODINEC, M.[3], ŠTURM, S.[1] & MIRTIČ, B.[4]
[1] Department for Nanostructured Materials, Jožef Stefan Institute, Jamova cesta 39, SI-1000 Ljubljana, Slovenia
[2] Department for Advanced Materials, Jožef Stefan Institute, Jamova cesta 39, SI-1000 Ljubljana, Slovenia
[3] Department for Material Physics, Ruđer Bošković Institute, Zagreb, Croatia
[4] Department of Geology, Faculty for Natural Sciences and Engineering, Ljubljana, Slovenia
* E-mail: alenka.lenart@ijs.si

Introduction

The transitions of amorphous silica via various metastable phases (cristobalites, tridymites, silica-X and silica-K) to α-quartz are important from the geological perspective, especially with regards to sedimentation and diagenesis. The transition depends on the starting material, type and concentration of mineralizers, temperature, pressure and time of synthesis (BETTERMANN & LIEBAU, 1975). In the framework of our research we have shown that morphologically well-developed, micron-sized, low-temperature or α-quartz crystals can be obtained directly from opal-A at 250°C and 40 bar, without any intermediate phases being present.

Methods

The isothermal method was used, where in the whole volume of an autoclave a constant temperature is applied. Tetraethylorthosilicate (TEOS) was used as the silica precursor, distilled water as the solvent and NaOH as the mineralizer. The experiments were performed at pH = 12, 250°C, 40 bar and for different hydrothermal synthesis times. The obtained products were investigated with scanning and transmission electron microscopy, X-ray diffraction (XRD) and Raman spectroscopy.

Results and discussion

With the extension of the synthesis time, different silica products were formed. With a synthesis time of 8 h, polydisperse spheres of non-crystalline opal-A, which was determined by XRD and Raman spectroscopy, were obtained (Fig. 1a). After 12 h of synthesis, the spheres coalesced and formed amorphous aggregates (Fig. 1b). With a prolongation of the experiment to 24 h, XRD patterns showed that the obtained product is still amorphous; however, the Raman spectre revealed the beginning of the formation of α-quartz. When a longer reaction time was applied, the XRD detected α-quartz and also a significant change in morphology was noticeable. After 72 h of synthesis the XRD revealed the prevalence of α-quartz, and some small amount of opal-A was additionally detected by Raman. The transition from rounded quartz particles to quartz with already developed certain crystal faces was recognised (Fig. 1c). After 144 h the XRD pattern showed that the obtained product is pure low-temperature quartz, with no other phases being present. The solid product consisted of double-terminated, short-prismatic 3–4 μm crystals of quartz with well-developed, rhombohedral and prismatic crystal faces (Fig. 1d).

Conclusions

We studied the development of α-quartz crystals from nanoscale silicon dioxide spheres of opal-A in relatively low p-T conditions. The formation mechanism can be explained over several growth steps. After the TEOS hydrolysis and condensation reactions the nucleation of opal spheres begins (MASALOV *et al.*, 2011). This is followed by their aggregation. The next step includes the crystallization and formation of α-quartz nanocrystals from opal-A. As their size increases, they develop crystal faces. In the above-mentioned p-T conditions the following reaction sequence is taking place: opal-A → coalescence of spheres → formation of nanocrystalline quartz → micron-sized quartz with well-developed crystal faces.

References

BETTERMANN, P. & LIEBAU, F. (1975): Contributions to Mineralogy and Petrology, 53: 25–36.
MASALOV, V.M., SUKHININA, N.S., KUDRENKO, E.A. & EMELCHENKO, G.A. (2011): Nanotechnology, 22: 275718 (9 pp).

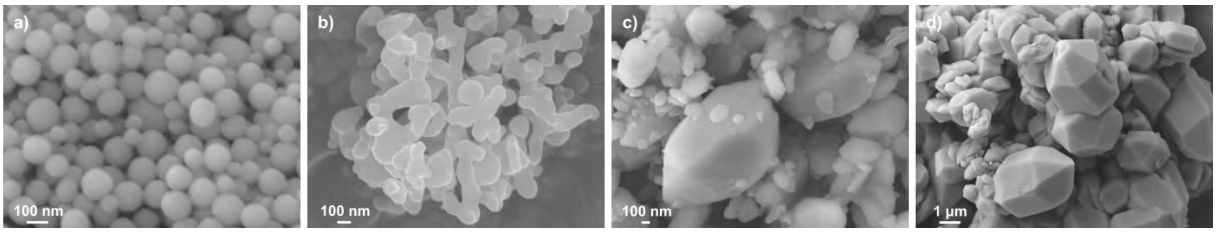

Fig. 1. *a) spheres of opal-A; b) coalescence of spheres; c) quartz with the beginning of formation of crystal faces; d) quartz with well-developed crystal faces.*

MODAL COMPOSITIONS AND TEXTURES OF ALKALI BASALT HOSTED UPPER MANTLE XENOLITHS FROM THE NORTHERN PART OF THE CARPATHIAN-PANNONIAN REGION (NÓGRÁD-GÖMÖR VOLCANIC FIELD, HUNGARY-SLOVAKIA)

LIPTAI, N.*, PATKÓ, L. & ARADI, L.
Lithosphere Fluid Research Lab, Department of Petrology and Geochemistry, Eötvös University, Pázmány Péter sétány 1/C, H-1117 Budapest, Hungary
* E-mail: n.liptai.elte@gmail.com

One possible way to understand upper mantle processes better is to study ultramafic xenoliths hosted in alkali basalt, kimberlite and lamprophyre. Upper mantle xenoliths from the five volcanic fields of Plio-Pleistocene alkali basalts in the Carpathian-Pannonian region (Styrian Basin, Little Hungarian Plain, Bakony-Balaton Highland, Nógrád-Gömör Volcanic Field, Perşani Mountains) have provided matter to petrologic and geochemical studies in the last few decades (e.g. EMBEY-ISZTIN *et al.*, 1989, 2001; DOWNES *et al.*, 1992; SZABÓ, 2004; DOBOSI *et al.*, 2010). In our work we concentrate on the Nógrád-Gömör Volcanic Field (NGVF), located at the northern part of the Carpathian-Pannonian region. We collected xenoliths from the central part of the area, including five quarries from Medves Plateau and Babi Hill that have barely been studied before.

From more than 200 collected xenoliths, over 80 samples were chosen for detailed petrographic examinations. The main aim was to determine texture types and modal compositions of the xenoliths regarding the rock-forming minerals, as well as describe fabrics of the mantle constituents (olivine, orthopyroxene, clinopyroxene and spinel). Based on the results, we present a detailed summary about the NGVF xenoliths, showing how they can be correlated with xenoliths originating from better researched marginal areas, introducing a texture type (poikilitic) (Fig. 1), as well as a rock type (wehrlite) (Fig. 2) that have not been reported before in earlier studies on the central part of the NGVF. It will also be presented that wehrlites show features of different texture types in the form of clinopyroxene-spinel aggregations sitting in the original texture, which indicates a possible mantle metasomatism that took place before the ascension of the host basaltic melt. Presence of amphibole in some of the xenoliths also confirms that this process enriched the upper mantle in incompatible elements.

References

DOBOSI, G., JENNER, G.A., EMBEY-ISZTIN, A. & DOWNES, H. (2010): Geological Society, London, Special Publications, 337: 177–194.

DOWNES, H., EMBEY-ISZTIN, A. & THIRLWALL, M.F. (1992): Contributions to Mineralogy and Petrology, 109: 340–354.

EMBEY-ISZTIN, A., SCHARBERT, H.G., DIETRICH, H. & POULTIDIS, H. (1989): Journal of Petrology, 30: 79–105.

EMBEY-ISZTIN, A., DOBOSI, G., ALTHERR, R. & MEYER, H.P. (2001): Tectonophysics, 331: 285–306.

SZABÓ, Cs., FALUS, Gy., ZAJACZ, Z., KOVÁCS, I. & BALI, E. (2004): Tectonophysics, 393: 119–137.

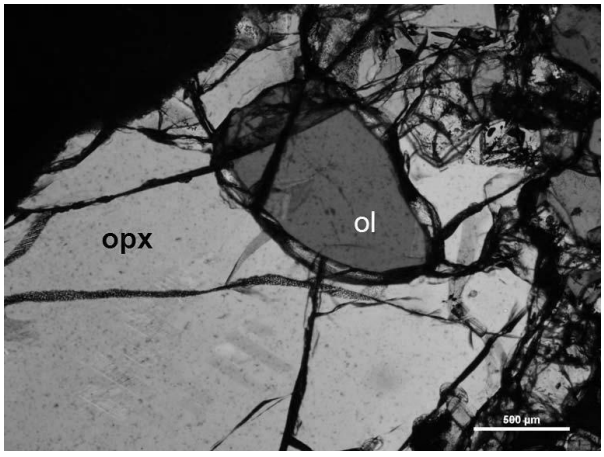

Fig. 1. *Olivine (ol) inclusion in orthopyroxene (opx) as an indication of poikilitic textured lherzolite; transmitted light, N+*

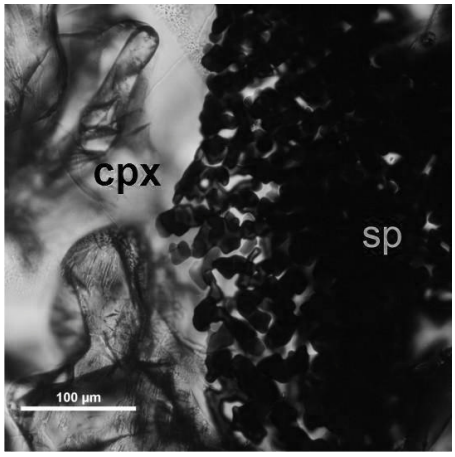

Fig. 2. *Aggregation of clinopyroxene (cpx) and vermicular spinel (sp) in a wehrlite; transmitted light, 1N*

STUDY OF SECONDARY MINERALS OF ABANDONED Cu DEPOSIT Ľ'UBIETOVÁ-PODLIPA (SLOVAKIA)

LUPTÁKOVÁ, J.*, MILOVSKÁ, S., BIROŇ, A., JELEŇ, S. & ANDRÁŠ, P.
Geological Institute, Slovak Academy of Sciences, Ďumbierska 1, 974 01 Banská Bystrica, Slovakia
* E-mail: luptakova@savbb.sk

This study presents preliminary results of detailed mineralogical investigation of sulphide oxidation products at abandoned Cu-Fe deposit at the Ľubietová-Podlipa (Central Slovakia). Our research goal is to determine release, migration and precipitation of metallic and non-metallic compounds under weathering conditions at the deposit. The Cu-Fe ore district Ľubietová has rich mining history and is nowadays famous as an interesting mineralogical locality. Environmental issues on this deposit comprise mainly oxidation of primary sulphides and forming of secondary phases such as those under this study. Our investigation was focused on Fe-oxy-hydroxides (known as good scavengers of many elements), Mn-oxides and supergene minerals of Cu by means of XRD, SEM-EDS, WDS.

The goethite of several generations and morphological types was recovered from the dump debris. It was identified as the main component of massive hard Fe-oxy-hydroxides ("limonite"). Usually it occurs in assemblage with libethenite, pseudomalachite, malachite and occasionally with hematite or Mn-oxides. Visible growth zoning corresponds to variation of main and trace elements in alternating layers. Fe content ranges from 30.43 to 52.43 wt% with minor concentration of Cu (< 6.89 wt%), P (< 2.49 wt%), Al (< 0.67 wt%), rarely Bi (< 5.70 wt%), Mn (< 0.19 wt%) and Si (< 1.06 wt%), traces of Co, Sb, As occur. The XRD study shows well ordered crystal structure of goethite. Bi-oxide (bismite?) was found in association with goethite. It forms irregular aggregates with skeletal texture or impregnations along growth zones within goethite. Covellite, idiomorphic natropharmacosiderite and pharmacosiderite were determined in microcracks, cavities and rims of tennantite. Covellite with goethite and chalcocite also replace primary chalcopyrite. Isolated grains of Ag_2S (< 5 μm) are frequently found in cavities and matrix of goethite and Cu secondary minerals. Studied Mn-oxides form fine grained aggregates in cavities of goethite, secondary Cu-phases and on quartz, or they occur as an interface between pseudomalachite and goethite. Several characteristic morphologies have also distinctive chemical composition: (1) aggregates of subtle acicular and fibrous crystals up to 1 μm show Mn (< 43.87 wt%), Ba (< 8.60 wt%), Cu (< 7.25 wt%), Fe (< 6.47 wt%), Co (< 1.84 wt%) and Ca, Ni, K, Al < 1 wt%; (2) chaotically arranged platy crystals, up to 5 μm, with Mn (< 28.02 wt%), Cu (< 16.89 wt%), Co (< 10.18 wt%), Fe (< 4.99 wt%) and Al, P, Ba, Ca, K < 1 wt%; (3) fine-grained porous aggregates with variable concentration of Mn, Cu, Co, Ba, Fe (EDS). The XRD revealed presence of romanèchite, hollandite and cryptomelane. These phases exhibit poorly defined (diffuse) diffraction maxima of low intensity characteristic of low degree of structural ordering and small size of diffraction domains. Definitive identification and refinement of crystal chemistry will be further performed by vibrational spectroscopy on well-defined mineral separates. Systematically increased contents of heavy metals in the Fe-oxy-hydroxides (goethite) and Mn-oxides suggest, that on the studied deposit they act as "natural" chemical barriers.

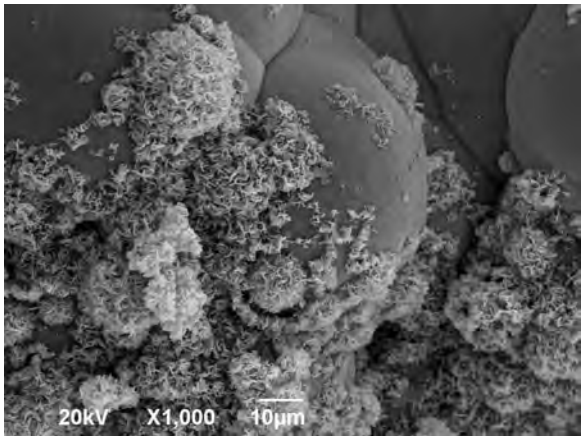

Fig. 1. *Platy crystals of Mn-oxides growing on goethite (SEM).*

During the study focused on secondary minerals, the ore minerals were also discovered. Some of them were already known (chalcopyrite, tetrahedrite, pyrite), others were expected (Ag_2S, gold, tennantite, bismuthinite, gersdorffite), but presence of others is surprising (cinnabar, cassiterite).

Acknowledgements. This study was financially supported by Slovak scientific agencies VEGA (contract No. 2/0065/11) and APVV (contract No. 0663-10) and by the Operational Programme Research and Development through the project: Centre of Excellence for Integrated Research of the Earth's Geosphere (ITMS: 26220120064), which is co-financed through the European Regional Development Fund.

LATE TOURMALINES AND THEIR UNUSUAL COMPOSITIONAL TRENDS IN GRANITIC PEGMATITES FROM THE BOHEMIAN MASSIF, CZECH REPUBLIC

MACEK, I.[1,2]* & NOVÁK, M.[2]
[1] Department of Mineralogy and Petrology, National Museum, Cirkusová 1740, 193 00 Prague, Czech Republic,
[2] Department of Geological Sciences, Masaryk University, Kotlářská 2, 611 37 Brno, Czech Republic
* E-mail: ivo_macek@nm.cz

The tourmaline-group minerals are useful geochemical indicators due to their refractory behaviour and chemical structure which can incorporate a lot of elements. We compared late tourmalines from three different types of granitic pegmatites in the Moldanubian Zone, Bohemian Massif. The first sample comes from NYF euxenite-type pegmatite Kožichovice III penetrating amphibole-biotite syenite of the Třebíč Pluton. The black core (schorl-dravite) with small dark blue rim (dravite) < 1 mm thick locally intergrowths with non-perthitic Kfs and Qtz. Chemical compositions of the rim with Al_{tot} 6.09–6.24 *apfu*, Mg 1.85–1.93 *apfu*, Fe_{tot} 0.69–0.80 *apfu* is Mg-Al enriched with $Fe_{tot}/(Fe_{tot} + Mg) \leq 0.30$ relative to the core with Al_{tot} 5.19–5.88 *apfu*, Mg 1.33–2.09 *apfu*, Fe_{tot} 0.90–1.60 *apfu* (Fig. 1). In desilicated LCT pegmatite near Dolni Bory situated on contact serpentinite and migmatic gneiss early black schorl with Al_{tot} 5.13–5.69 *apfu*, Mg 0.44–1.23 *apfu*, Fe_{tot} 1.99–2.67 *apfu* is overgrown by late fibrous dravite (enclosed in opal-CT) with Al_{tot} 6.07–6.37 *apfu*, Mg 1.45–1.62 *apfu*, Fe_{tot} 0.97–1.26 *apfu* (Fig. 1) and $F_{tot}/(Fe_{tot} + Mg) \leq 0.46$. The last examined sample was discovered in contaminated LCT elbaite-subtype pegmatite Bližná I, South Bohemia enclosed in dolomite-calcite marble. Late aggregate to fibrous blue dravite with Na 0.49–0.61 *apfu*, Ca 0.04–0.13 *apfu*, Mg 1.97–2.22 *apfu*, Fe_{tot} 0.20–0.34 *apfu*, Al_{tot} 6.15–6.36 *apfu* and $Fe_{tot}/(Fe_{tot} + Mg) \leq 0.15$ grows on olive green to brown aggregate of liddicoatite-elbaite with Na 0.16–0.71 *apfu*, Ca 0.23–0.79 *apfu*, $Mg \leq 0.76$ *apfu*, $Fe_{tot} \leq 0.39$ *apfu*, Al_{tot} 6.67–7.82 *apfu* (Fig. 1). These late tourmalines show similar compositions with moderate Al_{tot} (6.07–6.37 *apfu*) mostly low Ca (0.04–0.13 *apfu*), quite variable X-site vacancy (0.04–0.47 *apfu*) very low Ti (≤ 0.05 *apfu*), low F (≤ 0.17 *apfu*) and high activity of Mg (1.45–2.22 *apfu*).

Textural relations and chemical composition indicate change of crystallization conditions (decrease in temperature, transition of parental medium from melt to hydrothermal fluid, opening of the system to host rocks) during tourmaline evolution. Such dravitic composition (Fig. 1) might be stable in low-T conditions similar to authigenic tourmaline originated during diagenetic processes (e.g., SPERLICH *et al.*, 1996; AUBRECHT & KRIŠTÍN, 1995).

Acknowledgements. This work was supported by internal grant of National museum, Prague 2011/05/IG-PM to IM and research project GAČR P210/10/0743 to MN.

References

AUBRECHT, R. & KRIŠTÍN, J. (1995): Mineralia Slovaca, 27: 37–44.

SPERLICH, R., GIERÉ, R. & FREY, M. (1996): American Mineralogist, 81: 1222–1236.

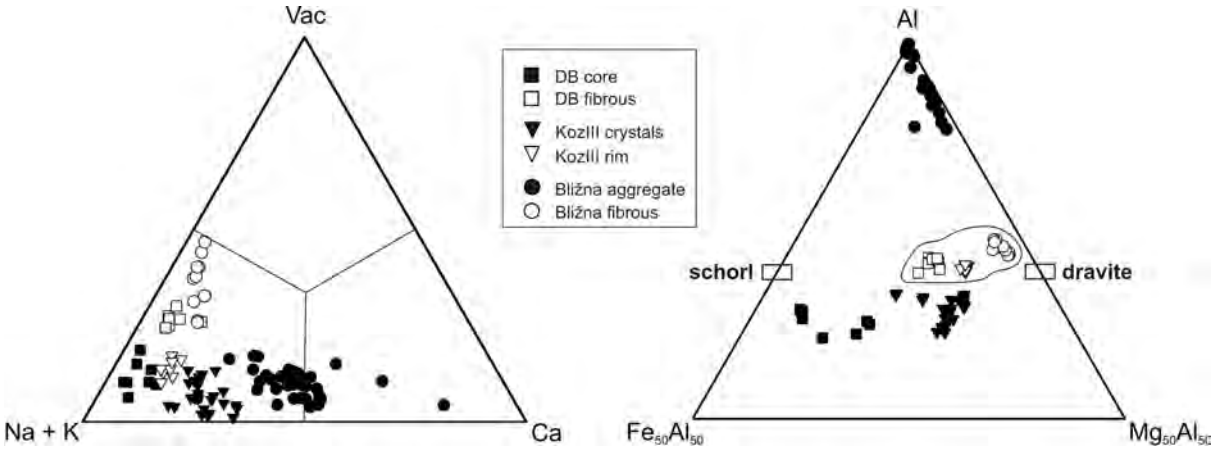

Fig. 1. *Chemical compositions of early to late tourmalines from three distinct localities in the Moldanubian Zone, Bohemian Massif, Czech Republic.*

COMPOSITION AND MICROSTRUCTURE PROPERTIES OF GEOPOLYMER MATERIAL MADE OF ACIDIC FLY-ASH WITH NaOH TREATMENT

MÁDAI, F.* & KRISTÁLY, F.
Institute of Mineralogy and Geology, University of Miskolc, H-3515 Miskolc-Egyetemváros, Hungary
* E-mail: askmf@uni-miskolc.hu

Utilization of industrial and mining wastes is an important issue all over the world, promoted also by the Directive 2006/21/EC (management of wastes from the extractive industry). In Hungary, the lignite-based Visonta thermal power plant generates 160–200 tons of slag and fly ash per year (KOVÁCS, 2001). A viable way of its utilization is the production of construction blocks using geopolymerisation hardening.

The term "geopolymer" was used first by Davidovits in 1972 for three-dimensional Al-silicates that are formed from naturally occurring Al-silicates at low temperature and short time by means of alkali activation (DAVIDOVITS, 1991). Treated by an alkali hydroxide solution, an amorphous poly(sialate) forms from SiO_4 and AlO_4 tetrahedra linked by shared oxygen atoms, while cations (Na^+, K^+ or Ca^{2+}) present in the framework, balancing the negative charges of the AlO_4 tetrahedra. The empirical formula is $M_n(-(SiO_2)_z-AlO_2)_n \cdot wH_2O$, where z is 1, 2 or 3, M is a monovalent cation such as K^+ or Na^+ and n is the degree of polycondensation (KOMNITSAS & ZAHARAKI, 2007). This polymerised gel material acts as an intergranular cementing phase, which consists of zeolitic nanocrystallites bound together by Al-silicate gel. The process of geopolymerisation involves leaching, diffusion, condensation and hardening (DAVIDOVITS, 1991).

Five test bodies treated by geopolymerisation had been produced at the Institute of Raw Material Preparation and Environmental Processing, University of Miskolc. Applied raw material was fly-ash from the Visonta power plant, additionally few percent of FGD gypsum was mixed. The test bodies differ in time of grinding: one was used without grinding, the other four were ground in ball mill for 10, 20, 30, 60 minutes respectively. After grinding the test materials were mixed with NaOH solution for 3 minutes, reaching moisture-saturated conditions and kept in cast for 4 hours, followed by a relaxation period for 16 hours at 20°C. Finally, heat treatment was applied for 4 hours at 150°C. Best average compressive strength (10.66 N/mm^2) was obtained for the test body ground for 30 minutes, however the test body ground for 10 minutes reached 5.15 N/mm^2 compressive strength.

Samples from the five test bodies were observed for microstructure characterisation using optical, SEM, EDS and XRPD methods. EDS element mapping and consecutively image processing was used to characterize the element distribution in the cementing phase and in leached fly-ash grains. Rietveld XRPD refinement has shown that about 88% of the ungrounded sample is X-ray amorphous material. It is justified by optical properties, too. The most abundant detected crystalline phase was mullite (7.5%) which was found also by its optical properties, forming a few aggregates of elongated crystals with 80–100 microns length. Another detected Al-silicate was sillimanite (1.5%). Few quartz (1.7%) and cristobalite (0.8%) grains and iron-oxide spherules present also as crystalline phases.

The chemical composition of the fly-ash grains and matrix was analysed by SEM and EDS. Beside Al, Si and O, five minor elements were detected: Na, Mg, Ca, K and Fe. In the Al-silicate grains the most abundant minor element is Na, most frequently reaching 3–4 at%, but in some grains and in the matrix up to 7.75 at%. The sum of other four minor elements (Mg, Ca, K, Fe) was usually less than 1 at%. Fig. 1. shows the Al vs. Si (+K, Ca, Fe, Mg) composition calculated for 13 oxygen of glassy fly-ash grains, solidified from the Al-silicate melt, from which some mullite and sillimanite crystallizes at higher temperature. Fig. 2. shows the elevated Na-concentration in sample ground for 30 minutes, indicating that Na appears in the intergranular cement and also by diffusion within some grains.

The work described was carried out as part of the TÁMOP-4.2.1.B-10/2/KONV-2010-0001 project in the framework of the New Hungarian Development Plan. The realization of this project is supported by the European Union, co-financed by the European Social Fund.

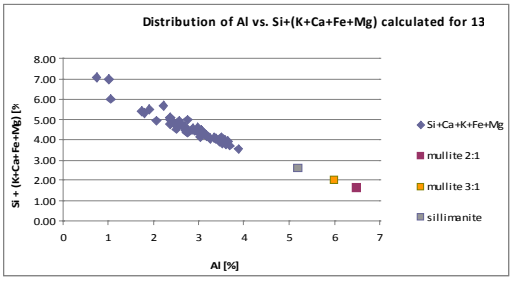

Fig. 1. *Distribution of Al vs. Si (+K, Na, Fe, Mg) in the glassy fly-ash grains.*

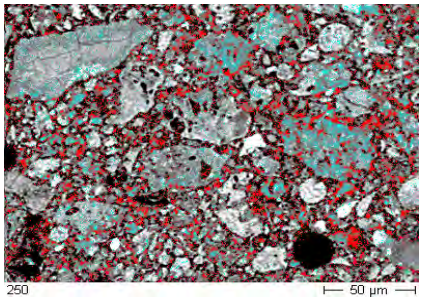

Fig. 2. *Distribution of elevated concentration of Na in the sample ground for 30 minutes. (BSE image combined with element map).*

References

DAVIDOVITS, J. (1991): Journal of Thermal Analysis, 37: 1633–1656.

KOMNITSAS, K. & ZAHARAKI, D. (2007): Minerals Engineering, 20: 1261–1277.

KOVÁCS, F. (2001): Publications of the University of Miskolc, Series A (Mining), 55: 67–76.

DETERIORATION OF DACITE FROM THE CSÓDI HILL QUARRY, DUNABOGDÁNY, HUNGARY

MÁDAI, F.* & KRISTÁLY, F.
Institute of Mineralogy and Geology, University of Miskolc, H-3515 Miskolc-Egyetemváros, Hungary
* E-mail: askmf@uni-miskolc.hu

The dacite laccolite of the Csódi-hill is a well-known object among mineralogists, petrologists and also rockhounds from Hungary. The quarrying in the Csódi-hill started in 1860, the present quarry has been operating since the 1980s, its main product is crushed stone, but there were attempts also to use it as a dimension stone. Hydrothermal alteration of the rock mass resulted in post volcanic cavity fillings that were investigated in detail by several authors (articles in PAPP, 1999). This monograph collected the information on mineralogy of different cavity fillings (zeolites, calcite) inclusions (serpentine-group minerals), petrogenesis of the dacitic rock mass as well as on appearance of iron-rich trioctahedral smectite.

In 2008 the operating firm indicated a specific problem of the hydrothermally altered rock type, asking some research from the Institute of Mineralogy and Geology of the University of Miskolc. It was observed that deponated crushed stone left for about a year in depot, has significantly lost its petrophysical quality after the sulphate crystallization test, while the freshly quarried stone fulfilled the quality requirements. Several methods, for instance, optical microscopy, whole rock XRPD, EDS, acoustic wave propagation, were used to characterize the differences among the freshly quarried unaltered (rock type 1), freshly quarried, hydrothermally altered (type 2) and the problematic, altered and deponated (type 3) rock types. Only very slight differences were found.

The alteration, appearance, composition, quantity of the main rock forming minerals (plagioclase, quartz, sanidine, biotite, amphibole) were very similar. Felsic minerals were fresh, while mafic minerals were intensively altered and interstitial smectite, nontronite and Fe-rich vermiculite, as well as iron oxides and hydroxides were found in all rock types. The hydrothermally altered samples contained more zeolites, and vermiculite. Significant difference was found however in acoustic wave propagation, showing that the deponated altered (type 3) rock has higher porosity than the freshly quarried ones (type 1 and 2): 3640 m/s vs. 4250 m/s respectively.

It was supposed that the interstitial smectite of the deponated, hydrothermally altered rock gradually changed to mixed-layer clay mineral, resulting in enhanced porosity.

Recently an other problem of the altered rock type from the same quarry was investigated: surface deterioration of dimension stone blocks made from this rock was observed. The blocks were used for pavement since 2006 and a 2–3 mm thick detachment crust has been formed.

Same methods were used for characterisation, accomplished with SEM element mapping. Detailed optical and SEM investigation of the detachment zone showed that the main detachment plane is accompanied by a zone of microcracks. Appearance of tiny (30–50 micrometers) Ca-sulphate grains were detected in the detachment plane by element mapping. Broken, cracked biotite and plagioclase crystals were found in the detachment zone, showing the result of salt-frost deterioration.

The interstitial smectite (reddish brown in thin section) in the detachment zone was replaced by blackish, loose aggregates of clay minerals, composition of which is characterised as follows by EDS. Combined with previous investigations, it was found that the smectite of the altered rock type changes by atmospheric interactions, resulting in quick deterioration of the stone.

Reference

PAPP, G. (Ed.) (1999): Minerals of Csódi Hill, Dunabogdány, Hungary. Topographia Mineralogica Hungariae, Vol. 6, Herman Ottó Museum, Miskolc.

Table 1. *Composition of interstitial clay mineral phases (EDS results) within and near the detachment zone.*

point number, phase	Na_2O	MgO	Al_2O_3	SiO_2	K_2O	CaO	FeO
2, blackish fine-grained aggregate	0.73	5.32	24.92	52.14	1.54	2.10	13.25
3, blackish fine-grained aggregate	0.51	4.82	22.10	56.43	0.87	1.89	13.38
5, blackish fine-grained aggregate	0.78	3.32	21.90	56.88	1.15	3.02	12.95
6, reddish-brown interstitial smectite	0.41	5.41	23.42	47.54	1.35	2.34	19.52
7, reddish-brown interstitial smectite	0.44	7.88	19.98	47.34	1.69	2.20	20.47

MINERALOGICAL CHARACTERISTICS OF WEATHERING CRUST ON THE POLISH FLYSCH CARPATHIAN SANDSTONES

MARSZAŁEK, M.[1]*, RZEPA, G.[1] & ALEXANDROWICZ, Z.[2]
[1] Department of Mineralogy, Petrography and Geochemistry, AGH – University of Science and Technology, A. Mickiewicza Ave. 30, 30-059 Kraków, Poland
[2] Institute of Nature Conservation, Polish Academy of Sciences, A. Mickiewicza Ave. 33, 31-120 Kraków, Poland
* E-mail: mmarszal@agh.edu.pl

The outer zones of protected sandstone landforms such as tors, crags, pillars, mushrooms and others, occurring in the area of the Polish Carpathians are covered by weathering crust with characteristic lamination running parallel to the rock surface (ALEXANDROWICZ & PAWLIKOWSKI, 1982; ALEXANDROWICZ, 2008). In the Carpathian Foothill these sandstones occur within Silesia Unit represented by thick bedded sandstone formations such as Istebna Beds (Upper Cretaceous to Paleogene) and Ciężkowice Sandstone (Lower Eocene). The results of the presented study concern the characteristics of the mineral composition of the surface zones of these natural sandstone forms.

Based on the results of previous work, 31 crust samples of Istebna and Ciężkowice sandstones from six locations were collected. Optical microscopy (Olympus BX 51), X-ray diffractometry (DRON-3.0), scanning electron microscopy with energy dispersive spectrometry (FEI Quanta 200 FEG with EDAX), electron microprobe (Cameca SX-100), Mössbauer spectroscopy (Wissel 360 spectrometer), thermal analyses (Derivatograph C) and sequential chemical extraction (see RZEPA *et al.,* 2011 for details) were used for examine the crust samples.

The main components of the studied sandstones are quartz, rock fragments, feldspars, micas and accessory heavy minerals. The cement is of a mixed nature and formed by a matrix and ferruginous phases – iron oxides and hydroxides sometimes accompanied by carbonate minerals. Ferruginous phases occur in intergranular spaces, comprise pigment in clay minerals, fill fractures in detrital minerals and form single grains of various morphology. Mineralogy of secondary Fe-bearing phases (mostly goethite and hematite) is responsible for the variable colouration and cementation of the sandstones. Goethite is present in yellow and brown-coloured zones, whilst hematite is responsible for red and pink hues. The latter is probably not a direct product of weathering of primary minerals, but is a product of goethite transformation (RZEPA *et al.,* 2011).

The external surface of sandstone is usually covered by a very thin, hard, black crust with a sharp-edged fracture. An amorphous film, up to ten plus micrometres thick, is carbon-rich and contains Si, Al, Fe, P, Cl and K. Aggregates of opal-type silica and small rings with a fairly uniform diameter of several micrometres, probably of biological origin are apparent. Spherical particles of aluminosilicate glass, and iron oxides particles (chiefly hematite) were also found. Their composition and morphology indicate that they originated from industrial emissions (MARSZAŁEK, 2008). Secondary crystalline phases, chiefly gypsum, barite, alunite-jarosite and halite also appear within this layer. The majority of these (except halite) were locally found in the form of a thin, interrupted laminae in a distance from the surface.

The presence of sulfate minerals: gypsum, barite, and alunite-jarosite in sandstones often result from weathering processes accompanied with air pollutants. Sulfur may come from the atmosphere where it occurs commonly as SO_2 in various concentrations but it may also be released in the weathering process of sulphides present in the sandstones (KUBISZ, 1964; ALEXANDROWICZ & PAWLIKOWSKI, 1982). Formation of sulfate minerals results from the reaction between the products of decomposition of sulphides and products of weathering of feldspars, and also biotite, glauconite, muscovite, and calcite. Jarosite formation is a common process in all iron sulphide containing rocks, or the rocks subjected to impact of AMD-type waters (BINGHAM & NORDSTROM, 2000). Minerals from the jarosite group often constitute the last sulfate link in the cycle of iron migration within the weathering zone.

Acknowledgments. This study was supported by State Committee for Scientific Research of Ministry of Science and Higher Education of Poland, grant no. NN 305 094635 and AGH-UST Project no. 11.11.140.158.

References

ALEXANDROWICZ, Z. (2008): Polish Geological Reviews, 56: 680–687.

ALEXANDROWICZ, Z. & PAWLIKOWSKI, M. (1982): Mineralogia Polonica, 13(2): 41–59.

BINGHAM, J.M & NORDSTROM, D.K. (2000): Reviews in Mineralogy and Geochemistry, 40: 351–403.

KUBISZ, J. (1964): Prace Geologiczne, 22: 1–96.

MARSZAŁEK, M. (2008): International Journal of Architecture Heritage, Conservation, Analysis and Restoration, 2(1): 83–92.

RZEPA, G., MARSZAŁEK, M., & ALEXANDROWICZ, Z. (2011): Mineralogia – Special Papers, 38: 160–162.

ELEMENTAL AND PHASE COMPOSITION OF ORES OF NORILSK TYPE

MASHUKOV, A.*, MASHUKOVA, A. & BISTRYAKOVA, S.
Institute of Fundamental Training, Siberian Federal University, Krasnoyarskiy Rabochiy 95, Krasnoyarsk, Russia
* E-mail: AVMashukov@sfu-kras.ru

Elemental and phase composition of ore samples were studied using the methods of X-ray microscopy and Mössbauer microscopy. It was done for the purpose of revealing the distribution of ions Fe, Ni, Cu, Co, S. The elemental composition of the studied samples changes from one sample to another (Table 1).

There were revealed embedded crystals of $CuFeS_2$ and $(Fe,Ni)_9S_8$ in the pyrrhotite matrix. The Fe distribution of the whole scanned area was uniform. However, there are some 30–60 μm size sections which are highly enriched in Fe. Some inclusions, have rectangular and rhomboid forms (2–4 μm) containing Ni with increased content of Fe. The concentration of Ni has its maximum in inclusions, which contain Cu.

The spin magnetic moment changes the magnetic stability of the samples and Curie temperature, which changes with the replacement of magnetic ions of Fe with Co ions. The step-type thermomagnetic curves indicate the presence of a mechanical mixture, consisting of two or more ferromagnetic phases. It is proved by the discrepancy of Curie temperature in the cycle "heating–cooling". As it was shown by the studies, the presence of the impurity ions leads to changing magnetic properties. Its presence also leads to changing thermomagnetic properties of pyrites at $t >$ 350°C at the expense of high ion Co and S mobility.

The samples have a complex and varied diverse composition, which includes bornite, pentlandite, magnetite, hematite, pyrrhotite having the composition of Fe_7S_8. Wroewolfeite was detected in some samples. In the synthesized samples of the system FeS–Fe_7S_8 after keeping them for 30 years at room temperature, there FeOOH was detected. In natural samples this phenomenon was not found.

Two sample groups have been established according to the Mössbauer spectra. The first group presents a superposition of two six-line spectra and single lines of paramagnetic states of the areas in the samples.

The position of absorption lines in the magnet-ordered areas show the presence of stoichiometric FeS and $CuFeS_2$. Some samples of this group have broadened lines, which testify the existence of different iron ion positions in sublattices.

For the other samples containing FeS and $CuFeS_2$ in the pyrrhotite matrix $Fe_{1-x}S_x$, the spectra are a superposition of insolved duplets, which testifies to the presence of paramagnetic areas.

The magnetic phase has a spectrum composed of two six-linear spectra. The peaks on the spectrum borders show the oxide presence.

The presence of native elements and the intermetallic compounds show a reducing mode of ore formation processes. The results of all the investigations are shown in the Table 2.

One can see that the given parameters vary in a wide range. It shows that the local electronic structure depends on the rock genesis. So, the presence of the character is the structures of the solid solutions decay, shows a wide temperature range of sulphide crystallization.

Table 1. *Elemental composition of the samples.*

Elements	Fe	Ni	Cu	S	Co
Maximum content (%)	50.0	5.0	25.0	36.0	0.4

Table 2. *The parameters of hyperfine interactions.*

Effective magnetic field, kA/m	Isomer shift, mm/sec	Quadrupole splitting, mm/sec
22.8–28.3	0.300–1.394	0.250–2.688

THE TEMPERATURE STABILITY OF QUATERNARY PRECIPITATIONS REMANENCE

MASHUKOV, A.*, MASHUKOVA, A. & BISTRYAKOVA, S.
Institute of Fundamental Training, Siberian Federal University, Krasnoyarskiy Rabochiy 95, Krasnoyarsk, Russia
* E-mail: AVMashukov@sfu-kras.ru

The value and direction of the ancient magnetic field as well as physico-chemical conditions of rock formation play a great role in those natural rocks where the iron compound formation is important.

To reveal the conditions determining the specific character of the Quaternary precipitation remanence of the Yenisey River, their magnetic and structural properties were investigated. The value of the alternating magnetic field, which half reduces the remanence of the samples, makes up 16 kA/m, the coercive force is 30 A/m and the saturation magnetization is more than 800 A/m. Samples contain C, Si, Al, Mg, Na, Ca, K, Fe, O, H, bearing minerals: muscovite, clinochlore, riebeckite, ankerite, albite, orthoclase, magnetite, hematite. Kaolinite content does not exceed 2%.

As an additional damaging factor, heating of the samples was used. The relative magnetization (I/I_0) and the relative resistivity (ρ/ρ_0) of the samples at different temperatures are shown in Table 1.

Magnetic separation method was used to reveal the minerals to three fractions: strongly magnetic (1), weakly magnetic (2) and non-magnetic (3) (Table 2).

One can see from Table 2 that the basic ferruginous mineral in the fraction (1) is magnetite. Hematite is probably located on the surface of magnetite grains. The isomer shifts testify different surrounding of radiating and absorbing nucleus and to different iron ion valency. The magnetic minerals of the fraction (2) are hematite grains. The compounds FeOOH and FeO do not give any contribution into the remanence. The isomer shift and the quadrupole splitting of these compounds are identical with those for the weakly magnetic fraction.

For the Fe nucleus in magnetite (fraction 1) the value of the isomer shift in octahedral location is 0.525 mm/sec. The effective magnetic field, which is on the Fe nucleus is $3.9 \cdot 10^4$ kA/m. And in tetrahedron location they make up 0.925 mm/sec and $3.8 \cdot 10^4$ kA/m respectively. With the rise of the temperature, the reflex intensity of Fe_3O_4 decreases to the temperature of 300°C. Then one can observe its increase (35°/2θ) to temperature 580°C. The magnetization carriers in fraction 2 are Fe_2O_3. The values of the isomer shift make up 0.424 mm/sec, and that of the effective magnetic field is $4.1 \cdot 10^4$ kA/m. The isomer shift values and the quadrupole splitting values for FeO are 0.672 mm/sec and 0.505 mm/sec, and for FeOOH, these values make up 1.434 mm/sec and 2.525 mm/sec, respectively.

Thus, the Mössbauer spectra make it possible to determine the types of magnetic minerals in complex compounds. Their identification enables to reveal the stability of remanence in geological time scales.

Table 1. *Relative magnetization and relative resistivity at different temperatures.*

°C	20	50	100	150	200	250	300	350	400	450	500	550	595
I/I_0	1	0.87	0.85	0.86	0.99	0.99	0.87	0.96	0.93	0.93	0.75	0.70	0
ρ/ρ_0	20	0.20	0.07	0.53	0.53	0.09	0.09	0.09	–	–	–	–	–

Table 2. *Mineralogical composition of different fractions.*

Fraction	Percentage			
	Fe_3O_4	Fe_2O_3	FeO	FeOOH
1	87.3 ± 0.2	0.7 ± 0.7	4.7 ± 0.3	8.0 ± 0.2
2	–	21.7 ± 0.7	36.4 ± 0.1	42.3 ± 0.2
3	–	–	53.1± 0.05	46.9 ± 0.05

BALL PEGMATITE FROM JELENIA GÓRA (KARKONOSZE MASSIF) – NEW OUTCROP

MATYSZCZAK, W.
Institute of Geochemistry, Mineralogy and Petrology, Faculty of Geology, University of Warsaw, al. Żwirki i Wigury 93, 02-089 Warszawa, Poland
E-mail: witold.matyszczak@gmail.com

Introduction

One of the most interesting rocks of the Karkonosze granitoid massif is so-called ball pegmatite. This rock was described for the first time by VON BUCH in 1802, and since that time until today it is of interest to researcher. The detailed description of the history of its discovery is given by KENNAN & LORENC (2008). From six ball pegmatite outcrops, described until 1941, only three of them were available at time. After the World War II until 2009 there was only one locality available (KENNAN & LORENC, 2008), despite searches (KARWOWSKI & KOZŁOWSKI, 1972).

In 2009, author found new ball pegmatite outcrop, unknown until now. In the following two years, two outcrops, missing after World War II were rediscovered. The new ball pegmatite locality was found near Jelenia Góra. It occupies an area few sq meters. Within the weathering crust, single orbs are found. In most cases the orbs are cracked, especially the relatively large ones. The orbs diameters vary from few to more than 30 cm. The biggest found specimen was 34 cm in diameter, but it was only part of an orb (core and a half of the mantle), which could reach even 50 cm in diameter.

Typical orb has concentric layer structure, in which one can distinguish: core, mantle and rim. The orbs cores are built with K-feldspar megacryst, often twinned, and few quartz crystals. Sometimes cores consist of porphyritic K-feldspar, quartz and aggregates of fine biotite flakes. Those aggregates build cores of big and very big orbs, occasionally middle-size orbs. Orb mantles consist of K-feldspar overgrowth poikilitic quartz, biotite, and less frequently of plagioclase. Rim is built with granophyre intergrowths of K-feldspar and quartz.

Orbs are cemented in two ways (i) by quartz-alkali-feldspar mass with biotite, similar to aplite or (ii) by pegmatite, which consists of euhedral crystals of quartz, K-feldspar, and albite? In contrast to pegmatite-type cement, which is present in most of specimens, poorly preserved aplite-type cement was found only around few orbs.

Based on fluid inclusions investigations from ball pegmatite from Czarne KARWOWSKI & KOZŁOWSKI (1972) suggested that it was formed from aplite melt, which contained K-feldspar megacrysts. Rapid cooling and probably degassing of such melt, resulted in crystals growth around megacrysts.

Preliminary mineralogical studies revealed following accessory minerals: magnetite, ilmenite, cassiterite, fergusonite-(Y), aeschynite-(Y) or polycrase-(Y), fluorapatite, monazite-(Ce), cheralite, xenotime-(Y), titanite, zircon, and thorite. Among all identified minerals a presence of aeschynite-(Y) or polycrase-(Y) is worth mentioning. According to the author's knowledge none of this pair of isochemical minerals was described from Poland until now. Unfortunately, there is no method, based on chemical composition, which would allow to assign this grain to the aeschynite- or euxenite-group minerals.

Conclusions

The new outcrop of ball pegmatite has been found and two others considered as missing have been rediscovered. The rock is very interesting due to record size of some orbs as well as its mineralogical composition. Further investigations are needed recognize in details its mineralogical composition likewise better understand of its origin.

References

KARWOWSKI, Ł. & KOZŁOWSKI, A. (1972): Acta Geologica Polonica, 22(1): 93–118.

KENNAN, P.S. & LORENC, M.W. (2008): Mineralogia, 39: 79–85.

VON BUCH, L. (1802): Geognostische Beobachtungen auf Reisen durch Deutschland und Italien, Band 1, Entwurf einer geognostischen Beschreibung von Schlesien, 13–28.

BEUDANTITE $[PbFe^{3+}_3(AsO_4)(SO_4)(OH)_6]$ – SEGNITITE $[PbFe^{3+}_3(AsO_4)_2(OH)_6]$ SOLID SOLUTION FROM LIKAS-KŐ, VELENCE HILLS, HUNGARY

MENYHÁRT, A.*, ZAJZON, N. & SZAKÁLL, S.
Institute of Mineralogy and Geology, University of Miskolc, H-3515 Miskolc-Egyetemváros, Hungary
* E-mail: adrienn.menyhart@gmail.com

Beudantite is a Pb-Fe arsenate with sulphate substitution, in a ratio As:S near to 1:1 (in atomic %) (SZYMANSKI, 1988), while segnitite has the same composition but without (or with minor amount of) sulphate substitution (BIRCH *et al.*, 1992). We studied the changes in the arsenate:sulphate ratio with scanning electron microscope (SEM) equipped with wavelength dispersive X-ray spectrometer (WDX). The samples were collected from the Likas-kő area, Velence Hills (Hungary), where in the oxidation zone of an enargite mineralization several secondary minerals were formed. The members of the beudantite-segnitite series are quite common arsenates in this area with characteristically yellow, brown or even black euhedral crystals. In most of the analyzed aggregates arsenates show zonality, epitaxial crystallization together with other minerals (e.g., jarosite, Fig. 1). The samples could be classified into two groups within the beudantite-segnitite solid solution series according to their sulphate content. At Type 1 the arsenate:sulphate ratio is near to the ideal 1:1 of beudantite (Fig. 1), while at Type 2 this ratio is higher than 1.5:0.5 of the sulphate-containing segnitite (Fig. 2). Beside Fe, in most samples we could also measure Al in variable amount (Table 1).

References

BIRCH, W.D., PRING, A. & GATEHOUSE, B.M. (1992): American Mineralogist, 77: 656–659.
SZYMANSKI, J.T. (1988): Canadian Mineralogist, 26: 923–932.

Table 1. *Mean compositions of beudantite-segnitite solid solution according to the WDX analyses (in atomic %). Sample **a**: average of 5 spot analyses; Sample **b**: average of 12 spot analyses; Sample **c**: average of 13 spot analyses; Sample **d**: average of 9 spot analyses. These values are the lowest (**a** and **c**) and highest (**b** and **d**) measured sulphate contents in each type. The last line of the table shows the arsenate:sulphate ratio, calculated from atomic percentage, normalized for 2.*

	Type 1		Type 2	
	a	***b***	***c***	***d***
Fe+Al	44.97+5.73	45.39+3.69	35.81+13.09	47.94+1.65
Pb	17.24	17.21	17.89	17.38
As	19.52	16.58	28.65	24.3
S	12.32	17.13	4.55	7.58
arsenate:sulphate ratio	*1.23:0.77*	*0.98:1.02*	*1.73:0.27*	*1.52:0.48*

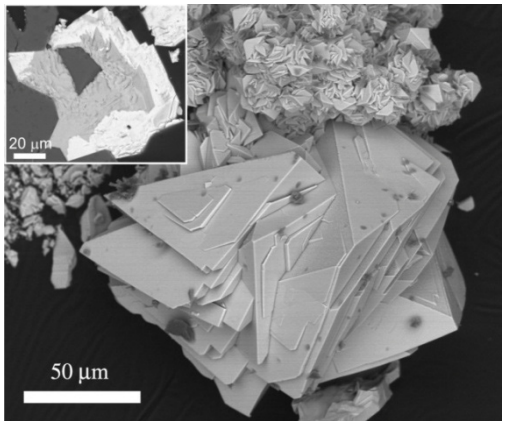

Fig. 1. *SEM image of a rhombohedral crystal aggregate. On the top left its cross section shows that around a jarositic core the beudantite shell was formed.*

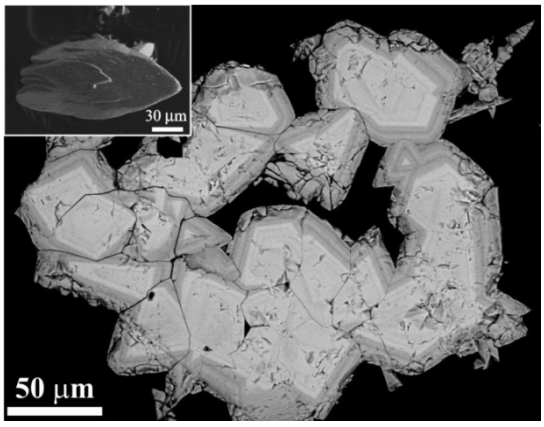

Fig. 2. *Cross section SEM image of sample **c** where around the segnitite core a 10–20 µm wide plumbogummite shell was grown. On the top left the scalenohedral morphology could be seen.*

DISSEMINATED CRYSTAL MUSH FRAGMENTS IN THE CIOMADUL DACITE (SE CARPATHIANS, ROMANIA)

MOLNÁR, K.[1]*, KISS, B.[1], HARANGI, Sz.[1] & NTAFLOS, T.[2]
[1] Volcanology group, Department of Petrology and Geochemistry, Eötvös Loránd University, Pázmány Péter sétány 1/c, H-1117 Budapest, Hungary
[2] Department of Lithospheric Research, University of Vienna, Althanstrasse 14, A-1090 Vienna, Austria
* E-mail: mkata90@gmail.com

The Ciomadul dacite, product of the latest (30–100 ka) volcanic eruptions in the Carpathian-Pannonian region, Eastern-Central Europe, is a crystal-rich rock with ubiquitous plagioclases and amphiboles. Combined, fine-scale textural and geochemical investigations indicate a complex origin of these minerals, formed partly in a low temperature dioritic-granodioritic crystal mush body, partly in a higher temperature hybrid magma. In addition, biotite, titanite, apatite, zircon, K-feldspar and quartz occur in various amounts in the dacites as well as crystal clots composed by these minerals. Most of these crystals are resorbed and are interpreted as antecrysts derived from a remobilised crystal mush body.

The nature of the crystal mush was investigated through the detailed analysis of the crystal clots. Their texture resembles plutonic rocks, such as microdiorites and granodiorites, however, they contain interstitial glasses. The glass could represent evolved melt between the mineral phases in the crystal mush body rather than originated by melting of the crystal phases. Thermobarometric calculations performed using the composition of coexisting plagioclases and amphiboles yield 2–3 kbar pressure and 700–730 °C temperature, which is close to the granitic solidus. In certain crystal clots, plagioclases show strongly resorbed margin with sieved texture and an overgrowth zone with distinct composition (e.g., higher FeO content resembling the plagioclase microphenocrysts in the host rock). The coexisting amphiboles here are strongly opacitized and often have a coarse-grained clinopyroxene corona. These features suggest a heating process presumably due to intrusion of hot mafic magma into the near-solidus magma body. This is consistent with the thermometric calculations for the amphibole-plagioclase pairs found in the host rock that resulted in a temperature range of 820–860 °C, significantly higher than the values got for the crystal clots.

In summary, the Ciomadul dacite contains vast amount of low-temperature, disseminated crystal mush fragments (up to 50 vol% of the “phenocrysts”), which are interpreted as a pre-existing near-solidus magma body at about 8–10 km depth. This was reheated and remobilised by intrusion of hot mafic magmas. This process could lead to the rejuvenation of the magmatic system and an eruption phase, possibly after a long repose time.

This study belongs to the research project supported by the OTKA No. K68587.

Au-PORPHYRY MINERALIZATION IN BELUJ (ŠTIAVNICA STRATOVOLCANO, SLOVAKIA)

MOLNÁR, L.[1]*, KODĚRA, P.[1] & BAKOS, F.[2]
[1] Department of Geology of Mineral Deposits, Faculty of Natural Sciences, Comenius University, Mlynská dolina, 842 15 Bratislava, Slovakia; [2] EMED – Slovakia, s.r.o. Nám. SNP 466/1, Detva, Slovakia
* E-mail: luismoloar@gmail.com

The studied area is located in the Central Slovakia Volcanic Field, in the mantle of the Neogene Štiavnica stratovolcano. Au-porphyry systems in this part of the stratovolcano are connected to intrusive andesite and diorite porphyry bodies, related to early stage of evolution of the stratovolcano. This porphyry system was recently explored by EMED – Slovakia, Ltd. including two inclined drill holes down to 254 m depth, discovering uneconomic potential of 58.4 Mt at 0.3 ppm Au ore (BAKOS *et al.,* 2010).

The host rock of the mineralisation is a medium grained andesite porphyry body. The intrusion is affected by Ca-Na silicate alteration in the form of actinolitisation of mafic minerals and replacement of rock forming feldspar by alkaline plagioclase (albite-anorthite) accompanied by minor titanite and apatite. K-silicate alteration is represented by biotitisation and magnetitisation of mafic minerals (amphibole) and replacement of plagioclases by K-feldspar. Later intermediate argillization is represented by illite, smectite, chlorite (diabantite, brunsvigite), epidote and pyrite. A post mineralization advanced argillic alteration occurs in elongated NW-SE trending zones up to several tens of meters thick, formed by argillised and silicified breccias with vuggy texture. The phyllic alteration locally appears on the margins of the intrusive centre. Broad surrounding of the centre is propylitized (BAKOS *et al.,* 2010).

Gold mineralisation is spatially connected to stockwork of quartz veinlets. Some of the veinlets are banded, while banding results from high content of vapour rich fluid inclusions and tiny grains of magnetite and ilmenite. Banded quartz veins are accompanied by Fe-rich smectite (nontronite, saponite) and chlorite. Relatively younger are quartz-calcite veins with chlorite, smectite, and chalcopyrite veins sporadically with sphalerite. Veinlets with cubic shaped zeolite (chabazite?) and clay minerals (smectite) are younger than quartz veins, and are dominant in the middle section of the studied drill core (from 136 to 172 meters), where Mn has a positive anomaly with an average of 875 ppm. Brecciation occurred from 118 to 140 meters in the form of a fine grained breccia pebble-dyke that cuts through the host rock. The breccia-dyke is affected by silicification and biotitisation and contains older fragments of quartz veins. Brecciation from 218 to 230 meters is affected by intense silicification, biotitisation, and argillization (illite, smectite). The main ore mineral is magnetite and ilmenite disseminated in veins and as grains in the host rock. Pyrite replaces magnetite and ilmenite and is disseminated in the rock and in quartz veins. Chalcopyrite, galena, sphalerite and molybdenite are less frequent. Gold forms isometric grains or grain clusters up to 5–10 μm (BAKOS *et al.,* 2010). Au is increased in the sections rich in banded quartz veinlets and in the brecciated zones, with a maximum of 1.2 ppm. Rare zoned garnet (andradite) was also found in the host rock, with outer rim enriched in grossular component. Tourmaline was found in the matrix with biotite, plagioclase and K-feldspar, and therefore it might be related to K silicate alteration. Other accessory minerals are monazite, allanite, thorite, xenotime and zircon (BAKOS *et al.,* 2010). According to geochemical analyses of drill core (provided by EMED) Cu has an average of 245 ppm, and is more enriched in the sections of banded quartz veinlets and in brecciated zones. Pb and Zn are enriched in zones of K-silicate alteration, and veins with zeolite with an average of 40 ppm for Pb and 250 ppm for Zn. Slight Mo enrichment occurs in the zone of a breccia dyke from 118 to 140 meters with an average of 7 ppm. Ag is always under detection limit (max. 0.9 ppm Ag).

Quartz veins contain predominantly vapour-rich fluid inclusions, both primary and secondary, sometimes forming irregular band of inclusions. Locally, trails of secondary vapour-rich inclusions with green anisotropic solid phases are present, interpreted as salt-melt bearing inclusions (by analogy with the Biely vrch Au porphyry; KODĚRA *et al.,* 2011). Quartz also hosts rare trails of oval opaque inclusions, possibly representing sulphide melt inclusions and secondary two-phase liquid-rich and vapour-rich inclusions, probably related to later stages of alteration processes. Plagioclase crystals contain rare secondary vapour rich fluid inclusions. Oxygen isotopes were measured on quartz from veinlets. Isotopic composition showed a narrow range of data from 9.0 to 9.6‰ $\delta^{18}O$, and show similar values measured to that measured on quartz from the Biely vrch Au porphyry deposit in the Javorie stratovolcano (7.6 to 12.4‰ $\delta^{18}O$; KODĚRA *et al*., 2011). Both localities also share similar mineralisation and alteration styles and fluid inclusion properties, indicating similar genesis despite location in different stratovolcanoes.

Acknowledgement. Support by APVV grant 0537-10 and EMED – Slovakia, Ltd. is acknowledged.

References

BAKOS, F., FUCHS, P., HANES, R., ŽITŇAN, P. & KONEČNÝ, V. (2010): Mineralia Slov., 42: 1–14.

KODĚRA, P., LEXA, J., HEINRICH, C.A., WÄLLE, M. & FALLICK, A.E. (2011): Proc. 11th SGA Meeting, 417–419.

POSSIBLE ACID ROCK DRAINAGE EFFECT ON NEUTRAL pH

MÓRICZ, F.[1]*, MÁDAI, F.[1] & WALDER, I.F.[2]
[1] Institute of Mineralogy and Geology, University of Miskolc, H-3515 Miskolc-Egyetemváros, Hungary
[2] Kjeøy Research & Education Center, Kjeøy, N-8412 Vestbygd, Norway
* E-mail: moriczferi@gmail.com

In the last two decades, the effect of Acid Rock Drainage (ARD) has become the leading environmental problem in metal mining. Weathering starts to degrade sulphidic type ore, which is unstable on the surface environment, resulting in low pH and mobilizing heavy metal contamination. The release of ARD to surface- and groundwater deteriorates the water quality and may cause depletion of alkalinity, acidification, bioaccumulation of metals, accumulation of metal in sediments, effects on habitats, elimination of sensitive species and unstable ecosystems.

Currently the handling, storage and monitoring of the abandoned mine sites, tailing and waste dumps are strongly regulated, which is a large step forward compared to the earlier sulphidic mining activity till the 90's. In case of mining activity the only short term environmental friendly thinking is not always exact because in the monitoring system the focus is on the first few years, or maximally a decade. However, the sulphide bearing material, in the first few years of the law regulated monitoring protocol, does not always show any acid producing activity and contamination, although the alteration of sulphide to sulphate are present. The occasion is that, the neutralizing minerals, such as calcite, dolomite or feldspars, can buffer the produced acidity, formed by the pyrite oxidation. In geology the sulphide oxidation is a normal process without serious pollution, because the amount of the sulphides, the water and the oxygen is limited in meaning of short term, compared to the huge amount of relative quickly exploited sulphide containing materials, produced by mining during years or decades. In the mining activity gives artificial environment, where the unit of the sulphide, mainly pyrite, oxidation exceeds the neutralizing or buffering capacity of the nature, thus causes ARD effect, which appears as acidic or strongly acidic seepage water, where the level of heavy metals concentration are elevated.

In September 2011, samples were collected from a waste dump, near Recsk, Hungary. The origin of the samples is the -900 level of the Western copper ore researching edit, number 3, which is in the contact of the exoskarn and the neighbouring carbonate rocks. This induced the high amount of the pyrite in the samples, which exceeds the 75 wt%, also more than 1 wt% of chalcopyrite, and pyrrhotite and the few percentage of calcite. On the surface of the 20 cm sized samples from the material of the waste damp, some iron oxides have already appeared, which were mechanically removed in the step of the sample processing. Samples were crushed to 1 and 2 mm for the column test. During this geochemical analysis, the sulphide oxidation is sped up to mimics of the long term behaviour of the mining material. In the present of water and oxygen, the pyrite starts oxidizing. The calcite, as quick neutralizing mineral, works well which is showed by the measured pH, between 7.1 and 7.2. Thus, the non acidic seepage lets the iron ions oxidize and form stable phases, which could continue until the pH goes under 4–4.5. Theoretically, the following stoichiometrycally exact equation takes place, which is made by the combination of several equations of the ARD process: $2FeS_2$ (s) + $3CaCO_3$ (s) + $9H_2O$ (l) + $8O_2$ (g) → $2Fe(OH)_3$ (s) + $3CaSO_4$ (s) • $2H_2O$ (l) + $(SO_4)^{2-}$ (aq) + $3CO_2$ (g).

Environmental problems will start, if the acid producing potential is higher than the neutralizing one, so beside the acidic environment, stable minerals cannot form and all the elements will be in dissolved phase, especially if the pH sinks under 1.5–2. In sample from Recsk, the amount of the pyrite is multiple higher than the calcite, thus environment pollution will take place in an uncertain time.

In this presentation the focus is on to prove the equation above, as well as to answer that thesis, whether there could happen oxidation in the zone of neutral pH. The proving process is to detect and measure the end members of part of the equation, thus the $iron^{III}$-hydroxide – which could be also iron oxides by dehydration, via phase of goethite – on the surface of the fresh pyrite grains, the gypsum coating on the surface of the calcite, detected by electron microprobe, the sulphate concentration in the seepage, measured by ion chromatograph and the carbon-dioxide gas in the air tightly closed sample keeper. As an evidence, the presence of iron containing minerals, gypsum, free sulphate ion and carbon dioxide proved that there is a sulphide oxidation. The low amount of calcite compared to that of pyrite determines ahead the environmental pollution in the future. The dropping amount of the calcite and the blocking of it by gypsum, justify the decreasing of the neutralizing capacity in the future, which will not be able to keep the balance, therefore the system will move toward acidic condition. The rate of oxidizing in the pyritic system increases exponentially, moreover it works as a chain reaction, thus moves itself ahead quicker and quicker. The ore mineralization is polymetallic, therefore copper, zinc, lead will also appear in the seepage, together with their replacement element, like cadmium or molybdenum.

With this presentation, the author would like to reflect on necessity of the circumspect handling and also on the accuracy planning in the storage system of the potentially dangerous waste and mine materials.

MINERALOGY AND GENESIS OF THE POWDER-LIKE SPHALERITE (BRUNCKITE) VEINS FROM THE OLKUSZ MINE, UPPER SILESIA, POLAND

NEJBERT, K.[1]*, BĄBEL, M.[1] & CIEŚLIK, B.[2]
[1] University of Warsaw, al. Żwirki i Wigury 93, 02-089 Warszawa, Poland
[2] ZGH "Bolesław" S.A., ul. Kolejowa 37, 32-332 Bukowno, Poland
* E-mail: knejbert@uw.edu.pl

Veins of the powder-like sphalerite (brunckite) occur in the Upper Silesia Zn-Pb deposits, representing the Mississippi-Valley type (MVT) (GÓRECKA *et al.,* 1996). Brunckite accumulations are known from the mines near Olkusz and Bytom (HARAŃCZYK, 1959; ZAWIŚLAK, 1970; SASS-GUSTKIEWICZ, 2007). Brunckite was described as a new mineral by HERZENBERG (1938), from the Cercapuquio Mine in Peru. Later XRD studies showed that it is a textural variety of sphalerite. HERZENBERG (1938) described brunckite as a white-grey cryptocrystalline highly porous mass, which easily adhere to a tongue and is easily crumbled into powder when rubbing with fingers. Some authors include also the well lithified, yellowish sphalerite showing colloform texture into brunckite (HARAŃCZYK, 1959). In this report we apply the original Herzenberg's definition of brunckite to describe unlithified accumulations of the powder-like sphalerite.

Studied brunckite was sampled in the Olkusz Mine, where it occurs in veins, as infillings of caverns within breccia-type Zn-Pb deposits, and as thin laminae within internal sediments recorded at the bottom of the Zn-Pb ore bodies in the Upper Silesia (ZAWIŚLAK, 1970; SASS-GUSTKIEWICZ, 2007). The brunckite veins (1–20 cm thick) are met mainly at the contact of the ore-bearing dolomite with the internal sediments. The veins commonly show massive texture. In some veins horizontal lamination and laminae of organic matter were recognized. The sedimentological structures indicate that the accumulation of brunckite took place in open free spaces. The examined brunckite veins represent the last generation of Zn-sulphides in this area. The brunckite occurs in close association with the accumulations of amorphous organic matter, recognized as highly oxidized dopplerite by SASS-GUSTKIEWICZ & KWIECIŃSKA (1999). These authors suggested that the organic matter precipitated from humic acids during their interaction with Ca-rich solutions. Field studies indicate that the brunckite and the amorphous organic matter were deposited simultaneously. The XRD examination revealed that the brunckite veins nearly entirely consist of sphalerite. In some samples Ca-Mg-carbonates and gypsum were recorded. The SEM-EDS studies showed that the sphalerite form separate randomly oriented euhedral crystals forming porous masses. The majority of crystals range from 0.5 to 3 (max. 15) μm in size. The grains are commonly isometric, the needle-like forms were not observed. Chemical composition of the sphalerite is close to stoichiometric, the Fe content is less than 0.2 wt% (data from EDS analyses in small areas).

The origin of the brunckite veins was so far explained by the two genetic models: (1) the spontaneous crystallization from low-temperature hydrothermal solutions at the end of Zn-Pb mineralizing processes (HARAŃCZYK, 1959; GÓRECKA *et al.,* 1996), (2) the result of granular disaggregation of the Zn-ores with well developed colloform texture (SASS-GUSTKIEWICZ, 2007). The euhedral habit of sphalerite crystals together with their uniform grain sizes, and lack of any needle-like sphalerite crystals, commonly met in the colloform Zn-ores (GÓRECKA *et al.,* 1996; SASS-GUSTKIEWICZ, 2007), strongly support the origin by direct spontaneous crystallization from hydrothermal solutions. This interpretation is also consistent with the sulphur isotope data (GÓRECKA *et al.,* 1996). The $\delta^{34}S$ of the Olkusz Mine brunckites ranges from -32 to -15‰, while the older generations of the Zn-Pb-Fe-sulphides are characterized by much heavier S-isotopes. Their $\delta^{34}S$ values are from 2 to 12‰ for sulphides from the yellowish sphalerite and galena, and from -15 to -2‰ for sulphides from the brown sphalerite and pyrite-marcasite (op. cit.). The low values of $\delta^{34}S$ ranging from -30 to -5‰ are recorded from many MVT deposits, and are commonly interpreted as the result of activity of sulphate-reducing bacteria during crystallization of Zn-Pb-Fe sulphides (FALLICK & ASHTON, 2001).

The origin of the studied brunckite is interpreted as the result of low-temperature hydrothermal crystallization of Zn-sulphides driven by activity of sulphate-reducing bacteria responsible for the reduction of the $(SO_4)^{2-}$ to S^{2-}. Spontaneous brunckite precipitation presumably took place during mixing of some genetically different hydrothermal fluids. The precipitated fine ZnS grains (brunckite), together with the amorphous organic matter, were immediately deposited in tectonic fissures and other free spaces common in the Zn-Pb deposits. Such interpretation explains close association of the Upper Silesian brunckite with the oxidized amorphous organic matter, being probably a product of bacterial degradation of the humic acids in the subsurface.

References

FALLICK, A.E. & ASTON, J.H. (2001): Economic Geology, 96: 885–890.
GÓRECKA, E., LEACH, D.L. & KOZŁOWSKI, A. (Eds.) (1996): Prace PIG, 154: 1–182.
HARAŃCZYK, C. (1959): Bulletin de l'Academie Polonaise des Sciences, 7(5): 359–362.
HERZENBERG, R. (1938): Zentralblatt für Mineralogie, A/12: 373–374.
SASS-GUSTKIEWICZ, M. (2007): Mineralogia Polonica, 38(2): 231–241.
SASS-GUSTKIEWICZ, M. & KWIECIŃSKA, B. (1999): Economic Geology, 94: 981–992.
ZAWIŚLAK, L. (1970): Rudy i Metale Nieżelazne, 15(6): 419–422.

STUDY OF FLUID-ROCK INTERACTIONS IN MAFIC GRANULITE XENOLITHS FROM THE BAKONY-BALATON HIGHLAND VOLCANIC FIELD, HUNGARY

NÉMETH, B. [1,2]*, TÖRÖK, K.[1,2] & SZABÓ, Cs.[2]
[1] Eötvös Loránd Geophysical Institute, Columbus u. 17-23, Budapest, Hungary
[2] Lithosphere Research Group, Department of Petrology and Geochemistry, Eötvös Loránd University, Pázmány Péter sétány 1/C, H-1117 Budapest, Hungary
* E-mail: bianca.nemeth@gmail.com, nemeth@elgi.hu

The Pannonian Basin is famous of its Plio-Pleistocene alkaline basalt hosted xenoliths derived from different depths of the lithosphere. We studied fluid-rock interactions in mafic, lower-crustal garnet granulite xenoliths from the Bakony-Balaton Highland Volcanic Field (BBHVF) by petrography, microthermometry, electron microprobe analyses, Raman and IR spectroscopy on silicate melt inclusions to find out the composition and origin of the migrating melts and fluids to assess their interaction with the granulitic lower crust.

The studied xenoliths have granoblastic texture and the main rock forming minerals are plagioclase, clinopyroxene, garnet ± orthopyroxene. The most common accessories are sphene and ilmenite. Some xenoliths contain hydrous minerals like amphibole and rarely biotite. This is the oldest mineral assemblage which could be detected. Texturally younger minerals occur in some samples originating from different reactions, like melting and subsequent crystallisation due to fluid-rock interaction.

Geothermobarometry shows that the equilibrium temperature of mafic garnet granulites was between 800 and 950°C, and the equilibrium pressure was 10–13 kbar. Two generations of silicate melt inclusions (SMI) were observed in the samples. There are primary silicate melt inclusions, in the original granulite facies rock forming minerals (plagioclase, clinopyroxene and sphene) and some of the minerals which were formed later on during fluid-rock interactions (e.g., Ilm, Cpx and Opx, new Amp and Pl) also trapped SMI during their growth.

The SMI contain glass phase ± bubble. Microthermometry was made on the bubbles of the SMI where low temperature phase changes were visible. Melting temperatures of the bubble content ranged from -56.6 to -57.6 It suggests that the bubbles contain CO_2-dominated liquid. The homogenisation temperatures (+29.9°C) show low-density liquid in the bubbles in the clinopyroxene hosted SMI. Raman spectroscopy shows other gas and liquid components associated with the CO_2 (81–100 mol%), such as N_2 (up to 7 mol%) and H_2O (up to 12 mol%). Raman spectroscopy was made on those inclusions where microthermometry was not possible due to the small size or dark appearance of the bubble. The detected components of these bubbles change between the following values: CO_2: 70.8–100 mol%; CO: up to 26.7 mol%; N_2: up to 4.4 mol%. The bubbles of plagioclase and clinopyroxene hosted SMI contain up to 6 mol% and 12 mol% H_2O, respectively. In SMI hosted by sphene, the bubbles do not contain H_2O.

We measured the composition of the glass phase in SMI by electron microprobe and compared them with experimental data to find out the origin of the melts. The composition of the glass of SMI trapped in clinopyroxene and plagioclase show similarities to the rhyolitic-dacitic glass derived by melting of biotite-quartz-plagioclase mineral assemblage or of metagraywacke but also might derived by melting of mafic granulites. The composition of the glass phase of SMI trapped in ilmenite is close to composition of a glass phase which derived by melting of alkaline basalt in the presence of additional CO_2-H_2O fluid. The glass phase of granulitic sphene hosted SMI has the same compositions as the ilmenite hosted ones. The glass of SMI trapped in later sphene has dacitic to rhyolitic composition similarly to those derived by melting of quartz-amphibolite or mafic granulite.

These results suggest that the SMI originated from partial melting of different lower crustal rocks of mafic and metasedimentary origin with an occasional presence of C-O-H-N fluids. According to the two different generations of host minerals and primary melt inclusions trapped by theses minerals, we can establish at least two events when melt percolated the lower crust and interacted with the lower crustal granulite rocks causing mineral reactions.

The research was supported by OTKA to K. Török, project number: NN79943 and for the REG_KM_INFRA_09 Gábor Baross Programme.

Zn-Pb MINERALIZATION IN RUDABÁNYA (HUNGARY): A RECOGNIZED NEW DEPOSIT TYPE

NÉMETH, N.*, FÖLDESSY, J., KUPI, L., ZAJZON, N. & ZELENKA, T.
Institute of Mineralogy and Geology, University of Miskolc, 3515 Miskolc-Egyetemváros, Hungary
* E-mail: foldnn@uni-miskolc.hu

The Rudabánya Ore Complex (ROC) is a traditional mining site of various ore types. In the modern times an iron ore mine was operated from the 1870's to 1985, opening a series of pits along the Rudabánya Range, where copper ore was also exploited, barite and lead ore resources has been registered too. Both primary and secondary oxidized ores were the target of the iron mining. The primary metasomatic hydrothermal siderite ore has been formed epigenetically in Mesozoic carbonate rocks. The secondary one is its near-surface oxidized zone of about 100 m thickness with supergene limonites. The recorded geological information concerns the exploration and mining facilities of this mine mainly, summarized by PANTÓ (1956).

The ROC is situated in the Darnó Zone, which is a regional, 2–5 km wide, NNE–SSW striking strike-slip fault zone. Its activity lasted probably from the Mesozoic times up to Quaternary. The ROC is an imbricated stack of horses, bounded by Darnó master faults on both sides. Permian–Lower Triassic rocks of the Silicikum stratigraphic unit host the polygenetic mineralizations.

The ROC has been target of subsequent base and precious metal prospecting after the closure of the iron ore mine. The hydrothermal galena mineralization in the barite dominated rim facies of the siderite blocks was known and described previously (PANTÓ, 1956; KOCH, 1985). During a recent exploration program the Institute of Mineralogy and Geology, University of Miskolc in cooperation with the Rotaqua Ltd. discovered significant sphalerite and galena resources. The assay of our rock chip and drill core samples showed the Zn content exceeds Pb by a factor of 4.5 on average, although it was hard to discern sphalerite in the host rock, even at high Zn grades. The sampling of further sphalerite-galena enrichments has given up to 15–20 wt% Zn and 4–5 wt% Pb contents in quartz and mica dominated, reductive facies calcareous siltstone (surrounding the iron ore bearing carbonate blocks). This has led to the recognition of a new, stratiform mineralization type ore.

The main components of this new paragenesis are pyrite, barite, sphalerite and galena, just like in the siderite rim facies, but the grain size here is smaller, 10 μm scale in general. Sulphide-rich beds show rhythmical layering of pyrite, then sphalerite and finally galena, but pyrite was formed also later. Pyrite is often framboidal and collomorph. The laminar texture of this ore has suffered ductile deformation. The mosaic texture of galena indicates dynamic recrystallization, in contrast with the hydrothermal ore. The stratiform ore type can also be distinguished from the hydrothermal one by chemical composition, its sphalerite having lower Cd- and Fe-content and its galena having lower Ag-content.

These characteristics indicate an early, low temperature, probably sedimentary-exhalative origin of this ore type, preceding the subsequent fracture-controlled mineralizations. Our observations may give rise to new economic ore potential of the analogous Lower Triassic sedimentary complexes.

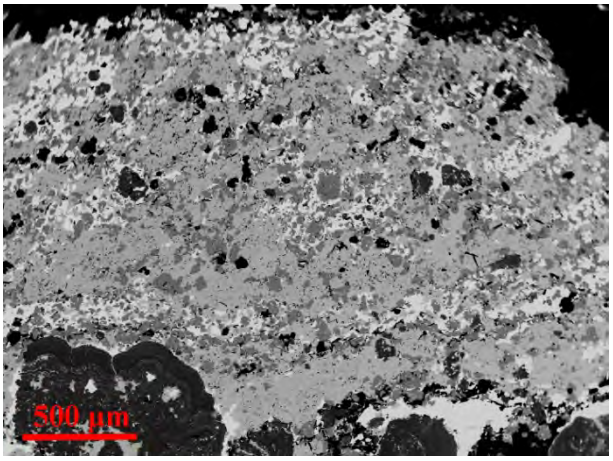

Fig. 1. *BSE image of a typical sedimentary-exhalative type ore texture from Rudabánya. Minerals from dark grey to white: pyrite, sphalerite, barite, galena.*

References

KOCH, S. (1985): Magyarország ásványai [Minerals of Hungary]. 2nd ed. Akadémiai Kiadó, Budapest, 562 p. (in Hungarian)

PANTÓ, G. (1956): Yearbook of the Hungarian Geological Institute, 44(2): 329–637.

PROCESSES OF FRACTIONATION VS. CONTAMINATION AT THE VĚŽNÁ I PEGMATITE, WESTERN MORAVIA, CZECH REPUBLIC

NOVÁK, M. & LOUN, J.*
Department of Geological Sciences, Masaryk University, Kotlářská 2, 611 37 Brno, Czech Republic
* E-mail: loun.jan@seznam.cz

The well-known Věžná I pegmatite of beryl-columbite subtype has been studied since 1960. It is situated 1 km S from Věžná village in a serpentinite body enclosed in migmatitic gneiss on the boundary between Strážek Moldanubicum and Svratka crystalline complex. The pegmatite dike, up to 3 m thick, shows usual internal structure with symmetric zoning: in its most differentiated part including from the margin to the center : (i) contact reaction rim with the host rock composed by phlogopite, chlorite, anthophyllite and actinolite, (ii) thin granitic wall zone (Kfs + Plg + Qtz + Bt), (iii) dominant intermediate zone of graphic Kfs + Qtz and Plg + Qtz intergrowths, (iv) intermediate unit (core margin) of blocky Kfs, (v) albite-rich unit, (vi) quartz core (isolated central pods, and (vii) very rare pod of Li,Cs-bearing minerals (pollucite, lepidolite, elbaite). The Věžná I pegmatite is currently uncovered at three isolated outcrops from less to more evolved from N to S: (I) fine- to coarse-grained granite, (II) simple pegmatite + granite, and (III) symmetrically zoned pegmatite body with the units (i), (ii), (iii) and (iv) on the currently accessible outcrops.

Chemical compositions of primary minerals (biotite, cordierite and tourmaline) and their evolutions at the outcrops were studied by EMPA. Biotite is present at all outcrops and the compositions show decreasing Ti and increasing F from the outcrop I to III but decreasing of Fe/(Fe + Mg) ratio in the same direction. Cordierite occurs only at the outcrop III as graphic intergrowths with quartz (iii) and rare crystals within blocky unit (iv) with a weak variation in the Fe/(Fe + Mg) ratio. Tourmaline occurs in simple pegmatite (outcrop II) and in several paragenetic and compositional types at the outcrop III: black in graphic intergrowths with quartz (iv), black crystals and aggregates in (v) and green to pink in (vi). Chemical composition shows generally decreasing of Ti and increasing of F and decreasing of Fe/(Fe + Mg) ratio from outcrop II to graphic unit in outcrop III as in biotite. Then Fe/(Fe + Mg) ratio increases to more evolved units in black schorl→ green Fe,Mn -elbaite → pink Mn-elbaite.

The overall diagram (Fig. 1) with Fe/(Fe + Mg) ratio of all presented minerals from three outcrops indicates this evolution: pegmatitic (granitic) melt likely intruded in the direction from outcrop I to III and was contaminated by host rock (serpentinite). After forming of wall zone (and partially graphic zone) in the outcrop III, the contamination finished, at blocky part the rest of Mg was consumed by cordierite and tourmaline, and fractionation continued until the end of crystallization of high fractionated small pods of Cs,Li,Mn-rich unit (vii) with Li-mica, Li-tourmaline, primary triplite, and pollucite. Combination of both principal processes – contamination, characterized by input of Mg, and fractionation, characterized by depletion of Mg, increase of Fe/(Fe+Mg) ratio and then depletion in Fe and enrichment in Li, Cs and Mn, – control chemical composition of minerals in the pegmatite.

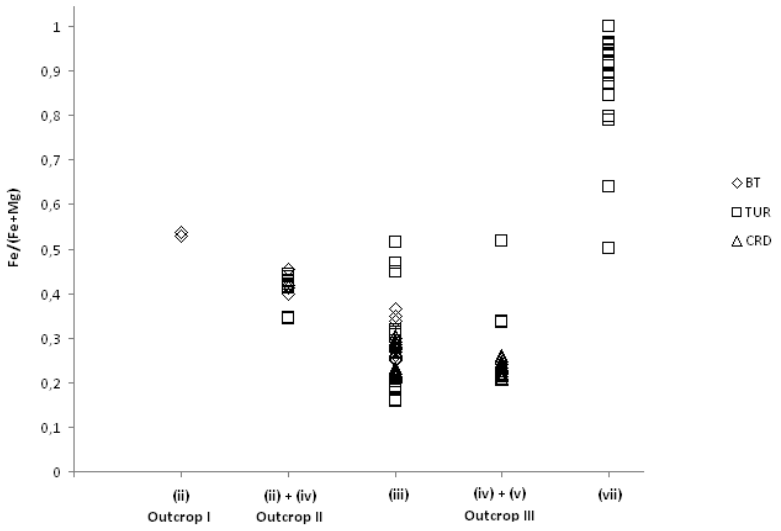

Fig. 1. *Fe/(Fe + Mg) diagram of biotite, tourmaline and cordierite from the outcrops I to III.*

CARBONATE PRECIPITATION UNDER THE ICE OF LAKE BALATON

NYIRŐ-KÓSA, I., ROSTÁSI, Á. & PÓSFAI, M.*
Department of Earth and Environmental Sciences, University of Pannonia; Egyetem u. 10, Veszprém, Hungary
* E-mail: mihaly.posfai@gmail.com

Calcite precipitation in hardwater lakes is a common phenomenon, as a result of the consumption of CO_2 by algae through photosynthesis. The mineralogical composition of the sediment of Lake Balaton is dominated by carbonate minerals that primarily formed by this biologically-influenced chemical process. Since the water of Lake Balaton is Mg-rich, the precipitating calcite contains significant and variable amount of Mg (MÜLLER & WAGNER, 1978; CSERNY, 1987). According to previous reports, "protodolomite", a structurally disordered carbonate with dolomite-like composition occurs in the deeper layers of Balaton sediments (MÜLLER, 1970). It is unclear whether the Mg content of calcite is randomly distributed in individual particles, or distinct carbonate types occur that have specific amounts of Mg in their structures. It is also unknown whether the morphologies of carbonate grains are affected by their Mg content.

The study of pristine, freshly-precipitated calcite is difficult because the suspended calcite grains are indiscriminately filtered by various zooplankton species, and then excreted as pellets, aggregates of the original carbonate crystals and of other, non-digestible material such as diatom tests (G.-TÓTH *et al.*, 1987). These pellets are deposited on the lakebed, but can again be stirred up by wave action and turbulence in shallow Lake Balaton, re-entering the lake's ecological cycle. Thus, the sediment contains mostly "reprocessed" carbonate mineral aggregates, the properties of which do not necessarily reflect those of the original precipitated particles.

In order to understand the structural and morphological consequences of the incorporation of Mg into the calcite that forms in Lake Balaton, we collected freshly precipitated carbonate particles in sediment traps that were placed under the ice. With this sampling setup we wished to avoid the effects of wind-driven turbulence and resuspension, and thus biological reprocessing of the sedimented material. The collected material was studied using X-ray powder diffraction (XRD) and scanning and transmission electron microscopy (SEM and TEM, respectively). Our preliminary observations indicate that the traps collected elongated, few μm-large aggregates in which the individual crystallites occurred in a consensus crystallographic orientation. In addition to the aggregates, smaller, euhedral particles (rhombohedra) were also present. Whereas the Mg/Ca ratio appeared to vary from grain to grain but remained below ~1/7 in the elongated aggregates, the Mg content was much higher in the euhedral crystals. In addition to carbonates, the sediment traps also collected clay minerals and diatoms, and the sampling vials contained a large number of copepods; thus, some biological reprocessing of the carbonates might have occurred. Further studies are in progress to understand the potential relationships between compositional and structural features of the precipitated carbonates, as well as the influence of the biota on the mineralogical character of the sediment.

Support from the EU/Hungarian grant TÁMOP-4.2.2.-B-10/1-2010-0025 is gratefully acknowledged.

References

CSERNY, T. (1987): Annual Reports of the Hungarian Geological Institute, 1985: 343–365.

G.-TÓTH, L., ZÁNKAI, N.P. & MESSNER, O.M. (1987): Hydrobiologia, 145: 323–332.

MÜLLER, G. (1970): Nature, 226: 749–750.

MÜLLER, G. & WAGNER, F. (1978): Special Publications of the International Association of Sedimentologists, 2: 57–81.

ARCHAEOMETRIC STUDIES OF POLISHED STONE ARTEFACTS FROM MECSEK-VILLÁNY MTS. (SOUTH HUNGARY)

OLÁH, I.[1], BENDŐ, Zs.[2]*, SZAKMÁNY, Gy.[2] & SZILÁGYI, V.[3]
[1] Hungarian National Museum, National Heritage Protection Centre; Daróci u. 1-3, H-1113 Budapest, Hungary
[2] Department of Petrology and Geochemistry, Institute of Geography and Earth Sciences, Eötvös Loránd University, Pázmány Péter sétány 1/C, H-1117 Budapest, Hungary
[3] Nuclear Analysis and Radiography Department, MTA Centre for Energy Research, Konkoly Thege u. 29-33, H-1121 Budapest, Hungary
* E-mail: bendozs@caesar.elte.hu

87 polished stone artefacts from the Korinek-collection were investigated. These artefacts were collected as stray finds by Prof. László Korinek from the southern part and southern foreland of Mecsek Mountains (South Hungary). The collection contains predominantly axes, but adzes, chisels, grinding stones, handstones, and perforated pendants can also be found. The majority of the artefacts are fragmented, although finished and semi-finished tools also occur. The semi-finished tools show very interesting preparation marks.

The source area of the collection partially overlaps with the area of a recently excavated archaeological site near Diósviszló. The pottery found here together with polished stone tools suggests that at least some of the latter artefacts originate from Transdanubian Linear Pottery culture.

Besides doing provenance analysis the authors have compared particular artefacts of the Korinek-collection and stone artefacts deriving from the nearby archeological site, Diósviszló.

Macroscopic description and magnetic susceptibility measurements were made on all samples, polarising microscopic petrography, mineral chemistry by SEM-EDX and PGNAA bulk chemical analyses were used on selected samples. Intact artefacts were analysed by non destructive methods only. In case of SEM-EDX analysis a newly developed, completely non destructive method was applied.

As regards the raw materials, the majority of the artefacts were made from late Cretaceous fine-grained dyke or subvolcanic alkaline magmatic rocks of the surrounding Mecsek Mountanis. However, a few alkaline magmatic rock samples come from other localities. The provenance of hainite-bearing sodalite phonolite is the Moravian-Moldanubian territory, most probably Zelenicky Vrch. There are relatively high amounts of several varieties of greenschists-metabasites-contact metabasites. Felsőcsatár and Zelezny Brod types of tools could also be identified, but there are still pieces of unknown origin. Other raw materials, such as sandstone, serpentinite, mylonite, siltstone, volcaniclastic siltstone, limestone and quartzite, represent only few pieces.

Links between artefacts of the Korinek-collection and samples from Diósviszló excavation site have been found. Regarding the raw materials of the collection and the excavation site alkaline magmatic rock types are very similar and two sandstone types are completely identical.

SOME DATA OF MINERAL RESOURCES IN SOUTHEASTERN ALBANIA, THE REGIONS KORCE-LIBRAZHD

ONUZI, K.[1]*, KOLLER, F.[2], HOECK, V.[3], GEGA, D.[1] & MARKU, S.[1]
[1] Instituti i Gjeoshkencave, Universiteti Politeknik i Tiranes, Albania
[2] Department of Lithospheric Research, University of Vienna, Altanstraße 14, A-1090 Vienna, Austria
[3] Department of Geography and Geology, Salzburg University, 34 Hellbrunner Str., A-5020 Salzburg, Austria
* E-mail: konuzi@yahoo.com

Librazhd-Korca region represents significant potential ore deposits, in some of which geological-mining activities are still carried out. Chromium, iron-nickel, copper, are the minerals of economic value in the region.

Chromium mineralization is concentrated mostly in the Shebenik-Pogradec ophiolitic massif, but fragmentary outcrops are detected also in ophiolitic massifs of Voskopoja, Vallamara and Morava. The mineralization is distributed in several lithological sequences.

In the fresh harzburgite sequence with rare dunite lenses, we meet podiform chromite mineralizations, for example in section Fushe, Madhe-Gjorduke. This mineralization is relatively poor, in relation to the mineralization found in the upper parts of the cross section, and the size of ore bodies is medium to small. In harzburgite-dunite sequence of the ultrabasic massif cross section, where the presence of the dunitic lenses varies in 10–20%, the main concentrations of chromium ore are placed. In its lower part the deposits of Katjeli, Pojska, Memelisht 4, Guri Pishkashit are situated. A series of other ore concentrations are those of Prenjas, Guri Pishkashit, Pishkash 4 and 5, Varri i Plakes, Poshte Govates, Buzgare, Mollez, Shape. These ore bodies are morphologically pseudo-layers, podiform, and partly folded. The sizes are relatively large. They have normally massive textures and high contents of above 4 wt% Cr_2O_3. In the ultramafic cumulate sequence only a weak mineralisation, in the form of "schlieren" or small bodies occur, but normally without any economic significance.

Also the ophiolitic complexes of the western belt are encountered some occurrences of chromium such as in the Voskopoja ophiolitic complex, in Pasha Tepe and Ura e Verbes Sector. Chemical composition of the Pasha Tepe occurrence is Cr_2O_3 = 39, Al_2O_3 = 22.8 and MgO = 16.5 wt%, while the occurrence of the Ura e Verbes results Cr_2O_3 = 14–30, Al_2O_3 = 8–17 and MgO = 25–32 wt%. In these deposits, elements of the platinum group can be found. In the studied region this ore formation is encountered only in the Voskopoja ophiolitic complex (Dersnik) where around 7 occurrences are known with content of Cr_2O_3 = 22–42 and Al_2O_3 = 30–35 wt%. They are located in dunitic rocks of upper parts of the ultramafic cross section.

Iron-nickel ores in Southeast Albania: significant reserves of iron-nickel and nickel-silicate ores are located, which have supported the mining activities and utilization of iron-nickel ore for export purposes and for production of steel in the Elbasan Metallurgical Plant. Products of the ancient weathering crust and deposits of iron-nickel and nickel silicate associated with this, are related to ultrabasic rocks of the Mirdita Tectonic Zone. Those ores are formed by the alteration of ultrabasic rocks during various time stages which started during Cretaceous period (in the central region), and pre-Eocene (in the southeastern region). Deposits of iron-nickel ores of the region Librazhd-Pogradec have a very wide spread, extending into two generations, and situated in both (a) northeast side and (b) northwestern side of the Shkumbini River upstream. For example in the Guri i Kuq deposit the true thickness ranges from 1–2 m to 30–40 m. Their values vary from 38.9 to 50 wt% for iron, from 0.8 to 1.11 wt% for nickel and from 0.06 to 0.10 wt% for cobalt.

Copper ore. Copper deposits have a considerable spreading in Rehova and Bregu i Geshtenjes, where they are located in a basaltic pillow lava packet. Type mineralization is disseminate (the most of ore bodies), and massive in the deeper levels, near the contact with diabasic basalts (diabase)

Geological reserves are approximately 240,000 ton, belonging to blocks, containing about 1.83 wt% Cu. In the Voskopoja ophiolitic complex and Vithkuq-Rehova allochthonous, this mineralization is located in the volcanic rocks of Shipcke, Lavdar, Polena Vithkuq, Column, Leshnje areas, and is represented by a quartz-pyrite-chalcopyrite mineralization type, often in the form of veins with limited size (2–10 m in length and 1–2 m of thickness), with Cu content = 0.52 wt%, Zn = 0.7 wt% and Au = 0.33 g/t. Mineralization is located between brecciated diabases and amygdaloidal basalts.

MINERALOGICAL RESEARCH OF THE KOŠICE CHONDRITE (SLOVAKIA)

OZDÍN, D.[1]*, UHER, P.[1], KAŇUCHOVÁ, Z.[2], SVOREŇ, J.[2], BARATTA, G.A.[3], PORUBČAN, V.[4] & TÓTH, J.[4]
[1] Department of Mineralogy and Petrology, Faculty of Natural Sciences, Comenius University, Mlynská dolina, 842 15 Bratislava, Slovakia
[2] Astronomical Institute of Slovak Academy of Sciences, 05960 Tatranská Lomnica, Slovakia
[3] INAF – Osservatorio Astrofisico di Catania, via S. Sofia 78, 95123 Catania, Italy
[4] Department of Astronomy, Physics of the Earth and Meteorology, Faculty of Mathematics, Physics and Informatics, Comenius University, Mlynská dolina G, 842 48 Bratislava, Slovakia
* E-mail: daniel.ozdin@gmail.com

On February 28, 2010 at 23:24:46 CET a very bright fireball over a wide area of the city of Košice in Eastern Slovakia, followed by a fall of meteorite was observed. Fireball was clearly visible from a distance of several hundred kilometres. In some parts of Eastern Slovakia and Northern Hungary also sound effects accompanying falling meteorite similar to thunder or the explosion, were recorded. Sonic booms were recorded at 7 seismic stations in Slovakia, Hungary, and Poland. Bolide was recorded also by radiometric sensors at six automatic bolide stations in the Czech Republic and one in Austria. On the basis of two private security cameras in Hungary (Örkény and Telki), which captured the fireball, trajectory and approximate location of the impact of meteorites, were calculated. Meteorite flew over Slovakia from west to east and disintegrated at explosion 35 km above the surface. Most of the meteorite fell on the area between Košice town and Vyšný Klátov village. By August 2010, 76 fragments of the meteorite were recovered of a total weight of 4.3 kg. The largest fragment is of the weight of 2.17 kg. Considering that individual meteorite fragments were found only a few weeks after the fall, the samples were only slightly affected by weathering. The Košice meteorite is the first Slovak meteorite and only the 15th with the known orbit in the interplanetary space. The meteorite Košice was officially approved by the Nomenclature Committee of the Meteoritical Society on June 27, 2011.

Mineralogical research was done mainly by using of polarized microscopy, electron microprobe (WDS, EDS, BSE, CL methods). From other analytical methods also Micro-Raman spectroscopy, ICP-MS, ICP-ES, Infrared spectroscopy, and powder X-ray diffraction, were applied.

In the thin sections meteorite is characterized by highly recrystallized fine-grained granular texture with abundant chondrules. Part of meteorite exhibits brecciated character, but individual breccia fragments show almost the same composition. Several types of chondrules are present; they are commonly indistinct and only a part of them are clearly visible. Most of chondrules contain forsterite but albite, augite and enstatite are also abundant. Rarely, some chondrules are formed predominantly by chromite. These chondrules have granular texture and usually are not of a perfect round shape. Size of chondrules is up to 1.1 mm. The Košice chondrite has a dark gray to black fusion crust with thickness up to 0.6 mm. Fusion crust is characteristic by remelting silicates, phosphates and oxides. Fe-Ni alloys were not remelting.

Based on the average compositions of forsterite (Fa_{19}) and enstatite (Fs_{17}), high metallic Fe and other criteria, the meteorite could be classified as the H-group ordinary chondrite. According to homogeneous compositions of forsterite (*olivine*) and enstatite, absence of igneous glass, presence of secondary albite predominately as crystalline aggregates and overall texture with (relatively high metamorphic grade) enable us to classify the Košice chondrite as petrologic type H5. Planar fractures in olivine and undulatory extinction of olivine and albite as well as opaque shock veins and locally melt pockets indicate S3 stage of shock metamorphism.

Mineralogy of the meteorite is characteristic for this type of chondrite. The major non-metallic minerals of the chondrite are forsterite, enstatite and albite ($Ab_{82}An_{12}Or_{06}$). Additional minerals comprise augite ($En_{45–59}Wo_{26–43}Fs_{08–15}$), chromite, chlorapatite, merrillite/tuite, graphite and Fe-oxides. Accessory graphite (<1 vol%) was confirmed by Micro-Raman spectrometry. Metallic phases are represented mostly by taenite, iron (*kamacite*) and tetrataenite. Sulphides are represented only by troilite. Iron and taenite form characteristic immiscible textures. Chemical composition of Fe, Ni alloys shows a rising of Ni + Cu contents with current recession of Fe + Co contents. Rarely, troilite forms veinlets with taenite skeletal crystals. These veinlets are one of the primary minerals in the chondrite and may indicate mobilization of metallic elements during metamorphism or local impacts-induced phenomena.

Acknowledgement. This work was supported by the Slovak Research and Development Agency under the contract No. APVV-0516-10 and VEGA – the Slovak Agency for Science, grant No. 2/0022/10.

GENESIS OF VEIN-STOCKWORK CRYPTOCRYSTALLINE MAGNESITE FROM THE DINARIDE OPHIOLITES

PALINKAŠ, L.[1]*, JURKOVIĆ, I.[2], STRMIĆ PALINKAŠ, S.[1] & GARAŠIĆ, V.[3]
[1] Institute of Mineralogy and Petrography, Faculty of Science, University of Zagreb, Horvatovac 95, Zagreb, Croatia
[2] Croatian Academy of Sciences and Arts, Zagreb, Croatia
[3] Faculty of Mining, Geology and Petroleum Engineering, University of Zagreb, Pierottijeva 6, Zagreb, Croatia
* E-mail: lpalinkas@geol.pmf.hr

Vein and stockwork depositions of cryptocrystalline magnesite, known also as Kraubath type, gelmagnesite, and Khalilovo type, are widespread phenomena in the Tethyan ophiolites from Alps to Zagros, including those in Dinarides, but also in other ophiolite suits like California, Bushveld, etc. Thirteen samples from the magnesite deposits: Čajetina, Kose, Krive Strane, Ćave, Mokra gora (Zlatibor Mt.), Trnava and Bela Stena (Raška, Kopaonik Mt.), Miličevci (Čačak), Goleš and Kamenica (Kosovo), and Banovići (Konjuh Mt.) in the Dinaridic and Vardar ophiolite belts were analyzed on C- and O isotopes, REE and trace elements, to shade more light on genesis of this specific genetic type, widespread along the whole Tethyan ophiolite belt.

From two controversial hypotheses on genesis, applying direction of flow of ore forming fluids – *per ascendum* and *per descendum* – the authors favour the latter. Pro and contra arguments for either models track the following reasoning:

1) Stable isotopic data on C- and O-isotopes in magnesite show significant regression line in all cryptocrystalline vein-stockwork deposits. It requires uniform conditions on a regional scale. Supply of light CO_2, needed for gaining low C-isotope values of the vein magnesite proposed by *per ascendum* model, can hardly derived by decarboxylation of organic rich sediments, in 2–3 km beneath the ophiolite, as a regional phenomenon. The *per descendum* model offers evolution of C-isotopes from heavy to light by gradual precipitation of heavier isotopes in magnesite in comparison to those of $(CO_3)^{2-}$ in the descending fluid. A closed, or semi-closed system regarding CO_2 supply in the fluid from lateritic weathering crusts downward is controlled by the Rayleigh equation. It does not require exceptionally light $\delta^{13}C_{CO2}$ and can satisfy the model with those of atmospheric origin with initial value of -7‰.

2) Extremely low values of REE and trace elements, as well as a simple monomineralic paragenesis, are results of precipitation from "clean descending fluid" already purified by weathering processes in the thick lateritic crust. *Per ascendum* hydrothermal fluids, mobilizing all elements accompanied in the ophiolitic precursor by the lateral-secretion model, would produce complex ferroan carbonate paragenesis, which appropriates to listvenites.

3) Degassing as a result of magnesite precipitation in the veins reaching 300 m depth requires a high partial pressure of the free CO_2 phase, and extremely unreal, high concentration of $\Sigma(CO_2)_{tot}$ under high pH conditions.

4) Mg-HCO_3 waters leaving the lateritic crust gradually precipitate magnesite on the way down, controlled by increasing pH. The final results are magnesium-poor waters of Ca-OH type. Magnesitization is a phenomenon similar to karstification in many respects.

REE chondrite-normalized patterns in magnesites reflect processes in the weathering lateritic crust. Mobilization of REE in saprolite by carbonate complexing, fixation and fractionation of LREE and HREE in the lateritic zone by adsorption on colloids and clays, and remobilization of REE in the ferruginous crust, shape the final patterns of the magnesite vein-stockwork system beneath.

DESERT ROSES – A CRYSTAL MORPHOLOGICAL STUDY

PAPP, R.[1]*, TÓTH, E.[2], BENDŐ, Zs.[3] & WEISZBURG, T.G.[1]
[1] Department of Mineralogy, Eötvös Loránd University, Pázmány P. sétány 1/C, H-1117 Budapest, Hungary
[2] Eötvös Museum of Natural History, Eötvös Loránd University, Pázmány Péter sétány 1/C, H-1117 Budapest, Hungary
[3] Department of Petrology and Geochemistry, Eötvös Loránd University, Pázmány P. sétány 1/C, H-1117 Budapest, Hungary
* E-mail: pappr@nhmus.hu

Desert roses are well-known crystallisation forms of the sulphates gypsum and barite: in arid climate, sulphate precipitating from evaporating fluids encloses grains of the surrounding sand. Evolved crystal groups usually consist of intergrown lens shaped "petals" or rosettes. The rosettes represent more or less simultaneous crystallisation centres that finally get connected in the course of multiple growth cycles.

Gypsum roses can be grouped according to the size and arrangement of the rosettes. Up to now, African gypsum samples have been studied in details, and three morphological groups have been distinguished. The first type is characterised by the presence of a big, central rosette and the other rosettes grow out from the middle of the central petal. At the second type plates grow randomly, and they cross other rosettes on many places. At both types, plate growth continues with the original orientation after crossing another plate, yet the growth of smaller rosettes usually stops at the contact with bigger rosettes. At the rare third type, plates do not grow through each other, but grow roughly parallel and they are only linked at the middle of the rosettes.

Gypsum roses from Chihuahua, Mexico, are spherical aggregates, built up of max. 5–6 mm long, colourless gypsum plates, and on the edge of the rosettes a white crust of anhydrite (possibly with some gypsum) is present, without any inclusions.

Many gypsum rosettes exhibit perfect cleavage, allowing a look inside the rosette. Stereomicroscopic and SEM observations suggest that the rosettes always cleave according to {010}, because we can observe two less perfect cleavage directions around the included sand grains, and the angle between these directions is close to 118.43° (or the 61.57°supplementary angle), corresponding to the angle between {100} (// *c* axis) and {011} (// *a* axis) on the (010) plane. This way the crystallographic orientation of the rosettes can be identified. Cleavage according to $\{11\bar{1}\}$ and $\{\bar{1}03\}$ (HINTZE, 1930) has not been observed on the desert rose samples.

Concerning the orientation of the rosettes (hypidiomorphic single crystals), the (010) plane is always perpendicular to the equatorial plane (the biggest circle cross section) of the rosette, the crystallographic axis *b* always being in the equatorial plane.

Gypsum roses can further be categorised upon their sand content: they can be rich or poor in sand grains. In the sand-poor rosettes, sand grains are aligned into growth zones. The middle of the rosette is mostly clear and inclusion-free, then towards the rim of the rosettes sand-rich zones alternate with clear, sand-free zones. Growth cycles probably start in a loose sandy environment, clear gypsum crystallising first, with the sand grains being pushed away from the growing crystal face, and subsequently, as the sand grains around the growing crystal get more closely packed, the crystal finally incorporates them. The growth zones usually have approximately rhombic cross section on the (010) plane, and the sand lanes run roughly parallel to the edges of the lens. The surface of the gypsum rosettes is uniformly coated with sand grains, and sand grains are accumulated at the connection zones of the rosettes.

Inclusion zones and perfect (010) cleavage are missing from the sand-rich rosettes. Inclusion zoning depends on the grain size of the sand, too: if the grains are larger than 2–3 mm, the gypsum simply grows around the grains, without forming grain-rich and grain-free growth zones.

Scanning electron microscopy equipped with energy-dispersive X-ray spectrometer (SEM-EDX) was applied for the identification of sand grains. More than 90% of the inclusions are quartz and alkali feldspar, but occasionally amphibole, TiO_2, iron (oxy)hydroxide, titanite, garnet, calcite, and zircon grains were identified, too.

Barite roses studied so far were full of sand and because of that we did not manage to make good cleavage planes on the petals. At some cases, at the edge of the rosettes and at the connection zone between petals, sand grains were aggregated by clay.

Reference

HINTZE, C. (1930): Handbuch der Mineralogie, 1.3.2., pp. 4274–4323.

FLUIDS IN UPPER MANTLE XENOLITHS FROM THE RIO GRANDE RIFT, NEW MEXICO, USA

PARK, M.[1]*, BERKESI, M.[2], JUNG, H.[1], KIL, Y.[3] & SZABÓ, Cs.[2]
[1] School of Earth and Environmental Sciences, Seoul National University, Seoul, Korea
[2] Lithosphere Fluid Research Lab, Eötvös University, Budapest, Hungary
[3] Geological Museum, Korea Institute of Geoscience and Mineral Resources, Daejeon, Korea
* E-mail: noproblem82@snu.ac.kr

Mantle-derived volatile-rich fluid inclusions can give important information on chemical features and physical condition on fluid regimes in the upper mantle. These volatiles may play also an important role in understanding the fluid/mantle rock interaction in the lithospheric mantle causing mantle metasomatism (BELKIN & DE VIVO, 1989; O'REILLY & GRIFFIN, 2000). Besides, the Rio Grande rift (abbreviated to as RGR) in New Mexico (USA) is an excellent place to study the evolution of the subcontinental lithospheric mantle to better explain its temporal and spatial heterogeneity. However, fluid inclusions study has not been carried out yet at the RGR.

Alkali basalt-hosted spinel peridotite xenoliths (~15 Ma age) were collected from Adam's Diggings in the RGR. We selected five representative spinel peridotite xenoliths which are the most abundant in fluid inclusions (FIs). Based on fluid inclusion petrography (e.g., ROEDDER, 1984), three kinds of FIs can be distinguished, which are: Type IA (healed, fracture-related, large negative crystal shape; 10–25 μm), Type IB (opaque-solid-bearing, less-small negative shape; 5–10 μm), and Type IC (exsolved spinel-related, spherical shape; 5–10 μm). We studied the FIs by the use of heating-freezing stage (microthermometry), high resolution Raman spectroscopy and FIB-SEM (Focused Ion Beam-Scanning Electron Microscopy) techniques. These FIs are characterized to be CO_2-dominated with other minor components (visible melting occurred at -58.0 to -56.8±0.2 ºC). The calculated CO_2 density for Type IC, IB and IA show 1.05–1.12 g/cm^3 and 0.98–1.08 g/cm^3, and 0.69–0.86 g/cm^3, respectively.

Raman analysis showed that, in addition to the CO_2-rich liquid, Type I FIs contains Mg-carbonate in each case. Furthermore, Type IA fluid inclusions showed a CO_2-H_2O system with hydrous solid (amphibole). Type IB and Type IC FIs showed a CO_2-N_2 system, but they also have a sulfur-bearing opaque solid.

FIB-SEM technique provided more information for solid phases within the FIs. In some FIs a thin glass film with vesicles can be observed at the wall of the FIs. Type IA FIs contain Ca-bearing sulphate, Fe-bearing oxide, Mg-carbonate, amphibole, but Type IB & IC have Fe (Ni-Cu-Co)-bearing sulphide.

Mantle fluids in RGR could experience at least three events in order to form three dominant FIs system indicating the complexity of mantle fluids in the RGR.

References

BELKIN, H.E. & DE VIVO, B., (1989): New Mexico Bureau Mines and Mineralogy Research Bulletin, 131: 20.

O'REILLY, S.Y. & GRIFFIN, W.L. (2000): Lithos, 53: 217–232.

ROEDDER, E. (1984): Fluid inclusions. Reviews in Mineralogy, 12: 1–646.

SUBMARINE HYDROTHERMAL AND SUPERIMPOSING GARNET FORMING METASOMATIC PROCESSES IN THE SZARVASKŐ BASALT FORMATION (NE-HUNGARY)

PÁSZTOR, D.[1]*, KISS, G.[1] & MOLNÁR, F.[2]
[1] Department of Mineralogy, Eötvös Loránd University, Pázmány P. sétány 1/c, H-1117 Budapest, Hungary
[2] Geological Survey of Finland, PO. Box 96, FI-02151 Espoo, Finland
* E-mail: carmelo.nuggets@gmail.com

The Bükk Mts. in NE-Hungary contains Triassic and Jurassic submarine basaltic rocks in the Szarvaskő Unit and in the Darnó Unit, which are related to the different evolutionary stages of the Neotethys. These rocks are considered to be fragments of Dinaridic origin and were displaced to northeast along the Periadriatic-Balaton-Darnó- and Mid-Hungarian Lineaments during the Oligocene-Early Miocene. These different magmatic blocks are found in the same accretionary mélange (HAAS & KOVÁCS, 2001; DIMITRIJEVIĆ *et al.*, 2003; KISS *et al.*, 2011).

This study focuses on a small quarry located in the Jurassic magmatic complex of the Szarvaskő Unit. This magmatic complex contains commonly gabbro, rarely ultramafic rocks as well as an extended pillow basalt series. According to HARANGI *et al.* (1996) and AIGNER-TORRES & KOLLER (1999), the formation of these series is most likely related to a back-arc basin, opened in the area of the Neotethian realm.

After completing fieldwork, in order to characterize the collected samples of the different pillows and their alteration mineral assemblage, macroscopic, stereomicroscopic, polarizing microscopic and SEM+EDX observations, XRPD measurements were performed.

The investigated rocks of the quarry represent the peperitic facies *s.l.* (i.e. local admixture of basaltic lava into water-soaked siliciclastic sediment) of a subaqueous lava-flow complex. However, a dolerite block was observed also, found in tectonic relationship with the pillow basalt series at the eastern part of the outcrop.

In the highly altered pillow basalt, channel-like cavities of 1–2 centimetres in diameter occur. In addition to the macroscopically observable pyrite, chalcopyrite, barite and gypsum (the latter formed as alteration product of the pyrite) were also found in the vugs. The formation of this mineral assemblage – together with the chlorite, albite, quartz and titanite hydrothermal alteration assemblage in the host rock –, were most likely formed in a submarine hot fluid circulation system of greater importance than a simple cooling-related hydrothermal process.

Completely altered basalt also occurs in some blocks of the outcrop. This rock is composed mainly of Ca-garnet (mostly grossular with high manganese content), chlorite and quartz. These minerals form a relict, porphyry-intersertal texture, replacing the original minerals of the basalt, however, the macroscopic appearance of the rock also resembles to its original pillow structure. This alteration parageneses can be explained by the effect of a Ca-metasomatic process, similar to the *sensu lato* rodingitization, superimposing the earlier, above discussed submarine hydrothermal mineralization. This is supported also by the rare presence of special minerals, like zircon and apatite, however, in our case, the formation of the garnet-bearing rock is more likely related to processes happened in a ridge-setting (reported also in Norway by AUSTRHEIM & PRESTVIK, 2008), different from formation of *sensu stricto* rodingite.

References

AIGNER-TORRES, M. & KOLLER, F. (1999): Ofioliti, 24: 1–12.

AUSTRHEIM, H. & PRESTVIK, T. (2008): Lithos, 104: 177–198.

DIMITRIJEVIĆ, M.N., DIMITRIJEVIĆ, M.D., KARAMATA, S., SUDAR, M., GERZINA, N., KOVÁCS, S., DOSZTÁLY, L., GULÁCSI, Z., LESS, Gy. & PELIKÁN, P. (2003): Slovak Geological Magazine, 9(1): 3–21.

HAAS, J. & KOVÁCS, S. (2001): Acta Geologica Hungarica, 44: 345–362.

HARANGI, Sz., SZABÓ, Cs., JÓZSA, S., SZOLDÁN, Zs., ÁRVA-SÓS, E., BALLA, M. & KUBOVICS, I. (1996): International Geological Review, 38(4): 336–360.

KISS, G., MOLNÁR, F., KOLLER, F. & PÉNTEK, A. (2011): Mitteilungen der Österreichischen Mineralogischen Gesellschaft, 157: 43–69.

APPLICATION OF AN INNOVATIVE BENEFICIATION TECHNIQUE TO KRASTA CHROMITE ORE (ALBANIA) FOR THE PRODUCTION OF HIGH GRADE – LOW SILICA CHROMITE SAND

PEDROTTI, M.*, GRIECO, G. & KASTRATI, S.
Dipartimento di Scienze della Terra "A. Desio", Università degli Studi di Milano; Via Botticelli 23, Milano, Italy
* E-mail: maria.pedrotti@unimi.it

The Mirdita ophiolite is located in the northern ophiolite belt of Albania. Based on differences in the internal stratigraphy and chemical composition of the crustal units, two types of ophiolites have been recognized in the Mirdita ophiolite, namely the Western Mirdita Ophiolite (WMO) and the Eastern Mirdita Ophiolite (EMO) (DILEK *et al.,* 2008). Boninitic dikes and lavas crosscut and/or overlie the older extrusive rocks in the EMO (BECCALUVA *et al.,* 1994). The crustal section of the WMO has MORB affinities, whereas that of the EMO predominantly shows SSZ geochemical affinities. The extrusive sequence in the EMO consists of pillowed to massive flows ranging in composition from basalt and basaltic andesite in the lower section to andesite, dacite, and rhyodacite in the upper part (BORTOLOTTI *et al.,* 1996). Large peridotite massifs are exposed at the western and eastern ends of the Mirdita ophiolite. Plagioclase-bearing peridotites are frequently observed in the WMO, whereas harzburgite is dominant in the EMO (BEQIRAJ *et al.,* 2000).

In this work, we focus on Bulqiza peridotite massif located in the EMO, because it has economically important chromite ores. Chromite is an important mineral used in the metallurgy, chemistry and refractory industries and often requires enrichment processes to achieve the chemical parameters for different markets.

This work deals with disseminated chromite ore samples collected at Krasta Mine, located in the central southern part of the Bulqiza Massif. First of all the samples, having an average Cr_2O_3 content of 23.66 wt%, were enriched using spirals and shaking tables at Krasta plant. The first chromite sand concentrate has 46.58 wt% Cr_2O_3 and 10.35 wt% SiO_2. In order to meet the very demanding chemical parameter requirements for refractory market, chromite first concentrate sand was re-enriched using a combination of dry magnetic and gravity separation at the pilot plant of Omega Foundry Machinery Ltd. in Peterborough (UK). In a second step sand was enriched using a drum magnet. New concentrate was then enriched in a third step by means of an Inclined Fluidised Separator (IFS) that works in dry conditions using an air cushion as fluidisation agent.

Preliminary results show that the pilot plant is able to strongly re-enrich the primary concentrate sand, producing a final concentrate sand with up to 60.01 wt% Cr_2O_3 and 2.43 wt% SiO_2 with a tail that is still suitable for the steel market (Fig. 1).

References

BECCALUVA, L., COLTORTI, M., PREMTI, I., SACCANI, E., SIENA, F. & ZEDA, O. (1994): Ofioliti, 19: 77–96.

BEQIRAJ, A., MASI, U. & VIOLO, M. (2000): Exploration and Mining Geology, 9: 149–156.

BORTOLOTTI, V., KODRA, A., MARRONI, M., MUSTAFA, F., PANDOLFI, L., PRINCIPI, G. & SACCANI, E. (1996): Ofioliti, 21: 3–20.

DILEK, Y., FUMES, H. & SHALLO, M. (2008): Lithos, 100: 174–209.

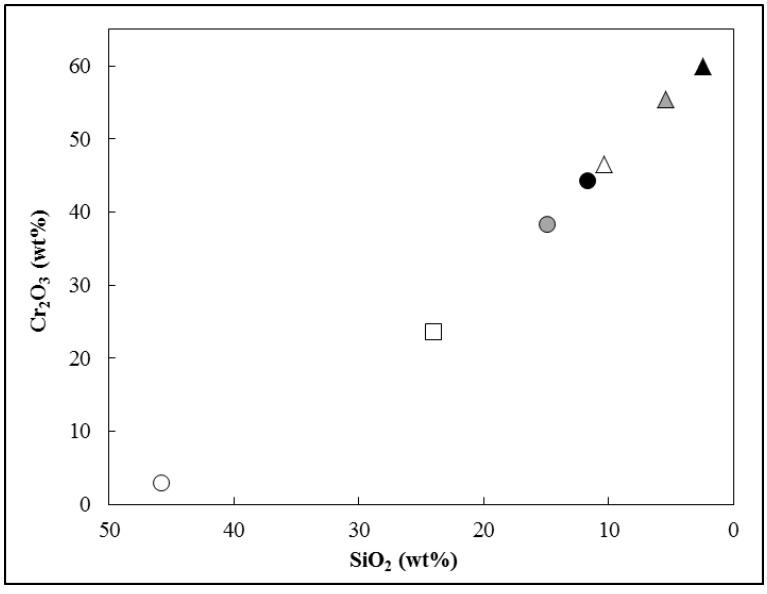

Fig. 1. *Three steps Krasta chromite ore enrichment: spirals and shaking tables at Krasta plant (white symbols), drum magnet (grey symbols) & IFS (black symbols) at Peterborough pilot plant. Square = feed, triangles = concentrates and circles = tails. First and second concentrates are the feeds of the following steps.*

THE SOWIE MTS. PEGMATITES (LOWER SILESIA, SW POLAND): A CURRENT KNOWLEDGE

PIECZKA, A.[1]*, ŁODZIŃSKI, M.[2], SZEŁĘG, E.[3], ILNICKI, S.S.[4], NEJBERT, K.[4], SZUSZKIEWICZ, A.[5], TURNIAK, K.[5], BANACH, M.[6], MICHAŁOWSKI, P.[6] & RÓŻNIAK, R.[6]
[1] Department of Mineralogy, Petrography and Geochemistry, AGH – University of Science and Technology, Mickiewicza 30, 30-059 Kraków, Poland
[2] Department of General Geology, Environmental Protection and Geotourism, AGH – University of Science and Technology, Mickiewicza 30, 30-059 Kraków, Poland
[3] Dept. of Geochemistry, Mineralogy and Petrography, University of Silesia, Będzińska 60, 41-200 Sosnowiec, Poland
[4] Inst. of Geochemistry, Mineralogy and Petrology, Univ. of Warsaw, Żwirki and Wigury 93, 02-089 Warszawa, Poland
[5] Institute of Geological Sciences, University of Wrocław, Cybulskiego 30, 50-205 Wrocław, Poland
[6] DSS S.A. Company, Piława Górna Quarry, Sienkiewicza 96, 58-240 Piława Górna, Poland
* E-mail: pieczka@agh.edu.pl

Pegmatites of the Sowie Mts. gneissic block are known for at least 150–200 years. In the 19th century, they were mined out in numerous localities, *e.g*. Owiesno, Różana, Piława, Bielawa, Kamionki, mainly as a feldspar raw material. Most data pertinent to the mineralogy of the pegmatites date back to that period. In the pegmatite of Michałkowa (*type locality*), WEBSKY (1868) described a new phosphate mineral, sarcopside, $(Fe,Mn,Mg)_3(PO4)_2$, accompanied by huréaulite and vivianite (fide LIS & SYLWESTRZAK, 1986). Another phosphate, triplite, $(Fe^{2+},Mn)_2PO_4F$, was reported in a railway crosscut northwards of Piława Górna (FIEDLER, 1863; DATHE & FINCKH, 1924; HINTZE, 1933; LIS & SYLWESTRZAK, 1986), while a mineral representing the columbite group, $(Fe,Mn)(Nb,Ta)_2O_6$, in form of plates up to 5 mm in diameter, was found in a pegmatite occurring also nearby Piława Górna (ROMER, 1864; ROTH, 1867; TRAUBE, 1888; HINTZE, 1933; LIS & SYLWESTRZAK, 1986). MIKUSZEWSKI *et al.* (1976), based on geochemical investigations about of 100 surface-available pegmatite bodies, concluded that the Sowie Mts. metamorphism (*ca*. 380–370 Ma) was not sufficient for the formation of zoned pegmatite bodies enriched in trace elements. However, PIECZKA *et al.* (2003, 2004) gave first indications on Li-bearing mineralization in pegmatites of the region. These are the presence of ferrisicklerite, $Li_{1-x}(Fe,Mn)PO_4$, forming lamellar intergrowths with graftonite, sarcopside, Ca-beusite, staněkite, alluaudite and numerous others phosphates in a pegmatite from Lutomia, as well as green elbaite found in the vicinity of Gilów. Moreover, the occurrences of columbite-(Fe) and Pb-bearing microlite, in the form of inclusions in beryl crystals, were reported by ŁODZIŃSKI & PIECZKA (2008) from the region Owiesno–Kietlice. It was more and more evident that at least some of the Sowie Mts pegmatites represent transitional varieties between the MS and REL classes in the pegmatite classification by ČERNY & ERCIT (2005). NOVÁK (2005), who characterized pegmatites in the Bohemian Massif, preclassified Sowie Mts. pegmatites as LCT, beryl pegmatites.

Six-year period of mining activity of the Company *Dolnośląskie Surowce Skalne S.A*. at Piława Górna, a supplier of crushed aggregates for the largest national infrastructure projects including first of all the construction of express roads and motorways, with an output of 20–25 million tons of various metamorphic rocks, resulted in formation of an immense open pit enabling viewing down to 100 m of the massif. The metamorphic rocks are frequently cut with pegmatite veins, especially of dyke nature (*Julianna-2008, Subtrio-2009, Lithium-2010*) reaching vertically to 30–40 m, horizontally to 80–100 m, in thickness to 4–6 m, with the tonnage reaching 40.000–50.000 tons, showing distinct zoning (border zone, graphic zone, massive feldspars zone, quartz nucleus). Such big pegmatite bodies have not been hitherto known. Beforehand, a vein-and-lens pegmatite system from Lutomia, approx. 20 m long, was considered as the biggest pegmatite in the Sowie Mts. region.

The pegmatites from Piława Górna exhibit diversified states of geochemical evolution, from almost completely barren, through poorly to highly evolved, with local concentrations of Li, Cs, Be, B, Nb, Ta and REE-bearing mineralization. They can be classified as LCT, MS-REL to REL pegmatites. The basic minerals are typical of pegmatite: quartz, microcline, albite, biotite, muscovite, frequently black tourmaline (schorl), garnet evolving from almost $Alm_{50}Spe_{50}$ in veins of poorly-evolved pegmatite to $Spe_{97}Alm_3$ in the most evolved Li-bearing pegmatite representing the albite-spodumene class. The mineral of **beryl**, $Be_3Al_2[Si_6O_{18}]$, the main carrier of **Be**, occurs in all pegmatite bodies, although in various forms and colours (greenish, yellowish, white, pinkish, bluish). In the most evolved Li- and Cs-bearing pegmatite *Lithium-2010*, it evolved into a composition typical for **pezzottaite**, $CsBe_2LiAl_2[Si_6O_{18}]$. Beryl is usually accompanied by small quantities of **bavenite**, $Ca_4Be_2Al_2Si_9O_{26}(OH)_2$ and **bityite**, $CaLiAl_2Si_2BeAlO_{10}(OH)_2$. **Phenakite**, $Be_2[SiO_4]$, **helvite**, $Mn_4Be_3Si_3O_{12}S$, and probably **liberite,** Li_2BeSiO_4, so far have been encountered only as accessory minerals. Beryl is not distributed uniformly in veins; apart from a pegmatite relatively poor in this mineral (*Julianna-2008* type), there was also exposed a big pegmatite vein (*Subtrio-*

2009 type, approx. 10,000–15,000 m^3 rock), in which the contact between the feldspar zone and the quartz nucleus was almost completely grown with crystals of this mineral.

In poorly evolved pegmatite, type *Julianna-2008*, **Nb** and **Ta** mineralization is encountered in the form of **columbite-(Fe)**, evolving toward **columbite-(Mn)**, **tantalite-(Fe)** and further toward **ixiolite** overgrown with Nb- and Ta-bearing **cassiterite**, and **titanian ixiolite**. Relics of the last phase were found in minerals of the samarskite group: prevailing **ishikawaite** and **samarskite-(Y)** in minor amounts. Grains of those minerals are usually overgrown with **polycrase-(Y)** and various minerals belonging to the **pyrochlore** and **betafite** groups of the pyrochlore supergroup (**pyrochlore**, **yttropyrochlore**, **uranpyrochlore**, **betafite** and **yttrobetafite**). In addition, the contents of Nb and Ta reach more than 5 wt% Ta and 3 wt% Nb in **cassiterite** and more than 4.0 wt% Ta and 3.0 wt% Nb in **titanite**. Columbite grain sizes are diversified. The largest crystal of columbite-(Fe) reached 6 cm; but usually crystals of the mineral are considerably finer. Grains of the samarskite-group minerals reach even 2 cm in size, but in most cases are smaller. Ixiolite is rather fine. The Li- and Cs-bearing pegmatite, type *Lithium-2010*, also contains **columbite-(Mn)** that evolves towards **tantalite-(Mn)**, forming plates and needle-shaped crystals, up to 2 cm in length, sometimes altered into **microlite**, **plumbomicrolite**, and **bismutomicrolite** (all of them belonging to the pyrochlore supergroup), Nb- and Ta-enriched **rutile** and **ilmenite** containing up to a dozen or so wt% Nb or Ta, **wodginite**, as well as Ta-rich members of the **roméite** group.

Carriers of alkali metals (**Li**, **Rb**, and **Cs**) are only connected with moderately and highly fractionated pegmatites (types *Subtrio-2009* and *Lithium-2010*). **Lepidolite** (pink mica) and **spodumene,** $LiAlSi_2O_6$, as well as coloured tourmalines (mainly **elbaite** to **olenite**, with **rossmanite and liddicoatite** domains) are main carriers of Li. Others, already aforementioned Li-bearing phases are represented by **bityite** (*Subtrio-2009*), **lithiophilite** and the most probably **liberite,** Li_2BeSiO_4 and **eucryptite**, $LiAlSiO_4$ (*Lithium-2010*). Rubidium is concentrated in feldspars (0.4–0.5 wt% Rb) and micas, especially of the highly fractionated *Lithium-2010* pegmatite because of its substitution for K. Cesium mineralization has been recognized in blocks of the Li-bearing pegmatite as separate nests of **pollucite**, $(Cs,Na)_2Al_2Si_4O_{12} \bullet H_2O$, reaching up to 30 cm in length. In the outermost parts of beryl crystals, coming from *Lithium-2010* pegmatite, there was diagnosed a zone containing up to 15 wt% Cs, whose composition corresponds to Cs-bearing variety of beryl named **pezzottaite**. Other beryl crystals contain up to 7 wt% Cs, but Cs is negligible in crystals coming from *Julianna-2008* and *Subtrio-2009* pegmatites. In addition, Cs was identified as an important substituent in K-feldspars (to 0.2 wt%) and in some dark micas (up to 18 wt% Cs), in which it prevails over K.

Rare earth elements, including Sc and Y, concentrate mainly in poorly fractionated pegmatites, type *Julianna-2008*, in which REE-containing phases are sometimes disseminated mainly around the border between the graphic zone and massive feldspar zones. The phases are represented mainly by **fluorapatite**, minerals of the **samarskite** group, containing from around 2 to more than 6 wt% Y and 4 wt% of other lanthanides. Lower REE contents correspond to **ishikawaite**, higher to **samarskite-(Y)**. **Polycrase-(Y)** that co-occurs with samarskite contains around 10.0–13.0 wt% Y and 7–8 wt% of other rare earth elements. Similar contents of REE are recorded in **yttropyrochlore** and **yttrobetafite**. Apart from the mentioned phases, REE are main components in **monazite,** $(Ce,Nd,Sm,La)PO_4$, and **xenotime,** $(Y,Yb,Er,Dy,Ga)PO_4$; while in **thorite** detected were approx. 3 wt% Y and 2–4 wt% LREE.

In the pegmatites, as well as in the surrounding amphibolite have been recognized trace sulfide mineralization including Ni-bearing pyrrhotite, pyrite, arsenopyrite, chalcopyrite, sphalerite, galena, bismuthinite and a still unrecognized Ag-Bi-sulfosalt, as well as bismutite and native Bi. This type of mineralization may be related to the hydrothermal stage, which had formed many small ore deposits mined within the Block area before many years ago.

The presented draw on the current knowledge of mineralogy of the Sowie Mts. pegmatites indicates that the bodies may be quite exceptional even in the scale of whole Bohemian Massif. Large dimensions of the bodies arise a question about economic significance of the pegmatites as K-feldspar raw material or as a potential source of some critical elements. The described pegmatites *Julianna-2008*, *Subtrio-2009* and *Lithium-2010* have been completely excavated during winning of migmatite and amphibolite rocks.

Acknowledgement. This work was supported by MNiSZW grant N N307 241737.

References

ČERNY, P. & ERCIT, T.S. (2005): Canadian Mineralogist, 43: 2005–2026.

LIS, J. & SYLWESTRZAK, H. (1986): Minerały Dolnego Śląska. Wrocław.

ŁODZIŃSKI, M. & PIECZKA, A. (2008): Mineralogia – Special Papers, 32: 108.

MIKUSZEWSKI, J., KANASIEWICZ, J. & JĘCZMYK, M. (1976): In: FEDAK, J. (Ed.): The current metallogenic problems of central Europe, 290–304.

NOVÁK, M. (2005): Acta Musei Moraviae, Scientiae geologicae, 90: 3–74

PIECZKA, A., GOŁĘBIOWSKA, B. & SKOWROŃSKI, A. (2003): Book of abstracts. International Symposium on Light Elements in Rock-forming Minerals. Nové Město na Moravě, Czech Republic, June 20 to 25, 63–64.

PIECZKA, A., ŁOBOS, K. & SACHANBIŃSKI, M. (2004): Mineralogia Polonica, 35(1): 3–14.

CONGOLITE FROM THE KŁODAWA SALT MINE (CENTRAL POLAND) AND ITS IMPORTANCE AT EVALUATION OF METAMORPHIC CONDITIONS IN THE SALT DOME

PIECZKA, A.[1]* & WACHOWIAK, J.[2]
[1] Department of Mineralogy, Petrography and Geochemistry, AGH – University of Science and Technology, al. Mickiewicza 30, 30-059 Kraków, Poland
[2] Department of Economic and Mining Geology, AGH – University of Science and Technology, al. Mickiewicza 30, 30-059 Kraków, Poland
* E-mail: pieczka@agh.edu.pl

Congolite, $(Fe,Mg)_3B_7O_{13}Cl$, a mineral belonging to the boracite group (boracite, trembathite, congolite, chambersite and ericaite), occurs in nature exceptionally rarely in marine evaporites. For the first time this mineral was described from Mesozoic salts of Kouilou Department in Republic of Congo, Brazzaville (WENDLING *et al.*, 1972), and then was only found in the Penobsquis and Millstream evaporate deposits of southern New Brunswick, Canada (ROULSTON & WAUGH, 1981; BURNS & CARPENTER, 1996; GRICE *et al.*, 2005), and in the Boulby potash mine, Loftus, Cleveland, England *(http://www.mindat.org*). The Kłodawa salt dome, with active underground salt mine, is a following occurrence of congolite.

Congolite has been recognized in the Underlying Halite and Youngest Halite units of the Zechsztein profile, separated with the Pegmatite Anhydrite unit. The Underlying Halite, forming the top of the PZ–3 cyclothem, is represented by three-meter-thick layer of grey-orange rock-salt containing 93.4–96.1 wt% NaCl. The Youngest Halite of the PZ–4 cyclothem forms *ca*. 70-meter-thick lode of almost pure halite (98.5–99.0 wt% NaCl), pale orange to pale pink in colour. Congolite occurs at the bottom of the layer, about 3–4 m from the contact with the Pegmatite Anhydrite, in an interval of further 4–5 m.

The Kłodawa congolite forms euhedral, pseudo-cubic crystals with dominant {100} and less prominent {111} forms, with sizes commonly ranging from 0.3 to 0.6 mm. Only a dozen crystals out of some hundred distinguished from the rock-salt samples proved to be bigger than 1 mm, but not more than 1.2 mm. The crystals are of vitreous lustre, commonly translucent to transparent, with colour varying from yellowish through pale-violet to pale-violet-brown and brownish, with zonal texture often visible in hand specimens. Back-scattered-electron (BSE) images show complex internal texture of the congolite crystals in detail. They are commonly composed of numerous Fe-rich endomorphs with delicately-marked oscillatory zoning, which emphasizes growth stages of the {100} rhombohedral form. The endomorphs are overgrown with numerous medium to dark grey zones grading into the {100} orthorhombic form. Furthermore, such orthorhombic subcrystals are overgrown with some distinct concentric zones parallel to faces of the {100} and, less commonly, {111} cubic forms. Compositions of all zones correspond to congolite with varying Fe, Mg and Mn contents, but always with Fe exceeding Mg. Such a crystal texture distinctly reflects phase-transitions from rhombohedral congolite to orthorhombic ericaite and finally to cubic, high-temperature Fe-dominant analogue of boracite during crystallization of the Fe-dominant borate at increasing temperatures. Currently, parts of the crystals exhibiting the orthorhombic and cubic morphology represent congolite paramorphoses after the higher-temperature orthorhombic and cubic borate, $(Fe,Mg)_3B_7O_{13}Cl$, unstable in the room-temperature.

Diversified composition of the congolite in the border zones, with morphology passing from rhombohedral to orthorhombic and from orthorhombic to cubic presented in the system *temperature–atomic proportion Fe* that reflects phase relations in the series boracite-trembathite-congolite (BURNS & CARPENTIER, 1996), gives an opportunity to evaluate temperature of the metamorphic processes within the salt dome (*ca*. 230–250°C and 310–320°C, respectively), initiating migration of $(BO_3)^{3-}$ and Mg^{2+}-bearing brines and fluids and crystallization of $(Fe,Mg,Mn)_3B_7O_{13}Cl$ in Fe-enriched, pinkish-coloured rock-salts (from *ca*. 100–150°C to *ca*. 350–360°C). Two stages, which can be related to inflows of Mg^{2+}-bearing fluids, are marked by decreasing Mn/(Mn + Fe) ratio during growth of the rhombohedral endomorphs and follow the cubic borate. Differentiation in composition of all the remaining zones connected with increasing Mn/(Mn + Fe) ratio is rather a result of Mn-Fe fractionation and different diffusion of Mg^{2+}, Fe^{2+} and Mn^{2+} to the crystals growing under disequilibrium conditions.

References

BURNS, P.C. & CARPENTER, M.A. (1996): Canadian Mineralogist, 34: 881–892.
GRICE, J.D., GAULT, R.A. & VAN VELTHUIZEN, J. (2005): Canadian Mineralogist, 43: 1469–1487.
ROULSTON, B.V. & WAUGH, D.C.E. (1981): Canadian Mineralogist, 19: 291–301.
WENDLING, E., HODENBERG, R.V. & KÜHN, R. (1972): Kali und Steinsalz, 6: 1–3.

MELT AND SUBDUCTION-RELATED FLUIDS IN THE PERŞANI MOUNTAINS, ROMANIA UPPER MANTLE XENOLITHS

PINTÉR, Zs., SZABÓ, Á.*, BERKESI, M., TÓTH, A. & SZABÓ, Cs.
Lithosphere Fluid Research Lab, Department of Petrology and Geochemistry, Eötvös University, Pázmány Péter sétány 1/C, H-1117 Budapest, Hungary
* E-mail: sz_abel@yahoo.com

The Plio-Pleistocene alkali basalts in the Carpathian–Pannonian Region brought a large amount of lithospheric mantle xenoliths to the surface. The easternmost and youngest alkaline basaltic volcanic field is developed in the Perşani Mountains (Eastern Transylvanian Basin, Romania), where numerous upper mantle xenoliths have been studied (SZABÓ *et al.*, 2004). By studying these xenoliths, we can insight into the lithospheric mantle regarding its chemical and physical processes such as partial melting, metasomatism, deformation. Compilation of the impact of these processes on the lithospheric mantle provides significant information about their relationship to the subduction of the European plate beneath the Eastern Carpathians, which is the major geodynamic event of the studied area.

Seven spinel lherzolite/hornblendite composite and four amphibole-clinopyroxenite xenoliths were selected for this paper to study the metasomatic process. The peridotites contain small amount of interstitial amphibole, whereas the hornblendites and amphibole-clinopyroxenites contain occasionally other OH-bearing minerals such as apatite and phlogopite. The amphiboles and clinopyroxenes in spinel lherzolites are depleted in incompatible trace elements, where the same minerals in hornblendites and amphibole-pyroxenites show elevated incompatible trace element content. These geochemical characteristics and their high La/Lu ratios suggest that the hornblendites and amphibole-pyroxenites were formed by an incompatible element enriched mafic silicate melt (POWELL *et al.*, 2004).

Three spinel lherzolite/hornblendite composite and one clinopyroxenite xenoliths were selected for fluid inclusion study. In the composite xenoliths two generations of fluid inclusions can be distinguished. Older generation (Type 1) fluid inclusions can be seen randomly in the hornblendite vein. These fluid inclusions show negative crystal shape with 30–70 μm average size, and they are partly decrepitated along the cleavage plains of amphiboles. Younger generation (Type 2) fluid inclusions occur in ortho- and clinopyroxenes near to the hornblendite vein. They trapped along healed fractures, which cross the hornblendite vein too. These fluid inclusions have also negative crystal shape with an average 15–30 μm size. Solid phases inside of the fluid inclusion are also observed under the petrographic microscope in both types. Microthermometric and Raman analyses (at room temperatures and elevated temperatures up to +150 °C, after BERKESI *et al.*, 2009) indicate that the two generations of fluid inclusions have different character. The Type 1 inclusions contain CO_2, however Type 2 fluids contain CO_2, N_2 and in some cases small peak of H_2O as a dissolved component. By Raman spectroscopy, magnesite as well as apatite, Mg- and Na-rich carbonate minerals and quartz were detected inside the fluid inclusions hosted in the hornblendite vein (Type 1). Solid phases in Type 2 fluid inclusions were identified as magnesite. Based on synchrotron coupled infrared spectroscopy, beside the CO_2, H_2O was also detected and mapped in hornblende hosted fluid inclusions from Type 1.

These features indicate a complex melt-mantle interaction beneath the study area, which can be related to a subducted slab.

References

BERKESI, M., HIDAS, K., GUZMICS, T., DUBESSY, J., BODNAR, R.J., SZABÓ, Cs., VAJNA, B. & TSUNOGAE, T. (2009): Journal of Raman Spectroscopy, 40: 1467–1463.

POWELL, W., ZHANG, M., O'REILLY, S.Y. & TIEPOLO, M. (2004): Lithos, 75: 141–171.

SZABÓ, Cs., FALUS, Gy., ZAJAC, Z., KOVÁCS, I. & BALI, E. (2004): Tectonophysics, 393: 119–137.

TESTING THE HEAVY MINERALS ACCUMULATION IN BOZEŞ SEDIMENTARY ROCKS (SOUTH APUSENI MTS., ROMANIA)

POJAR, I.* & ZAHARIA, L.
Department of Geology, Babeş-Bolyai University, Kogălniceanu Street 1, Cluj-Napoca, Romania
* E-mail: iuly_rew@yahoo.com

Hydraulic sorting is an important factor which may influence the sediments during transportation and deposition, resulting in mineralogical and chemical differentiations due to the preferential accumulation of weathering-resistant heavy minerals, such as zircon, apatite, monazite and titanite (sphene) (NESBITT & YOUNG, 1996). These accessory phases are the main hosts for some trace and RE elements (e.g. Zr, Y, U, Th, Nb, Ta; MASS & McCULLOCH, 1991), thus their fractionation may produce irregular chemical variations in rock composition, and furthermore may complicate the interpretation of sedimentary provenance, mainly based on RE and selected trace elements contents (LA FLÈCHE & CAMIRÉ, 1996). Even more, in some cases the hydraulic sorting may indicate the way and the direction of the detrital flow.

Therefore, the evaluation of the intensity of sorting is a very important task, and can be performed either through the shape of rock fragments and quartz grains or through the geochemical composition of the rocks, by examining the abundances and co-variations of selected elements (e.g., LI *et al.*, 2008).

The studied area, located in the SE part of the Metaliferi Mountains (Apuseni Mts.), was part of a Late Cretaceous basin in which siliciclastic material was deposited in turbiditic facies. Now the detrital rocks, as rhythmical alternations of clays and sandstones, with an overall thickness of 3000 m, constitute the Bozeş Formation. Twenty two sandstone samples were collected and investigated in terms of petrography and whole-rock geochemistry in order to test the intensity of sorting and its effects on heavy minerals accumulations.

Under the microscope, most of the samples show angular to subangular lithic fragments and quartz grains. There are few exceptions, with more rounded grains, but these are not preferential to any part of the basin. Thus, a short-term transportation and consequently, a lower sorting degree are inferred for Bozeş sediments.

Geochemically, constant abundances, as well as weak and unsystematic co-variation of selected elements, show a low degree of sorting (LI *et al.*, 2008), and this is the case for Bozeş sediments, with constant Zr, Nb, Y and Ta abundances. Furthermore, very weak correlations are observed between LREE and Th, Ta/La and Ti or HREE and Hf (LA FLÈCHE & CAMIRÉ, 1996). No fractionation of the Ta/La ratios excludes any significant accumulation of zircon and titanite (Fig. 1), which may increase the Th, Hf, and Ta contents of the sediment, besides Zr. In the same way, a very weak accumulation of apatite is shown by the Tb/Yb ratios.

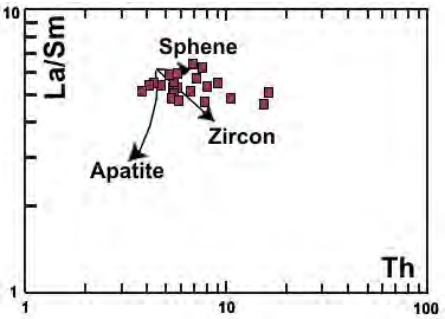

Fig. 1. *Plot showing the effects of heavy mineral accumulation on Th and La/Sm ratios in Bozeş sedimentary rocks (after LA FLÈCHE & CAMIRÉ, 1996).*

Therefore it can be concluded that heavy mineral accumulation did not influenced significantly the geochemical signature of the Bozeş sedimentary rocks, which can be used further for provenance interpretations.

Acknowledgements. This study was financially supported by the project PN II-RU_TE_ 313/2010 (CNCSIS-UEFISCSU, Romanian Ministry of Education and Research).

References

LA FLÈCHE, M.R. & CAMIRÉ, G.E. (1996): Canadian Journal of Earth Sciences, 33: 676–690.

LI, Q., LIU, S., WANG, Z., CHU, Z., SONG, B., WANG, Y. & WANG, T. (2008): International Journal of Earth Sciences (Geologische Rundschau), 97: 443–458.

MASS, R. & McCULLOCH, M.T. (1991): Geochimica et Cosmochimica Acta, 55: 1915–1932.

NESBITT, H.W. & YOUNG, G.M. (1996): Sedimentology, 43: 341–358.

SURFACE TOPOGRAPHY OF GLAUCONITE GRAINS: A PRELIMINARY INTERFEROMETRY STUDY

POP, D.[1]*, LUTTGE, A.[2,3], FISCHER, C.[4] & ARVIDSON, R.S.[2]
[1] Museum of Mineralogy, Babeş-Bolyai University; Kogălniceanu St. 1, Cluj-Napoca, Romania
[2] Department of Earth Sciences, Rice University; Main Street 6100, Houston, USA
[3] Department of Chemistry, Rice University; Main Street 6100, Houston, USA
[4] Geowissenschaftliches Zentrum, Georg-August-Universität; Goldschmidtstr. 3, Göttingen, Germany
* E-mail: dana.pop@ubbcluj.ro

Glauconite is an iron-rich, mica-type clay-sized mineral that forms as a rule in marine environments *via* successive diagenetic processes. It is commonly accepted that one prerequisite factor in glauconite genesis is the existence of a mineral or organic precursor, as microenvironment for the essential chemical exchanges (*e.g.*, ODIN, 1988). The typical granular or globular/pelletal shape of glauconite microcrystalline aggregates is considered to reflect the precursor's outline, at least up to a certain stage in the formation. Based on these constraints, morphological classifications of glauconite (*e.g.*, TRIPLEHORN, 1966) have distinguished diverse grain types such as faecal pellets, fossil casts, macrofossil debris, mineral/rock clasts, volcanic glass shards (based on the precursor type), or "cauliflower", "en accordion"/vermicular, fragmentary, spongy, film/ pellicle (based on the grain's final shape). Glauconite grains may also undergo multiple stages of transport and deposition, and thus their morphology at macroscopic and microscopic scales may record complex changes in their environment. Finally, the surface topography of glauconite grains may also reflect mechanical and chemical damage introduced by common methods of sample concentration and preparation, *e.g.*, centrifugation or acid leaching.

The purpose of our study is to understand how the surface topography of a glauconite grain relates to the nature of its precursor and its subsequent history of diagenesis and transport. We have thus used vertical scanning interferometry (VSI) to study glauconite grains sampled from the Transylvanian Depression (Romania), representing diverse depositional environments ranging in age from Cretaceous to Miocene. The mineralogical and geological features of these materials have already been characterized in detail (POP & BEDELEAN, 1996).

Interferometry quantitatively provides surface heights (*z*) with very high, near atomic scale vertical resolution and a wide vertical scan range from ~100 μm down to ~2 nm. The typical lateral (*x, y*) resolution ranges from 0.15 to 1.5 μm, depending mainly on the numerical aperture of the applied Mirau objective (LUTTGE & ARVIDSON, 2010). VSI's large scan range permits the study of materials whose high surface roughness (>> 1 μm) would preclude analysis by atomic force microscopy (AFM). Interferometry data consist of detailed digital surface maps of grain topography. These data permit compact surface characterization by calculation of, *e.g.*, heights' frequency distribution and of several surface roughness parameters. The latter can be used for defining surface building blocks characterized by specific wavelengths and heights (FISCHER *et al.*, 2008).

We have used two VSI instruments with different analytical configurations that allowed taking measurements at both large (overall grain-wise) and small (grain surface-wise) scales. In order to provide comparable data, we have selected for detailed analysis two fixed sizes for the fields of view: 20 x 20 μm (160x magnification) and 50 x 50 μm (50x magnification). Based on synthetic histograms, the typical glauconitic topographic "leitmotifs" have heights (*z*, in μm) of: 2.6, 1.6 (±1.1), 0.2, -0.2, -0.7 and -2.6; the maximum frequency corresponds to the 0.2 μm "hill". Among basic building blocks, negative topographic features ("valleys") are less frequent; they were better visualized by using the 50x objective. The grains having supposed faecal pellet precursors show the smoothest surfaces with the smallest *z* variation interval: 4 to -1 μm. Bioclasts generate more diverse grain topographies, with *z* ranging from 4 to -3 μm. "Vermicular" grains show strongly asymmetric, narrow histograms with *z* varying from 7 to -2 μm, probably reflecting the more complex topography of their supposed mica precursors. These preliminary data suggest that predictable relationship exist between the surface morphology and roughness of glauconite grains and the identity of their precursors.

References

FISCHER, C., KARIUS, V., WEIDLER, P.G. & LUTTGE, A. (2008): Langmuir, 24: 3250–3266.
LUTTGE, A. & ARVIDSON, R.S. (2010): Journal of the American Ceramic Society, 93(11): 3519–3530.
ODIN, G.S. (Ed.) (1988): Green marine clays. Developments in Sedimentology, 45: 1–444.
POP, D. & BEDELEAN, I. (1996): Acta Mineralogica-Petrographica, 37: 5–33.
TRIPLEHORN, D.M. (1966): Sedimentology, 6: 247–266.

POTENTIALLY TOXIC ELEMENT CONTAMINATION IN EARTH MATERIAL AND WILD FLORA AT THE ROŞIA MONTANĂ ANCIENT MINING AREA (ROMANIA)

PORRO, S.*, DE CAPITANI, L. & SERVIDA, D.
Dipartimento di Scienze della Terra, "Ardito Desio", Università degli Studi di Milano, Via Botticelli 23, I-20133 Milan, Italy
* E-mail: silvia.porro@unimi.it

Potentially Toxic Element (PTE) pollution from mining activities is a significant environmental problem, as mine dumps are source of heavy metal dispersion in the nearby ecosystems. In this work PTE contamination in the mining area of Roşia Montană (Romania) was investigated by bio-geochemical analyses that have affected both the Hop waste-rock dump and the valley of Roşia River.

The Roşia Montană hydrothermal ore deposit is hosted in andesites and dacites of Neogene age piercing the prevolcanic sedimentary basement as breccia pipes. They host polymetallic sulphides and Au-Ag-Te mineralizations that present in epithermal veins, mineralizing phreatomagmatic breccias and stockworks (WALLIER *et al*., 2006).

On the Hop waste dump (2.5 ha) 10 plant samples, belonging to Salix *spp*., *Popolus tremula* and *Betula pendula* species, were collected with the corresponding rizosphera. Moreover, other 12 mixed soil and plant samples, belonging to *Alnus glutinosa*, were collected, starting from the adit of the SF. Cruci din Orlea gallery up to the confluence between Roşia and Abrud Rivers. Earth material and soil samples were collected from 15 to 40 cm depth and the fraction < 2 mm was separated for pH and EC analyses. Cu, Zn and As concentrations were determined by ICP-AES on both soil and plant tissues. Bioaccumulation Factor (BF) and Translocation Factor (TF) were calculated for plants data set.

Results show that the plant species growing on the Hop waste-rock dump can tolerate acid substrates, with pH values ranging from 3 to 5. In earth materials, average element concentrations reach 28 ppm for Cu, 41 ppm for Zn and 470 for As. Cu and Zn contents in plant tissue is always higher than those in soils while As content is always lower. BF values are almost always greater than 1 for Cu and Zn and << 1 for As. TF calculation shows a preferential allocation of metals in leaves. In soils along the river, average element concentrations are one order of magnitude higher than those of non-contaminated soils (KABATA-PENDIAS & PENDIAS, 2001), reaching 150 ppm for Cu, 232 ppm for Zn and 57 ppm for As. The species *Alnus glutinosa* shows a special property: PTE average contents in leaves are always lower than in soils, reaching 17 ppm for Cu, 59 ppm for Zn and 2.6 ppm for As. BF values are < 1 and TF calculation shows a preferential allocation of Cu in roots.

These results appear interesting for phytoremediation purpose, also for the surrounding areas still not vegetated. On the other hand, they highlight that ecotoxic elements are actually moving from substrates to living beings, resulting in a potential geochemical hazard.

References

KABATA-PENDIAS, A. & PENDIAS, H. (2001): Trace elements in soils and plants. CRC, Boca Raton.

WALLIER, S., RAY, R., KOUZMANOV, K., PETTKE, T., HEINRICH, C.A., LEARY, S., O'CONNOR, G., CALIN, G.T, VENNEMAN, T. & ULLRICH, T. (2006): Economic Geology, 101: 923–954.

COMPOSITIONAL VARIATION IN Cs, Mg, Fe-ENRICHED BERYL FROM COMMON PEGMATITE IN KOVÁŘOVÁ, SVRATKA UNIT, CZECH REPUBLIC

PŘIKRYL, J.*, NOVÁK, M. & GADAS, P.
Department of Geological Sciences, Masaryk University, Kotlářská 2, 611 37 Brno, Czech Republic
* E-mail: hanzii@mail.muni.cz

Beryl, a typical accessory mineral in granitic pegmatites, has quite variable composition tending to (i) beryl close to its ideal formula $Be_3Al_2Si_6O_{18}$ with minor contents of Na, Fe, Mg and H_2O; (ii) T-beryl with dominant substitution in the T(2)-site and CH-site leading to pezzottaite ($CsBe_2LiAl_2Si_6O_{18}$); (iii) O-beryl with dominant substitutions in the O-site and CH-site leading to the simplified general formula $R^+Be_3R^{3+}R^{2+}Si_6O_{18}$, where R^+ = Na, Cs; R^{3+} = Al, Fe^{3+}, Sc; and R^{2+} = Mg, Fe^{2+}. Unusual Cs,Mg,Fe-enriched beryl was found in common pegmatite from Kovářová, Svratka unit. It is built by mica schists, paragneisses, migmatites, orthogneisses, amphibolites and anatectic (?) pegmatites. Abundant fragments of pegmatite occur ~0.5 km N from Kovářová village. Based on these fragments, the pegmatite dike, ~50 cm thick and ~10 m long, is concordantly enclosed in medium-grained amphibolite (Hbl + $Plg_{An26–79}$ > Ttn + Ilm) with sharp contacts. The pegmatite has simple internal structure of (i) medium- to coarse-grained outer unit ($Plg_{An7–31}$ > Kfs > Qtz > Mu > Bt), ~1–2 cm thick, (ii) thin quartz + muscovite-rich zone (Qtz > Mu > Ab+Kfs) with rare biotite, typically developed between outer unit and (iii) coarse-grained inner unit (Kfs > Qtz > Ab > Mu) locally with crystals of (iv) blocky K-feldspar, up to 15 cm in size, and rare masses of smoky quartz, up to 5 cm in diameter. Beryl and garnet ($Alm_{48–72}Sps_{22–47}Prp_{1–6}Grs_{2–4;}$ Y ≤ 0.5 wt% Y_2O_3) are common accessory minerals, whereas small grains (< 0.5-1 mm) of apatite, schorl, ilmenite, Th-enriched monazite-(Ce), xenotime-(Y) and zircon, and highly heterogeneous Nb,Ta,Ti-oxides are rare.

Two types of beryl variable in shape, size, position in pegmatite and composition were recognized based on EMPA and LA-ICP-MS study. Long prismatic crystals of **beryl I** (0.19–1.03 wt% Cs_2O, ≤ 0.05 Cs, 0.01–0.03 Na, 0.01–0.12 Mg, 0.04–0.16 Fe, all in *apfu*) with *c*/*a* ~5–10, (≤ 200 μm), are common in thin sections from the inner unit. They are homogeneous and do not contain inclusions of micas. Yellowish to greenish crystals of **beryl II** with *c*/*a* ~5, locally up to 1 cm long, are common in the inner unit and exhibit complex zoning. The complexly zoned crystals of **beryl II** studied in detail yielded several distinct compositional types (generations). Volumetrically dominant (~75–90 vol%) **beryl IIa** (1.07–1.23 wt% Cs_2O; 0.04–0.05 Cs, 0.04–0.05 Na, 0.03–0.06 Mg, 0.12–0.14 Fe, all in *apfu*) forms central parts of these crystals and contains numerous small inclusions of muscovite + Cs-annite (≤ 20 μm). Beryl IIa is heterogeneous in BSE images; Cs-enriched and Cs-poor portions are oriented parallel to *c*-axis and the latter are always close to the inclusions of muscovite + Cs-annite. Commonly thin outer rims (≤ 100 μm thick) of **beryl IIb** (0.04–0.14 wt% Cs_2O, 0.13–0.20 Na, 0.12–0.18 Mg, 0.05–0.08 Fe, all in *apfu*) are developed along prismatic and basal planes. Beryl IIb is heterogeneous, but no mica inclusions were identified. Both primary types of beryl IIa and IIb underwent later recrystallizations and were replaced by three younger beryl types (generations). **Beryl IIc** (0.13–0.17 wt% Cs_2O, 0.06 Na, 0.03–0.04 Mg, 0.07–0.09 Fe, all in *apfu*) forms irregular rather homogeneous masses, up to 200 μm in size, within beryl IIa. These masses, free of any inclusions, do not show any evident orientation to *c*-axes and have diffusive contacts to its precursor – beryl IIa. Small subhedral portions of **beryl IId** (Cs_2O b.d.l., 0.04 Na, 0.03 Mg, 0.01 Fe, all in *apfu*), ~50 μm in size, are oriented parallel to *c*-axis and replace host beryl IIb exclusively on basal planes. Late **beryl IIe** (≤ 0.14 wt% Cs_2O, 0.17 Na, 0.02 Mg, 0.01 Fe, all in *apfu*) forms very thin irregular veinlets, up to ~30 μm thick, cutting beryl IIa. Primary beryl I and beryl IIa have similar compositions, whereas primary beryl IIb in rims is evidently Na,Mg-enriched but Cs- and in part Fe-depleted. Recrystallization of primary beryl IIa,b yielded Cs-depleted compositions closer to the ideal formula (beryl IIc,d); late beryl IIe is evidently Na-enriched.

Several types of beryl distinct in textures (e.g., orientation to *c*-axes), presence of mica inclusions and chemical composition point out rather complex process of the beryl and pegmatite formation including primary zoning and late hydrothermal recrystallizations. The common pegmatite likely of anatectic origin shows rather simple internal structure; hence, combination of elevated contents of Mg + Fe and of Cs in beryl is very unusual. Moreover, high Cs in beryl and in Cs-annite, Mn in garnet, Ta in Nb,Ta,Ti-oxides and Th in monazite. They indicate quite a high degree of fractionation of the pegmatite, which is hardly consistent with its potential anatectic origin. Consequently, (i) the pegmatite has a magmatic source and high Mg in beryl is product of external contamination or evolved mica-rich rocks of the Svratka Unit underwent partial low-percentage anatexis producing such strange compositions (migmatites contain up to 103 ppm Cs, pers. comm. D. Buriánek).

This work was supported by the research project GAČR P210/10/0743 to MN and PG.

Fe-VERMICULITE PSEUDOMORPHS AFTER BIOTITE CRYSTALS FROM GRANODIORITES OF THE BRNO MASSIF (CZECH REPUBLIC)

PROKOP, J.[1], LOSOS, Z.[1]*, GADAS, P.[1] & VŠIANSKÝ, D.[2]
[1] Department of Geological Sciences, Masaryk University, Kotlářská 2, 611 37 Brno, Czech Republic
[2] Research Institute of Building Materials, JSC, Hněvkovského 65, 617 00 Brno, Czech Republic
* E-mail: losos@sci.muni.cz

The occurrence of columnar euhedral "biotite" crystals with focus on their crystallochemical properties, mineral inclusions and alteration products from granodioritic rocks of the "Kralovo Pole" unit, Brno Massif, have been studied. Micromorphological descriptions, microprobe analysis and X-ray powder diffraction were used to investigate the chemical and structural changes and the mechanism of biotite breakdown into Fe-rich vermiculite during the alteration processes.

Apatite, ilmenite, magnetite, K-feldspar and oligoclase (plagioclase I) that developed at stages of magma crystallization represent the most abundant mineral inclusions in vermiculitized biotite crystals. Growth of secondary inclusions, represented by Fe-oxy-hydroxides, albite (plagioclase II), rutile and titanite, was caused by low-temperature hydrothermal reactions.

Biotite alteration products display a wide range of chemical compositions. Two main types of alteration products have been distinguished. Textural relationships suggest that the prevailing alteration type I is isovolumetric, without the evidence of apparent chemical zonal distribution and it primarily involves exchange of the interlayer K. The empirical formulas indicate that the altered biotite are essentially relatively free of octahedral Al, and that the tetrahedral sheets of biotite have a similar Si:Al ratio.

Examples of the slightly altered biotite from Brno-Židenice and Brno-Líšeň occurrences (calculated on 11 O):

$(K_{0.56}\ Ca_{0.05}\ Ba_{0.01}\ Na_{0.01})_{\Sigma 0.63}\ (Fe_{1.45}\ Mg_{1.14}\ Ti_{0.23}\ Al_{0.12}\ Mn_{0.02}\ \square_{0.04})_{\Sigma 3}\ (Si_{2.85}\ Al_{1.15})_{\Sigma 4}\ O_{10}\ [(OH)_{1.99}\ Cl_{0.01}]_{\Sigma 2}$;
$(K_{0.33}\ Ca_{0.10}\ Na_{0.01})_{\Sigma 0.44}\ (Fe_{1.47}\ Mg_{1.14}\ Ti_{0.24}\ Al_{0.12}\ Mn_{0.02}\ \square_{0.01})_{\Sigma 3}\ (Si_{2.86}\ Al_{1.14})_{\Sigma 4}\ O_{10}\ [(OH)_{1.98}\ F_{0.01}\ Cl_{0.01}]_{\Sigma 2}$.

Examples of the most altered biotite from Brno-Židenice and Brno-Líšeň occurrences (calculated on 11 O):

$(Ca_{0.16}\ K_{0.03}\ Na_{0.02})_{\Sigma 0.21}\ (Fe_{1.90}\ Mg_{1.08}\ Al_{0.22}\ Ti_{0.03}\ Mn_{0.02})_{\Sigma 3.25}\ (Si_{2.85}\ Al_{1.15})_{\Sigma 4}\ O_{10}\ (OH)_2$;
$(Ca_{0.32}\ K_{0.13}\ Na_{0.02})_{\Sigma 0.47}\ (Fe_{1.40}\ Mg_{0.96}\ Ti_{0.31}\ Al_{0.12}\ Mn_{0.02}\ \square_{0.19})_{\Sigma 3}\ (Si_{2.86}\ Al_{1.14})_{\Sigma 4}\ O_{10}\ [(OH)_{1.93}\ F_{0.07}]_{\Sigma 2}$.

From the structural point of view, it is evident that only vermiculite is the alteration product of biotite crystals. On the basis of X-ray diffraction data, mixed structures are not present there.

During alteration type II some phases develop along cleavage planes, initially near the edges of biotite crystal, but then strongly permeating into the body and subdivided segments. This process involves intensive cation exchange generally resulting in the decrease in interlayer K, Fe^{VI}, Al^{VI} and increase in interlayer Ca and tetrahedral Si. The values of octahedral Mg and Al are variable.

This work was supported by the EU-project "Research group for radioactive waste repository and nuclear safety" (CZ.1.07/2.3.00/20.0052) to ZL.

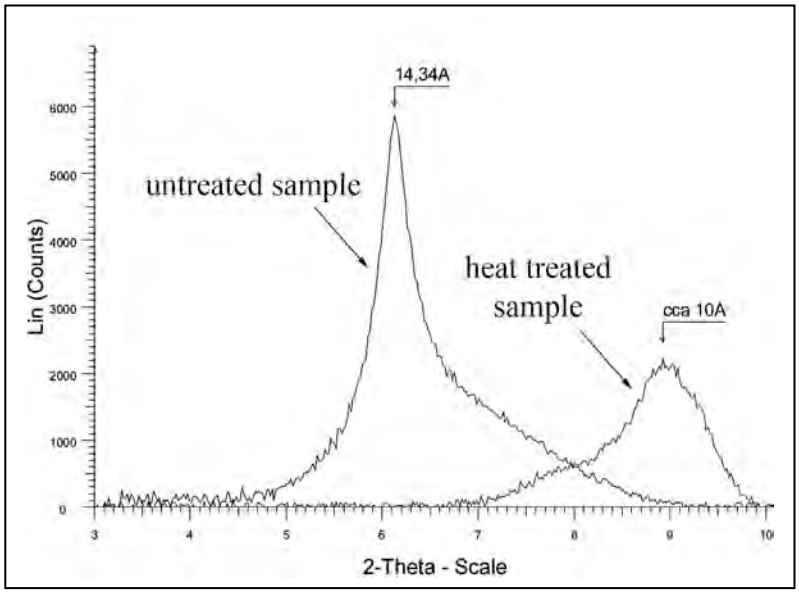

Fig. 1. *Shift of the basal 002 diffraction of vermiculite after heat-treatment of sample at 500°C and duration for 1 hour.*
Euhedral "biotite" crystal from Brno-Líšeň.

SILVER-BEARING MINERALS AT STAN TERG Pb-Zn DEPOSIT, REPUBLIC OF KOSOVO

PRŠEK, J.[1]*, KOŁODZIEJCZYK, J.[1], QELA, H.[2], ASLLANI, B.[2] & MIKUŠ, T.[3]
[1] Department of Economic Geology, Faculty of Geology, Geophysics and Environmental Protection, AGH - University of Science and Technology, al. Mickiewicza 30, 30-059 Kraków, Poland
[2] Trepça Mines Prishtine, Republic of Kosovo
[3] Geological Institute, Branch Banská Bystrica, Slovak Academy of Sciences, Ďumbierska 1, 974 01 Banská Bystrica, Slovakia
* E-mail: prsek@yahoo.com

Stan Terg Pb-Zn deposit is located in the northern part of Kosovo within Vardar zone. The studied deposit comprises two type of mineralization: skarn and hydrothermal. Ore genesis and minerals precipitation is connected with the Tertiary volcanic processes. Host rocks are marbles, schists and skarns. Mineralization filled up empty spaces within breccias as well. Gangue minerals are carbonates and quartz and the main ore minerals are sphalerite and galena (HYSENI *et al.*, 2010). Old suggestions and researches showed that silver is linked with galena, but no precious other studies had been done (FERAUD & DESCHAMPS, 2009 and literature therein).

Ag-bearing minerals were found in hydrothermal ore samples collected at 10th level of the mine. The samples were investigated by polarized microscope in reflected light and SEM-EDS analyses.

Our researches show that only a small amount of silver is bounded to galena (less than 0.4 wt%). Silver forms mainly its own minerals, like silver sulphosalts or minerals of the tetrahedrite group. In each case, silver mineralization is common within hydrothermal assemblages.

Several silver sulphosalts were distinguished: stephanite, pyrostilpnite and polybasite. Stephanite (Fig. 1) and pyrostilpnite (Fig. 2) occur as irregular crystals within massive galena or forms crystals in the galena vugs. Pyrostilpnite chemical composition is close to the theoretical, whereas stephanite has higher antimony (2.4–2.5 *apfu*). Polybasite was identified as irregular form within chalcopyrite, together with Ag-bearing tetrahedrite and freibergite. Its chemical composition is close to the theoretical, but increased content of copper (12 at%) and reduced content of silver (39 at%) can be observed.

Minerals from tetrahedrite group are represented by Ag-bearing tetrahedrite and freibergite. Tetrahedrite forms small grains within galena or grains and veinlets together within chalcopyrite. Content of Ag vary from 0.5 to 2 at%. Content of Zn and Fe is very variable from 3–6.5 at% of Zn and 0.5–3 at% of Fe. Freibergite intergrowths with pyrostilpnite (Fig. 2), or forms single grain with heteromorphite inclusions or veinlets in chalcopyrite. Ag content is much higher than in tetrahedrite and it varies between 15 and 24 at%. Fe content is 4–5.5 at% and Zn content is up to 2 at%.

The position of silver mineralization in vugs or in veinlets shows it younger origin. The further researches in silver mineralisation are needed.

References

FERAUD, J. & DESCHAMPS, Y. (2009): BRGM Report No RP-57204-FR, 92 p.
HYSENI, S., DURMISHAJ, B., FETAHAJ, B., SHALA, F., BERISHA, A. & LARGE, D. (2010): Geologija, 53(1): 87–92.

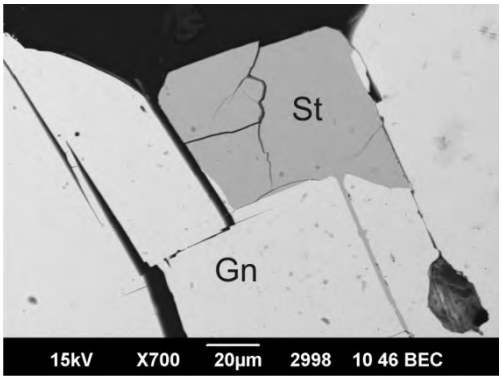

Fig. 1. *Stephanite (St) crystal within galena (Gn).*

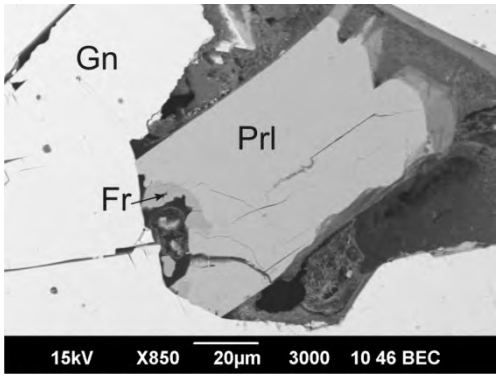

Fig. 2. *Pyrostilpnite (Prl)-freibergite (Fr) grain inside vug in galena (Gn).*

CAVE MINERALOGY AND STABLE ISOTOPE GEOCHEMISTRY OF LILIECILOR CAVE, ROMANIA

PUŞCAŞ, C.M.[1,2]*, EFFENBERGER, H.S.[3], STREMŢAN, C.C.[1] & ONAC, B.P.[1]
[1] Department of Geology, University of South Florida, Tampa, USA
[2] Department of Geology, Babeş-Bolyai University, Cluj-Napoca, Romania
[3] Institute of Mineralogy and Crystallography, University of Vienna, Vienna, Austria
* E-mail: cpuscas@mail.usf.edu

The karst of the Trascău Mts. (E Apuseni Mts., Romania) although extensive both at surface and underground, has received little attention from scientists so far. From a mineralogical point of view, the prospect of discovering rare cave minerals in this region is dim, due to its monotonous lithology and absence of overlying or adjacent ore deposits. However, applying stable isotope analysis to various cave minerals as carbonates, phosphates, or sulphates, could significantly advance the present understanding of the cave depositional environment at times when the mineral assemblages were precipitated.

Although the number of minerals discovered in the Liliecilor Cave is limited, the thick guano deposit (up to 2 m) covers most of the floor; it attracts scientific interest. The cave consists of a 113 m long, linear passage, with an elliptical cross-section, few short side passages, and no speleothems. Analytical methods, used in this study include powder X-ray diffraction (partly evaluated by Rietveld refinements), micro X-ray fluorescence, and isotope ratio mass spectrometry ($\delta^{34}S$ and $\delta^{18}O$ in sulphates and $\delta^{18}O$ in phosphates).

Based on the phosphate paragenesis in the Liliecilor Cave it appears that parts of the "ideal" sequence of phosphate deposition (HILL & FORTI, 1997) are repeated over and over from top to bedrock. All the required cations (Ca^{2+}, Na^{1+}, Al^{3+}, Mg^{2+}, and $Fe^{2+,3+}$) are available throughout the guano deposit that contains isolated limestone fragments and clay lenses. Consequently, the controlling factors for the precipitating species must be the pH and the humidity of the deposit. The succession of phosphate minerals indicates that leaching from the uppermost, fresh layer of bat guano must follows both vertical and horizontal gradients, with impervious layers hindering its dispersion at times. Percolating solutions are rich in guano-derived phosphate and sulphate; based on $\delta^{34}S$ values of gypsum from the cave, the dissolved $(SO_4)^{2-}$ is probably brought about by the oxidation of limestone-associated sulphides. The chemistry of leachates varies throughout the sediment pile due to the latter's compositional differences or as a result of alterations generated by precipitating species. Further changes in sediment pH and humidity (due, for example, to changes in the chemistry of the percolating solutions) may induce phase transformations to minerals that are more stable under these newly created conditions.

Reference

HILL, C.A. & FORTI, P., (1997): Cave minerals of the world, 2nd Ed. National Speleological Society, Huntsville.

MINERALOGY AND GEOCHEMISTRY OF THE CARNIAN (LATE TRIASSIC) OF THE GERECSE AND BALATON HIGHLAND BASINS, HUNGARY: IMPLICATIONS FOR PALEOENVIRONMENTAL CONDITIONS DURING THE CARNIAN PLUVIAL EVENT

RAUCSIK, B.[1]* & ROSTÁSI, Á.[2]
[1] Department of Geology, University of Pécs; Ifjúság útja 6, Pécs, Hungary
[2] Department of Earth and Environmental Sciences, University of Pannonia; Egyetem u. 10, Veszprém, Hungary
* E-mail: raucsik.bela@gmail.com

The Upper Triassic sediments both in NW Europe and in the Mediterranean region imply a generally arid climate regime which is reflected in the formation of evaporites and extensive dolomitization of platform carbonates. However, in the Carnian, a humid phase is assumed by many authors (e.g., RIGO *et al.*, 2007), based on various humidity-aridity paleoclimate proxies. In the western Paleotethys, it is more or less coeval with the demise of rimmed carbonate platforms and an exceptional high input of siliciclastics (GIANOLLA *et al.*, 1998). In the different parts of the Germanic Basin, deposition of mudstones, marls and evaporites of the Keuper was interrupted by sediments composed of dominantly fluvial sandstones (SIMMS *et al.*, 1994). Moreover, coal seams formed within Carnian deltaic successions of the Northern Calcareous Alps. This event was attributed to an increase in precipitation of regional significance (SIMMS & RUFFELL, 1989), and thus called "Carnian Pluvial Event" (CPE).

In this presentation, mineralogical and geochemical characteristics of Carnian (Late Triassic) marly sediments (Veszprém Marl Formation) of the Gerecse and Bakony (Transdanubian Range, W Hungary) are discussed and the results interpreted in a paleoenvironmental framework. 180 samples from four boreholes (Balatonfüred Bfü–1, Mencshely Met–1, Veszprém V–1 which are located in the Balaton Highland and Zsámbék Zs–14 from the Gerecse Mountains) were analysed by X-ray powder diffraction, XRF and ICP-MS to determine the mineralogical and chemical composition.

A relationship can be identified between lithology and clay mineral content in the studied successions; carbonate-rich intervals are enriched in illite/smectite mixed-layer phase (IS), while carbonate-poor intervals show illite-rich composition. This difference can be interpreted as a result of fluctuations of terrigenous input and/or sea-level changes. Kaolinite enrichments (~10–20%) in the clay fraction of the lower part of Mencshely Marl Member can be regarded as a manifestation of the climate shift from the prevailing aridity to the more seasonal climate with enhanced humid season. The large amount of smectitic clay (transformed to IS) could be partly derived from transport of weathering products from a distant source area and, subordinately, from diagenetic alteration of intermediate to basic volcanic rocks.

Based on different paleoredox and paleoproductivity proxies, periods of elevated degree of productivity and related poor oxygenated bottom water conditions can be proven in the studied successions located in the Balaton Highland. Contrarily, enhanced productivity is not evidenced in the Zsámbék Basin where the bottom water anoxia could be caused by a barrier related sluggish circulation. These features seem to be controlled by enhanced freshwater runoff, probably triggered by the CPE. Traces of transport of volcanic matter are apparent in the Mencshely Met–1 core as suggested by the presence of albite, elevated concentration of the rare earth elements and enrichment in Zr, Hf, Y, U, Ta and Nd.

On the basis of mineralogical and geochemical results of the Veszprém Marl Formation, a drastic change in the sedimentation is represented by these marl-dominated basinal sediments, which could have resulted from a composite effect of climatic change, sea-level variation and tectonism.

This study was supported by the Bolyai Research Scholarship of the Hungarian Academy of Sciences and by the "Developing Competitiveness of Universities in the South Transdanubian Region (SROP-4.2.1.B-10/2/KONV-2010-0002)" project.

References

GIANOLLA, P., RAGAZZI, E. & ROGHI, G. (1998): Rivista Italiana di Paleontologia e Stratigrafia, 93: 331–347.

RIGO, M., PRETO, N., ROGHI, G., TATEO, F. & MIETTO, P. (2007): Palaeogeography, Palaeoclimatology, Palaeoecology, 246: 188–205.

SIMMS, M.J. & RUFFELL, A.H. (1989): Geology, 17: 265–268.

SIMMS, M.J., RUFFELL, A.H. & JOHNSON, A.L. (1994): In: FRASER, N. & SUES, H.D. (Eds.): In the Shadow of the Dinosaurs. Cambridge University Press, 352–365.

CLAY MINERALOGY OF QUATERNARY LOESS–PALEOSOL SECTIONS AT BEREMEND AND PAKS, HUNGARY: A COMPARATIVE STUDY

RAUCSIK, B.[1]*, VARGA, A.[1], KOVÁCS, J.[1], UDVARDI, B.[2], KOVÁCS, I.[3], ÚJVÁRI, G.[4] & MIHÁLY, J.[5]
[1] Department of Geology, University of Pécs; Ifjúság útja 6, Pécs, Hungary
[2] Lithosphere Fluid Research Lab, Department of Petrology and Geochemistry, Eötvös Loránd University; Pázmány P. sétány 1/C, Budapest, Hungary
[3] Eötvös Loránd Geophysical Institute of Hungary; Kolumbusz u. 17-23, Budapest, Hungary
[4] Geodetic and Geophysical Institute of the RCAES, Hungarian Academy of Sciences; Csatkai E. u. 6-8, Sopron, Hungary
[5] Science Research Center, Hungarian Academy of Sciences; Pusztaszeri út 58, Budapest, Hungary
* E-mail: raucsik.bela@gmail.com

In this study, mineralogical composition of loess and paleosol samples collected from Beremend (SE Transdanubia, Villány Hills; 25 samples) and Paks (mid-Hungary, next to the right bank of the Danube River; 64 samples) sections were analyzed. Both sections represent partly the Old Loess Series (OLS; MIS 11–17? and 11–22, respectively) and partly the Young Loess Series (YLS; MIS 5–7? and 2–10, respectively) exposing four and ten paleosol layers, respectively. In the Beremend section, unconformities among sediments appear to be common.

The bulk mineral composition of sediments estimated from XRD data indicates that quartz, smectite (sme), and carbonate minerals (calcite and dolomite) are the dominant minerals in both studied sections. Illitic material (ill) with chlorite (chl) is present in all samples but usually in small proportion. Albite, K-feldspar, and kaolinite are the typical minor components with amorphous material. The bulk carbonate content of the YLS sediments is tendentiously higher than those of the OLS samples. Furthermore, the YLS loess samples of the Paks section are especially rich in dolomite (up to 25%). On the other hand, in the Beremend samples, goethite is also a frequent constituent but it is almost totally absent in the Paks section where sediments usually contain only a detectable amount of amphibole. The paleosol samples can be characterized by a smectite-dominance (Beremend: 30–60%; Paks: 10–40%) compared to loess samples (Beremend: 10–40%; Paks: 0–30%) which contain higher amounts of illite. Interestingly, in the loess samples from the Paks YLS, smectite can not be detected. Both sections show no systematic variation in kaolinite content.

ATR-FTIR observations on bulk rock specimens (11 samples from Beremend and 17 samples from Paks) support the qualitative mineralogical compositions determined by XRD measurements. Additionally, infrared spectra of samples show characteristic changes in the integrated areas, band positions and intensity for both locations. The integrated area of water and hydroxyl stretchings, i.e. the absorption band between 2800 and 3750 cm^{-1}, is usually larger for paleosol samples than loess samples. This is also true for the bending band of water which can confirm the higher swelling clay mineral content of the paleosol samples. These parameters are well correlated indicating that they are closely related. The detected water could only be derived from swelling clays due to the sample preparation which dried off adsorbed water. Characteristics of the IR bands at ~3620 and ~3400–3430 cm^{-1} in clays appear to indicate the dominance of aluminum in the octahedral layer and the presence of Na and Ca in the interlayer space. These observations are based on similarities to known standards, therefore, should be handled with precaution at this stage.

Paleoproxy indicators, based on semi-quantitative XRD data, such as sme/ill and sme/(ill+chl) ratios also show systematic variations with lithology. These ratios in paleosols show higher values than in loess samples. Furthermore, in the lower part of the Paks section (OLS), the sme/ill and sme/(ill+chl) ratios in paleosols are significantly higher than in YLS fossil soils. Changes in bulk kao/ill ratio show significant differences between the Beremend paleosol (bulk kao/ill > 1) and loess (bulk kao/ill < 1) samples. The same pattern related to lithology is apparent in the bulk kao/ill ratio for the Paks samples; however, all values remain below 1.

The relatively high sme/ill and sme/(ill+chl) ratios observed in paleosols, could suggest a strengthened chemical weathering and weak physical erosion. By contrast, lower ratios in loesses could indicate intensified physical erosion and weakened chemical weathering. Decreasing values of mineralogical proxy indicators from the OLS to the YLS, especially in the Beremend section, highlight the superimposed effects of climate and tectonism on the Danube loess. Additionally, the observed variations between the two sections can be regarded as a result of differences either in the provenance or in the paleoenvironmental history.

This study was supported by the "Developing Competitiveness of Universities in the South Transdanubian Region (SROP-4.2.1.B-10/2/KONV-2010-0002)" project (BR and JK), by a Marie Curie International Reintegration Grant (NAMS-230937) (IK) and by the Bolyai János Research Scholarship of the Hungarian Academy of Sciences (GÚ).

ELECTRON MICROSCOPY STUDY OF {110} INTERPENETRATION TWINS OF PYRITE

REČNIK, A.[1]*, JIN, L.[2], HOUBEN, L.[2], ZAVAŠNIK, J.[1] & DANEU, N.[1]
[1] Department for Nanostructured Materials, Jožef Stefan Institute, Jamova cesta 39, SI-1000 Ljubljana, Slovenia
[2] Ernst Ruska Centre and Institute for Microstructure Research, Jülich Research Centre, 52425 Jülich, Germany
* E-mail: aleksander.recnik@ijs.si

Interpenetration twins of pyrite were first described from Weserbergland in Germany. Owing to characteristic crosses coinciding with {100} faces they were named iron-cross twins. Crystallographically, iron-cross twins are produced by 180° rotation about the $[1\,\bar{1}\,0]$-axis, however there is very little known about the actual twin boundary structure at the atomic scale. Based on fringe contrast of a low-resolution TEM image recorded on an inclined twin boundary DONNAY *et al.* (1977) reported that twin boundaries in pyrite are curved extended defects not bound to any of the low-index lattice planes. They proposed an idealized twin boundary model with a continuous Fe-sublattice across (110) interface comprising unit-cell steps alternated between (100) to (010) planes. Although anticipated, no impurity elements could be detected on the twin boundary.

In our study we used twinned pyrite crystals from Mt. Katarina, Slovenia (REČNIK, 2007). The crystal habit is dominated by the pentagon-dodecahedral {210} form, which makes the interpenetration twinning macroscopically visible. Twinned crystals of pyrite were cut parallel to the (001) plane, maintaining the nucleation point of the two intersecting $(\bar{1}\,10)$ and (110) twin planes near the centre of the TEM specimen. A quick glance over the TEM specimen revealed that near the centre of the crystal the boundaries between interpenetrating twin domains generally follow {110} planes and make intermittent steps to {100} planes, whereas in the outer regions {100} interfaces become more and more common, while {110} boundaries gradually cease to exist. Due to the fact that twin boundaries can occupy 6 parallel pairs of {110} planes and 3 parallel pairs of {100} planes where only 2 of each are edge-on, while all other are either inclined or lie in-plane with respect to the selected viewing direction. For this reason, it is quite a challenge to find an area suitable for HRTEM investigations. According to our observations the primary {110} twin boundary (type-A) can deflect into secondary {100} interfaces (type-B), following a simple crystallographic relation: (110) → a·(100) + b·(010), where the fractions of both components are a = b for an idealized interpenetration twin, and a ≠ b in the case of realistic twins. EDS chemical analysis of individual interfaces showed that the primary (type-A) twin boundaries comprise a significant amount of Cu, whereas the secondary (type-B) twin boundaries are devoid of dopants. Using a concentric electron probe (CEP) method (WALTHER *et al.*, 2004) we have shown that 0.18 ± 0.03 nm of the type-A twin boundary is occupied by copper, which with respect to the structural density of pyrite, would correspond to one full monolayer of Cu. While the local atomic structure of {110} and {100} twin boundaries are not yet resolved, present results suggest that these are growth twins, which formation is triggered by the incorporation of Cu in the nucleation stage.

References

DONNAY, G., DONNAY, J.D.H. & IIJIMA, S. (1977): Acta Crystallographica, A33: 622–626.

REČNIK, A. (2007): Nahajališča mineralov v Sloveniji [Mineral localities of Slovenia]. Institut "Jožef Stefan", Ljubljana.

WALTHER, T., DANEU, N. & REČNIK, A. (2004): Interface Science, 12: 267–275.

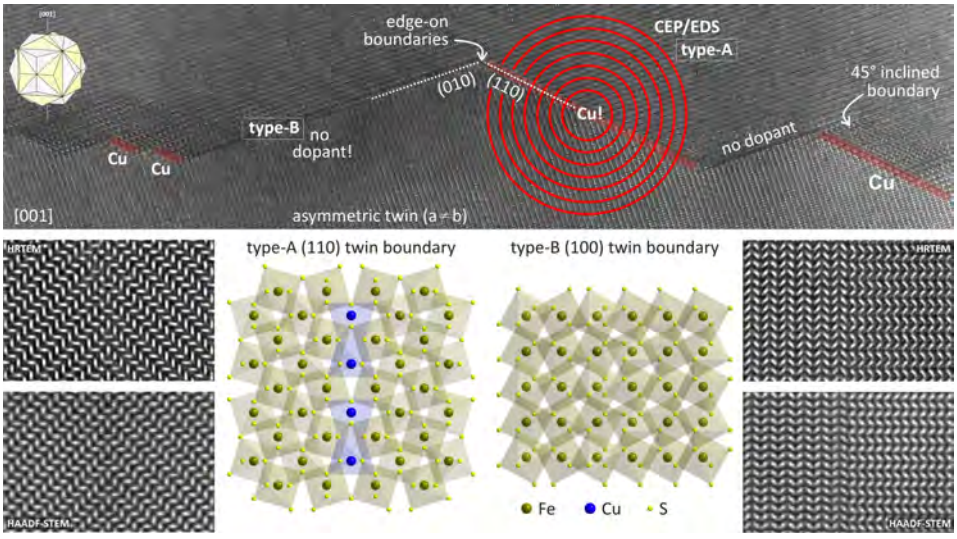

RELATIONSHIPS BETWEEN CLAY MINERALS AND WATER: INFLUENCE OF EXTERNAL AND STRUCTURAL FACTORS

ROBERT, J.-L.
Institut de Minéralogie et de Physique des Milieux Condensés, Université Pierre et Marie Curie, 4 place Jussieu, 75252 Paris Cedex 05, France
E-mail: jean-louis.robert@impmc.upmc.fr

The combination of diffractometric (X-rays and neutrons) and thermal (TGA and DTA) analyses has revealed the existence of seven hydration states in 2:1 clay minerals (synthetic saponites), as a function of the partial water vapour pressure (P/P_0). For low water vapour pressures, only layer edges and surfaces are concerned. With increasing P/P_0, a progressive hydration of the compensating cation is observed, with an increase, by steps, of the basal distance d_{001}, from about 10 Å to about 15 Å. However, the classical model "one-layer" and "two-layers" is much more complicated.

For high P/P_0 values (> 85%), pore water appears, indicating a saturation (edges, surface and interlayer space).

Compositional variations which strongly modify the clay mineral structures mainly influence the hydration properties. Structural factors like the ditrigonal distortion of the tetrahedral sheet and the layer stacking strongly affect the relationships between clay minerals and water. This has been demonstrated on the saponite group, with layer charge 0.33–1.0 [i.e., aspidolite, $NaMg_3(Si_3Al)O_{10}(OH)_2$] and on the aspidolite-preiswerkite join [$Na(Mg_2Al)(Si_2Al_2)O_{10}(OH)_2$].

On the whole, the influence of the layer charge is negligible, as well as the origin of the charge (tetrahedral and/or octahedral). The main factors are the local structure and the layer stacking which determine the coordination of the compensating cation. When the coordination number of the interlayer cation drops from [12] to [6], the hydration properties progressively decrease, and when the six-fold coordination is reached, no water molecule can enter the interlayer space. The minor hydration is only due to the adsorption of water molecules on edges and surface.

CLINOPTILOLITE TREATMENT OF AMD WATERS FROM AFRICA RESERVOIR IN THE ŁUK MUŻAKOWA, W POLAND

RZEPKA, P.*, BAJDA, T., BOŻĘCKI, P., MANECKI, M. & RZEPA, G.
Department of Mineralogy, Petrography and Geochemistry, AGH University of Science and Technology,
al. Mickiewicza 30, 30-059 Kraków, Poland
* E-mail: przemyslaw.rzepka@gmail.com

The Muskau Arc is a large horseshoe-shaped glaciotectonic belt formed during the Mid Polish Glaciation. Neogene lignite deposits containing pyrite were excavated there till the 80-ties of the 20th century. The abandoned mining pits filled up with water forming set of reservoirs called "anthropogenic Lakeland". Oxidation of sulfide-containing lignite, exposed to atmospheric oxygen and water leads to formation of acidic waters. The waters are characterized by relatively high Fe and SO_4 content. This chemical association and acidic pH of water constitutes main environmental problem in this region, which is typical for every AMD areas.

The objective of this study is effectiveness of neutralization abilities of treatments potentially applied to large reservoir called Africa (Fot). This is a meromictic lake with permanent stratification: the mixolimnion at the top (down to ca. 12 m depth), in which the water is well mixed and saturated with oxygen, and the monimolimnion in the deeper part, which is poor in oxygen and which did not mix with upper layer. The pH and concentration of major ions is strongly controlled by the stratification with lower pH = 2.5 and lower ion concentrations in the upper layer and higher pH = 4.5 and higher salinity in the bottom one.

We tested application natural zeolite as the treatment for improvement of the quality of lake waters. The zeolite used in this study is a clinoptilolite separated from Winston clay from New Mexico (HAGGERTY & BOWMAN, 1994). In the set of bench-top experiments zeolite was added to the water pumped from the depth of 6 m and 16 m (upper and lower layer). The amount of the zeolite was calculated based on the salinity and cation exchange capacity of the sorbent.

The treatment resulted in decrease in salinity, increase of pH and precipitation of various secondary phases. The major mineral component of the precipitate was gypsum. The effects of the precipitates on hydrochemical equilibrium of the waters are modeled using PHREEQC hydrochemical model.

This work was supported by Polish NCN through project No. 2011/01/M/ST10/06999.

Reference

HAGGERTY, G.M. & BOWMAN R.S. (1994): Environmental Science & Technology, 28(3): 452–458.

METAMORPHIC HISTORY OF LATE NEOPROTEROZOIC DOKHAN-TYPE VOLCANICS IN THE MEKNAS AREA, SE SINAI, EGYPT

SADEK GHABRIAL, D.[1]* & MINGHUA, R.[2]
[1] Department of Geological Science, National Research Centre, Egypt
[2] Department of Geological Sciences, University of Texas, USA
* E-mail: dghabrial@hotmail.com

The mineralogical and metamorphic features of the Neoproterozoic Meknas volcanics in south-eastern Sinai, Egypt, have been studied. These volcanics developed during the late stage of the Pan-African event and occur as successive sheets ranging in composition from andesite to rhyolite. Their mineral assemblages and mineral chemistry indicate these rocks underwent two metamorphic phases. The first is an early contact phase, which is characterized by the assemblage actinolitic hornblende + hornblende + biotite + oligoclase + quartz suggesting amphibolite facies metamorphism, with P-T conditions at 550±50°C and <2–3 kbar. This metamorphism was followed by a late hydrothermal phase under greenschist and sub-greenschist facies conditions as evidenced by formation of actinolite + chlorite + albite in andesite and dacite and chlorite + muscovite in rhyodacite and rhyolite.

EXPERIMENTAL DISSOLUTION OF ASBESTOS, AIMED ON PASSIVATION OF ASBESTOS WASTE DUMPS

SERGEEVA, I.* & KERESTEDJIAN, T.
Geological Institute, Bulgarian Academy of Sciences, Acad. G. Bonchev St., Bl. 24, BG-1113 Sofia, Bulgaria
* E-mail: Sergeevai@geology.bas.bg

A number of asbestos mines in the Rhodope Mountains, SE Bulgaria, were extensively exploited for anthophyllite asbestos in the middle of the 20th century. After the late 70-ies, when mining was discontinued for safety regulation reasons, a large number of unsecured asbestos dumps was left behind. These dumps are currently very hazardous, because of their location close to settlements and because neither remediation nor any kind of insulation have been done there.

From financial point of view, all existing approaches for securing asbestos dumps represent pure expenditure (DELLISANTI *et al*., 2009; YANAGISAWA *et al*., 2009; GUALTIERI, 2000). In contrast, the idea behind the experiments reported here is to convert asbestos into another, usable product, using cheap reactants and reasonable temperatures, in order to minimize the conversion cost. Additional motivation for the experiments was the fact that asbestos are calcium- and magnesium-bearing silicates. These cations readily react with CO_2, providing opportunities for the so called "mineral CO_2 sequestration" – another "greening" effect.

In this study complete decomposition of anthophyllite- and tremolite-asbestos was achieved by treatment with NaOH and formation of brucite, sodium carbonate hydrate and sodium silicate as run products. The experiments were performed in a Teflon covered stainless steel autoclave, where asbestos was reacted with NaOH in aqueous solution, at temperatures 90 and 200°C. Two types of experiments were conducted: with heat pretreated anthophyllite-asbestos and raw, non-treated anthophyllite and tremolite-asbestos. In the first case anthophyllite-asbestos was heated at 950°C for 4 hours and then reacted with highly concentrated solution of sodium hydroxide (25 M) at a temperature of 200°C. The run product was gelatinous substance without any trace of asbestos. In the second series of experiments, asbestos was reacted with the same concentrated solution of NaOH (pH = 15.4), but at temperatures 90 and 200°C. Complete decomposition of asbestos was achieved only in the experiments at 200°C. Brucite was the only one newly formed phase (Fig. 2), determined by powder XRD analysis.

In order to check the influence of concentration and pH of the aqueous solution over the degree of asbestos dissolution, a third series of experiments were accomplished, using concentrations in the range 1 M to 27.5 M NaOH. Considering the equation: $Mg_7Si_8O_{22}(OH)_2 + 16Na(OH) = 7Mg(OH)_2 + 8Na_2SiO_3 + 2H_2O$ our presumption was that a pH = 14 (provided by 1 M NaOH) would be enough to convert asbestos. However, the experiment with 1 M NaOH solution resulted in just partial dissolution of anthophyllite and formation of respectively small amount of brucite. The reason presumably was that the reaction leads to falling pH down to 11, where further reaction stops. Obviously, the extreme pH values are crucial for the complete dissolution of anthophyllite- and tremolite-asbestos in this experiment. The results of autoclave experiments demonstrate that under suitable conditions (pH > 11) asbestos are readily converted to brucite and sodium silicate (Fig. 3), which are both valuable by-products and could be used for industrial applications, or reacted with CO_2 for its mineral sequestration.

References

DELLISANTI, F., ROSSI, P. L. & VALDRÈ, G. (2009): International Journal of Mineral Processing, 91: 61–67.

GUALTIERI, A. F. (2000): Journal of Applied Polymer Science, 75: 713–720.

YANAGISAWA, K., KOZAWA, T., ONDA, A., KANAZAWA, M., SHINOHARA, J., TAKANAMI, T. & SHIRAISHI, M. (2009): Journal of Hazardous Materials, 163: 593–599.

Fig. 1. *BSE image of anthophyllite-asbestos.*

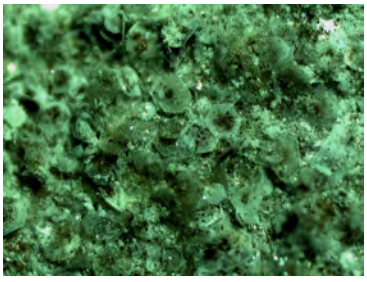

Fig. 2. *Microphotograph of brucite.*

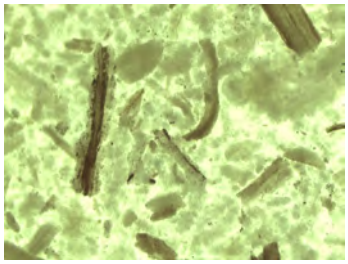

Fig. 3. *A gel of destroyed anthophyllite in sodium silicate sol.*

WASTE ROCK CHARACTERISATION SUPPORTING A BETTER EXPLOITATION AND REMEDIATION DECISION-MAKING

SERVIDA, D.[1]*, DE CAPITANI, L.[1], GRIECO, G.[1], PORRO, S.[1] & COMERO, S.[2]
[1] Università degli Studi di Milano, Via Botticelli 23, I-20133 Milano, Italy
[2] Institute for Environment and Sustainability, Via Enrico Fermi, I-21020 Ispra, Italy
* E-mail: diego.servida@unimi.it

The exploration and exploitation activities are fundamental to our society, as the demand for raw materials is high. By contrast, more than 95% of the material moved for the extraction of metals and metalloids is accumulated as waste (DA ROSA *et al.*, 1997). Within the mine wastes, the larger volume is made up of *waste rocks*, some of which are earth materials with metal and metalloid concentrations (many of which are *potential toxic elements PTE*) too low to be economic but high enough to be a source of environmental pollution. Waste rocks have a significant environmental impact, particularly since they are one of the main source of superficial and ground waters contamination. The process leading to this pollution is strictly related to a set of chemical reactions known as Acid Rock Drainage – ARD – or Acid Mine Drainage – AMD – (NORDSTROM & ALPERS, 1999; BLOWES *et al.*, 2003). Since companies are now turning to larger deposits with lower grade ores, the amount of mine wastes will increase more and more (HUDSON-EDWARDS *et al.*, 2011). For this reason, all the methodologies of prevention, reuse and recycling of mine wastes are encouraged (LOTTERMOSER, 2011).

To choose the best available methodology and technology, waste rock management should begin with the correct and complete characterisation, including both geochemical, mineralogical and geotechnical features (JAMIESON, 2011). Moreover, geostatistical analysis of the data set allows to optimize the information obtained with respect to time and the money invested. In particular, knowing the correlation among the waste rock features, it is possible to design the further sampling campaigns and extend the analytical results to all the stock piles.

In this study two case histories are reported:

1) The first is the characterisation of the mine dump of Rio Marina (SERVIDA *et al.*, 2009), which is an old abandoned mine site exploited for Fe.

2) The second is the characterisation of the mine dump of Roşia Montană (SERVIDA *et al.*, submitted), which is an already exploited mine site and where an evaluation is going on with the resumption of Au mining.

At Rio Marina, the results show the occurrence of 4.46 x 10^6 m^3 waste rocks with As, Cu, Pb and Zn concentrations higher than Italian law limits for PTE in soils and characterised by high *net acid production potential*. Nevertheless, just upstream of the mining site, a formation of carbonate rocks outcrops, having *acid neutralising capacity*, so a reasonable solution to minimize both the environmental hazard and the invasive remediation could be to mix waste rocks with "in situ" carbonates.

At Roşia Montană, results show that the waste rocks of the Hop dump are composed by two different lithologies, one of which is acid generating while the other one is acid neutralising. ARD could be avoided by a designed stockpiling of waste rocks. Moreover, it was assessed that the mine dump is composed by waste rocks where PTE concentrations are below the limits screening level calculated according to international law (e.g., EPA, 1996), so it could to form the hypothesis that this dump is not the main source of PTE.

References

BLOWES, D.W., PTACEK, C.J., JAMBOR, J.L. & WEISENER, C.G. (2003): Treatise on geochemistry, 9: 149–204.

DA ROSA, C.D., LYON, J.S. & HOCKER, P.M. (1997): Mineral Policy Center, Washington DC: 269 pp.

EPA (1996). Soil Screening Guidance: Fact Sheet.

HUDSON-EDWARDS, K.A., JAMIESON, H.E. & LOTTERMOSER, B.G. (2011): Elements, 7: 375–380.

JAMIESON, H.E. (2011): Elements, 7: 381–386.

LOTTERMOSER, B.G. (2011): Elements, 7: 405–410.

NORDSTROM, D.K. & ALPERS, C.N. (1999): Reviews in Economic Geology, 6a: 133–160.

SERVIDA, D., COMERO, S., DAL SANTO, M., DE CAPITANI, L., GRIECO, G., MARESCOTTI, P., PORRO, S., FORRAY, F.L., GÁL, Á. & SZAKÁCS, A. (submitted): Journal of Environmental Management, Manuscript number: JEMA-D-12-00671.

SERVIDA, D., GRIECO, G. & DE CAPITANI, L. (2009): Journal of Geochemical Exploration, 100: 75–89.

POTENTIAL TOXIC ELEMENT MOBILITY AT ROŞIA MONTANĂ GOLD MINE (METALIFERI MTS., ROMANIA)

SERVIDA, D.[1]*, DE CAPITANI, L.[1], GRECO, G.[1], PORRO, S.[1], COMERO, S.[2], MARESCOTTI, P.[3], FORRAY, F.L.[4], GÁL, Á.[4] & SZAKÁCS, A.[5]
[1] Università degli Studi di Milano, Via Botticelli 23, I-20133 Milano, Italy
[2] Institute for Environment and Sustainability, Via Enrico Fermi, I-21020 Ispra, Italy
[3] Università di Genova, Corso Europa 26, I-16132 Genova, Italy
[4] Babeş-Bolyai University, M. Kogălniceanu 1, Cluj-Napoca, Romania
[5] Sapientia University, Str. Matei Corvin 4, RO-400112 Cluj-Napoca, Romania
* E-mail: diego.servida@unimi.it

Roşia Montană, the largest gold mine in Europe, was closed in 2006 after a long mining history, dating back to Roman times. The possibility to re-open the mine is mostly related to finding a solution to severe environmental problems. Waters draining the mine site are characterised by low pH and high concentration of suspended or dissolved potential toxic elements (PTE), leading to severe pollution of the Roşia and Abrud Rivers (BIRD *et al.*, 2005).

The two principal sources of PTE are the piles of waste rock stored during the old exploitation operations and the unexploited ore bodies still occurring inside the tunnels and in the open pits. This study faces the problem of characterizing the mineralogical and chemical composition of the Hop dump, one of the main waste-rock dumps of the Roşia Montană gold mine. Twenty-five samples were collected on the eastern part of the Hop dump, following a virtual squared grid (knots distance of 25-30m). Geotechnical, geochemical and mineralogical features of each sample were investigated. Moreover, the chemical reactivity was tested by means of static tests, following AMIRA procedure (IWRI and EGI, 2002), and kinetic tests following the "modified EPA method 1312" (SPLP–EPA, 1994).

It was assessed, matching field and analytical data with Positive Matrix Factorisation processing, that the waste rocks are composed by two principal lithologies: one labelled as "andesitic breccia"; the other labelled as "dacite". A third independent factor was identified and related to the occurrence of "residual ore" in the waste rocks. The concentrations of PTEs in the waste rocks are below the regulatory limits, with the exception of As, which has concentrations up to 10 times higher than the threshold prescribed by international law. As a matter of fact, part of the As can be related to a natural background concentration in dacites, while another part is strictly related to the ore deposit. The SEM analyses showed that a part of the As content is associated to primary minerals occurring within the dacite-rich samples (particularly sulphides) and the remaining part is contained in the secondary authigenic mineral phases (mainly iron oxyhydroxides and oxyhydroxi-sulphates). The static test results and mineralogy indicate that, even if all the waste rock samples can produce acid, due to the occurrence of reactive sulphides, only the dacite-rich samples are expected to really generate acid mine drainage (AMD), since the andesite-rich samples contain enough carbonate minerals to determine an acid-neutralizing capacity (ANC) higher than the maximum potential acidity (MPA).

Kinetic tests showed that PTE contents in filtered solutions are generally low and under the law threshold: As ranges between 1 and 7 ppb, Cu ranges between 0 and 98 ppb and Zn ranges between 21 and 570 ppb. pH values of leachates greatly varies, from 2.9 to 8.9, and their sulphate content ranges between 13.5 and 475 ppm thus exceeding the European limit for drinking water standards. Comparison between the geochemical features of leached waters and bulk chemistry of waste-rocks shows that the release of As in aqueous solutions is very poor, despite its hazardous concentrations in the solid material (range 80–107 ppm). On the other hand, Cu and Zn contents in the rocks are lower, ranging between 30 and 47, and between 31 and 44 ppm, respectively, but they are characterized by a higher geochemical mobility.

Given the evidence of field and preliminary analysis on waters, the Hop dump contributes only to some extent to environmental pollution related to AMD processes, whereas it is conceivable that most of the potentially hazardous processes take place in the underground tunnels of the mine or in other waste-rock dumps which have not yet been analyzed.

References

AMIRA INTERNATIONAL (2002): ARD Test Handbook. IWRI and EGI.

BIRD, G., BREWER, P.A., MACKLIN, M.G., SERBAN, M., BALTEANU, D. & DRIGA, B. (2005): Journal of Geochemical Exploration, 86: 26–48.

U.S. ENVIRONMENTAL PROTECTION AGENCY (1994): SW-846 online.

Ag-Sb-Pb MINERALIZATION OF THE VEIN H14F3, SHAFT 21, PŘÍBRAM URANIUM AND BASE-METAL ORE DISTRICT (CZECH REPUBLIC)

ŠKÁCHA, P.[1,2]*, SEJKORA, J.[3], KNÍŽEK, F.[4], SLEPIČKA, V.[5], LITOCHLEB, J.[3] & JEBAVÁ, I.[3]
[1] Mining Museum Příbram, Hynka Kličky Place 293, CZ-261 01 Příbram VI - Březové Hory, Czech Republic
[2] Institute of Geochemistry, Mineralogy and Mineral Resources, Charles University, Faculty of Science, Albertov 6, CZ-128 43 Prague 2, Czech Republic
[3] Department of Mineralogy and Petrology, National Museum, Cirkusová 1740, CZ-193 00 Prague 9, Czech Republic
[4] CZ-261 02 Příbram VII/127, Czech Republic
[5] CZ-261 02 Příbram VII/405, Czech Republic
* E-mail: skacha-p@muzeum-pribram.cz

There are two significant ore districts in the Příbram ore region (Czech Republic, Central Bohemia) – the Březové Hory base-metal ore district and the Příbram uranium and base-metal ore district. Ore veins of the Příbram uranium and base-metal district are mostly concentrated in exocontact of the Central Bohemian Plutonic Complex in the Neoproterozoic and Cambrian volcanosedimentary formations. Příbram ore area is the most important Ag-Pb-Zn-Sb-U deposit in Czech Republic, and one of the most important hydrothermal vein deposits of this type on the world. In Příbram area was mined about 3450 tons of Ag, 420 000 tons of Pb and about 48 000 tons of U (AUTHORS COLLECTIVE, 2003). Shaft 21 is located in the central part of the Příbram uranium and base-metal ore district in the "ore node" called Háje (after Háje village). The ore vein H14F3 (mined from the shaft 21) is known because of the occurrence of the interesting silver - antimony mineralization, especially rich dyscrasite accumulations (KNÍŽEK *et al.*, 1990).

By the revision of the specimens from this vein, interesting association of Ag-Sb-Pb minerals, Hg-silver and pyrargyrite were found in deeper parts of the vein (8^{th} level of the shaft, -400 m). Both minerals are common as pseudomorphosis after dyscrasite; the Sb-rich arsenic was usually hydrothermally leached in this place. The most common ore mineral near the 7^{th} level of the shaft (-350 m) is Sb-rich arsenic, which forms at least two generations, at some places also common sphalerite, galena and löllingite occur. Dyscrasite forms there large morphological scale of varieties from thin needles, thin plates to thick columnar crystals covered by younger Sb-arsenic. The younger type of dyscrasite forms coatings and aggregates growing directly in the calcite. The average large of crystals is about 1–2 cm and the maximum large of thin columnar crystals reached up to 6 cm. The (Ag + Hg)/(Sb + As) ratio for thin tabular bent crystals is between 3.53 and 4.06, for thin tabular crystals 3.60–3.93, for thick columnar crystals 3.45–4.03, for hydrothermal altered thick columnar crystals 3.43–4.22 and for younger regenerated tin white coatings is ratio between 2.89 and 3.23. We know at least three types of dyscrasite in the Příbram area (ŠKÁCHA *et al.*, 2006). The Ag/Sb ratio of oldest dyscrasite from Příbram varies between 3.4–3.6 (type I), 3.6–4.2 (type II including dyscrasite from the ore vein H14F3) and 3.5–3.6 (youngest type III). At studied mineralization, allargentum is rarer than dyscrasite with usually closely intergrowth; x for allargentum formula $Ag_{1-x}Sb_x$ varies from 0.14–0.16. Dyscrasite crystals and rarely Sb-arsenic aggregates can be replaced by younger miargyrite, which also forms crystals up to 0.5 cm and its chemical composition can be expressed as $Ag_{1.03}(Sb_{1.01}As_{0.01})_{\Sigma 1.02}S_{1.95}$. Rare freieslebenite with chemical composition $Ag_{1.03}Pb_{0.99}Sb_{1.01}S_{2.97}Cl_{0.01}$ forms crystals up to 0.5 mm growing on pseudomorphosis of miargyrite after Sb-arsenic. Tiny elongated andorite crystals up to 0.2 mm with empirical formula $(Pb_{0.98}Fe_{0.06})_{\Sigma 1.04}Ag_{1.07}(Sb_{2.96}As_{0.02})_{\Sigma 2.98}S_{5.88}$ and semseyite (grains up to 30 μm in andorite crystals) with empirical formula $(Pb_{8.64}Ag_{0.26})_{\Sigma 8.90}Sb_{8.15}S_{20.94}$ were found in association with dyscrasite and miargyrite. Andorite crystals are significantly zoned with %And (MAKOVICKY & KARUP-MØLLER, 1984) 91–102 (mean 96) and N 4.17–4.63 (mean 4.42). Crystals of pyrrhotite and stibnite in calcite gangue represent the younger mineral phases of the vein.

This described occurrence of Ag-Sb-Pb mineralization is similar to the well-known dyscrasite occurrence on the vein H14F (6^{th} level, shaft 21) in the same area (KOLESÁR, 1990). The main difference is in the chemistry of the late hydrothermal solutions and in the variability of mineral phases. Whereas on the H14F ore vein, the only known mineral phases originated from the hydrothermal alteration of dyscrasite are Hg-silver and allargentum, on the H14F3 ore vein was found interesting association comprised of Hg-silver, allargentum, miargyrite, andorite, semseyite and freieslebenite.

References

AUTHORS COLLECTIVE (2003): Rudné a uranové hornictví ČR. 647 p.

KNÍŽEK, F., LITOCHLEB, L. & ŠREIN, V. (1990): Bulletin of the Czech Geological Survey, 65: 321–328.

KOLESÁR, P. (1990): Lapis, 15(9): 19–26.

MAKOVICKY, E. & KARUP-MØLLER, S. (1984): Neues Jahrbuch für Mineralogie – Monatshefte, 175–182.

ŠKÁCHA, P., SEJKORA, J. & LITOCHLEB, J. (2006): Mineralogica Polonica, 28: 205–207.

GRANITIC PEGMATITES OF THE TŘEBÍČ SYENITE PLUTON, MOLDANUBIAN ZONE, CZECH REPUBLIC; AN EXAMPLE OF NYF TO MIXED PEGMATITES RELATED TO THE OROGENIC PLUTON

ŠKODA, R.* & NOVÁK, M.
Institute of Geological Sciences, Masaryk University, Kotlářská 2, CZ-611 37 Brno, Czech Republic
* E-mail: rskoda@sci.muni.cz

The current petrogenetic classification of granitic pegmatites includes two main petrogenetic families – orogenic LCT (enriched in lithium + cesium + tantalum) and anorogenic NYF (enriched in niobium + yttrium + fluorine). Several pegmatites share MIXED geochemical and mineralogical characteristics; however, their geotectonic position is not commonly discussed (ČERNÝ & ERCIT, 2005).

A large tabular body of the Třebíč Pluton (TP; ~540 km^2) is emplaced in medium- to high-grade metamorphic rocks of the Gföhl unit in the eastern part of the Moldanubian Zone. Porphyric (orthoclase), amphibole-biotite melasyenite to quartz melasyenite and melagranite show metaluminous composition (ASI = 0.85–0.93) with high concentrations of K_2O (5.2–6.5 wt%), MgO (3.3–10.4 wt%), P, Rb, Ba, U, Th, Cr, Cs, but unusually low Ca and Sr. Geochemical signature as well as isotopic Sr ($^{87}Sr/^{86}Sr_{337}$ = 0.709–0.7125) and Nd (εNd_{337} = -6.3) data suggest mixing of mantle-derived durbachite magma with (leuco)granitic melt derived from crustal rocks undergoing anatexis during rapid decompression (e.g., ŽÁK *et al.*, 2005).

The TP is characterized by abundant intragranitic NYF pegmatites with common biotite, tourmaline, titanite, allanite-(Ce) and Y,REE,Nb,Ta,Ti-oxides. The pegmatites have been divided on three distinct varieties: (i) Subhomogeneous allanite-type pegmatites forming small irregular nests and segregations commonly with transitional contact to the host syenogranite. (ii) Lenses, dikes and irregular bodies of simply zoned euxenite-type pegmatites (with Y,REE,Nb,Ta,Ti-oxides), are up to 2 m thick and several meters long, with transitional to sharp contacts. Typical minor to subordinate minerals include biotite (X_{Mg} = 0.49–0.70), black tourmaline (Ca,Ti-rich dravite-schorl to schorl) and a wide spectrum of accessory minerals present mainly in euxenite-type pegmatites, i.e. aeschynite- and euxenite-group minerals, allanite-(Ce), ilmenite, titanite, (Na,Cs,Mg,Fe,Sc)-enriched beryl, phenakite, niobian rutile, pyrite, and zircon. (iii) The euxenite-type pegmatite Klučov I with aeschynite-group minerals exhibits very similar geological position, internal structure and mineralogy. However, it is characterized by a higher degree of fractionation manifested by more abundant B-bearing minerals, chemical composition of tourmaline and presence of Sn-bearing (cassiterite, herzenbergite) and B-bearing (tinzenite) minerals relative to the other euxenite-type pegmatites. Low contents of P_2O_5 in feldspars as well as scarcity of phosphates (apatite, monazite) in pegmatites are typical.

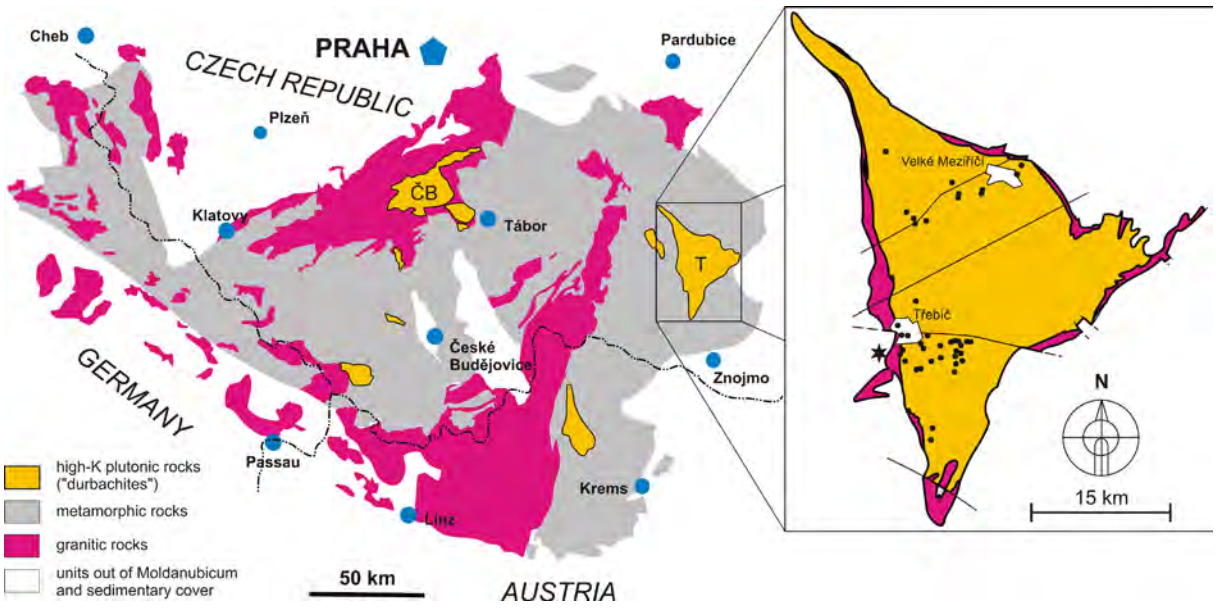

Fig. 1. *Schematic geological map of the part of Moldanubian zone (left) and Třebíč Pluton (right) including pegmatite districts; dots = NYF pegmatite occurrences, star = Kracovice MIXED pegmatite. In part modified from NOVÁK et al. (2012).*

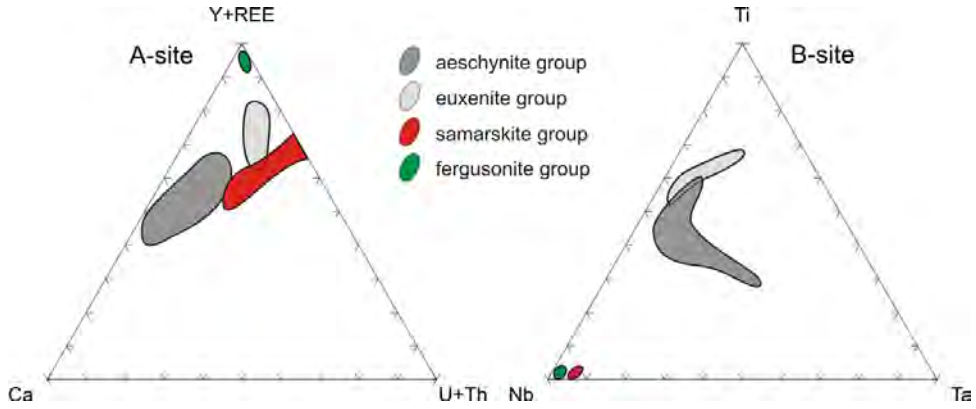

Fig. 2. *Chemical composition of aeschynite-, euxenite-, samarskite-group minerals and fergusonite (A-site and B-site occupancy). In part modified from ŠKODA & NOVÁK (2007).*

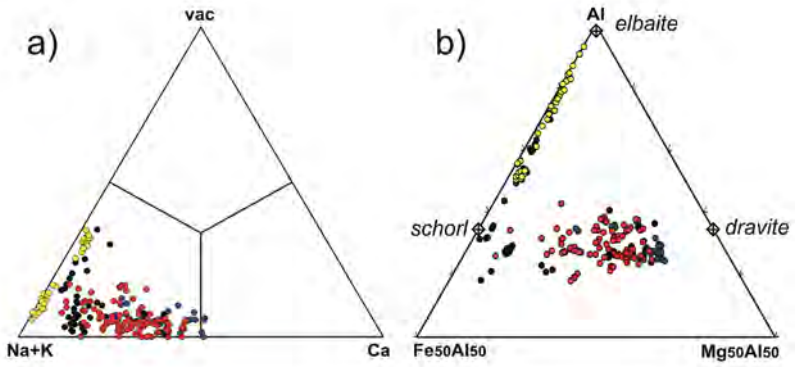

Fig. 3. *Composition of tourmaline from allanite-type pegmatites = blue symbol, euxenite-type pegmatites = red symbol, pegmatite Klučov I = black symbol, pegmatite Kracovice = yellow symbol: a) Na+K–Ca–X-site vacancy triangle; b) Fe_{tot}–Mg–Al triangle (NOVÁK et al., 2012)*

The most evolved lithium-bearing Kracovice pegmatite forms symmetrically zoned dike, about 1 m thick and 30 m long, which cuts graphitic gneiss located about 300 m from the edge of the TP. The most differentiated part of pegmatite consists inwards of: a granitic unit (Kfs + Plg + Qtz + Bi + Msc), graphic unit (Kfs + Qtz ± Bi) evolving to minor blocky K-feldspar, and albite complex situated close to small quartz core. Major minerals are represented by quartz, K-feldspar (locally amazonite) and albite (saccharoidal and rare *cleavelandite*). Typical subordinate minerals include micas (muscovite, biotite, zinnwaldite, masutomilite, polylithionite), tourmalines (schorl, elbaite); topaz, Y-rich spessartine, F-rich hambergite, monazite-(Ce), xenotime-(Y), zircon (Zr/Hf = 20.1–5.8), fergusonite-(Y), samarskite-(Y), calciosamarskite, hinnganite-(Y), columbite-(Mn), wolframoixiolite (MnNb >> FeTa), pyrochlore-(Y), titanite, cassiterite, scheelite, beryl, fluorite and löllingite. Close spatial, geochemical and mineralogical relations of this pegmatite to the intragranitic NYF pegmatites of the Třebíč Pluton suggest them to be a single pegmatite population (NOVÁK *et al.*, 2012).

The Třebíč Pluton is evidently orogenic body, which intruded to mid-crustal levels (at ~343–335 Ma) shortly after exhumation of the host high-grade rocks of the Gföhl unit. Apparent (geochemical and mineralogical) NYF signature of the itragranitic pegmatites (disregarding high Mg/Fe in minerals and low activity of F, typical for pristine anorogenic NYF pegmatites) is in contrast with the orogenic origin of the parental granite. The pegmatite from Kracovice with the MIXED signature, a member of the same granite-pegmatite system, confirms a strange character of this unique granite-pegmatite system of the Třebíč Pluton – orogenic with NYF > MIXED signature.

References

ČERNÝ, P. & ERCIT, T.S. (2005): Canadian Mineralogist, 43: 2005–2026.

NOVÁK, M., ŠKODA, R., GADAS, P., KRMÍČEK, L. & ČERNÝ, P. (2012): Canadian Mineralogist, 50: in print.

ŠKODA, R. & NOVÁK, M. (2007): Lithos, 95: 43–57.

ŽÁK, J., HOLUB, F.V. & VERNER, K. (2005): International Journal of Earth Sciences, 94: 385–400.

MINERALOGICAL IMPLICATIONS IN SYENITES FROM THE DITRĂU ALKALINE MASSIF, ROMANIA

SOGRIK, E.*, PÁL-MOLNÁR, E. & BATKI, A.
Department of Mineralogy, Geochemistry and Petrology, University of Szeged, Egyetem street 2, H-6722 Szeged, Hungary
* E-mail: sogrik.edina@geo.u-szeged.hu

The Ditrău Alkaline Massif [DAM], situated in the Eastern Carpathians, Romania, is a Mesozoic alkaline igneous complex, which was formed by an extensional tectonic event at the south European passive continental margin. It consists of different rock types from ultramafic, mafic rocks through diorites, granites, nepheline syenites and syenites to dykes (lamprophyres, tinguaites and alkali feldspar syenites). This paper presents new data on the mineralogy of the syenites.

DAM syenites have holocrystalline, hypidiomorphic and medium-grained texture. They are silica-saturated and oversaturated alkaline, miascitic rocks with 59.63–62.41 wt % SiO_2. These rocks are peraluminous (A/CNK = 1.28–1.53, A/NK/ = 1.48–1.70), which is confirmed by the dominance of K-feldspars (microcline, orthoclase) as the main Al phases. Syenites have a relative enrichment in LREE, the $(La/Yb)_N$ values range from 13.8 to 43.1. Some of them display positive Eu anomaly (Eu/Eu* = 1.53–3.81), reflecting the presence of plagioclase ($An_{0.47–16.52}$) and titanite. Syenites show enrichment in Ba, Sr and Zr. The high Ba-content reflects prevalent K-feldspar as a main rock-forming mineral, while Sr and Zr are associated with apatite and zircon, respectively, as abundant accessories in the studied syenites. Additional accessory minerals are magnetite and ilmenite. Secondary minerals are represented by calcite, epidote, muscovite and chlorite.

Mineral chemical analyses were determined by JEOL JXA-733 electron microprobe equipped with WDS and EDS at the Institute for Geological and Geochemical Research, Research Centre for Astronomy and Earth Sciences of Hungarian Academy of Sciences, Budapest.

The main mafic minerals are biotite and subordinate amphibole. Biotites are generally euhedral to anhedral and often chloritised. Some of them are intergrown with other minerals (amphibole, titanite). Inclusions are usually titanite, zircon, rutile and baddeleyite in biotites. They are Fe-rich biotites, annites with Fe/(Fe+Mg) values of 0.5–0.7.

Three types of amphiboles are determined in the DAM syenites. They all have subhedral shape but usually highly shattered and altered. Amphiboles are Ca-amphiboles, pargasite [$Na_{0.8}K_{0.3}Ca_{1.8}Fe^{2+}_{2.1}Fe^{3+}_{0.1}Mg_{2.3}Mn_{0.04}Al_{0.1}(Al_{1.9}Si_{6.1}O_{23})$], ferropargasite [$Na_{0.8}K_{0.3}Ca_{1.8}Fe^{2+}_{2.2}Fe^{3+}_{0.1}Mg_{2.0}Mn_{0.1}Al_{0.2}(Al_{1.9}Si_{6.1}O_{23})$] and hastingsite [$Na_{0.7–1.2}K_{0.3–0.4}Ca_{1.6–1.8}Fe^{2+}_{2.1–2.8}Fe^{3+}_{0.2–0.9}Mg_{1.2–2.0}Mn_{0.1–0.2}Al_{0–0.3}(Al_{1.8–2.2}Si_{5.8–6.2}O_{23})$]. Hastingsites are Fe-rich (Fe^{2+} = 2.05–2.82, Fe^{3+} = 0.05–0.87, mg# = 0.31–0.52) and potassian (K = 0.29–0.41), which corresponds with the miascitic affinity of the DAM syenites. The compositional trends of amphiboles in alkaline systems tend from ($Ca+Al^{IV}$)-rich and (Si+Na+K)-poor (early crystallisation) towards ($Ca+Al^{IV}$)-poor and (Si+Na+K)-rich (late crystallisation) content (GIRET *et al.*, 1980). Based on the composition of amphiboles in syenites, they are crystallised in the early magmatic stage (Fig. 1). Based on Al-in-hornblende of SCHMIDT (1992), the estimated crystallisation pressure for amphiboles is approximately 5–8 kbar, which suggests that the crystallisation of amphibole occurs ca. 15–25 km deep in the lithosphere.

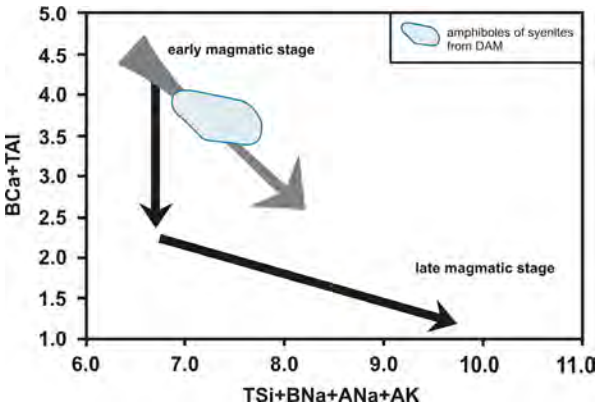

Fig. 1. *Compositional trend of amphiboles in syenites from DAM (GIRET et al., 1980).*

References

GIRET, A., BONIN, B. & LEGER, J.M. (1980): Canadian Mineralogist, 18: 481–495.

SCHMIDT, M.W. (1992): Contributions to Mineralogy and Petrology, 110: 304–310.

RUTILE AND HEMATITE PSEUDOMORPHS FROM MWINILUNGA (ZAMBIA)

STANKOVIĆ, N.*, DANEU, N. & REČNIK, A.
Department for Nanostructured Materials, Jožef Stefan Institute, Jamova 39, 1000 Ljubljana, Slovenia
* E-mail: nadezda.stankovic@ijs.si

Samples of rutile and hematite pseudomorphs from Mwinilunga (Zambia), were investigated by optical microscopy, X-ray powder diffraction, scanning and transmission electron microscopy. The pseudomorphs retained the plate-like morphology of the original crystals. Their surfaces are covered by fresh euhedral crystals of rutile, following a semi-epitaxial orientation relationship $[001]_{rut} \parallel \langle 11\bar{2}0\rangle_{ilm}$ where *c*-axes of the rutile crystals are lying parallel to the basal planes of the precursor. In-plane {101} twins of rutile are frequent. Cross-sections cut parallel to the basal plane of the precursor were prepared from the interior of the pseudomorphs. Optical microscopy of polished thin sections shows sub-microcrystalline texture of transparent rutile areas within a matrix of opaque phase. XRD analysis confirmed the presence of rutile and hematite. Although polycrystalline, rutile grains form distinct 120° domains, induced by a topotaxial growth on the corundum-type precursor. Within nanocrystalline domains of rutile macroscopic, often twinned crystals of rutile are emerging. These crystals adopt the orientation of the originally polycrystalline matrix. In nature, twins are commonly associated with a topotactic replacement of hematite or ilmenite by rutile, due to structural similarity. They do not have a definite three-dimensional form and the transformation is governed by rearrangement of the cations across the interface, while a hexagonal stacking of the oxygen sublattice remains unaltered (FORCE *et al.,* 1996; DANEU *et al.,* 2007). On submicron scale we have confirmed a nanocrystalline nature of rutile and hematite precipitates by TEM. The possible mechanism of recrystallization includes the action of acidic hydrothermal solutions (JANSSEN *et al.,* 2010). Under low pH values ilmenite rapidly alters to fine crystalline rutile following a dissolution-precipitation mechanism. First ilmenite is dissolved in acidic solution. With decreasing temperature hydrothermal solution reaches a point of supersaturation, which triggers precipitation of rutile. The volume difference between the ilmenite and rutile causes the formation of porosity, which is then filled-up by nanocrystalline hematite. Throughout the alteration process morphology of the precursor ilmenite crystal is preserved. A high degree of coherency between the precursor and precipitated rutile grains suggests a progressive recrystallization from the surface to the interior. This is indicated by finer crystallinity and higher coherency of the surface areas and coarse crystallinity in the interior as the acidity drops. In the final stage, macroscopic rutile crystals developed on the open surfaces and in the pores of ilmenite precursor. Twinning, where present, tends to follow the 120° domain texture of the fine crystalline rutile.

References

DANEU, N., SCHMID, H., REČNIK, A. & MADERC, W. (2007): American Mineralogist, 92: 1789–1799.

FORCE, E.R., RICHARDS, R.P., SCOTT, K.M., VALENTINE, P.C. & FISHMAN, N.S. (1996): Canadian Mineralogist, 34: 605–614.

JANSSEN, A., PUTNIS, A., GEISLER, T. & PUTNIS, C.V. (2010): Mineralogical Magazine, 74: 633–644.

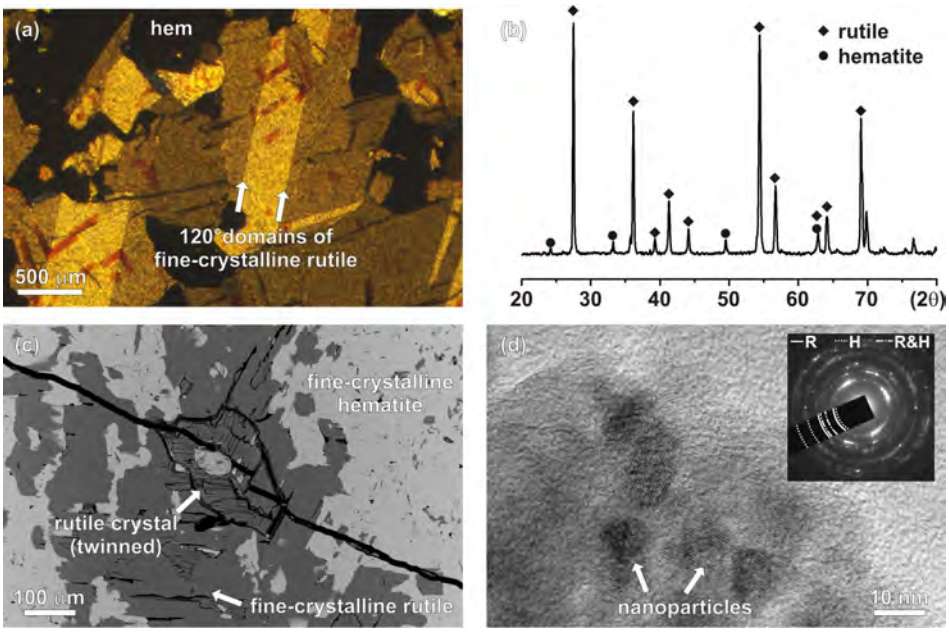

SUPERGENE ARSENATES OF COPPER FROM THE PIESKY DEPOSIT, ŠPANIA DOLINA, CENTRAL SLOVAKIA

ŠTEVKO, M.[1]* & SEJKORA, J.[2]
[1] Department of Mineralogy and Petrology, Comenius University, Mlynská dolina G, 842 15 Bratislava, Slovakia
[2] Department of Mineralogy and Petrology, National Museum, Cirkusová 1740, 193 00, Prague 9, Czech Republic
* E-mail: stevko@fns.uniba.sk

The abandoned Piesky deposit is part of Špania Dolina ore district and is situated approximately 1.2 km to the north from Špania Dolina village in the Starohorské Mts., Central Slovakia. In the past, Špania Dolina ore district was one of the most prominent producers of copper in Europe and there is evidence at the Piesky deposit that copper was mined there already during the Bronze Age (TOČÍK & BUBLOVÁ, 1985). Hydrothermal quartz-carbonate-sulphide mineralization is hosted mostly in sandstones and conglomerates of Permian age. The main primary minerals are quartz, siderite, dolomite, chalcopyrite and tetrahedrite (ILAVSKÝ, 1976; MICHŇOVÁ & OZDÍN, 2010a, b). There is an extensive supergene zone, especially at the near-surface part of the Piesky deposit. Most common supergene minerals are azurite, antlerite, brochantite, cuprite, chalcophyllite, devilline, gypsum, langite, malachite, native copper and posnjakite (e.g., FIGUSCHOVÁ, 1977, 1978; ŘÍDKOŠIL, 1978, 1981; ŘÍDKOŠIL & POVONDRA, 1982).

Studied samples with supergene copper arsenate minerals were recently collected from the dumps and mineralized outcrops at the Piesky deposit. All mentioned minerals were identified using a Bruker D8 Advance X-ray powder diffractometer and quantitative chemical data were collected using Cameca SX100 electron microprobe operating in the wavelength-dispersive mode from polished samples mounted in epoxy resin.

Together with other supergene minerals, clinoclase, cornwallite, chalcophyllite and sulfate rich tyrolite were identified. Clinoclase forms dark blue well developed columnar crystals up to 1 mm, sometimes grouped to the radial aggregates. It is associated with azurite, malachite, cornwallite and tyrolite. Refined unit-cell parameters of clinoclase are: a = 7.237(1) Å, b = 6.444(1) Å, c = 12.356(2) Å and V = 568.247(7) Å^3. Chemical composition of clinoclase is rather simple, only minor contents of Fe (up to 0.01 *apfu*), Al (up to 0.01 *apfu*), P (up to 0.03 *apfu*) and F (up to 0.02 *apfu*) were detected. Cornwallite occurs as pale to emerald-green botryoidal aggregates which usually replace aggregates of azurite. The refined unit-cell parameters of cornwallite are: a = 4.523(1) Å, b = 5.732(1) Å, c = 17.106(4) Å and V = 443.461(3) Å^3. An extensive As ↔ P substitution as well as minor contents of Al (up to 0.04 *apfu*), Sb (up to 0.07 *apfu*), Si (up to 0.02 *apfu*), S (0.02 *apfu*) and F (0.05 *apfu*) are characteristic for cornwallite. Chalcophyllite is most common supergene arsenate and it forms emerald to pale green tabular crystals up to 5 mm, which are mostly associated with azurite and baryte. Its refined unit-cell parameters are: a = 10.748(1) Å, c = 28.586(2) Å and V = 2697.335(12) Å^3. Contents of Fe (up to 0.11 *apfu*), Sb (up to 0.22 *apfu*), Si (up to 0.12 *apfu*), P (1.18 *apfu*) and Cl (up to 0.06 *apfu*) were observed in chalcophyllite. Sulphate-rich tyrolite occurs as blue-green to emerald-green radial aggregates up to 3 mm associated with azurite, malachite and clinoclase. The refined unit-cell parameters are: a = 27.425(5) Å, b = 5.564(2) Å, c = 10.496(4) Å and V = 1587.086(24) Å^3. Content of sulphate groups in tyrolite reaches up to 0.40 *apfu*. Minor amounts of Zn (up to 0.02 *apfu*), Sb and Si (both up to 0.04 *apfu*) and P (up to 0.09 *apfu*) were detected. Interesting are also contents of Cl (up to 0.03 *apfu*) and F (up to 0.13 *apfu*). All described copper arsenate minerals from the Piesky deposit represent decomposition products of tetrahedrite, which is locally arsenic-enriched.

References

FIGUSCHOVÁ, M. (1977): Hornická Příbram ve vědě a technice, 55–70.
FIGUSCHOVÁ, M. (1978): Mineralia Slovaca, 10: 383–384.
ILAVSKÝ, J. (1976): Economic Geology, 71: 423–432.
MICHŇOVÁ, J. & OZDÍN, D. (2010a): Mineralia Slovaca, 42: 69–78.
MICHŇOVÁ, J. & OZDÍN, D. (2010b): Acta Mineralogica-Petrographica, Abstract Series, 6: 237.
ŘÍDKOŠIL, T. (1978): Časopis pro Mineralogii a Geologii, 23: 436–437.
ŘÍDKOŠIL, T. (1981): Časopis pro Mineralogii a Geologii, 26: 263–271.
ŘÍDKOŠIL, T. & POVONDRA, P. (1982): Časopis pro Mineralogii a Geologii, 27: 79–84.
TOČÍK, A & BUBLOVÁ, M. (1985): Štúdijné Zvesti Acheologického ústavu, 21: 47–135.

MANTLE VERSUS CRUSTAL PROTOLITHS IN POST-COLLISIONAL MAGMATISM: THE VARISCAN FURCĂTURA PLUTON, ROMANIAN SOUTHERN CARPATHIANS

STREMȚAN, C.C.[1]*, RYAN, J.[1], ATUDOREI, V.[2], SAVOV, I.[3] & CHERATA, I.[4]
[1] Department of Geology, University of South Florida, Tampa, USA
[2] Department of Earth and Planetary Sciences, University of New Mexico, Albuquerque, USA
[3] School of Earth and Environment, University of Leeds, Leeds, UK
[4] Department of Geosciences, University of Poitiers, Poitiers, France
* E-mail: cstremta@mail.usf.edu

Numerous granitoid plutons intruded the Neoproterozoic basement of the Danubian domain (Romanian Southern Carpathians) during the Variscan orogeny. The age distribution recorded from the plutons indicates that this essentially granitic/granodioritic (lacking associated basic rocks almost completely) activity is of post-collisional origin.

The Furcătura (317.1±2.8 Ma) pluton, albeit volumetrically small, is remarkably heterogeneous, showing wide ranges for most of the petrological and geochemical parameters. These metaluminous to strongly peraluminous (A/CNK of 0.76 to 1.91) granites, granodiorites, and quartz monzonites are calc-alkaline to high-K calc-alkaline (with some excursions in the shoshonitic field) and are characterized by a wide range of Mg# (15 to 84). They lack significant Eu anomalies (average Eu/Eu* of 0.94) and have sub-parallel REE patterns, with REE ranging from 51.11 to 203.7.

The heterogeneous character of the Furcătura pluton is further reflected in the $\delta^{18}O$ values of the mineral separates. Isotopic values of quartz separates range from 7.37 to 11.59‰, with the highest values measured in the late magmatic aplitic veins. Radiogenic isotope ratios ($^{87}Sr/^{86}Sr$ ranging from 0.707428±8 to 0.722204±6 and $^{143}Nd/^{144}Nd$ from 0.512075±11 to 0.512331±5) are indicative of discrete sources contributing to the formation of the melts, with both crustal and mantle-like signatures. In conventional discrimination diagrams, as well as reflected by their trace elemental compositions, Furcătura granitoids show both I- and S-type granites features, with no particular geographic zonation.

Geochemical evidence suggests the pluton was derived from a heterogeneous, primarily (lower?) crustal source, with subordinate additions of mantle-generated melts (*e.g.*, low Nb/U and Ce/Pb, low $\delta^{18}O$ values and $^{87}Sr/^{86}Sr$ ratios). The presence of mantle signatures in post-collisional magmas requires mechanisms that allow mantle melts to pond on the interface or to intrude the lower crust. These mechanisms generically referred to in the literature as delamination, have played an important role in the Variscan post-collisional magmatism preserved in the Romanian Southern Carpathians.

THE ČANIŠTE EPIDOTE-BEARING PEGMATITE, FYRO MACEDONIA: AN EXAMPLE OF THE MAGMATIC-HYDROTHERMAL TRANSITION

STRMIĆ PALINKAŠ, S.[1]*, BERMANEC, V.[1], PALINKAŠ, L.[1] & BOEV, B.[2]
[1] Institute of Mineralogy and Petrography, Faculty of Science, University of Zagreb, Horvatovac 95, Zagreb, Croatia
[2] Faculty of Mining, Geology and Polytechnic, Krste Goce Delčev University, Misirkov bb, Štip, FYRO Macedonia
* E-mail: sabina.strmic@inet.hr

The Čanište pegmatite is situated approximately 150 km south from Skopje, Republic of Macedonia, on the western slopes of the Selečka Mts. which represents a part of the Eastern Pelagonian tectonostratigraphic unit. The Pelagonian Massif exposes Precambrian crystalline basement made of ortho- and paragneisses, micaschists and amphibolites and includes numerous pegmatites, which differ according to their size, the mineralogical features, the internal structures and the differentiation degree.

The Čanište pegmatite attracts attention due its peculiar Ca-enriched mineral assemblage with unique occurrence of up to 2 meters long epidote crystals. Up to a 10 m wide pegmatite lens-shaped body and adjacent Upper Carboniferous granodiorites cut Precambrian gneisses. The pegmatite exhibits zoned internal structure with the following sub-units: 1) The wall zone; 2) The first intermediate zone; 3) The second intermediate zone, and 4) The massive quartz core.

The wall zone consists predominantly of amazonitic microcline with following unit cell characteristics a = 8.584(4) Å, b = 12.980(6) Å, c = 7.219(3) Å, α = 90.79(6)°, β = 115.96(3)°, γ = 87.60(4)° and V = 721.5(4) Å^3. Minor quartz and biotite occur as well.

The first transitional zone comprises euhedral columnar, up to 2 m long, crystals of epidote, embedded in a medium- to coarse-grained matrix of hematite, muscovite, quartz, microcline and garnet. Zircon and beryl occur sporadically. The epidote lattice parameters, calculated on the basis of XRD patterns [a = 8.890(2) Å, b = 5.634(2) Å, c = 10.147(2) Å, β = 115.40(2)° and V = 459.1(2) Å^3] corresponds well to the data previously reported for epidote from other localities. According to the electron-microprobe data epidote from the Čanište pegmatite belongs to the clinozoisite subgroup with general formula of $Ca_2Al_2Fe^{3+}(Si_2O_7)(SiO_4)O(OH)$.

The second intermediate zone, composed of albite, quartz and microcline, grades into the monomineralic massive quartz core.

Textural features, melt and fluid inclusion data suggest that the Čanište epidote-bearing pegmatite formed as a result of subsequent and successive crystallization from a granodioritic melt. The absence of aplites suggests a steady pressure condition during the course of pegmatite crystallization. A combination of fluid inclusion data and Na/K geothermometer gained pressure of about 4 kbar (depth ≈ 10.8 km). The primary wall zone mineral assemblage (microcline ± biotite, quartz) crystallized from the melt between 480 and 640°C. Cooling of the melt below 420°C at oxygen fugacity around 10^{-28} bars ran up deposition of the first intermediate zone (epidote + hematite + grossular + muscovite + quartz ± almandine, zircon, beryl). The progress of crystallization increased the Na/Ca ration in the residual melt. Consequently, the second intermediate zone, predominantly composed of albite, crystallized at temperature around 390°C. The massive quartz core was deposited around 360°C from the very last melt residue strongly enriched in silica, water and CO_2 content.

MINERALS OF TURQUOISE GROUP FROM SÂNDOMINIC, GURGHIU MTS., ROMANIA AND FROM PARÁDFÜRDŐ, MÁTRA MTS., HUNGARY

SZAKÁLL, S.*, KRISTÁLY, F. & ZAJZON, N.
Institute of Mineralogy and Geology, University of Miskolc, H-3515 Miskolc-Egyetemváros, Hungary
* E-mail: askszs@uni-miskolc.hu

1) The Sândominic occurrence (Dorma Hill) is located in the southern termination of Gurghiu Mts, Eastern Carpathians, Romania, in the vicinity (~5 km from Fagul Cetății deposit) of the Bălan copper ore mineralization. The site is located on the contact of the Rebra metamorphic limestones and Tulgheş Lithogroup. Turquoise (Fig. 1) was found as incrustations in a highly fractured and oxidized, quartz dominated part of a milonitic rock. In the cracks and voids of quartz it is associated with goethite, occasionally with mm-size euhedral quartz. Here the meteoric fluids permeated the metamorphic rocks creating oxidizing environment, where turquoise formed of supergene origin. The pale blue or pale greenish blue mamillary form crusts (up to 0.2 mm thickness), according to the BSE images, consist of globular aggregates up to 5–10 μm in diameter. The samples are of poor crystallinity, according to X-ray powder diffraction (XRD; Cu$K\alpha_1$). The main observed peaks were 6.193 Å, 4.791 Å, 3.682 Å, 3.427 Å, 3.279 Å and 2.905 Å, which correspond to the (011), ($\bar{1}$01), (1$\bar{1}$1), (210), (200) and (123) peaks of ferroan turquoise (ICDD 00-025-0260). According to wavelength dispersive microprobe measurements (WDX) the crusts are chemically homogenous. The empirical formula (water calculated from the difference) is $(Cu_{0.58}Fe_{0.37}Ba_{0.06}Zn_{0.04})Al_{5.94}(PO_4)_4(OH)_{7.92} \bullet 4.45H_2O$. The B-site of the structure contains Al, the A-site is fully occupied by Cu and Fe^{2+}. (The measured data in wt%: Al_2O_3 33.05, P_2O_5 32.86, Fe_2O_3 3.60, CuO 5.63, ZnO 0.37, BaO 1.13, H_2O 23.35.)

2) At the Parádfürdő polymetallic ore deposit, Mátra Mts., Hungary the main sulphides are chalcopyrite, sphalerite and tetrahedrite/tennantite. Here the turquoise group mineral is of late-stage hydrothermal origin, it occurs in the cavities of quartz veinlets and is associated with quartz, barite, variscite, wavellite, jarosite and illite. The source of the hydrothermal fluids was likely meteoric water that was heated up during interaction with the sulphide-rich plutons at depth. This interaction with Cu-Zn-Fe-rich sulphides produced acidic fluids with leached out ions (Cu-Zn-Fe), which were necessary to form turquoise group minerals. The source of phosphorus could be the hydrothermally altered rock-forming apatite. Here the turquoise mineral (Fig. 1) is a solid solution of aheylite $(Fe^{2+},Zn)Al_6(PO_4)_4(OH)_8 \bullet 4H_2O$, faustite $(Zn,Cu)Al_6(PO_4)_4(OH)_8 \bullet 4H_2O$ and planerite $\square Al_6(PO_4)_2(PO_3OH)_2(OH)_8 \bullet 4H_2O$. Similar situation was already observed elsewhere (FOORD & TAGGERT, 1998). The mineral appears as pale yellowish brown hemispheres, up to 0.5 mm in diameter. The inner part of the spheres is massive, while the rim is formed of porous aggregates of crystals (up to 1–2 μm in size). These hemispheres build up loose aggregates (up to 1–2 cm in size). Good quality XRD patterns (Cu$K\alpha_1$) gave peaks at 6.773 Å, 3.088 Å and 2.931 Å which correspond to the (001), (0$\bar{2}$2) and ($\bar{1}$12) peaks of planerite (ICDD 00-050-1654). Aheylite was also identified by the reflections 4.802 Å, 2,057 Å and 2.014 Å representing the ($\bar{1}$10), (231) and (202) *hkl* planes (ICDD 00-050-1653). The strongest peaks are overlapping at 6.185 Å, 3.690 Å and 3.436 Å. The hemispheres, both their inner part and their rim, are chemically homogenous. The empirical formula is $(Zn_{0.21}Fe_{0.18}Cu_{0.11})Al_{5.91}(PO_4)_4(OH)_{6.73} \bullet 5.07H_2O$. The B-site is occupied by Al, however, the A-site is only half-occupied by Zn ≈ Fe^{2+} > Cu cations, thus the mineral is between aheylite, faustite and planerite. [The measured WDX data in wt%: Al_2O_3 38.51, P_2O_5 36.27, FeO 1.65, CuO 1.14, ZnO 2.20, H_2O 22.23 (calculated from difference)]. Seemingly this is a complicated, but characteristic solid solution in the turquoise group.

Reference

FOORD, E.E. & TAGGERT, J.E., Jr. (1998): Mineralogical Magazine, 62: 93–110.

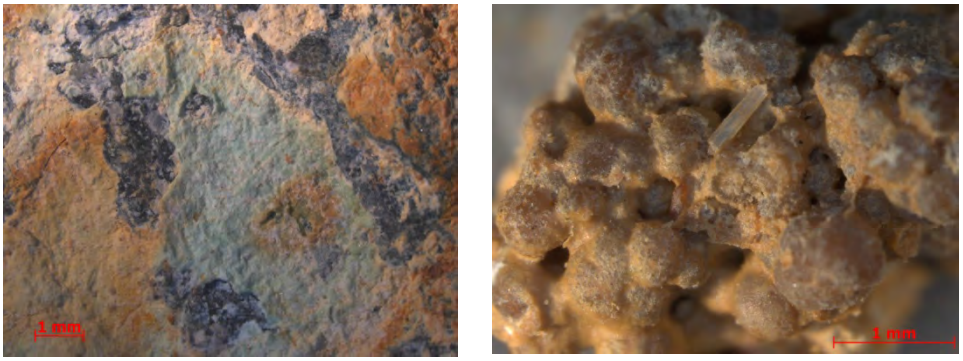

Fig. 1. *Light green crust of turquoise from Sândominic, Romania (left) and yellowish brown hemispheres of aheylite-planerite from Parádfürdő, Hungary.*

UNUSUAL IKUNOLITE FROM NAGYBÖRZSÖNY ORE DEPOSIT, BÖRZSÖNY MTS., HUNGARY

SZAKÁLL, S.*, ZAJZON, N. & KRISTÁLY, F.
Institute of Mineralogy and Geology, University of Miskolc, H-3515 Miskolc-Egyetemváros, Hungary
* E-mail: askszs@uni-miskolc.hu

The famous Nagybörzsöny ore deposit, Börzsöny Mts., Hungary, is hosted by Miocene calc-alkaline volcanic rocks and occurs as a stockwork in a dacite breccia pipe (NAGY, 2002). It is the type locality of pilsenite and jonassonite. The mineralization is multistage, from mesothermal to epithermal: Cu-Fe-(Au-Mo); Zn-Pb-Cu; Bi-Pb-As-W-(Au-Ag-Te); Zn-Pb-Ag-(Cu-Sb); Au-Ag. Ikunolite-containing ores were found in the Alsó- and Felső-Rózsa adits, Rózsa Hill. The ikunolite assemblage belongs to the third stage of mineralization. In this stage the main sulphides are bismuthinite and arsenopyrite, accompanying minerals are native bismuth, pyrite, marcasite, ferberite, hübnerite, gold, jonassonite, Bi-Pb-(Ag) sulphosalts (cosalite, lillianite, cannizzarite, pavonite, gustavite) and rare Bi-Te-sulphides (joséite-A, ingodite). Ikunolite, $Bi_4(S,Se)_3$, occurs together with arsenopyrite and bismuthinite in quartz veinlets. It forms well-developed plates and foliated masses up to 3–4 cm in size. Accompanying bismuth sulphides may alter to cannonite and other secondary minerals. The lamellae of ikunolite are lead grey in color, black in streak color. It has perfect cleavage parallel to {0001}.

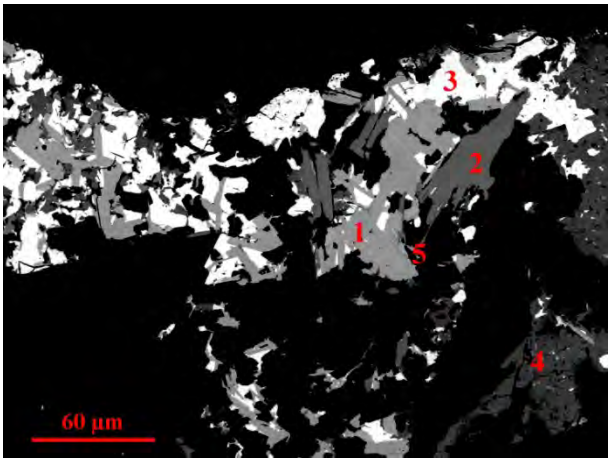

Fig. 1. *Typical assemblage of ikunolite from Nagybörzsöny (Se-zoning of ikunolite). 1 = ikunolite, 2 = lillianite, 3 = bismuth, 4 = bismuthinite, 5 = electrum (BSE image, 15kV, 20nA).*

Ikunolite was identified by X-ray powder diffraction and electron-microprobe analyses. X-ray powder diffraction was performed on a Bruker D8 Advance diffractometer (Cu$K\alpha_{1-2}$, 40 kV and 40 mA) in parallel-beam geometry (Goebel mirror 2) with 0.12° long-Soller on detector side. The careful sample preparation resulted in pure ikunolite specimens, with reduced preferred orientation. Variations in peak positions were observed, the main peaks for 3 specimens [*hkl*: $d_1/d_2/d_3$ (d_{calc}) Å]: 107: 3.024/3.027/3.029 (3.024); 0.1.14: 2.214/2.216/2.215 (2.208); 015: 3.272/3.269/3.280 (3.267); 110: 2.071/2.073/2.074 (2.075). Ikunolite is trigonal, space group $R\bar{3}m$. The cell parameters measured for the three specimens: (1) a = 4.149 Å, c = 39.261 Å, V = 585.34 Å^3; (2) a = 4.143 Å, c = 39.449 Å, V = 586.44 Å^3; (3) a = 4.149 Å, c = 39.397 Å, V = 587.39 Å^3.

Wavelength dispersive microprobe analyses show a wide variability of the chemical composition of ikunolite Results of our analyses document a continuous range of Se-for-S substitution. According to selenium content, the two observed end types of ikunolites are: first type contains up to ca. 1–2 wt% Se, while the second type contains up to ca. 9 wt% Se. The latter data may indicate a continuous solid-solution series with laitakarite, $Bi_4(Se,S)_3$. Similar ikunolite was mentioned from Rędziny, Poland (PARAFINIUK *et al.*, 2011). Most ikunolite compositions reveal substantial amounts of Pb substituting for Bi, in the range 0.15–0.44 *apfu*. The lead can substitute bismuth in the structure (MARKHAM, 1962). The tellurium content is up to ca. 0.3 wt%. The chemical formulae of the two Se-end types are the following (average of 5 and 3 analyses): $(Bi_{3.71}Pb_{0.26})_{\Sigma 3.97}(S_{2.86}Se_{0.14})_{\Sigma 3}$ and $(Bi_{3.40}Pb_{0.44})_{\Sigma 3.84}(S_{2.34}Se_{0.66})_{\Sigma 3}$.

References

MARKHAM, N.L. (1962): American Mineralogist, 47: 1431–1434.
NAGY, B. (2002): Földtani Közlöny, 132: 401–422.
PARAFINIUK, J., PIECZKA, A. & GOLĘBIOWSKA, B. (2008): Canadian Mineralogist, 49: 1305–1315.

THE FIRST OCCURRENCE OF NATIVE SELENIUM IN THE CARPATHIANS

SZEŁĘG, E.*, METELSKI, P. & JANECZEK, J.
Department of Geochemistry, Mineralogy and Petrography, Faculty of Earth Sciences, University of Silesia; Będzińska 60, 41-200 Sosnowiec, Poland
* E-mail: eligiusz.szeleg@us.edu.pl

Native selenium was found during investigation of hydrothermal assemblages in sandstones of the Godulskie Beds in the Wisła-Obłaziec sandstone quarry (Outer Carpathians, the Beskidy Mts., Poland). Major minerals of the hydrothermal assemblage are: calcite, barite, quartz and pyrite. Elongated crystals of pyrite and goethite pseudomorphs after pyrite occur within calcite druses. Pseudo-tetragonal pyrite crystals, up to 5 mm in length, exhibit well developed (100), (010), (001) and (111) or (100), (010), (110) and (111) faces (Figs. 1–2). In reflected light, the crystals are anisotropic. BSE imagery revealed both sector and oscillatory zoning. Acicular native selenium crystals up to 25 μm occur on the surface of the goethite pseudomorphs after pyrite in association with platy barite (Figs. 3–5).

EDS spectra revealed very strong selenium peak (Fig. 6). Weak peaks of oxygen and iron seen in the spectra, most probably originated from the background goethite. Sample preparation for EPMA turned out to be challenging due to the small size of selenium crystals and their strong adherence to the highly porous surface of goethite (Fig. 5). That may explain low analytical totals in electron microprobe analyses (Table 1).

Table 1. *EPMA data for native selenium from Wisła.*

Elements	wt%
Se	80.18
Fe	0.94
Ca	0.46
S	0.21
total	81.79

The origin of native selenium can be explained either by releasing traces of selenium from pyrite during its replacement by goethite and subsequent precipitation of selenium crystals or by the action of low-temperature Se-bearing fluids, from which selenium crystals precipitated on the porous surface of goethite. Spatial relationship between secondary goethite and native selenium favours the first possibility.

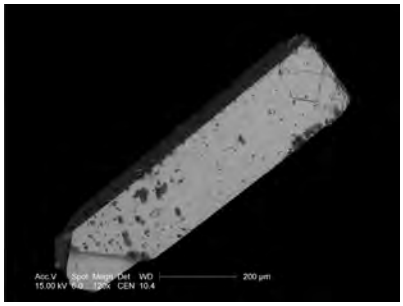

Fig. 1. *Elongated pyrite crystal with (100), (010), (001) and (111) faces. BSE image.*

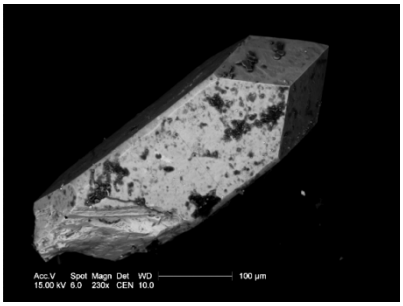

Fig. 2. *Elongated pyrite crystal with (100), (010), (110) and (111) faces. BSE image.*

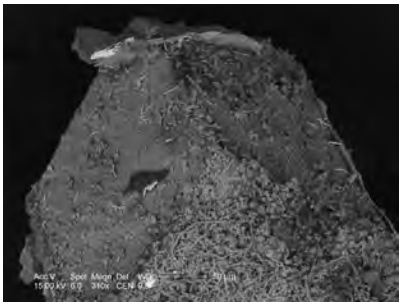

Fig. 3. *Acicular native selenium crystals on the surface of the goethite pseudomorphs. BSE image.*

Fig. 4. *Close-up of the aggregates of acicular native selenium crystals. BSE image.*

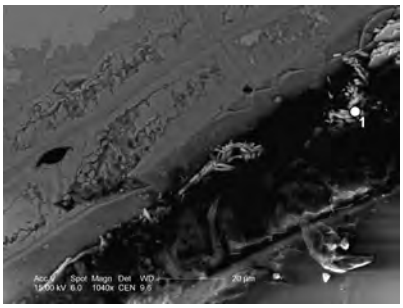

Fig. 5. *Native selenium (bright) on the surface of goethite. (1) marks analysis 1 in Table 1. BSE image.*

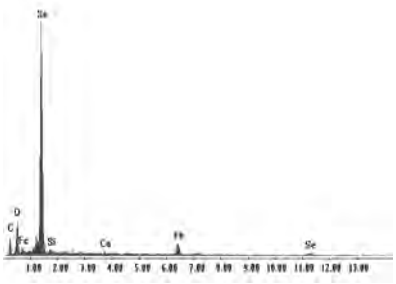

Fig. 6. *EDS spectrum of native selenium analyzed in spot 1 on Fig. 5.*

LUMINESCENCE CHARACTERISTICS OF QUARTZ SEPARATED FROM LATE PLEISTOCENE-HOLOCENE SEDIMENTS OF THE CARPATHIAN BASIN

THAMÓ-BOZSÓ, E.
Department of Geological Research, Geological Institute of Hungary, Stefánia út 14, H-1143 Budapest, Hungary
E-mail: bozso@mafi.hu

Quartz is a frequently used mineral in the luminescence age dating, first of all in the optically stimulated luminescence (OSL) dating method. OSL age of the sediment gives the date of its last exposure to sunlight. After deposition and burial the ionizing radiation of the surrounding sediments and the cosmic radiation generate free electrons, some of which become trapped in impurities and structural defects within quartz grains, and they store the absorbed energy. Initially the number of the trapped electrons is proportional to the dose of absorbed ionizing radiation. During heating or light exposure, the excited electrons escape from the traps, and the stored energy is released as luminescence light, TL or OSL signal respectively. There is a linear relationship between the absorbed dose and the luminescence signal for low doses. However, in the period of burial, the traps gradually become saturated, and the further ionizing radiation does not cause growth in the luminescence, limiting the age dating usually about 100 ka at the case of quartz. The higher values of the environmental dose rate cause earlier saturation. Usually only a small percentage of grains emit luminescence light, and the weak OSL signals give rise to problems in dating.

Late Pleistocene and Holocene sediments from different parts of the Carpathian Basin were studied, e.g. fluvial sediments near the Danube, Tisza, Körös, Lápos and Ér rivers, from the Transdanubian Hills, and South Transdanubia; eolian dune sands from the Transdanubian Central Range, and Transtisza Region; loess and loess-like sediments from Transdanubia, and valley of Ér River. Most of the fluvial sediments are medium or fine sands, and there are only a few sandy clay and gravel samples among them. Samples were collected by opaque PVC tubes. Sample preparation was done under subdued red light in dark room. Quartz was extracted mainly from within the grain size fraction 90–160, or 100–200 µm using H_2O_2 to remove the organic material, and 10% HCl to dissolve carbonates. Aqueous solution of sodium polytungstate was used for density separation of the quartz-rich fraction, which was then etched with 40% HF for 60 or 90 min to remove any remaining feldspars and the outer layer from the quartz grains (AITKEN, 1998). The clean quartz grains were mounted on stainless-steel discs in an 8 mm diameter (large aliquot) monolayer using silicone spray. OSL measurements were made using a Riso TL/OSL DA-15C/D reader with a calibrated 90Sr/90Y beta source. Blue light-emitting diodes (LEDs) were used for the optical stimulation of quartz for 40 s, at 125 °C. Preheat temperature was 220, 240, or 260 °C according to the results of preheat plateau tests. A single-aliquot regenerative-dose (SAR) protocol (WINTLE & MURRAY, 2006) was applied during the measurements. Environmental dose rates were calculated based on laboratory high-resolution gamma spectrometry analyses (Canberra GC3020, Eötvös Loránd Geophysical Institute of Hungary) of about 0.7–1 kg bulk samples from the sediments surrounding the OSL samples. To characterise the luminescence of the separated quartz fractions their growth curves, saturation doses, and luminescence intensity were compared.

Growth curves show the growth of luminescence response to increased doses of ionizing radiation up to 240 Gy in this study. Samples with fast-growing OSL reach the saturation level earlier, at about 80–100 Gy, e.g. some sediments from Transdanubia. Meanwhile samples with slowly growing luminescence become saturated later, above 200 or 240 Gy, e.g. fluvial sediments of Lápos, Tisza, Danube, Körös, and Ér rivers.

Comparing the luminescence intensity, quartz fractions separated from some sediment of Ér Valley, Transdanubia, and near Tisza River exhibit the brightest OSL signals. But sediments of the Danube which were collected in the Vienna Basin have very dim OSL signal with consequent difficulties in age estimation. Some sands in the Transdanubian Central Range also show quite dim luminescence. Environmental dose rates of the studied sediments range between 0.7 and 3.8 Gy/ka. Due to the high radioactive Th, U, and K content the sediments of the Lápos River and loess samples from different areas have higher dose rates (above 2 Gy/ka) than the sands do.

The research was supported by the Hungarian National Research Fund OTKA K-75801.

References

AITKEN, M.J. (1998): An introduction to optical dating. The dating of Quaternary sediments by the use of photon-stimulated luminescence. Oxford University Press, Oxford, etc., p. 280.

WINTLE, A.G. & MURRAY, A.S. (2006): Radiation Measurements, 41: 369–391.

THE [9]-COORDINATED *X* SITE IN THE CRYSTAL STRUCTURE OF TOURMALINE-GROUP MINERALS

TILLMANNS, E.* & ERTL, A.
Institut für Mineralogie und Kristallographie, Universität Wien, Althanstrasse 14, A-1090 Wien, Austria
* E-mail: ekkehart.tillmanns@univie.ac.at

Tourmalines are complex aluminium borosilicates with strongly varying compositions because of isomorphous replacements (solid solutions). The tourmaline mineral group which crystallises in space group *R*3*m* (No. 160; Z = 3) is chemically one of the most complicated groups of silicate minerals, with the general formula $X\ Y_3\ Z_6\ [T_6O_{18}]\ (BO_3)_3\ V_3\ W$ (HENRY *et al.*, 2011). The tetrahedral sites in tourmaline are primarily occupied by Si, and usually also by small amounts of Al and B. Planar rings of tetrahedra are linked by two types of octahedra, *Z* and *Y***,** which share edges to form brucite-like fragments. The *Z* octahedra are relatively small, somewhat distorted, and are occupied predominantly by trivalent cations such as Al^{3+}, Fe^{3+}, Cr^{3+} and V^{3+}, but can contain significant amounts of the divalent cation Mg^{2+}. The *Y* site is a relatively regular octahedron occupied by a wide array of mono- or multivalent cations, most commonly Li^{1+}, Mg^{2+}, Fe^{2+}, Mn^{2+}, Cu^{2+}, Al^{3+}, Cr^{3+}, V^{3+}, Fe^{3+}, Mn^{3+} and Ti^{4+}. Most structural refinements indicate that a minor *Y*-site vacancy can exist. The *X* site is a nine-coordinated trigonal antiprism, located along the three-fold axis of symmetry. It is most commonly occupied by Na and Ca, or vacant, and in rare cases occupied by K. Recently Pb was also described on this site (ERTL *et al.*, 2007; LUSSIER *et al.*, 2011).

FOIT & ROSENBERG (1979) plotted a positive correlation between Na occupancy and the <*X*–O> distance in Ca-poor tourmalines (7 samples with ≤0.1 *apfu* Ca). Interestingly, they stated that, if the <*X*–O> distance is plotted against the effective radius of the cations occupying that site, no correlation can be observed. FOIT (1989) plotted the <*X*–O> distances in correlation to (Na + *X*-site vacancies) of 13 tourmaline samples with different chemistry. He found a positive correlation with $r = 0.83$. GRICE & ERCIT (1993) characterised 12 tourmaline samples of various composition and described a relatively high scatter between <*X*–O> and the arithmetic mean of the constituent radii which they attributed to the fact that the calculation of mean ionic radii cannot account for the effect of *X*-site vacancies. BOSI *et al.* (2005) mentioned that usually <*X*–O> is linearly correlated with the *X*-site vacancies, whereas it is almost constant in samples with OH at the O2 site. BOSI & LUCCHESI (2007) described that <*X*–O> decreases with Ca content and increases with Na and *X*-site vacancy contents, a fact that could of course be expected.

To learn more about the role of the *X*-site cations and vacancies in relation the <*X*–O> distance we investigated 81 tourmaline samples (from the literature) with different *X*-site occupation. These samples show strongly varying <*Y*–O> and <*T*–O> distances. In contrast to earlier statements in the literature this evaluation has clearly shown that the <*X*–O> distance, as could have been expected, is positively correlated to the average effective ionic radius of the *X*-site occupants ($r = 0.98$ for 81 tourmaline samples, with Al_6 at the *Z* site and $(OH)_3$ at the *V* site). *X*-site vacancies (up to ~0.7 *apfu*), as well as a significant variation of <*T*–O> and <*Y*–O> distances, do not seem to have a significant effect on the <*X*–O> distance.

Olenite and "oxy-rossmanite" samples, in which the *V* site is not completely occupied by OH, show a significant deviation to this correlation. Tourmalines of the elbaite-olenite-rossmanite series (with Al_6 at the *Z* site) show a positive correlation between the <*X*–O> and the <Z–O> distance ($r = 0.80$; 40 samples) due to inductive effects in the structure.

This work was funded by the Austrian Science Fund (FWF) project no. P20509-N10 to ET and project no P23012-N19 to AE.

References

BOSI, F., ANDREOZZI, G.B., FEDERICO, M., GRAZIANI, G. & LUCCHESI, S. (2005): American Mineralogist, 90: 1784–1792.

BOSI, F. & LUCCHESI, S. (2007): American Mineralogist, 92: 1050–1063.

ERTL, A., HUGHES, J.M., PROWATKE, S., LUDWIG, T., BRANDSTÄTTER, F., KÖRNER, W. & DYAR, M.D. (2007): Canadian Mineralogist, 45: 891–899.

FOIT, F.F., Jr. (1989): American Mineralogist, 74: 422–431.

FOIT, F.F., Jr. & ROSENBERG, P.E. (1979): American Mineralogist, 64: 788–789.

GRICE, J.D. & ERCIT, T.S. (1993): Neues Jahrbuch für Mineralogie – Abhandlungen, 165: 245–266.

HENRY, D.J., NOVÁK, M., HAWTHORNE, F.C., ERTL, A., DUTROW, B.L., UHER, P. & PEZZOTTA, F. (2011): American Mineralogist, 96: 895–913.

LUSSIER, A.J., ABDU, Y., HAWTHORNE, F.C., MICHAELIS, V.K., AGUIAR, P.M. & KROEKER, S. (2011): Canadian Mineralogist, 49: 63–88.

MINERALOGICAL AND ENVIRONMENTAL STUDY ON SERPENTINE AND AMPHIBOLE ASBESTOS IN THE PARÂNG MOUNTAINS, ROMANIA

TOPA, B.A.[1]*, TÓTH, E.[2] & WEISZBURG, T.G.[1]
[1] Department of Mineralogy, Eötvös Loránd University, Pázmány Péter sétány 1/C, H-1117 Budapest, Hungary
[2] Eötvös Museum of Natural History, Eötvös Loránd University, Pázmány Péter sétány 1/C, H-1117 Budapest, Hungary
* E-mail: topabogi@gmail.com

The term asbestos is used for fibrous minerals that have been widely used in industry due to their special properties. It is a natural nanomaterial – a single fibre often has a diameter of only a few 100 nm. These fibres easily become airborne and respirable, and the inhalation of asbestos fibres in large quantity poses a serious risk to health. That is why the use of asbestos is now forbidden in most developed countries and asbestos is being removed from the built environment. Asbestos gained a regulatory definition (morphological and mineralogical criteria), enabling this way the measurement of its concentration in the main exposure medium (air) and the establishment of permissible exposure limits.

Being a morphological variety of certain minerals, asbestos surrounds us not only in our built environment, but also in nature. Natural asbestos occurrences can also be health risk sources, depending on a number of factors, including the size of the outcropping area, the probability of dust formation and the human presence.

We studied three, partly natural, partly artificial outcrops in the northern part of the Southern Carpathians, Romania, to assess their potential health risk. The first two localities are next to the Transalpina road (DN 67C), crossing the ridge of the Parâng Mountains, to the north of the peak Urdele. Recent road constructions have made these natural outcrops easily accessible by car. By cutting through the metamorphic (serpentinite, amphibolite and chlorite schists) rocks on the upper part of the ridge, the asbestos-bearing rocks got more exposed and their erosion rate increased. The first studied locality is the few 100 meters long road cut itself, a favourite break place of increasing transient tourism, the second is a nearby waterfall. The third occurrence is next to a dirt road in the valley of the Polatiştea River (tributary of the Jiu River), with similar rock types.

Following macroscopic observations in the field, samples were taken from the exposed and eroding rock veins, composed of white or green, lath-shaped and fibrous minerals, that were either perpendicular (cross-fibre) or parallel (slip-fibre) to the plane of the veins. Loose white filament bundles from the roadside and soil samples (with whitish fibres) near the waterfall have also been sampled. Air sample was taken on a gold-coated filter next to the uppermost exposure, where respirable dust formation is highly probable due to the open, almost always windy location and the presence of loose fibre bundles. Being at the same time a tourist outlook area, this location is supposed to carry the greatest health risk (by the inhalation of asbestos fibres).

We used X-ray powder diffraction (XPD) and scanning electron microscopy (SEM+EDX) for the qualitative phase analysis, and SEM to study the micromorphology of the selected minerals and soil aggregates. Airborne fibre concentration was quantified by SEM+EDX.

The collected white fibrous material is tremolite (with varying iron content), with many fibres fitting the legal asbestos size-range (illustrations are given in TÓTH & WEISZBURG, 2012). Other dominant phases of the samples are serpentine group minerals (antigorite, lizardite). Antigorite laths are in the asbestos range, too, and although it is not classified as asbestos by law, it may carry health risk (CARDILE *et al.*, 2007).

Air asbestos concentration was calculated two ways: if only legal asbestos (tremolite) is considered, airborne asbestos concentration is 17.5 fibre/dm^3, if also serpentine fibres are counted, the concentration is 35 fibre/dm^3. Both fibre concentrations exceed the current Hungarian environmental background (1 fibre/dm^3) and indoor asbestos clearance control limits (10 fibre/dm^3). It means that asbestos exposure is too high here for permanent living and/or working. For tourists driving through the transalpine road and stopping for a few minutes to enjoy the panorama, these outcrops are not regarded as major health risk, as exposure to asbestos dust is short. However, the paved road is getting more popular among cyclists, who inhale very intensively, thus sampling the air more efficiently and for longer time than motorised tourists. An additional risk may be associated with future permanent buildings (restaurant, hotel *etc.*) on the pass, therefore, coverage of the most asbestos-rich rock surfaces might prove useful. For better health risk assessment, the application of TEM is suggested to better discriminate between the serpentine minerals in air samples of mineralogically complex natural environments.

References

CARDILE, V., LOMBARDO, L., BELLUSO, E., PANICO, A., CAPELLA, S. & BALAZY, M. (2007): International Journal of Environmental Research and Public Health, 4(1): 1–9.

TÓTH, E. & WEISZBURG, T.G. (2012): Acta Mineralogica-Petrographica, Abstract Series, 7: this volume.

ASBESTOS: A REVIEW WITH SPECIAL EMPHASIS ON NATURAL CARPATHIAN-DINARIC OCCURRENCES

TÓTH, E.[1]* & WEISZBURG, T.G.[2]
[1] Eötvös Museum of Natural History, Eötvös Loránd University, Pázmány Péter sétány 1/C, H-1117 Budapest, Hungary
[2] Department of Mineralogy, Eötvös Loránd University, Pázmány Péter sétány 1/C, H-1117 Budapest, Hungary
* E-mail: zsike@abyss.elte.hu

A technological material with drawbacks

Asbestos used to be an industrial term for fibrous silicate minerals with a large number of industrial applications, including insulation (heat, electricity, noise, *etc.*) and friction materials (brake linings), engineered materials (fibre-reinforced composites like asbestos cement) and textiles (fire-resistant clothing) among others. The first use of these minerals dates back to the Stone Age, probably as earthenware reinforcing additive, followed by applications like lamp wicks, cremation clothes and other textiles. Since that time, asbestos has been in use continuously, with large scale mining and applications blooming in the first half of the 20th century.

Dusty environment has often accompanied the mining, processing and occasionally also the end-use of asbestos. Data on the deleterious health effects of asbestos dust, in the first place related to the inhalation of asbestos fibres (the main associated diseases are asbestosis, lung cancer and mesothelioma), accumulated gradually. Consequently, workplace asbestos dust permissible exposures got gradually limited, and asbestos-bearing products have been first limited, later prohibited in most industrialised countries. Asbestos removal from the built (man-made) environment has become a major issue, removal, waste treatment and safe deposition requiring large expenditure from the industrialised societies. Large sums are spent on compensations for asbestos-related diseases, too. While asbestos is being removed from the man-made environment in the developed countries, it is still widely applied and built into the man-made environment in the developing and undeveloped countries, due to its cheapness and good technological performance. In these latter countries, safe working conditions are often lacking, too. Whatever the final fate of these minerals, it is clear that asbestos plays an important role also in the 21st century.

Current legislation in Europe and Hungary

Based on the long and broad-range experience of mankind with asbestos, one would surely think that asbestos is a clear term. From the human health-concerned, legal point of view (Directive 83/477/EEC, repealed by 148/2009/EC), fibres of the serpentine mineral chrysotile and the amphiboles "crocidolite", grunerite ("amosite"), actinolite, anthophyllite and tremolite are to be called asbestos, if they are longer than 5 µm, thinner than 3 µm and their length : diameter (aspect) ratio is larger than 3 : 1 (WHO, 1997; Fig. 1). Simple as it sounds, it includes a lot of ambiguities and confusions, both on the mineralogical and the morphological side.

The only allowed activities related to asbestos are treatment and disposal of products resulting from demolition and asbestos removal (148/2009/EC; Hungarian legislation: 4/2011. (I. 14.) VM order), mining and processing is prohibited in Europe. Workplace exposure limit for asbestos fibre concentration in air is set at 100 fibre/dm^3, as an 8-hour time-weighted average (TWA). If workers are exposed to higher concentrations, they shall be issued with suitable respiratory and other personal protective equipment. In Hungary, additional permissible exposure limits are defined, too (12/2006. (III. 23.) EüM order): 10 fibre/dm^3, as control after asbestos removal; 1 fibre/dm^3, as general background.

Fig. 1. *Morphological definition of asbestos fibre, white "a" on red background being the international symbol of asbestos.*

Asbestos concentration in air should be determined by phase contrast microscopy (PCM, 148/2009/EC), measurement and fibre counting guidelines according to WHO (1997). Hungarian legislation also includes control analysis by scanning electron microscopy (4/2011. (I. 14.) VM order; not yet in daily practice).

Currently, all the declared asbestos minerals are regarded as Type I carcinogens by the WHO International Agency for Research on Cancer (IARC, 2012), irrespective of the fact that chrysotile is far less harmful than the fibrous amphiboles. Luckily enough, around 90% of asbestos use involved chrysotile, and the rest is mainly crocidolite and amosite.

Gaps between current legislation and current knowledge on asbestos

In spite of the large expenditure related to the "asbestos issue", legislation is decades behind the current knowledge on these minerals.

The mineralogical criterion is poorly defined. The six "declared" asbestos minerals are chrysotile (white asbestos; CAS# 12001-29-5) from the serpentine group, and five members of the amphibole group, namely, riebeckite (common name crocidolite or blue asbestos; CAS# 12001-28-4), grunerite (common name amosite or brown asbestos; CAS# 12172-73-5), anthophyllite (CAS# 77536-67-5), tremolite (CAS# 77536-68-6) and actinolite (CAS# 77536-66-4). These minerals are identified in most laws by their CAS registry numbers (CAS#), a US chemical database identifier with practically no structural data and only approximate chemical composition. The recently used CAS registries were created in 1984, and are based on the industrially applied fibrous silicates. Since then, amphibole nomenclature has been largely restructured (LEAKE *et al.*, 1997, 2003). As a consequence of the discrepancy, the Bolivian "blue asbestos", used in industrial applications, is classified as magnesioriebeckite (RRUFF database) by the current amphibole nomenclature, offering a potential escape route in legal cases. Legislation is also behind the scientific knowledge in terms of minerals that were "accidentally used" as minor components of industrial raw materials, and have similar health effects to the "classic" asbestos fibres. These include the fibrous variety of the amphibole fluoroedenite in the hydrothermally altered tuffaceous rocks of Biancavilla (Sicily, Italy), and the fibrous forms of the amphiboles richterite and winchite (mixed under the vermiculite of Libby, Montana, USA). Recently, health concerns have also been raised about fibrous antigorite (CARDILE *et al.*, 2007).

The morphological definition of an asbestos fibre seems straight forward, though amphiboles complicate fibre counting, as amphibole cleavage fragments overlap with the fibre size range. These fragments can thus contribute to the apparent fibre concentration in air, yet having a rather inert health impact, risk can be overestimated. Amphibole cleavage fragments usually derive from natural sources, not from anthropogenic materials.

Asbestos in the natural environment: a growing concern

Asbestos fibres form part of our natural environment, too, and both natural and disturbed outcrops (*e.g.*, road-cuts, open-pit asbestos mines) may pose health risks to the inhabitants. Asbestos fibres are different from most risk agents: they do not carry chemical risk (no soluble toxic element content, no acidic dissolution), risk is purely associated with the fibres becoming airborne and inhalable, and to a lesser extent, contaminating waters and becoming ingestible.

In Europe, these occurrences are mainly related to serpentinised ultramafic-mafic rocks of ophiolitic origin. As these occurrences are not engineered, anthropogenic fibre sources, with usually well-known (easy to identify) asbestos type(s), they need special attention and a clear environmental mineralogical approach. To assess the real health risks related to natural outcrops, the routine phase contrast microscopy fibre counting method may not be sufficient, especially as a number of minerals exist in acicular to fibrous form. Both morphological and chemical (structural) information is needed to identify the airborne fibres, best performed with the combination of scanning electron microscopy (SEM) and transmission electron microscopy (TEM).

In this work, the first results will be presented on disturbed outcrops of the Carpathian-Dinaric region.

The first example is a disturbed natural outcrop (Fig. 2), the east-west trending ridge of the Parâng Mountains, Southern Carpathians, Romania, cut by the north-south trending road 67C (Transalpina). The few 100 meters long roadcut exposes tectonically deformed serpentinite blocks that contain pale green, splintery to fibrous antigorite (weathering to thin laths fulfilling the size criteria of asbestos fibre, Fig. 3) and vein filling, silky white, slip-fibre tremolite (Fig. 1). The young (2–3 years old) roadcut is not consolidated, weathering goes on, bunches of tremolite up to 10 cm length can be found along the road. The soil (regolith) is occasionally a fibrous mass of antigorite and a subordinate amount of tremolite, and both minerals produce airborne particles. The surroundings are not inhabited, road construction / maintenance workers, tourists and local shepherds may be exposed to the fibrous dust on the open, often windy road. The first air analysis yielded 17 fibre/dm^3 (tremolite counted only), 35 fibre/dm^3 (tremolite and antigorite counted), suggesting that covering of the most weathering rock surfaces may be useful. Further information on the locality is given by TOPA *et al.* (2012).

Of special interest are the former asbestos mines, some of which, right in the Carpathian-Dinaric region, are still awaiting rehabilitation (*e.g.*, Dobšiná, Slovakia; Korlaće and Stragari, Serbia). Here, uncovered serpentinite rock surface, unprocessed serpentinite debris, "rock flour" (crushed and ground, processed serpentinite with residual asbestos content) and process dust may be the source of asbestos fibres. Most of the unprocessed debris and processed material are deposited as waste dumps in the mine surroundings. Processing (crushing and grinding) of the serpentinite enhances the possibility of fibrous dust formation. Fibre dissemination by means of erosion and water needs to be tested, too. The first environmental mineralogical studies on these localities are presented by GROZDICS *et al.* (2012, this volume − Dobšiná, Slovakia) and HARGITAI *et al.* (2012, this volume − Korlaće and Stragari, Serbia).

In the European Union, examples exist for almost complete asbestos mine rehabilitation (*e.g.*, MABE, Kozani Prefecture, Northern Greece), too, offering a good opportunity to compare the environmental impact of rehabilitated and non-rehabilitated mines.

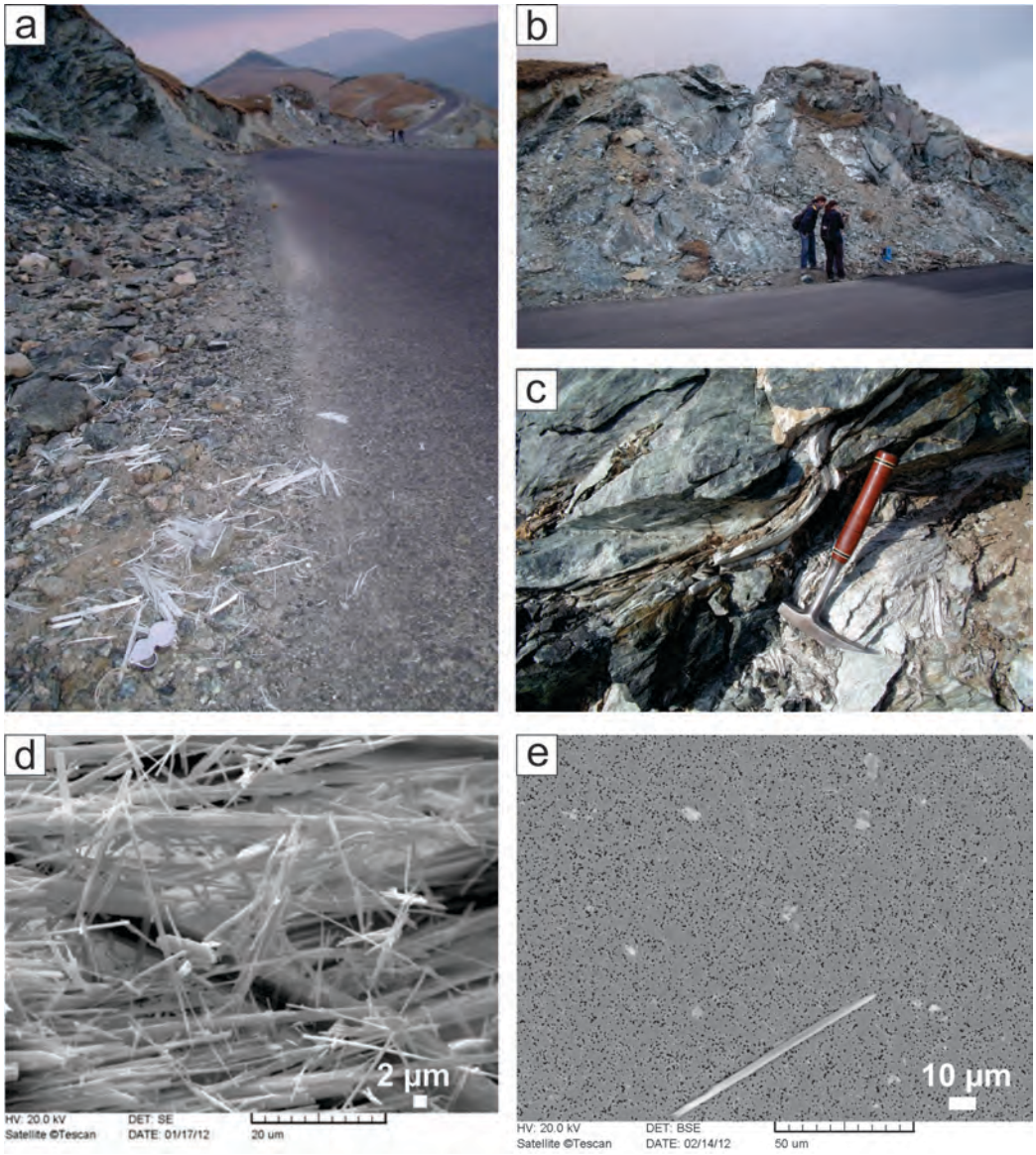

Fig. 2. *a: Eastwards oriented photo of the Parâng pass with white tremolite asbestos bunches at the roadside. b: Road cut with white tremolite veins in the greenish serpentinite. c: Slip-fibre tremolite. d: Tremolite bunch, with most long fibres fulfilling the size criteria of an asbestos fibre (SE image). e: Tremolite asbestos fibre on the air sampling gold filter (BSE image). Work of TOPA et al. (2012).*

References

CARDILE, V., LOMBARDO, L., BELLUSO, E., PANICO, A., CAPELLA, S. & BALAZY, M. (2007): International Journal of Environmental Research and Public Health, 4(1): 1–9.

GROZDICS, T., TÓTH, E. & WEISZBURG, T.G. (2012): Acta Mineralogica-Petrographica, Abstract Series, 7: this volume.

HARGITAI, A., TÓTH, E., VASKOVIĆ, N., MILOŠEVIĆ, M. & WEISZBURG, T.G. (2012): Acta Mineralogica-Petrographica, Abstract Series, 7: this volume.

IARC Monographs on the Evaluation of Carcinogenic Risks to Humans (2012): 100/C, 499 pp.

LEAKE, B.E., WOOLLEY, A.R., ARPS, C.E.S., BIRCH, W.D., GILBERT, M.C., GRICE, J.D., HAWTHORNE, F.C., KATO, A., KISCH, H.J., KRIVOVICHEV, V.G., LINTHOUT, K., LAIRD, J., MANDARINO, J.A., MARESCH, W.V., NICKEL, E.H., ROCK, N.M.S., SCHUMACHER, J.C., SMITH, D.C., STEPHENSON, N.C.N., UNGARETTI, L., WHITTAKER, E.J.W. & YOUZHI, G. (1997): Canadian Mineralogist, 35: 219–246.

LEAKE, B.E., WOOLEY, A.R., BIRCH, W.D., BURKE, E.A.J., FERRARIS, G., GRICE, J.D., HAWTHORNE, F.C., KISCH, H.J., KRIVOVICHEV, V.G., SCHUMACHER, J.C., STEPHEN-

SON, N.C.N. & WHITTAKER, E.J.W. (2003): Canadian Mineralogist, 41: 1355–1362.

TOPA, B.A., TÓTH, E. & WEISZBURG, T.G. (2012): Acta Mineralogica-Petrographica, Abstract Series, 7: this volume.

WHO (1997): Determination of airborne fibre number concentrations, a recommended method, by phase-contrast optical microscopy (a membrane-filter method). ISBN 92 4 154496 1, 53 pp.

12/2006. (III. 23.) EüM order (2006): Magyar Közlöny, 2006/32: 2673–2679.

2009/148/EC: Directive 2009/148/EC of the European Parliament and of the Council of 30 November 2009 on the protection of workers from the risks related to exposure to asbestos at work. Official Journal of the European Union, L 330 (16.12.2009): 28–36.

4/2011. (I. 14.) VM order (2011): Magyar Közlöny, 2011/4: 487–533.

83/477/EEC: Council Directive 83/477/EEC of 19 September 1983 on the protection of workers from the risks related to exposure to asbestos at work (second individual Directive within the meaning of Article 8 of Directive 80/1107/EEC). Official Journal of the European Communities, L263 (24.09.1983): 25–32.

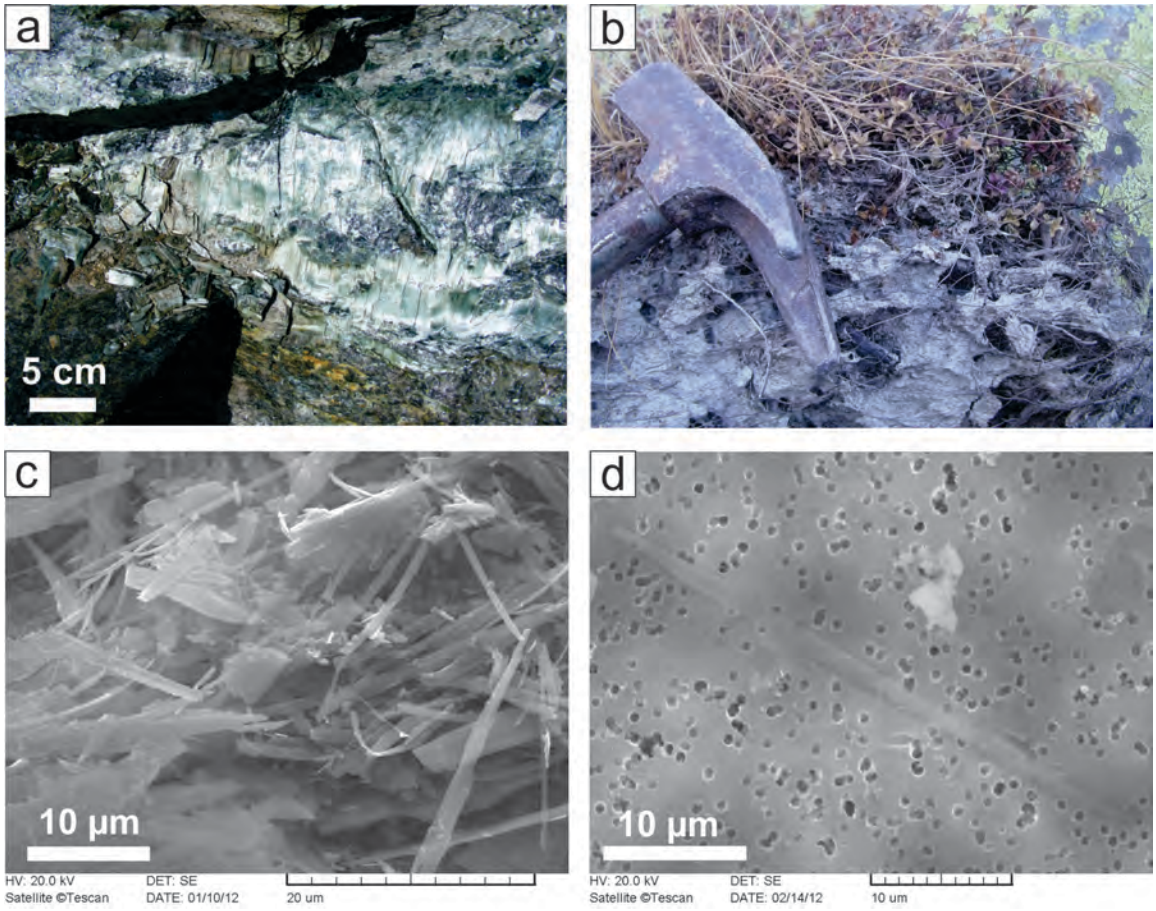

Fig. 3. *a: Silky green antigorite at the Parâng pass. b: Fibrous regolith (primitive soil) form the surroundings of the road. c: Antigorite laths from a soil sample, most long laths on the picture fulfilling the size criteria of a fibre (SE image). d: Antigorite lath (fibre size) on the air sampling gold filter (SE image). Work of TOPA et al. (2012).*

A COMPREHENSIVE INFRARED DATABASE TO RECOGNIZE THE WATER CONTENT OF MINERALS: PANNON UNIFORM LITHOSPHERIC INFRARED SPECTRAL DATABASE (PULI)

UDVARDI, B.[1], PINTÉR, Zs.[1], KOVÁCS, I.[2]*, HIDAS, K.[2], KUTASSY, L.[2], ZELEI, T.[2], FALUS, Gy.[2], LENDVAY, P.[2], FANCSIK, T.[2] & SZABÓ, Cs.[1]

[1] Lithosphere Fluid Research Lab, Department of Petrology and Geochemistry, Eötvös Loránd University, Pázmány Péter sétány 1/C, H-1117 Budapest, Hungary

[2] Eötvös Loránd Geophysical Institute of Hungary; Kolumbusz u. 17-23, Budapest, Hungary

* E-mail: kovacsij@elgi.hu

Over the last decades several papers and books, dealing with various aspects of water content of minerals by Fourier transform infrared spectroscopy, have been worldwide published. Advancements in technology and methods have resulted in an explosion of mineral infrared spectroscopy (PATERSON, 1982; LIBOWITZKY & ROSSMAN, 1996; SAMBRIGE *et al.*, 2008, KOVÁCS *et al.*, 2010). To keep up with this exponentially rising knowledge in infrared spectroscopy of minerals, an electronic spectral database was needed. This can assist us in understanding better both the qualitative and quantitative aspects of incorporation in minerals structures, and this could provide a reference for the interpretation of future infrared analysis of minerals.

This is the reason why we construct the Pannon Uniform Lithospheric Infrared (PULI) Spectral Database, which would include large amount of infrared spectra of nominally anhydrous silicate minerals (olivine, pyroxenes, garnet), diamonds and clay minerals. This is because there is internationally a great demand for a thematic reference spectral database, where the absorption bands of water incorporated in different minerals are summarized in a uniform format, which may be also suitable for quantitative re-evaluation.

Fundamentals of our analytical setup (i.e. sample preparation, microscope settings) and evaluation protocol (i.e. background subtraction, integration and calibration factors) results of the re-evaluation for upper mantle and experimentally derived olivine spectra are presented, which contribute to recognition of water content in the Earth's mantle and the multiple role of water in mantle processes. Furthermore, we tested a standard olivine by different infrared spectroscopy instruments to provide us clear and objective instructions regarding the analytical settings and spectrum evaluation. Such a spectral comparison has not been previously critically performed.

This study was supported by the OTKA, Hungarian Scientific Research Fund (PD 101683) and by a Marie Curie International Reintegration Grant (NAMS-230937) to IK.

References

KOVÁCS, I., O'NEILL, H. ST. C., HERMANN, J. & HAURI, E.H. (2010): American Mineralogist, 95: 292–299.

LIBOWITZKY, E. & ROSSMAN, G.R. (1996): Physics and Chemistry of Minerals, 23: 319–327.

PATERSON, M.S. (1982): Bulletin de Minéralogie, 105: 20–29.

SAMBRIDGE, M., FITZGERALD, J., KOVÁCS, I., O'NEILL, H. ST. C. & HERMANN, J. (2008): American Mineralogist, 93: 751–764.

BERYL IN GRANITIC PEGMATITES OF THE WESTERN CARPATHIANS (SLOVAKIA): COMPOSITIONAL VARIATIONS, MINERAL INCLUSIONS AND BREAKDOWN PRODUCTS

UHER, P.*, BAČÍK, P., OZDÍN, D. & ŠTEVKO, M.
Department of Mineralogy and Petrology, Comenius University, Mlynská dolina G, 842 15 Bratislava, Slovakia
* E-mail: puher@fns.uniba.sk

Beryl is characteristic mineral of Hercynian (ca. 350 Ma) granitic pegmatites associated with S- and I-type granites-granodiorites of the Tatric Unit, Western Carpathians, Slovakia (UHER *et al.*, 2010; OZDÍN, 2010). The pegmatite dikes belong to LCT-suite and beryl-columbite subtype of the rare-element class (*sensu* ČERNÝ & ERCIT, 2005). The beryl-bearing pegmatites occur mainly in the Malé Karpaty (Bratislava Massif), Považský Inovec, and Nízke Tatry Mountains. Beryl represents the only essential rare-element phase in majority of the pegmatites, whereas accessory Nb-Ta-(Sn) oxide minerals occur in the most evolved ones (e.g., Moravany nad Váhom, Jezuitské Lesy, Sopotnica Valley). Beryl forms columnar pale green crystals (up to 15 cm across), usually on the boundary between blocky K-feldspar + muscovite zone and quartz core (beryl I), or locally in saccharoidal and cleavelandite albite unit (beryl II).

The EMPA, LA-ICP-MS and XRD data show mostly the presence of alkali-poor beryl. However, Na, Fe, and Mg-enriched domains are locally present (up to 2.7 wt% Na_2O, 5.1 wt% FeO, and 2.7 wt% MgO; Prašivá, Švábsky Hill, Sitina). Trace element compositions of the studied beryl show relatively wide variations. Concentrations of Li are typically 120 to 830 ppm, locally 1400 to 1800 ppm (Švábsky Hill and Kamzík II). The highest Li contents are in beryl from the Moravany nad Váhom pegmatite (up to 5600 ppm). On the other hand, the highest concentrations of Cs (5700 to 9800 ppm, 1 to 2 wt% Cs_2O in some zones) occur in beryl I from the Jezuitské Lesy pegmatite (BM), whereas other investigated samples contain only ~50 to 1400 ppm Cs. Locally beryl contains slightly elevated contents of K (1300 to 2300 ppm) and Zn (~900 to 1700 ppm; Jezuitské Lesy, BM). Rb and Mn concentrations are generally low (≤ 170 ppm Rb, ≤ 280 ppm Mn), contents of Sc, Ga and Ni are lower than 100 ppm. Distribution and mutual relationships between major elements (Al, Fe, Mg, Na, and Cs) show the dominant role of $Na(Fe^{2+},Mg)\square_{-1}Al_{-1}$ channel-octahedral substitution mechanism in beryl. However, elevated Li or Cs contents also indicate the presence of channel-tetrahedral substitutions in beryl from the most evolved pegmatites: $(Na,Cs)Li\square_{-1}Be_{-1}$ (Moravany nad Váhom) and $(Cs,Na)Al\square_{-1}Si_{-1}$ (Jezuitské Lesy).

A common patchy internal zoning of magmatic beryl I crystals indicates a late-magmatic to subsolidus, partial dissolution-reprecipitation processes. The primary evolution trend in beryl I shows increasing Cs and Cs/Na with decreasing Mg and Mg/Fe from less evolved to more fractionated pegmatites. However, a secondary evolution trend probably connected with post-magmatic partial dissolution-reprecipitation shows decreasing Cs and increasing Mg/Fe in the beryl I. Beryl II show almost homogeneous internal texture and lower content of Cs than beryl I.

The powder XRD data support the compositional results and substitution mechanisms. The *c/a* ratio (AURISICCHIO *et al.,* 1988) reflects the presence of tetrahedral type in the Na,Cs-enriched beryl I (*c/a* = 0.9997; Jezuitské Lesy) and octahedral type in Na,Fe,Mg-rich beryl I (*c/a* = 0.9916; Sitina), in contrast to normal beryl type with mixed octahedral-tetrahedral substitutions in the other samples (*c/a* = 0.9975 to 0.9985).

Numerous microscopic inclusions of cassiterite, "hydroxycalciomicrolite", gahnite, pyrite, sphalerite, galena, and muscovite were detected in some beryl I crystals (Moravany nad Váhom, Švábsky Hill). Gahnite inclusions in beryl contain high iron concentrations (14 to 18 wt% FeO, 37 to 47 mol% of hercynite), which are unusual for pegmatite environment. Uranoan "hydroxycalciomicrolite" (7–9 wt% UO_2) forms zonal crystals in quartz-microcline veinlets in beryl.

Partial to almost complete breakdown of beryl I to secondary assemblage of phenakite ± bertrandite + quartz II + muscovite II ± K-feldspar II have been identified by CL, EMPA, XRD, and EBSD methods in almost all studied pegmatites. The beryl breakdown originated during subsolidus pegmatite alteration, probably by hydrothermal fluids.

References

AURISICCHIO, C., FIORAVANTI, G., GRUBESSI, O. & ZANAZZI, P.F. (1988): American Mineralogist, 73: 826–837.

ČERNÝ, P. & ERCIT, T.S. (2005): Canadian Mineralogist, 43: 2005–2026.

OZDÍN, D. (2010): Bulletin Mineralogicko-Petrologického Oddělení Národního Muzea (Praha), 18: 78–84.

UHER, P., CHUDÍK, P., BAČÍK, P., VACULOVIČ, T. & GALIOVÁ, M. (2010): Journal of Geosciences, 55: 69–80.

INITIAL RESULTS OF TEXTURAL AND FLUID INCLUSION ANALYSES OF GYŰRŰFŰ RHYOLITE FORMATION (PERMIAN, SW HUNGARY)

VARGA, A.[1]*, DABI, G.[2] & BAJNÓCZI, B.[3]
[1] Department of Geology, University of Pécs; Ifjúság útja 6, Pécs, Hungary
[2] Department of Mineralogy, Geochemistry and Petrology, University of Szeged; P.O. Box 651, Szeged, Hungary
[3] Institute for Geological and Geochemical Research, Research Centre for Astronomy and Earth Sciences, Hungarian Academy of Sciences; Budaörsi út 45, Budapest, Hungary
* E-mail: andrea.varga.geol@gmail.com

Facies interpretation of volcanic rocks is of critical importance for the reconstruction of eruptive processes, particularly in ancient and sometimes strongly altered successions with limited outcrop. However, this is often a difficult task since some pyroclastic rocks such as high-grade ignimbrites and felsic lavas may develop similar textures during emplacement, cooling and post-depositional alteration.

In this study, we investigate drill cores and thin sections of the subsurface Permian volcanic rocks (Gyűrűfű Rhyolite Formation, boreholes D 9015, D 9018 and XV) from southern Transdanubia, Mecsek Mountains which represent a felsic igneous province in the post-collisional Variscan foreland. In the study area, the Gyűrűfű Rhyolite has been interpreted traditionally as a rather monotonous complex of lava flows.

The most conspicuous feature of the studied core samples is the apparent porphyritic texture comprising abundant, but unevenly distributed, mostly broken feldspar and quartz phenocrysts. An important indicator of volcaniclastic origin is, however, the presence of relict coarsely porphyritic pumice lapilli, which has been flattened during compaction. In thin section the studied Gyűrűfű samples are thoroughly recrystallised. Using cathodoluminescence (CL), however, recrystallised shards are clearly evident in the matrix showing original vitriclastic textures. Some shards have recognisable rod and bubble-wall shapes, but those at the edges of quartz and feldspar crystals are strongly deformed and indicate welding compaction. The formerly glassy shards show remnants of axiolitic devitrification texture. In the relict pumice clasts, the internal vesicular microstructure has been destroyed. The brown rims of pumice clasts show axiolitic and spherulitic devitrification. Their central parts consist of a mosaic of fine-grained quartz and feldspar. Axiolitic devitrification develops during primary cooling and crystallisation of hot volcanic glass, and is a good indicator of primary emplacement of volcaniclastic deposits. Our data show that previously identified lavas are best interpreted as ignimbrites and that, as a result, the importance of explosive volcanism has been underestimated in the western part of the Mecsek Mts.

With respect to the petrographic character of the fluid inclusion assemblages, the studied samples from drill core XV display very similar features. Fluid inclusions are situated along arcuate trails in fragmented quartz grains indicating the pervasive nature of parent fluids. The direct connection of these trails to fractures of fragmented quartz grains is obvious at some places. Thus it is plausible to interpret these inclusions to contain fluids present after deposition of the formation and responsible for the cementation of the quartz grains. According to our preliminary microthermometric results, fluid inclusions homogenize to the liquid phase in a range between 89 and 125 °C (N = 33) with a maximum between 98 and 103 °C which is a minimum of the fluid temperature. Assuming the percolative nature of the fluid, and thus low fluid-rock ratio, it is plausible to consider that the fluid temperature was governed by the rock itself. Thus the measured range of homogenisation temperatures is also a minimum for the igneous mass at the time of fluid entrapment. Final melting temperatures are in a range between -4.5 and -2.8 °C, consistent with salinities between 7.17 and 4.8% *w*NaCl equivalent. These measurements, however, were successful only in four inclusions due to prevalent metastable behaviour.

This research has been supported by the Hungarian Scientific Research Found (OTKA; No. PD 83511) and by the János Bolyai Research Scholarship of the Hungarian Academy of Sciences (AV).

NEW U–Pb DATING AND Hf-ISOTOPE COMPOSITION OF THE GORNJANE GRANITOIDS (SOUTH CARPATHIANS, EAST SERBIA)

VASKOVIĆ, N.[1]*, BELOUSOVA, E.[2], O'REILLY, S.Y.[2], GRIFFIN, W.L.[2], SREĆKOVIĆ-BATOĆANIN, D.[1], CHRISTOFIDES, G.[3] & KORONEOS, A.[3]

[1] Faculty of Mining and Geology, University of Belgrade, Belgrade, Serbia

[2] ARC Centre of Excellence for Core to Crust Fluid Systems and GEMOC, Macquarie University, Sydney, Australia

[3] Aristotle University of Thessaloniki, Greece

* E-mail: nada.vaskovic@rgf.bg.ac.rs

The main feature of the South Carpathian geotectonic framework is the Getic and Danubian nappes (generated during the Cretaceous Alpine crustal convergence and shortening). Their Neoproterozoic-Paleozoic (Cambrian to Early Carboniferous) basement is intruded by Late Variscan granitoids, mostly of Pennsylvanian to Early Permian age. Within the Getic nappe, these granitoids define one N-SE alignment (up to 150 km length) that can be traced from Romania (Sichevita-Poniasca) to Eastern Serbia (Brnjica, Neresnica, Gornjane). Although the Romanian granitoids are relatively well-studied (DUCHESNE *et al.,* 2008) the investigation of the East Serbian ones is still in progress (cf. VASKOVIĆ *et al.,* 2004).

The present study provides the first U-Pb and Hf isotope results obtained on zircons from the main rock types of the Gornjane pluton (GP): porphyritic monzogranite [MG], fine-grained granite [FG], medium-grained granodiorite [GD] and fine-grained diorite [FD]. The analyzed zircons are zoned and some of them are older inherited zircons. U-Pb and Hf isotope analyses were done in the GEMOC Key Center (Macquarie University, Sydney) using LA-ICP-MS (Model HP 4500, Series 300) and a Merchantek EO LUV LA microprobe, attached to a Nu Plasma multi-collector ICP-MS. The U-Pb ages obtained for the MG (307.1 ± 4.5 Ma), FG (307.6 ± 2.5 Ma and 323.3 ± 2.6 Ma), GD (307.1 ± 2.9 Ma) and FD (305.8 ± 3.6 Ma) confirm the emplacement and magmatic crystallization of the GP during Late Variscan events. The ages of inherited zircons from all rock types confirm the involvement of Neoproterozoic (701–672 Ma) and Paleozoic material of Cambrian (502–407 Ma) and Devonian-Early Carboniferous (378–342 Ma) age in the magma genesis. The initial $^{176}Hf/^{177}Hf$ ratios in zircons from all rock types range from 0.282443 to 0.282690 and lie close to CHUR (Fig. 1). Most of the analyzed zircons show moderately juvenile Hf-isotope composition (ε_{Hf} is from +2 to +5), with some negative values (mainly in fine-grained granites, ε_{Hf} down to -5). The mean crustal model age (which assumes a source with the mean crustal Lu/Hf) is ca 1.1 Ga and a maximum crustal model age is ca 1.5 Ga (Fig. 1). Therefore, the GP magmas can be interpreted as being largely derived by remelting of Neoproterozoic to Mesoproterozoic lower crust.

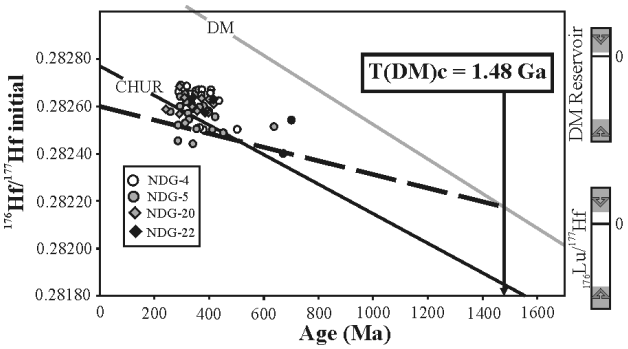

Fig. 1. *Hf-isotope data for the Gornjane pluton: NDG-4 = porphyritic monzogranite, NDG-5 = fine grained granite, NDG-20 = medium grained granodiorite, NDG-22 = fine grained diorite.*

The ages for the GP fit well the results obtained for the Romanian Sichevita-Poniasca pluton (311 ± 2 Ma; DUCHESNE *et al.,* 2008) as well as the late Variscan granites distributed throughout the Danubian nappe (e.g. San Nikola 311.9 ± 4.1 Ma) and the Balkan terrane (e.g. Petrohan 304.6 ± 4.0 Ma; Smilovene 304.1 ± 5.5 Ma; Hisara 303.5 ± 3.3 Ma; Koprivshtitza 312.0 ± 5.4 Ma; CARRIGAN *et al.*, 2005). If we take into consideration an older phase found in FG (sample NDG5 with 323 ± 2.6 Ma age) we can deduce that these granitic magmas were created within a relatively short time span, probably < 20 Ma.

This research was supported by project No 176016 of the Serbian Ministry of Science and ARC Centre of Excellence for Core to Crust Fluid Systems and GEMOC, Macquarie University, Sydney, Australia.

References

CARRIGAN, C.W., MUKASA, S.B., HAYDOUTOV, I. & KOLCHEVA, K. (2005): Lithos, 82: 125–147.

DUCHESNE, J.-C., LIÈGEOIS, J.-P., IANCU, V., BERZA, T., MATUKOV, D.I., TATU, M. & SERGEEV, S.A. (2008): International Journal of Earth Sciences (Geologische Rundschau), 97: 705–723.

VASKOVIĆ, N., KORONEOS, A., CHRISTOFIDES, G., SREĆKOVIĆ-BATOĆANIN, D. & MILOVANOVIĆ, D. (2004): Bulletin of the Geological Society of Greece, 36: 615–624.

COMPOSITIONAL VARIATIONS OF THE TENNANTITE-TETRAHEDRITE SERIES FROM THE MADAN Pb-Zn DEPOSITS, BULGARIA: OSCILLATORY ZONING AND CONDITIONS OF FORMATION

VASSILEVA, R.D.[1]*, ATANASSOVA, R.[1] & KOUZMANOV, K.[2]
[1] Geological Institute, Bulgarian Academy of Sciences, BG-1113 Sofia, Bulgaria; [2] University of Geneva, Switzerland
* E-mail: rosivas@geology.bas.bg

The tennantite-tetrahedrite solid solution series is the most common among the sulphosalt minerals in the Madan base metal deposits, Central Rhodopes, Bulgaria. Found in veins and metasomatic orebodies of the Petrovitsa and Gradishte deposits, these minerals closely associated with the main sulphides – galena, sphalerite, chalcopyrite and pyrite. Textural characteristics, mineral relationships and fluid inclusion studies suggest that tennantite-tetrahedrite$_{ss}$ at Madan precipitated in the late stages of mineralization at temperatures close to 200°C. Large compositional variations are responsible for the observed fine oscillatory zoning of the crystals, according to EPMA and LA-ICP-MS investigations.

A generalized formula for the tennantite-tetrahedrite$_{ss}$ was proposed by JOHNSON *et al.* (1986): $(Cu,Ag)_6\,Cu_4\,(Fe,Zn,Cu,Hg,Cd)_2\,(Sb,As,Bi,Te)_4(S,Se)_{13}$. Although in the Madan samples Cu content is always higher than 10 *apfu*, Cu can be considerably substituted by Zn, and less commonly by Fe and Ag. Such compositions correspond to zincian varieties (1.7–1.95 *apfu* Zn) with low Fe-content (0.08–0.45 *apfu*). Silver is characteristic of the Petrovitsa samples, reaching 0.30 *apfu*. The Gradishte samples reveal highly variable As/Sb ratios, mostly belonging in composition to the tennantite and intermediate members of the solid solution (Fig. 1). Tennantite-tetrahedrite$_{ss}$ from Petrovitsa have As/Sb ratio < 0.78, generally in the range of 0.10–0.55, corresponding to tetrahedrite. Bismuth and tellurium were below the limit of detection of the EPMA, however detected by LA-ICP-MS analyses at a ppm level. Selenium commonly substitutes for S.

Based on microprobe analyses the following average crystal-chemical formulae can be assigned: *Gradishte*: $(Cu^{+}_{5.99–6.00}Ag_{0–0.01})_{\Sigma6}Cu^{2+}_{4}(Fe_{0.08–0.45}Zn_{1.61–1.93}Cu^{2+}_{0.06–0.2}Cd_{0.01})_{\Sigma2}(Sb_{0.03–2.85}As_{1.12–3.98})_{\Sigma4}(S_{12.73–12.93}Se_{0–0.05})_{\Sigma13}$. *Petrovitsa*: $(Cu^{+}_{5.70–5.86}Ag_{0.11–0.30})_{\Sigma6}Cu^{2+}_{4}(Fe_{0.06–0.21}Zn_{1.81–1.95}Cu^{2+}_{0.10–0.25})_{\Sigma2}(Sb_{2.23–3.66}As_{0.33–1.74})_{\Sigma4}(S_{12.71–12.90}Se_{0-0.03})_{\Sigma13}$.

The presence of tennantite-tetrahedrite$_{ss}$ in the hydrothermal mineralization suggests increased activity of Sb and As in the fluids, as well as increased fS_2. Important Zn-incorporation in the studied samples is indicative for high fO_2 (SPIRIDONOV *et al.* 2005), resulting in enhanced Cu^{2+}/Me^{2+} ratios. A vertical zonation in the Madan hydrothermal system is observed, consisting of As-rich members (mostly zincian tennantite), typically found at depth (Gradishte ~400 m.a.s.l.), while in the upper levels (Petrovitsa mine ~970 m.a.s.l.) tetrahedrite compositions tend to prevail. Silver incorporation is often related to the late stage of formation of tetrahedrite, compared to the main sulphide paragenesis.

Acknowledgements. This study is part of the SCOPES IZ73Z0-128089 and SNF 20021-127123/1 projects of the Swiss National Science Foundation. The authors are grateful for the financial support of the BG051PO001-3.3.05-0001 Project of the Bulgarian Ministry of Science and Education.

References

JOHNSON, N.E., CRAIG, J.R. & RIMSTIDT, J.D. (1986): Canadian Mineralogist, 24: 385–397.

SPIRIDONOV, E., MALEEV, M., KOVACHEV, V., KULIKOVA, I., NAUMOVA, G. & FILIMONOV, S. (2005): Proceedings of the Bulgarian Geological Society, 80th Anniversary, 79–82.

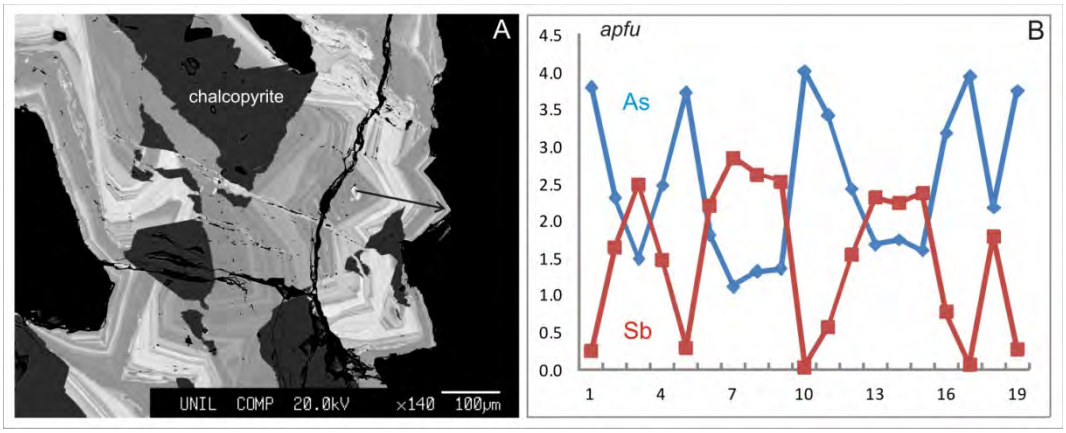

Fig. 1. *BSE image of Gradishte tennantite-tetrahedrite$_{ss}$ reveals typical oscillatory zoning (A), controlled by As and Sb fluctuation (B). Location of the profile is indicated on the BSE image.*

PETROGRAPHIC STUDY ON MAGNETITE CARBONATITE FROM JACUPIRANGA, BRASIL

VETLÉNYI, E.*, GUZMICS, T. & SZABÓ, Cs.
Lithosphere Fluid Research Lab, Department of Petrology and Geochemistry, Eötvös Loránd University, Pázmány Péter sétány 1/C, H-1117 Budapest, Hungary
* E-mail: eniko.vetlenyi@gmail.com

Carbonatite and associated silicate rocks occur in more than 520 localities in the Earth (WOOLEY & KJARSGAARD, 2008). One of significance of these igneous rocks is that they usually associated with mineral resources of rare earth + Y (REY) and some high field strength elements (e.g. Nb, Ta, Zr) (MORBIDELLI *et al*., 1995). Our main aim is to give a detailed petrographic observation on the magnetite carbonatite, collected in Jacupiranga (Brazil), in order to have solid base for further petrogenetic study.

Optical microscopy, scanning electron microscopy and Raman microanalyses were carried out on the studied samples. The rock shows cumulate texture and consists mainly of calcite, dolomite and Ba-zoned phlogopite with abundant inclusions. Accessories are strontianite, celestine, apatite, forsterite, barite, chlorite, baddeleyite, geikielite, pyrophanite, uranpyrochlore, carbocernaite, vigezzite, ancylite, Mg-Al-hydrocarbonate, sphalerite and galena. It is characteristic for the sample that inclusions are containing fluid bubble and solid phases like carbocernaite, Na-Ca-carbonate and REE carbonate.

The rock-forming carbonates occur as complex intergrowth of calcite-dolomite, strontianite-calcite and strontianite-dolomite. The latter one is rather characteristic in the magnetite-hosted dolomite inclusions. Two textural variations of calcite-dolomite intergrowth can be distinguished. One is seen as large (10–50 µm) exsolution lamellae of dolomite occurring according to crystal direction of calcite or vice verse (Fig. 1). The other can be observed small (1–5 µm) and randomly distributed dolomite patches appearing in calcite and vice versa. Strontianite crystals are randomly associated to these lamellae.

On the basis of known phase diagrams, the intergrowth texture of the different carbonates (calcite, dolomite and strontianite) may be resulted in a high-T (T > 700°C) subsolidus exsolution happened in an originally Sr- and Mg-bearing calcite. In a comparison with other studies, the rock seems to be crystallized from a carbonate melt that is richer in MgO than carbonate magma from other localities.

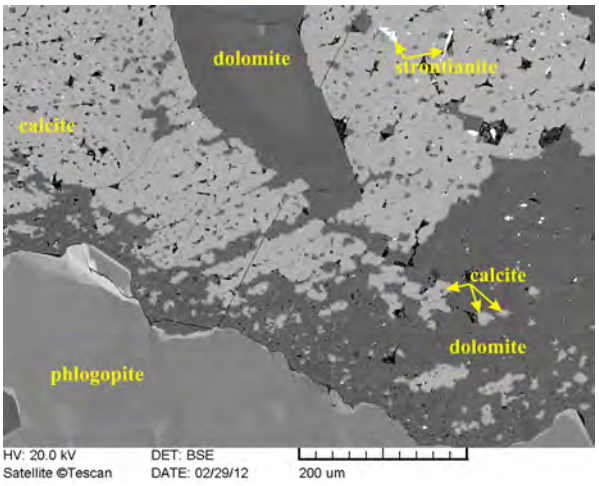

Fig. 1. *The picture shows exsolution lamellae of dolomite occurring according to crystal direction of calcite and vice versa.*

References

MORBIDELLI, L., GOMES, C.B., BECCALUVA, L., BROTZU, P., CONTE, A.M., RUBERTI, E. & TRAVERSA, G. (1995): Earth Science Reviews, 39: 135–168.

WOOLEY, A.R. & KJARSGAARD, B.A. (2008): Open file 5796, 1 CD-ROM, 1 map.

MINERALOGY AND K-Ar GEOCHRONOLOGY OF ILLITE-RICH FAULT GOUGES IN THE MÓRÁGY GRANITE, HUNGARY

VICZIÁN, I.[1]*, KÓNYA, P.[2], KOROKNAI, B.[2], KOVÁCS-PÁLFFY, P.[2], MAROS, Gy.[2], BALOGH, K.[3] & PÉCSKAY, Z.[3]
[1] Debrecen University, Egyetem tér 1, H-4032 Debrecen, Hungary
[2] Geological Institute of Hungary, Stefánia út 14, H-1143 Budapest, Hungary
[3] ATOMKI Institute of Nuclear Research, Bem tér 18/c, H-4026 Debrecen, Hungary
* E-mail: viczian@mafi.hu

The products of syntectonic fluid/rock interaction were studied in the Mórágy Granite, an Early Carboniferous pluton (~ 340 Ma) in the Variscan crystalline basement (Tisza unit) of the Pannonian basin. Following a Variscan regional metamorphism during cooling accompanied with the formation of a regional, NW-dipping foliation and localized ductile shear zones, the pluton suffered intense brittle deformation in several phases. In this granite body the final disposal of low and intermediate level radioactive waste is planned.

The analyzed clay gouge samples contain an illite + smectite + mixed-layer illite/smectite + chlorite + palygorskite + kaolinite + quartz + K-feldspar + plagioclase + calcite + dolomite assemblage with highly various ratios of the individual minerals. Clay minerals and chlorite are clearly newly formed phases formed at the expense of feldspars and mafic minerals of the original granitoid protolith. According to detailed XRD analyses, the polytypic variety of illite in clay gouges containing illite in considerable amount is almost exclusively 1*M*, suggesting the hydrothermal origin of illite. In some samples minor amounts (<10 %) of $1M_d$ and/or $2M_1$ polytypes also occur, whereas the former may represent the low-temperature alteration product of the 1*M* hydrothermal illite. The $2M_1$ polytype presumably display inherited component from primary magmatic biotite and/or metamorphic muscovite. The Kübler index values scatter mostly in the range of 0.51–0.61º 2θ for discrete illite structures and 0.73–1.02º 2θ for assemblages containing mixed-layer illite/smectites. Even broader basal reflections occur in smectite-rich assemblages.

K/Ar dating of illite-rich fine fractions (<10, <2, <1 μm) was carried out in the Institute of Nuclear Research (ATOMKI), Debrecen, Hungary. Strongly scattering Mesozoic ages were obtained (Middle/Late Triassic–Late Cretaceous) that are, however, in correlation with the degree of alteration of illite. Considering the absence of I/S and smectite, the oldest (Triassic–Early Jurassic) ages seem to represent indeed the time of important brittle tectonic activity accompanied with syntectonic fluid flow. Also the youngest (Late Cretaceous) age seems to indicate illite formation accompanied with a tectonic deformation. The Middle Jurassic and Early Cretaceous ages, however, are most probably mixed ages formed by low-temperature alteration of the hydrothermal illite-1*M* phase, if one regards the considerable amounts of illite/smectite and smectite in these samples.

The K-Ar ages obtained are compared with other age determinations and possible tectonic events in the territory of the Tisza tectonic unit and with the ages of illites in the Permian Boda Siltstone Formation in the vicinity of the granite body studied.

CHEMICAL COMPOSITION AND INCLUSION STUDY OF PRIMARY ACCESSORY PYRITE FROM GRANITOIDS OF THE WESTERN CARPATHIANS

VOJTKO, P.* & BROSKA, I.
Geological Institute, Slovak Academy of Sciences, Dúbravská cesta 9, 840 05 Bratislava, Slovakia
* E-mail: peter.vojtko@savba.sk

Pyrite is a common accessory mineral in West-Carpathian granites, but the I-type granite association is more typical indicating higher sulphur activity in primary melts. Several ppm of pyrite in I-type granites is typical, but sometimes the enrichment is to tens and locally hundreds to thousands ppm (g/t). Main elements, iron and sulphur show molar proportions close to ideal composition – 1 mol of iron and 2 mol of sulphur. The most important trace elements are Co, Ni and As. Their concentrations vary from a few ppm to several %, but Co dominates. Common content of Co in pyrites is around 0.4 wt% and Co and Ni substitute Fe because size of Co^{2+} and Ni^{2+} ions are similar to Fe^{2+}, and structure of NiS_2 and CoS_2 is identical to that of pyrite (VAUGHAN & CRAIG, 1978; TOSSELL *et al.*, 1981). Correlation between Co-Ni and As contents in pyrite are not explicitly discussed, although it was widely known that trace elements in pyrite increases with an increasing proportion of As (GRIFFIN *et al.*, 1991, HUSTON *et al.*, 1995). Correlation among Co/Ni between pyrite and bulk rock wasn't observed.

Character of inclusions in pyrite can be understood as a tracer of genesis and type of granite environment. The hydrothermal pyrite origin indicates presence of sulphosalt and sulphide inclusions, such as sphalerite and galena. Muscovite, K-feldspar, pure albite and apatite was characteristic in specialized S-type granites from Gemeric unit showing late-magmatic and hydrothermal conditions of origin. The rock-forming and accessory minerals typical for granite environment point to pyrite magmatic formation. The I-type granite types are indicated by inclusions of titanite and plagioclase with amount of An component up to 29.4%. The most complex mineral association with magnesiohornblende, plagioclase with increased amount of An component (31.75 up to 52.2%), epidote, titanite and chlorite show hybrid I-type granite genesis. On the other hand, also pyrite inclusions in zircons have been observed. Pyrite inclusions in zircons are locally with Fe-oxides rims. Intimate overgrowth of zircon and pyrite phase was identified in diorite rocks, whereas composition of pyrite inclusions was similar to those occurred in rock as accessory pyrite.

Remarkable is relationship between sulphates and sulphides in granitic rocks of Western Carpathians. Primary anhydrite ($CaSO_4$) is known as igneous from south Californian amphibole-biotite plutonic rocks associated with the regime of island arc (BARTH & DORAIS, 2000). In similar circumstances the primary anhydrite has been identified as inclusion in pyrite in granodiorite to tonalite from locality Dúbrava (Low Tatra Mts.) and in diorite body from Žiar Mts. as an inclusion in zircon. The primary anhydrite demonstrates a higher oxygen fugacity in early stage of granite evolution because the stability of anhydrite is above the NNO buffer. In granites Fe-Ti oxide breakdown process oscillated along NNO buffer, but usually is often significantly lower. Pyrite with anhydrite inclusion from Dúbrava probably has been originated from precipitation of iron halides and H_2S in magmatic stage.

References

BARTH, A.P. & DORAIS, M.J. (2000): American Mineralogist, 85: 430–435.

GRIFFIN, W.L., ASHLEY, P.M., RYAN, C.G., SOEY, H.S. & SUTER, G.F. (1991): Canadian Mineralogist, 29: 185–198.

HUSTON, D.L., SIE, S.H., SUTER, G.F., COOKE, D.R. & BOTH, R.A. (1995): Economic Geology, 90: 1167–1196.

TOSSELL, J.A., VAUGHAN, D.J. & BURDETT, J.K. (1981): Physics and Chemistry of Minerals, 7: 177–184.

VAUGHAN, D.J. & CRAIG, J.R. (1978): Mineral Chemistry of Metal Sulfides. Cambridge University Press, Cambridge.

SASA TAILINGS DAM CHARACTERIZATION (MACEDONIA)

VRHOVNIK, P.[1]*, ŠMUC, N.R.[1], DOLENEC, T.[1], DOLENEC, M.[1], SERAFIMOVSKI, T.[2], DANEU, N.[3], BUKOVEC, P.[4] & ZUPANČIČ, M.[4]

[1] Department of Chemistry and Biochemistry, Faculty of Natural Sciences and Engineering, University of Ljubljana, Aškerčeva cesta 5, SI-1000 Ljubljana, Slovenia

[2] Faculty of Mining, Geology and Polytechnics, University "Goce Delčev-Štip", Goce Delčev 89, 2000 Štip, Macedonia

[3] Department for Nanostructured Materials, "Jožef Stefan" Institute, Jamova 39, SI-1000 Ljubljana, Slovenia

[4] Department of Chemistry and Biochemistry, Faculty of Chemistry and Chemical Technology, University of Ljubljana, Aškerčeva cesta 5, SI-1000 Ljubljana, Slovenia

* E-mail: petra.vrhovnik@gmail.com, petra.vrhovnik@ntf.uni-lj.si

Purpose

This research is aimed to investigate the mineralogical characteristics and heavy metal contents as also their bioavailability in the Sasa tailings dam material, deposited close to the Sasa Pb-Zn mine in the Osogovo Mountains (eastern Macedonia).

Methods

Mineralogy of the surficial samples was determined at the Department of Geology, Ljubljana (Slovenia) by X-ray powder diffractometry using a Philips PW 3710 diffractometer and Cu*K*α radiation. Diffraction patterns were identified with the Powder Diffraction File (1977) JPDS system. Scanning electron microscopy (SEM) and energy-dispersive X-ray spectroscopy (EDS) were carried out on a Jeol JSM 5800 scanning electron microscope, equipped with a Si-Li detector (LINK ISIS 300, Oxford Instruments) at the Jožef Stefan Institute in Ljubljana, Slovenia. Geochemical analysis of the elements Mo, Cu, Pb, Zn, Ni, As, Cd, Sb, Bi, Ag, Al, Fe, Mn and S was obtained in a certified commercial laboratory in Canada (ACME Analytical Laboratories, Ltd.). 0.5 g of each sample was leached in hot (95ºC) Aqua Regia and analysed by ICP Mass Spectrometry, for evaluating the fractionation of metals (Co, Ni, Cr, Cu, As, Cd, Zn and Pb) in Sasa tailings dam material. For sequential extraction procedure, modified BCR scheme was used to evaluate the bioavailability of heavy metals in investigated waste material. During the procedure the metals were extracted into four fractions: acid soluble fraction (B1), reducible fraction (B2), oxidizable fraction (B3) and residual fraction (B4). To check the accuracy of the analytical procedure, the certified reference material BCR-701 was used.

Geology and environmental setting of the study area

The Sasa lead-zinc deposit lies within the Sasa-Toranica mining district in the Osogovo Mountains, eastern Macedonia. The geology of the Toranica-Sasa ore field comprises various rocks of both metamorphic and igneous origin, with the latter of Tertiary age. The most economically valuable mineralization is closely related to quartz-graphite schists, with the ore consisting mainly of galena, sphalerite, chalcopyrite and pyrite.

Results and discussion

According to XRD and SEM/EDS analyses the investigated material was dominated by the following minerals: quartz, calcite, mica, cordierite, epidote, clinochlore, sphalerite and clinopyroxene. Sample three (H-3) include pyrite and sample four (H-4) also contained magnetite, galena, hematite and chlorite. TASEV *et al*. (2005) classified the afore-mentioned minerals as belonging to the Sasa-Toranica zone. Sphalerite and galena, two of the most important minerals in the Sasa ore district, were not found at all in the samples as it was expected. One explanation for this may have been because samples were collected from the upper oxidation zone, where reduction minerals are absent. In addition, SERAFIMOVSKI *et al.* (2006) reported that in the Zletovo ore district, located near the Sasa mine, sphalerite is usually found only in a few generations and it is sometimes interstitially replaced by quartz, galena and other minerals. According to geochemical analyses the average contents of studied toxic metals in Sasa tailings dam material are as follows: Ag 20.49, As 111.3, Cd 151.93, Cu 928.12, Mo 3.04, Pb 6496.22, Sb 5.62, Bi 18.26, Zn 5121.89, Ni 31.2 and Co 24.97 mg/kg. Compared to average concentrations from Barroca Grande tailings dam (ÁVILA *et al.*, 2008), it can be seen that concentrations of almost all toxic metals are much higher in surficial material from Sasa tailings dam. Sequential extraction analysis revealed that Pb is the most mobile metal in Sasa tailings dam material since only 15% of total Pb is associated with residual fraction, while 50% of total Pb found in the acid soluble fraction. Ni, Cd and Zn showed far less mobility according to the first step of BCR scheme, with acid soluble concentration of less than 7%.

Conclusions

XRD and SEM-EDS analyses showed that detected mineral assemblage from Sasa tailing dam consists most of the minerals from the background rocks of the studied mining area. Results shown that due to high contents of metals and high mobility of metals, tailings dam material from Sasa mine represent a serious threat to the surrounding environment. Further research activities are urgent to find a potential remediation strategy to reduce the metal contents and their mobility in Sasa tailings dam.

References

ÁVILA, P.F., FERREIRA DA SILVA, E., SALGUEIRO, A.R. & FARINHA, J.A. (2008): Mine Water and the Environment, 27: 210–224.

SERAFIMOVSKI, T., DOLENEC, T. & TASEV, G. (2006): RMZ – Materials and Geoenvironment, 52(3): 535–548.

TASEV, G., SERAFIMOVSKI, T. & LAZAROV, P. (2005): Mineral Deposit Research: Meeting the Global Challenge, Session 7, 837–840.

CO_2-MINERAL SEQUESTRATION AND THE POTENTIAL FOR EXTRACTION OF ECONOMIC BY-PRODUCTS

WALDER, I.F.
Kjeøy Research & Education Center, Kjeøy, N-8412 Vestbygd, Norway
E-mail: ifwalder@kjeoy.no

There has been a lot of research development in recent years of different types of leaching techniques (acid leach, alkaline leaching, hydro-bio leaching, etc.). Most of this research has focused on leaching of sulphides and oxides for metal extraction. At the same time, there has been a lot of research taking place on CO_2-mineral sequestration, which has enhanced the understanding of mineral leaching in general. CO_2-mineral sequestration focuses on silicate minerals that release elements that can form (Ca, Mg, Fe) carbonate minerals for permanent CO_2-storage.

Silicate minerals show a very large range of reaction rates, where olivine is one of the most reactive silicate minerals. The reaction rate of olivine is quite high. However, a common obstacle is that secondary minerals form on the surface of the olivine and inhibit a continuation of the high reaction rate. To maintain a high reaction rate, therefore, high pressure and temperature is implied.

The release of CO_2 from combustion of fossil fuels and from industrial processes such as cement production, roasting of ores, and steel production has gained much interest in recent years due to the influence of CO_2 on the environment and effects such as global warming. Many of the sources of CO_2 such as emissions from power plants comprise only a few percent CO_2 and accordingly huge emissions volumes have to be managed to separate the CO_2 formed during combustion. Much focus has been on methods for CO_2 capture using liquid absorbents. These processes, so far, have had a high energy demand and have resulted in a CO_2 stream for which permanent storage or reuse has to be secured in a secondary process. However, the increasing focus on CO_2 emission as a tradable commodity opens opportunities for utilizing the emission gases for mineral leaching not only for CO_2-mineral sequestration, but also for element extraction.

The natural sequestration of atmospheric CO_2 in mine wastes has been studied with the focus to document the sequestration with respect to the total carbon dioxide impact of the mining process. The natural occurring passive reaction between atmospheric CO_2 and mine tailings may result in a reduction in the overall CO_2 impact of the mining (WILSON *et al*, 2009). Natural sequestration of CO_2 is facilitated by silicate mineral weathering and carbonate precipitation, taking place *in-situ* in soils and rocks e.g. caliche, and *ex-situ* in oceans in soils e.g. limestone formations.

Investigations have also been carried out involving the mechanical activation by milling of rocks to increase the available surface area and, thereby, obtaining increased reaction between gas containing CO_2 and solid minerals. However the reactions rates have still been too slow for application in an industrial process (HAUG, 2010).

Leading researchers in the field (O'CONNOR *et al.*, 2005; GERDEMANN *et al.*, 2007) concluded that ex-situ mineral carbonatisation is too expensive (high energy consumption) to be viable even though considerable mineral dissolution and carbonate precipitation was obtained within a few hours by using olivine in some of their experiments. Different types of pre-treatment (ligands, preheating, mechanical activation by milling etc) were tried in high temperature high-pressure reaction chambers (O'CONNOR *et al.*, 2005). GERDEMANN *et al.* (2007) further evaluated dissolution rate of finely ground olivine and serpentine in a supercritical CO_2–water solution in a high temperature and pressure vessel, and converted 81% of the olivine to magnesium carbonate in a few hours and 92% of preheated serpentine also to magnesium carbonate in one hour.

It is necessary, as described above, to dissolve (or alter with element release) minerals in order to achieve mineral CO_2 sequestration. When these mineral dissolve, there may be elements released that can form economically valuable products, e.g. calcite ($CaCO_3$), magnesite ($MgCO_3$), silica (SiO_2), and nickel. Different rock types will have different leaching potentials depending upon both the reaction rate of the minerals and the mineral chemistry. Carbon dioxide is then used to precipitate carbonate minerals with the elements released (Ca, Mg, Fe).

Olivine rich rocks (dunite) may be iron or magnesium rich with little or no calcium, but with potentially high concentrations of nickel. Pyroxene and amphibole rich rocks have lower reaction rates than olivine, but may have relatively high calcium content in addition to iron and magnesium. Anorthite rich rocks (anorthosite) have high calcium and aluminium content but little or no magnesium and iron.

Carbonic acid has been shown to be effective for long-term leaching for actinolite and carbonate minerals (WALDER, 2011; WALDER & LUNDKVIST, *in prep*; TANGWA *et al.*, 2011). Further research is necessary for developing economically viable methods or processes for using CO_2 as a leaching agent at atmospheric conditions.

References

GERDEMANN, S.J., O'CONNOR, W.K., DAHLIN, D.C., PENNER, L.R. & RUSH, H. (2007): Environmental Science & Technology, 41: 2587–2593.

HAUG, T.A. (2010): Dissolution and carbonation of mechanically activated olivine. Investigating CO_2 sequestration possibilities. PhD thesis, NTNU.

O'CONNOR, W.K., DAHLIN, D.C., RUSH, G.E., GERDEMANN, S.J., PENNER, L.R. & NILSEN, D.N. (2005): Aqueous mineral carbonation – Mineral availability, pre-treatment, Reaction parametric, and process studies. Final report. DOE/ARC-TR-04-002, Albany Research Center, US-DOE.

TANGWA, E.K., WALDER, I.F. & LUNDKVIST, A. (2011): Mineral CO_2 sequestration in mine waste rocks, column experiments. Abstract for Goldschmidt, Conference, Prague, Czech Republic, August 2011.

WALDER, I.F. (2011): CO_2 mineral leaching, Patent pending, No. 20110872.

WALDER, I.F. & LUNDKVIST, A. (in prep): CO_2-mineral sequestration using coarse crushed rocks from the extractive industry.

EXPERIMENTAL INVESTIGATION OF TITANIUM STABILITY IN NATURAL SAGENITIC PHLOGOPITES FROM FENNOSCANDIAN LAMPROPHYRES

WOODARD, J.[1]*, SJÖBLOM, S.[2], FRÖJDÖ, S.[2] & SELBEKK, R.[3]
[1] Department of Geography and Geology, University of Turku, FI-20014 Turku, Finland
[2] Department of Geology and Mineralogy, Åbo Akademi University, Domkyrkotorget 1, FI-20500 Turku, Finland
[3] Natural History Museum, University of Oslo, Sars Gate 1, N-0562 Oslo, Norway
* E-mail: jdwood@utu.fi

Shoshonitic (calc-alkaline) lamprophyres are mafic lamprophyres containing feldspar as a matrix phase, which typically occur in late- to post-orogenic tectonic settings. Precise knowledge of the pressures of both magma generation and dyke emplacement can be of great benefit for developing models of orogenic evolution. However in cases where mantle and lower crustal xenoliths are lacking, options for determining source pressures and temperatures are severely limited. Several shoshonitic lamprophyre dyke swarms are found in the margin between the Palaeoproterozoic Svecofennian Domain and the Archaean Karelia Craton. The dykes intrude large-scale normal fault structures within a NW-SE trending palaeosuture at ca. 1790 Ma, indicative of a change from a compressional to an extensional tectonic regime (WOODARD, 2010). These dykes contain abundant Ba- and Ti-rich mica, both as a phenocrystic and matrix phase. Mica (biotite or phlogopite) phenocrysts occur as castellated grains, with a core-to-rim increase in Mg# and ubiquitous sagenitic texture. Sagenitic texture refers to the occurrence of needle-like inclusions of rutile or titanite, in this case exclusively titanite, occurring parallel to (001) of the host biotite in preferred crystallographic orientation (e.g., SHAU *et al.*, 1991). Using the phlogopite-melt Ti- and Ba-partitioning thermobarometer (RIGHTER & CARMICHAEL, 1996), matrix phlogopite indicate crystallisation at 1000–1150ºC and 0.2–0.3 GPa, corresponding to emplacement at 7–10 km depth (WOODARD & BOETTCHER, 2010). This is in good agreement with previous depth estimates from this area (NIIRANEN, 2000). Thermobarometry from the phenocrysts imply PT conditions as high as 1200ºC and 6.2 GPa, well beyond the calibration range of the method, albeit in a linear trend (WOODARD & BOETTCHER, 2010).

Many studies have shown that Ti solubility in phlogopite increases with temperature (e.g., ROBERT, 1976; ARIMA & EDGAR, 1981; ESPERANCA & HOLLOWAY, 1987), implying that sagenitic texture could form as a result of exsolution of the Ti-rich phase at lower temperatures. However, some experiments have shown a decrease in Ti solubility with temperature, which is most likely a result of complex substitutions coupled with other trace elements, most notably Ba (e.g., GUO & GREEN, 1990; RIGHTER & CARMICHAEL, 1996). Ba solubility in phlogopite decreases with pressure but increases with both temperature and coupled Ti substitution (GUO & GREEN, 1990). In order to form sagenitic titanite by exsolution, the picture is further complicated by the stability Ca in phlogopite. Experimental studies have shown that like Ti, Ca solubility in phlogopite increases with temperature (OLESCH, 1979). Ca-rich phlogopite associated with orthopyroxene was interpreted as a prograde phase in ultrahigh pressure rocks (LI *et al.*, 2011), implying that Ca solubility may also increase with pressure.

For this study, we selected natural sagenitic mica phenocrysts from Fennoscandian shoshonitic lamprophyres for experiments in an attempt to reverse the exsolution process. Experiments were conducted in a piston cylinder apparatus over a range of temperatures (800–1100 ºC), pressures (1–2.5 GPa) and time (30–160 h) at Natural History Museum, Oslo. Preliminary results indicate that at the highest temperatures, titanite inclusions only became larger and more rounded. Across the whole temperature range at low pressure, breakdown of titanite resulted in crystallisation of perovskite at grain boundaries. Finally, at the highest pressures and moderate to low temperatures, titanite inclusions decreased in size or disappeared altogether with no evidence of formation of new Ti- or Ca-bearing phases. While additional experiments are needed over a greater range of pressures, the successful reversal of the exsolution process implies that these phenocrysts crystallised at high pressures and moderate temperatures.

References

ARIMA, M. & EDGAR, A.D. (1981): Contributions to Mineralogy and Petrology, 77: 288–295.
ESPERANCA, S., & HOLLOWAY, J.R. (1987): Contributions to Mineralogy and Petrology, 95: 206–216
GUO, J. & GREEN, T.H. (1990): Lithos, 24: 83–95.
LI, X.P., YANG, J.-S., ROBINSON, P., XU, Z.-Q. & LI, T.-F. (2011): Journal of Asian Earth Sciences, 42: 661–683.
NIIRANEN, T. (2000): Master's Thesis, University of Turku, Turku, Finland.
OLESCH, M. (1979): Bulletin de Minéralogie, 102: 14–20.
RIGHTER, K. & CARMICHAEL, I.S.E. (1996): Contributions to Mineralogy and Petrology, 123: 1–21.
ROBERT, J.L. (1976): Chemical Geology, 17: 213–227
SHAU, Y.H., YANG, H.Y. & PEACOR, D.R. (1991): American Mineralogist, 76: 1205–1217.
WOODARD, J. (2010): Ph.D. Thesis, University of Turku, Turku, Finland.
WOODARD, J. & BOETTCHER, I. (2010): Mineralogia – Special Papers, 37: 65–66.

INTEGRATED URBAN GEOCHEMICAL STUDY IN AJKA, HUNGARY

ZACHÁRY, D.[1]*, VÖLGYESI, P.[1], JORDÁN, Gy.[2] & SZABÓ, Cs.[1]
[1] Lithosphere Fluid Research Lab, Department of Petrology and Geochemistry, Eötvös Loránd University, Pázmány Péter sétány 1/C, H-1117, Budapest, Hungary
[2] Environmental Geology Department, Geological Institute of Hungary, Stefánia út 14, H-1143, Budapest, Hungary
* E-mail: zachary.dora@gmail.com

Urban environment may concentrate contaminants in large quantities deriving from industry, traffic, fertilizers, tailings and wastes. In Hungary, during the 20th century, industrial activity (e.g., mining, alumina industry, coal fired power plants) produced huge amount of by-products and pollutants. Both of these contaminants can be enriched in toxic metals and radioactive isotopes as a result of the treatment technology. Consequences could be toxic element and radionuclide enrichment in urban public and private areas such as soil of playgrounds and parks or dust in dwellings. In addition, technological by-products (particularly coal slag) were often used in construction technologies as building and insulation materials on their own or as additives to building materials.

The major objective of this research was to study and map the spatial distribution of toxic element (As, Hg, Pb, Cu, Zn, Cd, Ni) contamination of urban soil and airborne attic dust and to measure the radionuclide (^{226}Ra, ^{232}Th and ^{40}K) concentrations of urban soil and coal slag samples.

In order to figure out a link between contamination sources and the receiving urban areas, 46 soil samples were collected at 44 locations, 30 attic dust samples at 27 houses and 6 coal slag samples at 6 houses from the old-established industrial city, Ajka in western Hungary. Ajka has multiple contamination sources of glass industry, as well as heavy alumina industry and coal-based power plants supplied by the nearby bauxite and coal mines, respectively. The project area covers an 8x8 grid of 1 x 1 km cells with a total area of 64 km^2. The soil samples have been collected at a depth of 0–10 cm at public areas (mostly playgrounds and parks). Attic dust was sampled in houses with attics kept undisturbed for at least 30–40 years in order to represent long-term industrial pollution. The gamma dose rate was measured on the sampling sites with FH 40G L10 detector at the surface and at 1m height. The laboratory analyses include grain size distribution and ICP-OES measurements for soil and attic dust samples, whereas HPGe gamma-spectroscopy was used for soil and coal slag samples.

Results show spatial correlation of environmental contamination and the contamination sources. The applied integrated urban geochemical method is efficient to study the impact of contamination and it may help with revealing the possibly associated human health risk in an industrial area.

BOZEŞ SEDIMENTARY UNIT (APUSENI MTS., ROMANIA) – GEOCHEMICAL CONSTRAINTS ON PROVENANCE AND TECTONIC SETTING

ZAHARIA, L.[1]*, SOCACIU, A.[1] & BĂLC, R.[2]
[1] Department of Geology, Babeş-Bolyai University, Kogălniceanu Street 1, Cluj-Napoca, Romania
[2] Department of Environmental Science, Babeş-Bolyai University, Fântânele Street 30, Cluj-Napoca, Romania
* E-mail: luminita.zaharia@ubbcluj.ro

The Upper Cretaceous Bozeş Formation is a sedimentary unit located in the south-eastern part of the Apuseni Mts. Lithologically it consists of rhythmically alternating clays and sandstones, deposited in a turbiditic facies, with an overall thickness of 3000 m (GHIŢULESCU & SOCOLESCU, 1941). Based on macro- and microfauna, its age was defined as Santonian–Campanian (BĂLC *et al.*, 2012 and the references therein).

Sixteen samples of various sandstones were collected and analyzed for whole-rock geochemistry in order to investigate the source area of weathering, sorting effects and to constrain the provenance and tectonic setting.

The chemical compositions are similar for all investigated samples, with limited ranges for both, major oxides and trace and RE elements. The sandstones are potassic ($Na_2O/K_2O < 1$) and can be classified as arenites and greywacke. The SiO_2/Al_2O_3 ratios, ranging between 2.63 and 11.24, as well as the high values of Sr/Rb indicate a high immaturity of the samples. Lack of hydraulic sorting during transportation is supported by the constant REE and Th contents (which usually vary according to the preferential accumulation of heavy minerals). The chemical index of alteration (CIA) (NESBITT & YOUNG, 1982) has values between 56 and 81, pointing out a weak to medium chemical weathering/alteration of the source rocks, the process including only feldspar transformation.

A dominant intermediate igneous provenance is constrained based on the major oxides petrology, but with a consistent contribution from a quartzose sedimentary source. Trace elements (La, Th and Hf) indicate an acidic arc as source for Bozeş sediments.

On various tectonic discrimination diagrams based on trace and RE elements, developed by BHATIA & CROOK (1986), Bozeş sediments are grouped within the continental arc source (Fig. 1), showing that their deposition took place on a convergent margin in a continental volcanic arc setting. Thus, Bozeş unit was originally a sedimentary basin located in an environment of a volcanic arc developed over thin continental crust (as inter-arc, back-arc or fore-arc).

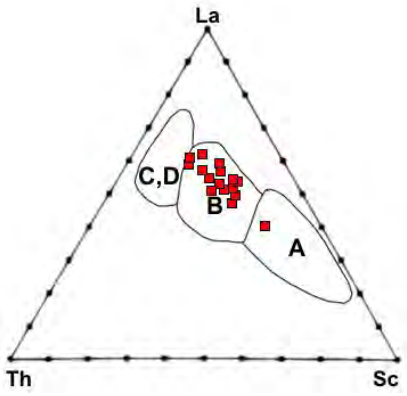

Fig. 1. *Tectonic setting discrimination diagram for the Bozeş sediments based on trace elements (A – oceanic island arc; B – continental island arc; C – active continental margin; D – passive margin) (after BHATIA & CROOK, 1986).*

Acknowledgements. This study was financially supported by the project PN II-RU_TE_ 313/2010 (CNCSIS-UEFISCSU, Romanian Ministry of Education and Research).

References

BĂLC, R., SILYE, L. & ZAHARIA, L. (2012): Studia Universitatis Babeş-Bolyai, Geologia, 57(1): 23–32.
BHATIA, M.R. & CROOK, K.A. (1986): Contributions to Mineralogy and Petrology, 92: 81–193.
GHIŢULESCU, T.P. & SOCOLESCU, M. (1941): Anuarul Institutului Geologic, 21: 181–463.
NESBITT, H.W. & YOUNG, G.M. (1982): Nature, 299: 715–717.

PRIMARY *VERSUS* METASOMATIC TOURMALINE FROM ELBAITE-SUBTYPE PEGMATITE IN PIKÁREC NEAR KŘIŽANOV, CZECH REPUBLIC

ZAHRADNÍČEK, L.[1]*, NOVÁK, M.[2] & GADAS, P.[2]
[1] Department of Mineralogy and Petrology, National Museum, Cirkusová 1740, 193 00 Prague, Czech Republic
[2] Department of Geological Sciences, Masaryk University, Kotlářská 2, 611 37, Brno, Czech Republic
* E-mail: lukas_zahradnicek@nm.cz

High compositional variability of tourmaline in the individual textural-paragenetic units of granitic pegmatites makes tourmaline excellent and widely used indicator of geochemical evolution from magmatic to hydrothermal stage and of external contamination of pegmatite melt as well. However, discerning of primary tourmalines and metasomatic ones are ignored in most cases. The elbaite-subtype pegmatite Pikárec is located in the easternmost part of the Moldanubian region, western Moravia, Czech Republic. Symmetrically zoned dike, ~ 3 m thick, is enclosed in amphibolite and consists of thin (i) coarse-grained outer granitic unit (Plg + Kfs + Qtz + Bt), volumetrically dominant (ii) graphic unit (Kfs + Qtz > Ab + Qtz) evolving to (iii) albite unit with blocky K-feldspar (Ab + Kfs + Qtz) and locally with (iv) small pockets. Tourmaline is a typical minor mineral evolving from the assemblage annite + schorl in outer parts of graphic unit through black schorl-foitite to Mn-rich foitite rimmed by pink elbaite in the inner part of graphic unit (Fig. 1a,b). Crystals of red, pink and green Mn-rich elbaite-rossmanite occur in pockets. Rare to common accessory minerals include fluorapatite, löllingite, spessartine, beryl, cassiterite, columbite, microlite, muscovite, polylithionite and pollucite. Alteration of early tourmaline (+ feldspars) by metasomatic tourmaline (Fig. 1a,b) is a typical feature of most tourmaline grains and crystals except those from pockets.

The reaction rims are always developed on the contact with plagioclase, albite or K-feldspar; no changes were found on the contact with quartz (Fig. 1a; left upper part). They originated in part instead of early tourmaline and in part instead of surrounding feldspars. These replacement processes may be expressed by the simplified reactions: Fig. 1a – Mg-schorl → schorl – (1) $Mg \rightarrow Fe^{2+}$; anorthite component in plagioclase → liddicoatite – (2) $7An + 2Li_2O + 3B_2O_3 + H_2O \rightarrow 2$ liddicoatite $+ 5CaO + 2SiO_2$; Fig. 1b – Na-rich Mn-foitite → X-site vacant, F-enriched elbaite – (3) foitite + $Na_2O + Li_2O + Al_2O_3 + F \rightarrow$ elbaite + H_2O + 2FeO; elbaite → elbaite (slightly Ca,F-enriched). Stoichiometry of the reactions is quite complicated; hence, some reactions are only approximate. Nevertheless, the reactions evidently require fluids rich in Li_2O, B_2O_3, F, and H_2O, what we can expect in early subsolidus stage at such complex (Li) pegmatite. The plot on Fig. 1c shows enrichment of metasomatic tourmaline by F relative to its primary precursors. In addition, slight to strong enrichment in Ca of metasomatic tourmaline is typical. Consequently, slight to moderate Ca,F-enrichment in late tourmaline may be an indication of its metasomatic origin in complex granitic pegmatites.

Acknowledgements. This work was supported by internal grant of National museum, Prague 2011/05/IG-PM to LZ and research project GAČR P210/10/0743 to MN and PG.

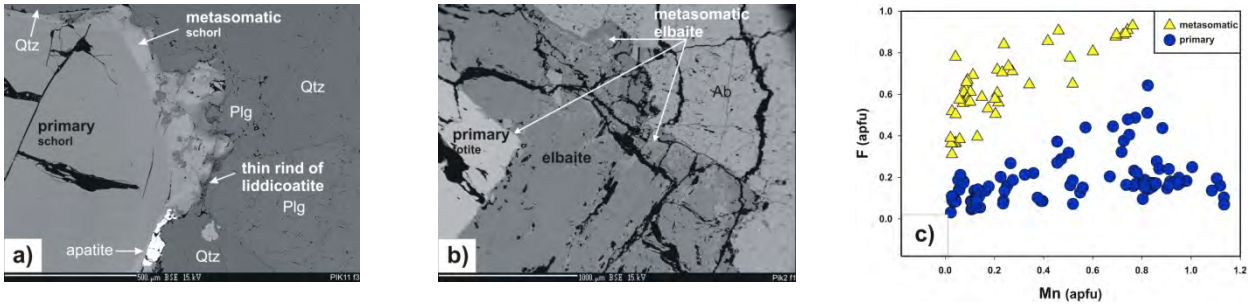

Fig. 1. *Textural relations (a, b) and F/Mn plot (c) of primary and metasomatic tourmalines. Replacement of early tourmaline + feldspars and surrounding feldspars by metasomatic tourmaline: a) outer part of graphic unit with plagioclase An_{15}; b) inner part of graphic unit with albite $An_{01–00}$.*

DETAILED CLAY MINERALOGY OF THE TRIASSIC-JURASSIC BOUNDARY IN THE EIBERG BASIN, AUSTRIA AT TWO LOCATIONS (KENDLBACHGRABEN AND THE GSSP AT KUJOCH)

ZAJZON, N.[1]*, KRISTÁLY, F.[1], PÁLFY, J.[2] & NÉMETH, T.[3]
[1] Institute of Mineralogy and Geology, University of Miskolc, H-3515 Miskolc-Egyetemváros, Hungary
[2] Department of Physical and Applied Geology, Eötvös Loránd University, Pázmány Péter sétány 1/C, H-1117 Budapest, Hungary and Research Group for Paleontology, Hungarian Academy of Sciences–Hungarian Natural History Museum–Eötvös University, Budapest, Hungary
[3] Institute for Geochemical Research, Hungarian Academy of Sciences and Department of Mineralogy, Eötvös Loránd University, Budapest, Hungary
* E-mail: nzajzon@uni-miskolc.hu

To help constrain scenarios for the Triassic-Jurassic boundary events, we obtained a temporally highly resolved, multidisciplinary dataset from the Kendlbachgraben section in the Northern Calcareous Alps in Austria, and also investigated a few samples from the same stratigraphic position from the newly selected base Jurassic GSSP (Global Stratotype Section and Point) at Kuhjoch. Both sections belong to the same paleogeographic unit (Eiberg Basin) and share similar stratigraphies. Here we present our observations on clay mineral.

Samples from the Kendlbachgraben section were investigated for detailed clay mineral determination (ZAJZON *et al*., 2012). Swelling and heating experiments and cation exchange (Mg and K) were carried out on oriented samples. Observed clay minerals are ~15 Å smectite (Mg > Fe), together with vermiculite (K-bearing) and chlorite (Fe > Mg) (14.2–14.5 Å), illite and kaolinite. The identified "14 Å type" minerals are Mg-dominant, with varying Fe, K and Ca content. Chlorite is evident only after heating the samples to 560°C and diminishes upwards in the section. Kaolinite is dominant in the boundary marl, and shows a decrease in quantity and degree of crystallinity upwards in the section. Cation exchange and glycerol saturation indicates the mixing of high and low layer charge smectites with the dominance of the high-charge type. Vermiculite is of the low layer charge, expanding type.

The topmost sample of the Triassic Kössen Formation has a very different clay mineral content compared to the other samples. It contains dominantly high-charged smectite and also vermiculite. These clay minerals may be formed by the alteration of mafic and ultramafic rocks. Upwards in the section smectites has a Ca–Na enrichment and vermiculite (chlorite) becomes dominant. In the boundary shale the clay mineral distribution is the following: kaolinite≥ illite + muscovite >> smectite. This suggests weathering under humid climate, and intensive terrigenous input. Above the boundary interval the clay mineral pattern changes to illite + muscovite >> kaolinite >> smectite, which corresponds to a less humid, mainly moderate climate.

Some pale-green, opaque or slightly transparent grains, 70–80 µm in size, are found in the topmost layer of the Triassic Kössen Formation. Their shapes vary from the perfectly spherical (Fig. 1) to the angular. They are identified as illite/aluminoceladonite, their average EDX composition is $K_{0.49}Na_{0.08}Ca_{0.07}Mg_{0.65}Fe^{2+}_{0.07}Al_1 Fe^{3+}_{0.41}[Al_{0.4}Si_{3.6}O_{10}(OH)_2]$. They presumably represent alteration products of volcanic material, on the basis of their shape and size. Most probably the rounded grains were altered from volcanic glass material.

Similar features can be observed also at Kujoch, the GSSP section. The mineral and clay mineral spectra are similar to the Kendlbachgraben section. The kaolinite content gradually increases in the basal part of the boundary shale ("Grenzmergel"). Similar pale-green spherules with the similar shape and size also can be found in this section in the same horizon (bottom of the boundary shale). The clay mineralogical features correlate well between the two sections, thus the observed features have at least regional extent throughout the Eiberg basin, but they likely represent global changes at the Triassic-Jurassic boundary interval.

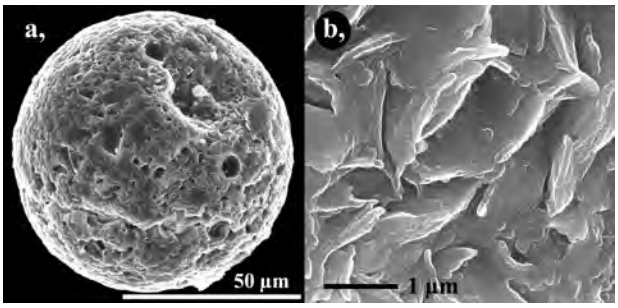

Fig. 1. *a: SE image of a pale-green clay spherule; b: enlarged surface of the same spherule.*

Reference

ZAJZON, N. *et al.* (2012): Clay Minerals, 47: in press.

KRUPKAITE FROM AVRAM IANCU MINE, BĂIȚA (BIHOR) METALLOGENIC DISTRICT, ROMANIA

ZAJZON, N.[1]*, SZENTPÉTERI, K.[2], FEHÉR, B.[3], SZAKÁLL, S.[1] & KRISTÁLY, F.[1]
[1] Institute of Mineralogy and Geology, University of Miskolc, H-3515 Miskolc-Egyetemváros, Hungary
[2] MINART Mineral Exploration Ltd., Húr str. 5, H-1227 Budapest, Hungary
[3] Department of Mineralogy, Herman Ottó Museum, Kossuth u. 13, H-3525 Miskolc, Hungary
* E-mail: nzajzon@uni-miskolc.hu

Ore samples were collected on the dumps of the Avram Iancu mine, Bihor Mts., Romania, before the recultivation. It is a five-element mineralization with uranium, sulphide and arsenide mineral paragenesis. Krupkaite ($PbCuBi_3S_6$) occurs abundantly as disseminated 20–100 μm sized inclusions in cobaltite (Fig. 1). It is always associated with the Co-Ni-Fe-Bi-U assemblage, which is characteristic host for this sulphosalt (MOËLO *et al*., 2008, MUMME, 1975).

In reflected light microscope, krupkaite is greyish white, has moderate reflectance 43% and strong bireflectance (39.1–47.0% at 560 nm). Under crossed polars anisotropy is strong but uncoloured, grey to dark grey. It is softer (4) than enclosing cobaltite (5.5) therefore grains have lower relief and observable Kalb line.

Only krupkaite was found among sulphosalts. Its WDX composition is the same from grain to grain (wt%): S 17.19, Cu 5.67, Pb 19.26, Bi 57.51, Se 0.61 (EDX), sum. 100.24. The calculated empirical formula is $Pb_{1.03}Cu_{0.98}Bi_{3.04}S_{5.91}Se_{0.09}$. It is very homogenous, zonation is not visible, and no other sulphosalts are associated. Gandolfi X-ray diffraction from the same area (Fig. 1) also supports identifying the sulphosalt as krupkaite. The reflections of the krupkaite on the X-ray film are: 4.013 Å, 3.643 Å, 3.540 Å, 3.139 Å, 2.652 Å, 2.562 Å and 2.79 Å and 1.976Å overlap with cobaltite (all the strong reflections are identified). The mineral is rarely associated with minute (5–10 μm in size) native bismuth blebs in cobaltite.

Krupkaite is reported from a number of epithermal deposits in the Carpathians: Baia Borşa (Maramureş, E-Carpathians) (COOK, 1997) and Larga hydrothermal system, Metaliferi Mts. (COOK & CIOBANU, 2004) as well as from other intrusive-related deposits in Europe: Karkonosze granite (GOLEBIOWSKA *et al*., 2006) and Loch Shin monzogranite (LOWRY *et al*., 1994). Based on the above mentioned mineral deposits, krupkaite usually forms at high to moderate temperature, i.e. 400–270°C range.

References

COOK, N.J. (1997): Mineralogical Magazine, 61: 387–409.

COOK, N.J. & CIOBANU, C.L. (2004): Mineralogical Magazine, 68: 301–321.

GOLEBIOWSKA, B., PIECZKA, A. & PARAFINIUK, J. (2006): Mineralogia Polonica, Special Papers, 28: 78–80.

LOWRY, D., STEPHENS, W.E., HERD, D.A. & STANLEY, C.J. (1994): Mineralogical Magazine, 58: 39–47.

MOËLO, Y., MAKOVICKY, E., MOZGOVA, N.N., JAMBOR, J.L., COOK, N., PRING, A., PAAR, W., NICKEL, E.H., GRAESER, S., KARUP-MØLLER, S., BALIC-ŽUNIC, T., MUMME, W.G., VURRO, F., TOPA, D., BINDI, L., BENTE, K. & SHIMIZU, M. (2008): European Journal of Mineralogy, 20: 7–46.

MUMME, W.G. (1975): American Mineralogist, 60: 300–308.

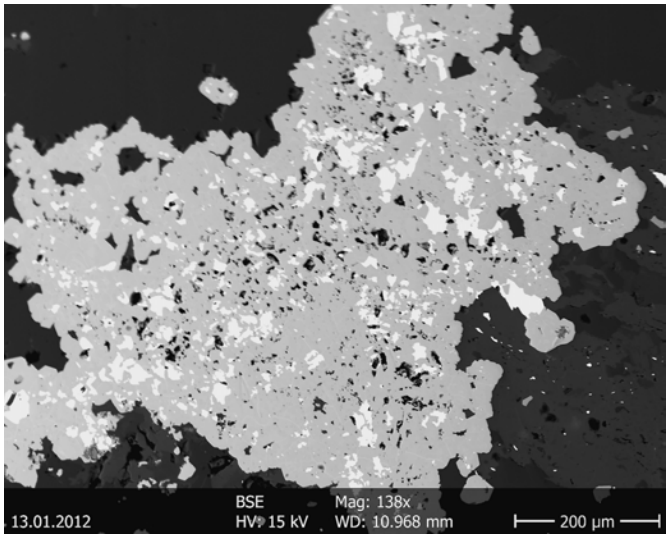

Fig. 1. *Krupkaite (white) in cobaltite (light grey), with silicate and carbonate minerals (BSE image).*

NEW DATA ON Cu-AMALGAMS, KOLYMITE AND BELENDORFFITE FROM RUDABÁNYA, HUNGARY

ZAJZON, N.[1]*, SZENTPÉTERI, K.[2], FEHÉR, B.[3], SZAKÁLL, S.[1], KUPI, L.[1] & BARKÓCZY, P.[4]
[1] Institute of Mineralogy and Geology, University of Miskolc, H-3515 Miskolc-Egyetemváros, Hungary
[2] MINART Mineral Exploration Ltd., Húr str. 5, H-1227 Budapest, Hungary
[3] Department of Mineralogy, Herman Ottó Museum, Kossuth u. 13, H-3525 Miskolc, Hungary
[4] Dept. of Physical Metallurgy and Metalforming, University of Miskolc, H-3515 Miskolc-Egyetemváros, Hungary
* E-mail: nzajzon@uni-miskolc.hu

Copper amalgam is known for a while, which was described according to chemical composition and optical characteristic as kolymite at Rudabánya, Hungary (SZAKÁLL, 2001). Cu-amalgams can be found as 20–200 µm anhedral inclusions in native copper, or cuprite. Grains are isotropic, highly reflective, 74.27% at 560 nm, and have tin white color. The amalgams are harder than enclosing native copper and have a positive flat relief. They are brittle and weakly fractured. New investigations of Cu-amalgam suggested the presence of belendorffite, instead of kolymite on the basis of different X-ray powder diffraction line intensities and line splitting (KUPI *et al.*, 2010). Chemistry is not relevant as both minerals having the Cu_7Hg_6 composition.

Optical spectroscopic measurements were performed on new polished sections. It could identify the phase as kolymite because the belendorffite has higher reflectance at low wavelengths (below 500 nm) than kolymite (Fig. 1). The measured spectrum is (wavelength in nm/reflectance %): 400/55.50; 420/59.94; 440/62.72; 460/56.76; 480/68.21; 500/70.20; 520/71.70; 540/72.82; 560/74.27; 580/75.34; 600/76.42; 620/76.72; 640/77.02; 660/77.46; 680/78.59; 700/78.55. Our spectrum is slightly elevated compared to the literature (MARKOVA *et al.*, 1980) which could be the result of the minor silver content in our samples. WDX composition of the same samples is Cu 26.21, Ag 0.31, Hg 73.10 with a total of 99.83 wt%. This corresponds to the formula of $Cu_{6.87}Ag_{0.05}Hg_{6.08}$. It has a Vickers hardness of 340 ± 8 (3–5 g load). XRD Gandolfi-camera pictures from the same crystals do not show diffraction line splitting, which is characteristic for belendorffite, as it showed at the previously studied material (KUPI *et al.*, 2010). On the basis of our data, we prove that both kolymite and belendorffite exist at Rudabánya.

References

BERNHARDT, H.J. & SCHMETZER, K. (1992): Neues Jahrbuch für Mineralogie – Monatshefte: 21–28.

KUPI, L., SZAKÁLL, S., ZAJZON, N., KRISTÁLY, F. & FEHÉR, B. (2010): Acta Mineralogica-Petrographica, Abstract Series, 6: 430.

MARKOVA, E.A., CHERNITSOVA, N.M., BORODAEV, Y.S., DUBAKINA, L.S. & YUSHKO-ZAKHAROVA, O.E. (1980): Zapiski Vsesoyuznogo Mineralogicheskogo Obshchestva, 109: 206–211.

SZAKÁLL, S. (2001): Rudabánya ásványai [Minerals of Rudabánya]. Kőország Kiadó, Budapest (in Hungarian).

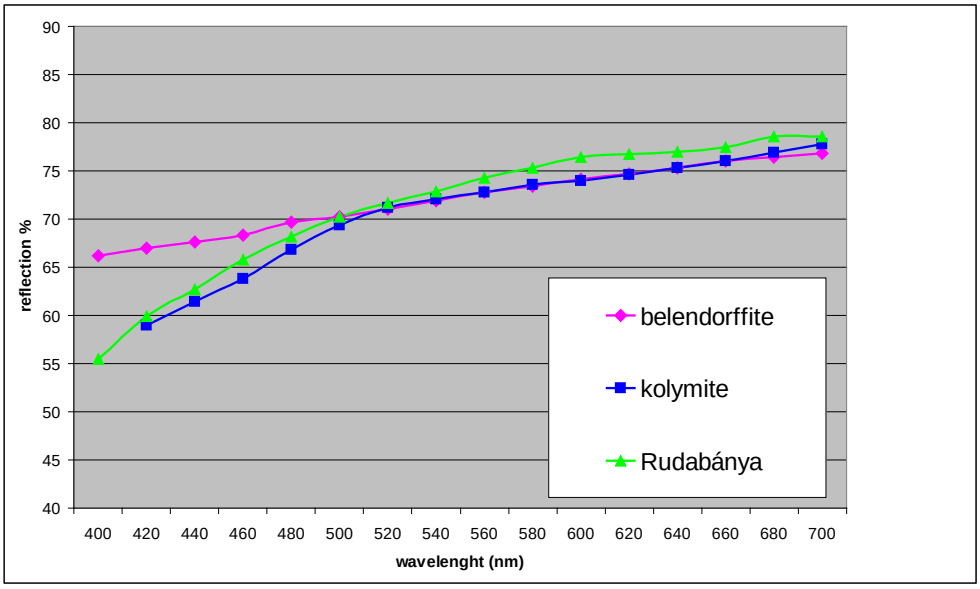

Fig. 1. *Optical spectra of kolymite from Rudabánya, compared to reference data of belendorffite (BERNHARDT & SCHMETZER, 1992) and kolymite (MARKOVA et al., 1980).*

SYNTHESIS OF Fe-SULPHIDES BY CHEMICAL VAPOUR TRANSPORT METHOD

ZAVAŠNIK, J.*, ŠOBAK, M., PODLOGAR, M. & REČNIK, A.
Department for Nanostructured Materials, Jožef Stefan Institute, Jamova cesta 39, SI-1000 Ljubljana, Slovenia
* E-mail: janez.zavasnik@ijs.si

In natural pyrite, a small amount of copper was shown to induce twinning (DANEU *et al.*, 2005). In order to verify this hypothesis we prepared iron sulphides by chemical vapour transport (CVT) method using halides as transporting agents (BUTLER & BOUCHARD, 1971). Equimolar parts of $FeCl_2$, and $FeBr_3$ precursors and small amount of $CuCl_2$ were heated to 600°C in an evacuated quartz tube in a horizontal single-zone furnace. Vapour phase migrated through a sulphur trap within a temperature gradient from 600 to 550°C for 72 hours. Nucleation of iron sulphides occurred in two temperature zones. As soon as the temperature reaches 600°C, iron immediately reacts with sulphur in the main temperature zone to form up to 3 mm large simple hexagonal plate-like crystals of pyrrhotite. During this reaction some of the iron halides are transported to the lower temperature zone at 550°C where they react with sulphur to produce pyrite and pyrrhotite, both nucleating from the vapour phase. Pyrite crystals in this second zone have a cubo-octahedral morphology with a porous core and an unusual homoepitaxial overgrowth on cubic and octahedral faces. In addition to pyrite, secondary crystallization of pyrrhotite in form of star-like twins is observed. A six-fold symmetry of twins suggests either an interpenetration twinning in basal {001} planes or 120° rotational twinning with the [001] twin axis and {110} prism planes as twin contact planes. EDS analysis of pyrrhotite, normalised to pyrite composition, indicates a slightly substoichiometric composition of Fe:S = 47:53, which suggests that pyrrhotite formed after pyrite as a result of sulphur deficiency. Corresponding electron diffraction pattern indicates that pyrrhotite is incommensurable. TEM study of twinned pyrrhotite revealed alternation of *ccp* and *hcp* sequences, coherently intergrown on a unit-cell scale (PÓSFAI & BUSECK 1997); *ccp* sequences are prevailing in the structure and may be the main cause of apparent twinning.

References

BUTLER, S.R. & BOUCHARD, R.J. (1971): Journal of Crystal Growth, 10: 163–169.
DANEU, N., REČNIK, A. & DOLENEC, T. (2005): 7th Multinational Congress on Microscopy: 197–198.
PÓSFAI, M. & BUSECK, P.R. (1997): EMU Notes in Mineralogy, 1: 193–235.

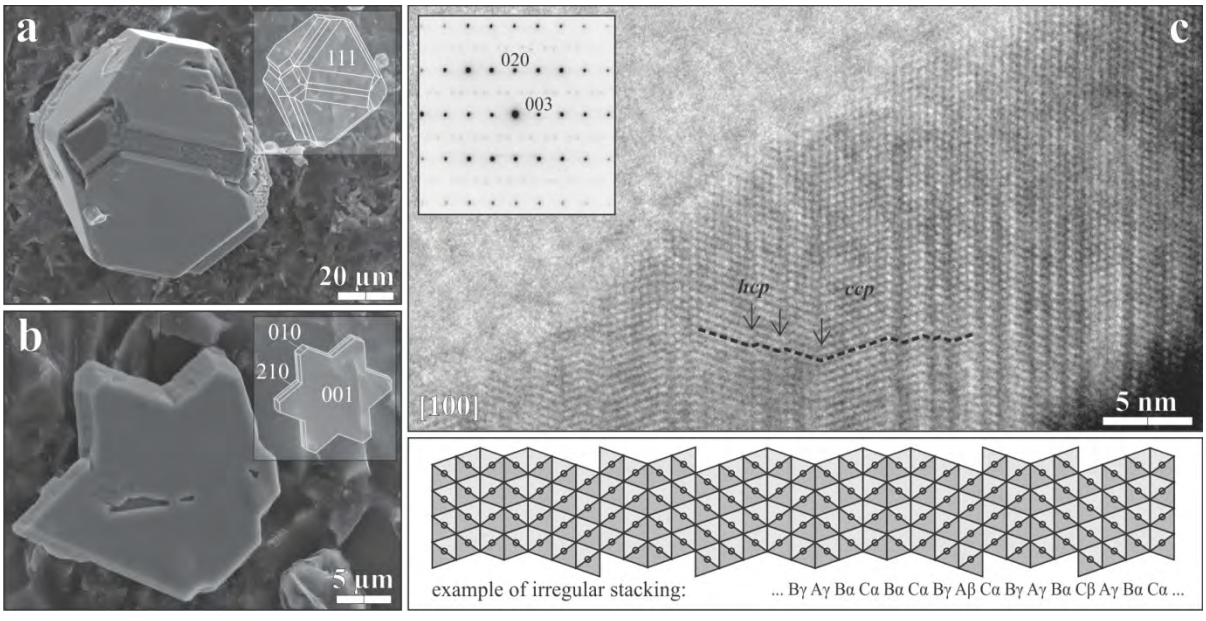

Fig. 1. *CVT synthesized Cu-doped Fe-sulphides. (**a**) SEM image of cubo-octahedral pyrite with epitaxial overgrowth of secondary generation of pyrite; (**b**) SEM image of interpenetration twinned pyrrhotite, grown in sulphur deficient environment at 600K; (**c**) HRTEM image of pyrrhotite in [100] projection. Irregular alternation of ccp and hcp stacking is visible near the thin edge of the crystal. The electron diffraction pattern (inset) shows weak incommensurable reflection pairs along [0kl], $k = 2n + 1$, $l \neq 3n$.*

GRANITIC ROCKS AS A SOURCE OF K_2O + Na_2O FOR CERAMIC APPLICATIONS IN BOLIVIA

ZEBALLOS, A.[1]*, WEIHED, P.[1], BLANCO, M.[2] & MACHACA, V.[2]
[1] Division of Geoscience, Luleå University of Technology, S-97187 Luleå, Sweden
[2] Instituto de Geología y del Medio Ambiente, Universidad Mayor de San Andrés, La Paz, Bolivia
* E-mail: Ariana.Zeballos @ltu.se

Based on geological mapping, sampling and mineralogical/petrological characterization, significant feldspar resources have been defined in Quimsa Cruz intrusive in the Choquetanga area and in the Sorata intrusive in the La Fabulosa area, Eastern Range, Bolivia. The petrographical studies performed on the samples show a granitic composition and the feldspar resources are hosted by granites in the Choquetanga area and in granitic pegmatites in the La Fabulosa area.

The potential of feldspathic rocks as a raw material for the ceramic industry is largely dependent on the alkali content present in the feldspars. Feldspars are used in ceramic industry for manufacturing of glass and pottery, both in the body of the ware and in the glaze, providing alumina (JENSEN & BATEMAN, 1979), and in the fine ceramic industry as a flux to form a glassy phase in the ceramic bodies, thus promoting vitrification and translucency. However, feldspars are also used as a source of alkalis and alumina in glazes (POTTER, 2006). The content of feldspars in ceramic goods varies between 15 and 80 wt% depending on the finished product (SINGER & SINGER, 1963). For sanitary ware (bathroom fittings) manufacturing of ceramics requires a significantly higher amount of feldspars (25–35 wt%) than in most other ceramic bodies. For example, wall and floor tiles industry uses 10–55 wt% feldspars for the finished products (HUGHES, 2006). Aplites, alaskites, granites, sands and pegmatites are commonly regarded as potential sources of feldspar (BATES, 1983; POTTER, 2006).

The ceramic industry in Bolivia has been growing in the last few years, more and more feldspathic raw material is needed and most is imported. The deposits were studied with focus on the feldspar content and in order to evaluate the quantity and quality of feldspars.

Figs. 1A and 1B show the texture, grain size and mineralogical composition of the samples. The results of the chemical analyses carried out by ICP show a ΣK_2O + Na_2O content of 7.84 wt% for Choquetanga samples and 14.25 wt% for La Fabulosa specimens, thus providing an alternative source of alkalis in both deposits.

References

BATES, R. (1983): Industrial minerals and rocks, 5(1): 711–722.
HUGHES, W. (2006): Minerals and metals availability in New South Wales Australia. 28.
JENSEN, M. & BATEMAN, A. (1979): Economic mineral deposits, 3: 496–505.
POTTER, M. (2006): Feldspars – Industrial Minerals & Rocks, 7: 451–460.
SINGER, F. & SINGER, S. (1963): Industrial Ceramics. New Delhi, India: Oxford and IBH.

Fig. 1. *Photographs of rock types in the studied areas. A) Choquetanga area: Feldspar bearing granites with typical orientation of feldspar megacrysts (5–10 cm in size); B) La Fabulosa area: The fine-grained granitic Sorata intrusive is surrounded and intruded by multiple pegmatitic dykes.*

SANIDINE TWINS FROM ZVEGOR, REPUBLIC OF MACEDONIA

ZEBEC, V.[1], ŽIGOVEČKI GOBAC, Ž.[2]*, MIKULČIĆ PAVLAKOVIĆ, S.[1], ŠIJAKOVA-IVANOVA, T.[3], ČOBIĆ, A.[2] & BERMANEC, V.[2]
[1] Croatian Natural History Museum, Demetrova 1, Zagreb, Croatia
[2] Institute of Mineralogy and Petrography, Department of Geology, Faculty of Science, University of Zagreb, Horvatovac 95, Zagreb, Croatia
[3] Department of Petrology, Mineralogy and Geochemistry, Faculty of Natural and Technical Sciences, University "Goce Delčev", Štip, Republic of Macedonia
* E-mail: zeljkaz@geol.pmf.hr

Introduction

Sanidine crystals were collected from quartz latite rocks east of the village Zvegor, in eastern part of the Republic of Macedonia. Morphology of these crystals was already described, but so far, among these crystals, only Carlsbad twins were observed (ŠIJAKOVA-IVANOVA *et al.,* 2011). X-ray powder diffraction analysis of these crystals confirmed the sanidine crystal structure (ŠIJAKOVA-IVANOVA *et al.*, 2011).

Experimental

Representative crystals were chosen for a goniometric measurement, which was done by two-circle reflecting goniometer. Crystallographic forms {010}, {110}, {130}, {001}, $\{\bar{1}11\}$, $\{\bar{2}01\}$ and {021} were identified using axial ratio a:b:c = 0.6585:1:0.5554 (GOLDSCHMIDT, 1897).

Results

According to observation and measurements performed, together with the already observed Carlsbad twins (ŠIJAKOVA-IVANOVA *et al.,* 2011), two new types of twins have been discovered. First, there are twins according to Manebach twin law, where twin plane is (001) and second, (110) Prism law, where twin plane is (110). Among all twins present, Carlsbad twins are most abundant. Left- (Fig. 1a, b, c) and right-handed Carlsbad twins are almost equally present. In several cases just one twining formation a left- or a right-handed twinning is present (Fig. 1d). A complex multiple twinning is also observed, where Carlsbad twins are between themselves grown according to (110) Prism twin law (Fig. 1e). Manebach twins are elongated along [100] (Fig. 1f).

Discussion and conclusion

Although all these types of twins are already mentioned in literature (SMITH, 1974), twins according to (110) Prism law are not so common, and, therefore, their finding is notable.

References

GOLDSCHMIDT, V. (1897): Krystallographische Winkeltabellen. Springer, Berlin, 432 p.
SMITH, J.V. (1974): Feldspar minerals, 2: 303–398.
ŠIJAKOVA-IVANOVA, T., ČOBIĆ, A., ŽIGOVEČKI GOBAC, Ž., ZEBEC, V. & BERMANEC, V. (2011): 2nd International Workshop on the UNESCO-IGCP Project: "Anthropogenic effects on the human environment in the Neogene basins in the SE Europe", 1–5.

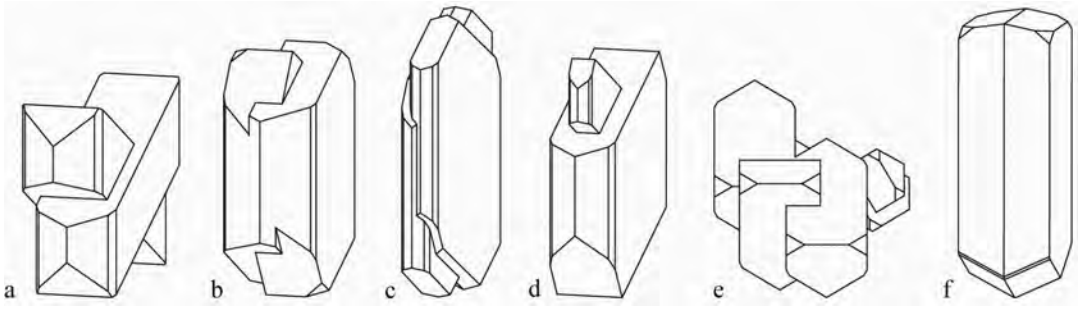

Fig. 1. *Sanidine twins. (a) Left-handed Carlsbad twins; (b) Left-handed Carlsbad twins: twinned crystals flattened along [010]; (c) Left-handed Carlsbad twins: twinned crystals elongated along [001]; (d) Carlsbad twins: a left- and a right-handed twinning in a just one twinning formation; (e) complex multiple twinning: Carlsbad twins grown according to (110) Prism law; (f) Manebach twins.*

AUTHOR INDEX

Alexandrowicz, Z. 84
Almási, E.E. 3
Anason, A. 4, 58
Andersen, J.C. 54, 55
Andráš, P. 80
Aradi, L. 5, 79
Arató, R. 6
Arehart, G. 13
Arvidson, R.S. 110
Asllani, B. 114
Atanassova, R. 7, 147
Atudorei, V. 131
Azzali, E. 8
Bąbel, M. 92
Bačík, P. 9, 144
Bajda, T. 120
Bajnóczi, B. 10, 145
Bakos, F. 90
Bălc, R. 156
Balica, C. 23
Balintoni, I. 23
Balogh, K. 149
Banach, M. 105
Baratta, G.A. 99
Baretto, S. de B. 11, 27
Barkóczy, P. 160
Bartha, A. 73
Batki, A. 3, 12, 128
Begić, V. 11
Belotti, F.M. 24
Belousova, E. 146
Bendő, Zs. 45, 97, 101
Benkó, Zs. 13
Beqiraj, A. 14, 15
Beqiraj (Goga), E. 14, 15
Berkesi, M. 16, 50, 102, 108
Bermanec, V. 11, 24, 27, 132, 163
Bertle, R.J. 17
Berzina, A.N. 18
Berzina, A.P. 18
Biernacka, J. 19
Bilal, E. 4, 46
Biroň, A. 80
Bistryakova, S. 85, 86
Blanco, M. 162
Bodor, S. 20
Boev, B. 132
Bondarenko, S. 67
Bors, V. 21
Bożęcki, P. 120
Bračko, I. 78
Brätz, H. 42
Broska, I. 22, 150
Buda, Gy. 69
Bukovec, P. 151
Buriánek, D. 30
Campeanu, M. 23
Cândido Filho, M. 24
Carbone, C. 8
Cherata, I. 131
Chernyatieva, A.P. 25
Cho, H.G. 26
Choi, H. 26
Chovan, M. 76
Christofides, G. 146
Chukanov, N.V. 55
Cieślik, B. 92
Čobić, A. 11, 27, 163
Comero, S. 123, 124
Čopjaková, R. 28, 29, 30
Cora, I. 39
Crandell, O.N. 31
Cristescu, C. 44
Czuppon, Gy. 16
Dabi, G. 145
Daneu, N. 32, 40, 118, 129, 151
de Capitani, L. 8, 111, 123, 124
Dinelli, E. 8
Dobos, T. 38
Dódony, I. 39
Dolenec, M. 151
Dolenec, T. 151
Drábek, M. 77
Drahokoupil, J. 77
Drev, S. 40
Dumitras, D.G. 4, 58
Effenberger, H.S. 115
Ertl, A. 42, 137
Fairhurst, R.J. 54, 55
Fallick, A.E. 70
Falus, Gy. 143
Fancsik, T. 143
Fehér, B. 43, 159, 160
Filipescu, R. 44
Fischer, C. 110
Földessy, J. 20, 94
Földvári, M. 74
Forray, F.L. 124
Fröjdö, S. 154
Gadas, P. 112, 113, 157
Gál, Á. 75, 124
Garašić, V. 100
Gega, D. 98
Georgiev, S. 48
Gherdán, K. 45
Ghineț, C. 46, 58
Giester, G. 42
Gimon, V.O. 18
Göttlicher, J. 76
Grakova, O.V. 47
Grieco, G. 68, 104, 123, 124
Griffin, W.L. 5, 146
Grigoraș, R. 52
Grinchenko, O. 67
Grozdev, V. 48
Grozdics, T. 49
Guzmics, T. 16, 50, 148
Haifler, J. 51
Har, N. 52
Harangi, Sz. 66, 89
Hargitai, A. 53
Hattori, K. 5
Hauck, S. 13
Heinrich, C.A. 70
Hidas, K. 143
Hirtopanu, P. 54, 55
Hoeck, V. 56, 65, 98
Horvat, M. 57
Houben, L. 118
Iancu, A.M. 4, 46, 58
Ilinca, G. 59
Ilnicki, S.S. 105
Ionescu, C. 56, 65
Jakab, Gy. 54, 55
Janeczek, J. 135
Jankovics, M.É. 66
Járó, M. 45
Jebavá, I. 125
Jeleň, S. 67, 80
Jin, L. 118
Jordán, Gy. 155
Jung, H. 102
Jurković, I. 100
Kacsó, C. 56
Káldos, R. 16
Kampić, Š. 11
Kaňuchová, Z. 99
Kastrati, S. 68, 104
Kerestedjian, T. 122
Kil, Y. 102
Kis, A. 69
Kiss, B. 66, 89
Kiss, G. 6, 103
Klötzli, U. 69
Knížek, F. 125
Koděra, P. 70, 90
Koller, F. 17, 69, 71, 72, 98
Kołodziejczyk, J. 114
Kónya, P. 73, 74, 149
Koroknai, B. 149
Koroneos, A. 146
Kouzmanov, K. 147
Kovács, I. 117, 143
Kovács, J. 117
Kovács-Pálffy, P. 74, 149
Kristály, F. 38, 75, 82, 83, 133, 134, 158, 159
Krivovichev, S.V. 25
Kučerová, G. 76
Kupi, L. 94, 160
Kutassy, L. 143
Kynický, J. 40
Lalinská-Voleková, B. 76
Laufek, F. 77
Lenart, A. 78
Lendvay, P. 143
Liptai, N. 79
Litochleb, J. 125
Łodziński, M. 105
Losos, Z. 113
Loun, J. 95
Ludusan, N. 54
Luptáková, J. 80
Luttge, A. 110
Macek, I. 81
Machaca, V. 162
Mádai, F. 82, 83, 91
Majzlan, J. 76
Manecki, M. 120
Marescotti, P. 8, 124
Marincea, Șt. 4, 46, 58
Markl, G. 12
Marku, S. 98
Maros, Gy. 149
Marszałek, M. 84
Mashukov, A. 85, 86
Mashukova, A. 85, 86
Matyszczak, W. 87
Meisel, T. 71
Melcher, F. 17
Menyhárt, A. 88
Metelski, P. 135
Metzner-Nebelsick, C. 56
Michałowski, P. 105
Mihály, J. 117
Mikulčić Pavlaković, S. 163
Mikuš, T. 67, 114
Milošević, M. 53
Milovská, S. 80
Minghua, R. 121
Mirtič, B. 78
Mogessie, A. 13
Molnár, F. 6, 13, 103

Molnár, K. 89
Molnár, L. 90
Móricz, F. 91
Nagy, G. 10
Nebelsick, L.D. 56
Nejbert, K. 92, 105
Németh, B. 93
Németh, N. 94
Németh, T. 158
Niedermayr, G. 71, 72
Novák, M. 29, 81, 95, 112, 126, 157
Ntaflos, T. 66, 89
Nyirő-Kósa, I. 96
Okrusch, M. 42
Oláh, I. 97
Onac, B.P. 115
Onuzi, K. 98
O'Reilly, S.Y. 5, 146
Ozdín, D. 9, 99, 144
Pálfy, J. 158
Palinkaš, L. 100, 132
Pál-Molnár, E. 3, 12, 128
Papp, R. 101
Park, M. 16, 102
Pásztor, D. 103
Patkó, L. 79
Pécskay, Z. 74, 149
Pedrotti, M. 68, 104
Pekker, P. 39
Petersen, O.V. 71
Petrescu, L. 55
Petrík, I. 22
Peytcheva, I. 48
Pieczka, A. 105, 107
Pintér, Zs. 16, 72, 108, 143
Plodinec, M. 78
Podlogar, M. 161
Pojar, I. 109
Ponomarenko, O. 67
Pop, D. 110
Porro, S. 8, 111, 123, 124
Porubčan, V. 99
Pósfai, M. 96
Přikryl, J. 112
Prokop, J. 113
Pršek, J. 67, 114
Puşcaş, C.M. 115
Qela, H. 114
Ratter, K. 45
Raucsik, B. 116, 117
Rečnik, A. 32, 40, 118, 129, 161
Robert, J.-L. 119
Rostási, Á. 96, 116
Różniak, R. 105
Ryan, J. 131
Rzepa, G. 84, 120
Rzepka, P. 120
Sadek Ghabrial, D. 121
Savov, I. 131
Scholz, R. 24
Schüssler, U. 42
Scott, P.W. 55
Sejkora, J. 125, 130
Selbekk, R. 154
Serafimovski, T. 151
Sergeeva, I. 122
Servida, D. 8, 111, 123, 124
Severson, M. 13
Šijakova-Ivanova, T. 163
Simon, V. 44, 65
Sjöblom, S. 154
Škácha, P. 125
Skakun, L. 67
Škoda, R. 30, 51, 126
Slepička, V. 125
Slovenec, Da. 57
Šmuc, N.R. 151
Šobak, M. 161
Socaciu, A. 156
Sogrik, E. 128
Spiridonova, D.V. 25
Srećković-Batoćanin, D. 146
Stanković, N. 129
Steininger, R. 76
Števko, M. 9, 130, 144
Stremțan, C.C. 23, 115, 131
Strmić Palinkaš, S. 100, 132
Šturm, S. 78
Svoreň, J. 99
Szabó, Á. 5, 108
Szabó, Cs. 5, 16, 50, 72, 93, 102, 108, 143, 148, 155
Szakács, A. 75, 124
Szakáll, S. 43, 73, 75, 88, 133, 134, 159, 160
Szakmány, Gy. 45, 97
Szegő, É. 74
Szełęg, E. 105, 135
Szentpéteri, K. 159, 160
Szilágyi, V. 97
Szuszkiewicz, A. 105
Takács, Á. 45
Thamó-Bozsó, E. 74, 136
Tillmanns, E. 42, 137
Topa, B.A. 138
Török, K. 93
Tóth, A. 108
Tóth, E. 49, 53, 101, 138, 139
Tóth, J. 21, 99
Tóth, M. 10
Turniak, K. 105
Udvardi, B. 117, 143
Uher, P. 9, 22, 99, 144
Újvári, G. 117
Váczi, T. 45
Varga, A. 117, 145
Varga, G. 45
Vašinová Galiová, M. 29
Vasković, N. 53, 146
Vassileva, R.D. 7, 147
Vetlényi, E. 148
Viczián, I. 149
Vojtko, P. 150
Völgyesi, P. 155
Von Quadt, A. 48
Vrhovnik, P. 151
Všianský, D. 113
Vymazalová, A. 77
Wachowiak, J. 107
Walder, I.F. 91, 152
Wälle, M. 70
Wegner, R. 11
Weihed, P. 162
Weiszburg, T.G. 45, 49, 53, 101, 138, 139
Wenzel, T. 12
Woodard, J. 154
Zacháry, D. 155
Zaharia, L. 44, 52, 109, 156
Zahradníček, L. 157
Zajzon, N. 43, 45, 88, 94, 133, 134, 158, 159, 160
Zavašnik, J. 118, 161
Zeballos, A. 162
Zebec, V. 11, 163
Zelei, T. 143
Zelenka, T. 74, 94
Žigovečki Gobac, Ž. 24, 163
Zupančič, M. 151

established in 1922

ACTA MINERALOGICA-PETROGRAPHICA
ABSTRACT SERIES

VOLUME 7 2012
HU ISSN 0365-8066
HU ISSN 1589-4835

Ikunolite, Nagybörzsöny, Hungary. Width of the picture 2 cm.
Photo and collection: L. Tóth.

Produced in Hungary by the University of Miskolc